Optimization of dicarboxylic acid production with *Methylorubrum extorquens* AM1 and further developments for future use as a methylotrophic cell factory

Dissertation
zur Erlangung des Doktorgrades
der Naturwissenschaften

vorgelegt beim Fachbereich 15 - Biowissenschaften
der Johann Wolfgang Goethe-Universität
in Frankfurt am Main

von
Laura Marie Pöschel
aus Aschaffenburg

Frankfurt am Main (2023)
(D30)

Vom Fachbereich 15 der
Johann Wolfgang Goethe-Universität als Dissertation angenommen.

Dekan:
Prof. Dr. Sven Klimpel
Goethe-Universität Frankfurt, Institut für Ökologie, Evolution und Diversität

Gutachter:
Prof. Dr. Jens Schrader
(ehemals) DECHEMA-Forschungsinstitut

Prof. Dr. Eckhard Boles
Goethe-Universität Frankfurt, Institut für Molekulare Biowissenschaften

Datum der Disputation:

"There is nothing like looking, if you want to find something (or so Thorin said to the young dwarves). You certainly usually find something, if you look, but it is not always quite the something you were after."

The Hobbit, John Ronald Reuel Tolkien, 1937

This thesis is based on the following publications and manuscripts:

Pöschel L, Gehr E, Buchhaupt M (2022a)
Improvement of dicarboxylic acid production with *Methylorubrum extorquens* by reduction of product reuptake.
Appl Microbiol Biotechnol 106:6713–6731. DOI: 10.1007/s00253-022-12161-0
→ incorporated as Chapter 6.1

Pöschel L, Guevara-Martínez M, Hörnström D, van Maris AJA, Buchhaupt M
Engineering of thioesterase YciA from *Haemophilus influenzae* for production of carboxylic acids.
Appl Microbiol Biotechnol (accepted)
→ incorporated as Chapter 6.2

Pöschel L, Gehr E, Buchhaupt M (2022b)
A pBBR1-based vector with IncP group plasmid compatibility for *Methylorubrum extorquens*.
MicrobiologyOpen 11:e1325. DOI: 10.1002/mbo3.1325
→ incorporated as Chapter 6.3

Pöschel L, Gehr E, Jordan P, Sonntag F, Buchhaupt M
Expression of toxic genes in *Methylorubrum extorquens* with a tightly repressed, cumate-inducible promoter.
submitted
→ incorporated as Chapter 6.4

Zusammenfassung

In Anbetracht des steigenden Konsums einer wachsenden Weltbevölkerung sowie der drohenden Endlichkeit fossiler Brennstoffe ist die Entwicklung von ressourcenschonenden Produktionsprozessen ein integraler Bestandteil der Transformation hin zu einer nachhaltigen Industrie. Als Rohstoff für Brücken- und Zukunftstechnologien empfiehlt sich insbesondere Methanol, welches sowohl petrochemisch als auch aus erneuerbaren Ressourcen hergestellt und auch in biotechnologischen Verfahren als Substrat eingesetzt werden kann. Die Methanolproduktion konkurriert weder mit der Nahrungs- und Futtermittelproduktion, noch benötigt sie große Agrarflächen, wie es für die meisten klassischen, zuckerbasierten Substrate der Fall ist. Obwohl Methanol bisher hauptsächlich aus fossilen Rohstoffen hergestellt wird, nimmt der Marktanteil an nachhaltig produziertem Methanol (Bio-Methanol und e-Methanol) stetig zu. Als Substrat in biotechnologischen Prozessen senkt die Verwendung von Methanol das Kontaminationsrisiko. Darüber hinaus kann es in definierten synthetischen Medien eingesetzt werden, was die Aufarbeitung potenzieller Zielprodukte stark vereinfacht.

Ein vielversprechender Plattformorganismus für die Etablierung methanolbasierter biotechnologischer Prozesse ist *Methylorubrum extorquens* AM1 (ehemals *Methylobacterium extorquens* AM1). Dieses Alphaproteobakterium dient seit über 60 Jahren als Modellorganismus für die Erforschung der Methylotrophie, der Fähigkeit, C_1-Moleküle wie Methanol als alleinige Energie- und Kohlenstoffquelle unter Anwesenheit von Sauerstoff zu nutzen. Obwohl durch die jahrzehntelange Erforschung umfangreiches Wissen über das Genom, das Transkriptom und die Stoffwechselwege erworben, sowie bereits verschiedene homologe und heterologe Produktionswege für eine Vielzahl von Produkten für *M. extorquens* im Labormaßstab beschrieben wurden, konnte bisher kein Prozess im industriellen Maßstab realisiert werden. Dafür können drei maßgebliche Gründe identifiziert werden: (1) Eine relativ limitierte Auswahl von Werkzeugen zur gentechnischen Modifizierung des Bakteriums, (2) fehlendes Verständnis für Kohlenstoffflüsse und auftretende Nebenreaktionen in modifizierten Stämmen, wie beispielsweise Produktreimporte, und (3) das Fehlen von maßgeschneiderten Produktionsstämmen für finanziell ertragreiche Zielprodukte sowie eine für diese speziell optimierte Bioprozessführung. Das Ziel der vorliegenden Arbeit war es, Entwicklungen für die drei genannten Bereiche zu tätigen, um zur Weiterentwicklung von *M. extorquens* hin zu einer methylotrophen Zellfabrik

beizutragen, die potenziell im industriellen Maßstab eingesetzt werden kann. Die Entwicklungen, die in dieser Arbeit erzielt wurden, sind in Abbildung 1 zusammengefasst.

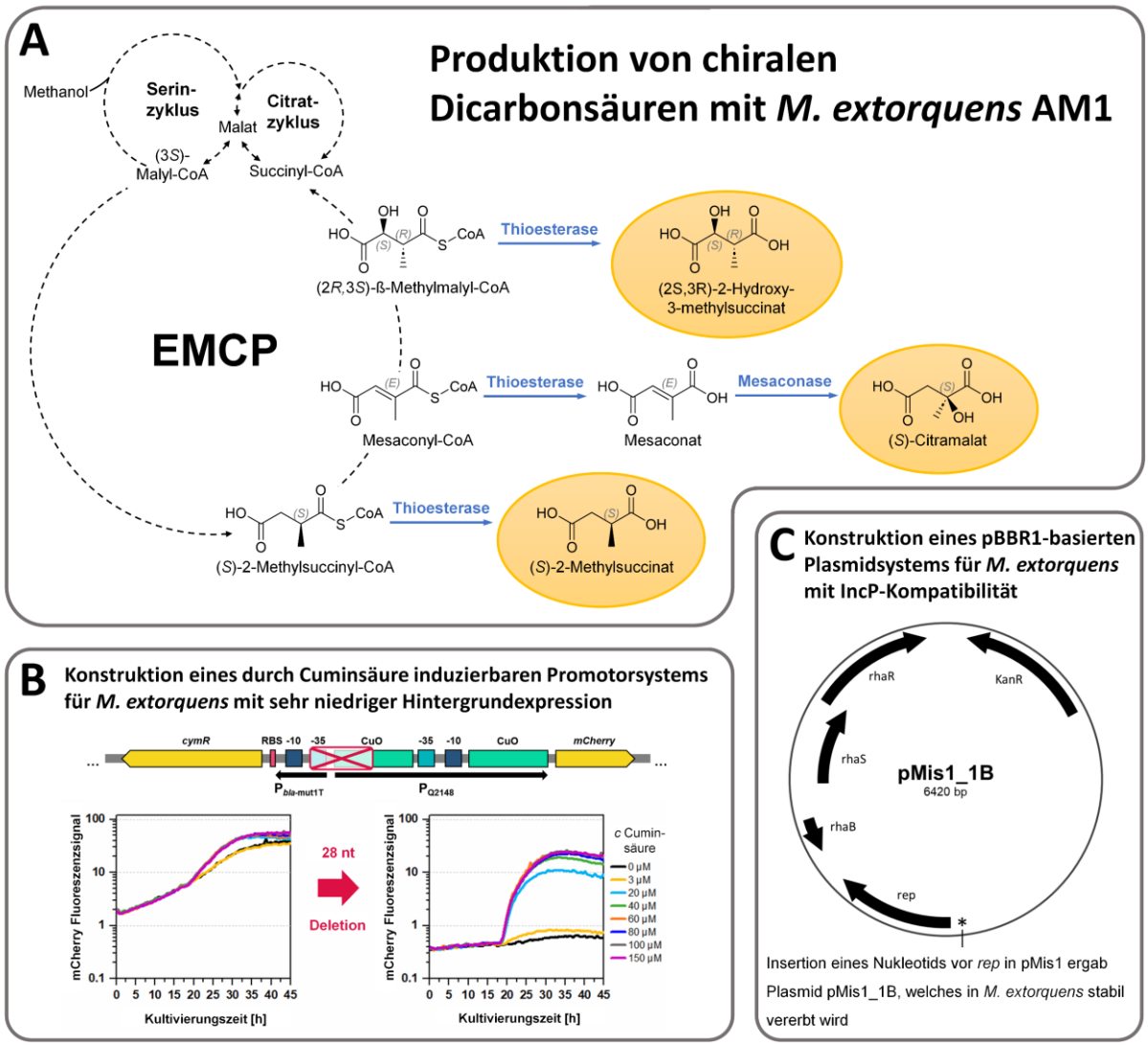

Abbildung 1 Übersicht des Promotionsprojektes - In dieser Arbeit erzielte Entwicklungen zur Verbesserung der Anwendbarkeit von *M. extorquens* AM1 als künftige methylotrophe Zellfabrik für die Produktion von chiralen Dicarbonsäuren und weiteren Spezialchemikalien aus Methanol. **A** Die Freisetzung von chiralen Verbindungen aus dem Ethylmalonyl-CoA-Stoffwechselweg (EMCP) wurde durch das Einbringen heterologer Enzyme (blaue Pfeile) erreicht. Zur Vereinfachung wurden in der Abbildung die Dicarbonsäuren mit den Namen der jeweiligen Anionen bezeichnet. Die gezeigten absoluten Konfigurationen der Produkte wurden entweder durch entsprechende Analysen belegt oder aus der Stereoselektivität der verwendeten Enzyme abgeleitet. **B-C** Zwei neuartige Werkzeuge wurden für die Herstellung von *M. extorquens* Stämmen entwickelt, ein mit Cuminsäure induzierbarer Promotor, der auf die Expression von Genen mit toxischen Produkten zugeschnitten ist (**B**), sowie ein Plasmidsystem, welches zusammen mit Plasmiden der IncP-Gruppe verwendet werden kann (**C**).

Maßgeschneiderte Produktionsstämme und -prozesse für wertvolle Zielprodukte, sowie Steigerung der Ausbeute durch Verminderung der Produktwiederaufnahme

Um das Potenzial von *M. extorquens* als methylotrophe Zellfabrik zu verdeutlichen, sollten für das Forschungsprojekt Zielprodukte gewählt werden, die auch industrielle und gesellschaftliche Interessen widerspiegeln. Kandidaten für solche Zielprodukte sind beispielsweise enantiomerenreine, chirale Substanzen, da diese von großer Bedeutung als Bausteine für pharmazeutische Wirkstoffe sind. In der Regel ist eine vollchemische stereoselektive Synthese oder Aufarbeitung chiraler Moleküle mit hohen Kosten und einem gesteigerten Arbeitsaufwand verbunden. Daher kann die Herstellung von chiralen Bausteinen auf biotechnologischem Weg eine kosteneffiziente Alternative bieten.

Im Ethylmalonyl-CoA-Stoffwechselweg (EMCP), der Teil des Primärstoffwechsels von *M. extorquens* ist, finden sich spezielle, teils chirale CoA-Ester-Intermediate. Derivate dieser CoA-Ester können durch das Einbringen von heterologen Enzymen freigesetzt werden. Die Dicarbonsäuren Mesaconsäure und 2-Methylsuccinylsäure (zur Vereinfachung werden im Folgenden die Bezeichnungen Mesaconat und 2-Methylsuccinat verwendet) wurden in einer früheren Studie durch Einbringen der heterologen Thioesterase YciA aus *Escherichia coli* in *M. extorquens* produziert[1)]. Da die chirale Integrität bei der Hydrolyse von (*S*)-2-Methylsuccinyl-CoA erhalten bleibt (Abbildung 1A), konnte trotz fehlender chiraler Analytik davon ausgegangen werden, dass 2-Methylsuccinat als *S*-Enantiomer vorliegt. Die verwendeten Stämme produzierten in der besagten Studie eine Mischung von Mesaconat und 2-Methylsuccinat mit einem maximalen kombinierten Produkttiter von 0,65 g/L in Schüttelkolbenexperimenten. Diese Experimente dienen als Grundlage für die Entwicklungen der vorliegenden Arbeit.

Die zuvor beschriebenen Stämme sollten weiterentwickelt werden, um höhere Ausbeuten zu erreichen und um neue, biotechnologisch bisher nicht zugängliche Dicarbonsäuren herzustellen. Zur Erhöhung der Produktausbeute sollte zunächst die zuvor beschriebene Produktwiederaufnahme von Mesaconat und 2-Methylsuccinat adressiert werden. In vorherigen Studien[1)] wurde ein deutlicher Abfall der Produktkonzentration beobachtet, sobald die produzierenden Bakterienkulturen in die stationäre Wachstumsphase übergingen. Zum Zeitpunkt der Studien war unklar, ob die Aufnahme der Produkte erst zu diesem Zeitpunkt einsetzt oder ob sie über die

1) Sonntag F, Müller JEN, Kiefer P, Vorholt JA, Schrader J, Buchhaupt M (2015) High-level production of ethylmalonyl-CoA pathway-derived dicarboxylic acids by *Methylobacterium extorquens* under cobalt-deficient conditions and by polyhydroxybutyrate negative strains. Appl Microbiol Biotechnol 99:3407–3419. https://doi.org/10.1007/s00253-015-6418-3

ganze Kultivierungsphase hinweg abläuft und durch die höhere Freisetzung maskiert wird. In der hier vorliegenden Arbeit wurden verschiedene Ansätze genutzt, um mögliche Faktoren für die Produktwiederaufnahme zu identifizieren. Eine Transkriptomanalyse von Zellen in verschiedenen Wachstumsstadien lieferte keine eindeutigen Ergebnisse hinsichtlich möglicher Importfaktoren. Auch konnte kein direkter Mutagenese/Screening Ansatz genutzt werden, da es nicht möglich war, *M. extorquens* auf Medien zu kultivieren, die ausschließlich Mesaconat oder 2-Methylsuccinat als Kohlenstoffquelle enthielten. Stattdessen wurde das halogenierte Analogon 2,2-Difluorosuccinat als Selektionsmittel eingesetzt, welches wachstumshemmend auf Methanol-metabolisierende *M. extorquens*-Zellen wirkt. Mit diesem Ansatz konnte schließlich das Gen *dctA2* als Ziel für die Verringerung der Aufnahme von Dicarbonsäuren identifiziert werden. Durch die Deletion des *dctA2* Gens, welches mit hoher Wahrscheinlichkeit für einen Säuretransporter codiert, konnte die Produktwiederaufnahme von Mesaconat und 2-Methylsuccinat deutlich reduziert werden. Weiterhin wurde die Wiederaufnahme von Mesaconat durch die Umwandlung zu einem von *M. extorquens* nicht-metabolisierbaren Produkt durch das Einbringen eines weiteren heterologen Enzyms unterbunden. Das achirale Produkt Mesaconat wurde dabei mithilfe einer Mesaconase/Fumarat Hydratase aus *Paraburkholderia xenovorans* zu (*S*)-Citramalat umgesetzt und somit ein weiteres chirales Produkt zugänglich gemacht (Abbildung 1A).

Zur Freisetzung der genannten Dicarbonsäureprodukte wurde YciA, eine Thioesterase mit breitem Substratspektrum, gewählt, die eine Vielzahl von CoA-Estern unterschiedlicher Kettenlänge akzeptiert. Somit sollte das Enzym in der Theorie alle im EMCP vorkommenden CoA-Ester von Interesse (Crotonyl-CoA, (*S*)-2-Ethylmalonyl-CoA, (*R*)-2-Ethylmalonyl-CoA, (*S*)-2-Methylsuccinyl-CoA, Mesaconyl-CoA, (2*R*,3*S*)-β-Methylmalyl-CoA, (*S*)-2-Methylmalonyl-CoA und (*R*)-2-Methylmalonyl-CoA) hydrolysieren können. In den Kulturüberständen von *M. extorquens*-Stämmen, die das entsprechende Thioesterase-Gen überexprimierten, konnten allerdings nur Mesaconat und 2-Methylsuccinat nachgewiesen werden. Um das Substratspektrum der YciA Thioesterase zu erweitern, wurde semi-rationales Enzym-Engineering eingesetzt. Da die potenziellen Substrate eine hohe strukturelle Ähnlichkeit aufwiesen und nicht klar war, welche Faktoren die Selektivität des Enzyms beeinflussen, war ein rein rationales Vorgehen wenig zielführend. Mithilfe eines Strukturmodells und der publizierten Literatur zu YciA und verwandten Thioesterasen wurde eine Reihe von

Aminosäurepositionen identifiziert, die bei der Enzym-Substrat-Bindung potenziell eine Rolle spielen. Basierend auf diesen Analysen wurde eine kleine Bibliothek von Expressionsplasmiden für YciA-Varianten erstellt, die an den identifizierten Stellen in der Aminosäuresequenz von der Wildtyp-Enzymvariante abwichen. Im Screening der entsprechenden Stämme konnte für keine der Varianten ein neuartiges Dicarbonsäureprodukt identifiziert werden. Allerdings wirkten sich Veränderungen der F35 Position stark auf die Produktion von Mesaconat und 2-Methylsuccinat aus. Der Einsatz von YciA F35N und YciA F35L steigerte die maximal erreichten Produkttiter im Vergleich zur unmodifizierten YciA-Variante deutlich. Der Einfluss der F35 Position konnte ebenfalls in einem *Escherichia coli*-Stamm nachgewiesen werden, der für die Produktion von 3-Hydroxybutyrat konstruiert wurde. Hierbei führte der Einsatz der F35L YciA-Variante zu dreifach höheren Produkttitern als der Einsatz des unmodifizierten Enzyms. Der Versuch, die F35L-Variante weiter zu charakterisieren, scheiterte daran, dass Zellextrakte, sowie das aufgereinigte Enzym der F35L-Variante keine oder nur sehr geringe Aktivitäten gegenüber den getesteten Substraten *in vitro* zeigten. Dies ließ darauf schließen, dass die Enzymvariante nur *in vivo* stabil ist. F35 befindet sich am N-Terminus einer α-Helix, die den Substratbindekanal definiert. Ein Vergleich mit anderen nahe verwandten Thioesterasen (Thioesterase Familien 4, 6, 7, 8, 11 und 31) zeigte, dass diese Position hochkonserviert ist. Dies spricht dafür, dass mit der besagten Position ein Target identifiziert wurde, welches potenziell auch zur Modifikation verwandter Thioesterasen verwendet werden kann. In der vorliegenden Arbeit wurden zwar mit YciA F35N und YciA F35L wesentlich produktivere Enzymvarianten für die Herstellung von Mesaconat und 2-Methylsuccinat generiert, zuvor unzugängliche Dicarbonsäureprodukte wurden durch den Einsatz der Enzymvarianten jedoch nicht freigesetzt. Die angestrebte Erweiterung des Dicarbonsäure-Produktspektrums von *M. extorquens* um ein weiteres chirales Molekül wurde schließlich durch die Verwendung einer alternativen Thioesterase aus *Corynebacterium glutamicum* erreicht. Der Einsatz dieser alternativen Thioesterase führte zur Freisetzung von 2-Hydroxy-3-methylsuccinat (siehe Abbildung 1A).

Für die beiden neuartigen Dicarbonsäureprodukte Citramalat und 2-Hydroxy-3-methylsuccinat liegen keine Analysen zur Enantiomerenreinheit vor, allerdings kann aufgrund der Substratcharakteristika sowie der Stereoselektivität der verwendeten Enzyme von der Produktion der Enantiomere (*S*)-Citramalat und (2*S*,3*R*)-2-Hydroxy-3-methylsuccinat in hoher Reinheit ausgegangen werden. Für 2-Methylsuccinat

wurden in Kooperation mit der Firma Chiracon GmbH (Luckenwalde, Deutschland) erste Analysen durchgeführt und ein Enantiomerenüberschuss des *S*-Enantiomers von 95 - 97,8 % berichtet.

Für die Skalierung der Dicarbonsäureproduktion mit *M. extorquens* AM1 wurden abschließend speziell zugeschnittene Fermentationsstrategien entwickelt. Eine besondere Herausforderung stellte dabei die präzise Steuerung der Methanolzufuhr dar. Konzentrationen von über 1 % (v/v) Methanol wirken sich negativ auf das Wachstum von *M. extorquens* AM1 Kulturen aus, während zu niedrige Methanolkonzentrationen die Wiederaufnahme von Dicarbonsäureprodukten fördern. Für die kontrollierte Methanolzufütterung wurde daher ein skriptgesteuertes Fed-Batch-Verfahren entwickelt, das ausschließlich auf Messungen des gelösten Sauerstoffes basiert und so eine aufwändige Online-Messung der Methanolkonzentration überflüssig macht. Für die Zielverbindungen Mesaconat, 2-Methylsuccinat, Citramalat und 2-Hydroxy-3-Methylsuccinat wurden Titer von 3,8 g/L bis 5,8 g/L erzielt, was die bisher höchsten Titer für die mikrobielle Produktion dieser Produkte auf Methanolbasis darstellt.

Entwicklung von neuen Werkzeugen für die Konstruktion von *M. extorquens* AM1-Produktionsstämmen

Eine breite Auswahl von Methoden für die Modifizierung von Produktionsstämmen ist eine Voraussetzung für die Anwendbarkeit von *M. extorquens* als methylotrophe Zellfabrik. Darunter fallen verschiedene molekulargenetische Werkzeuge für Genexpression, Gen-Transfer, Gen-Deletion, Gen-Integration, sowie für die Mutagenese. Allerdings sind viele gut etablierte Plasmid- und Promotorsysteme nicht geeignet für die Verwendung in *M. extorquens*.

Bislang werden hauptsächlich Plasmide für *M. extorquens* eingesetzt, die auf einem einzigen Plasmidsystem (pCM) basieren. Um die Expression von heterologen Genen in *M. extorquens* zu erleichtern und insbesondere um die Testung von Genkombinationen zu vereinfachen, sollte in der vorliegenden Arbeit die Anwendung eines neuartigen, zu pCM-Plasmiden kompatiblen, Vektors getestet werden. Bei diesem Vektor handelt es sich um eine Variante des pBBR1-basierten Plasmids pMis1 (Abbildung 1C). Aus pMis1-Transformanten wurde die Plasmidvariante pMis1_1b isoliert, die eine Insertion im Bereich des *rep*-Gens enthielt. Auch wenn die Co-Transformation von *M. extorquens* mit pMis1_1b und pCM zu Wachstumsdefekten

führte, konnte eine hohe Kopienzahl des neuen Plasmids sowie eine starke Plasmid-basierte Genexpression nachgewiesen werden.
Als zweites Werkzeug wird in der vorliegenden Arbeit ein synthetischer Promotor vorgestellt und charakterisiert. Das von der ETH Zürich beschriebene induzierbare Promotorsystem P_{Q2148} zeigte, anders als in der entsprechenden Publikation beschrieben, eine hohe Hintergrundexpression bei der Verwendung in *M. extorquens* AM1. Bei der Testung von Terpen-Produktionsstämmen wurde eine Variante des Promotors mit einer deutlich reduzierten Hintergrundexpression identifiziert. Diese Promotorvariante (P_{s6}), die eine Deletion weniger Basenpaare enthielt, wurde mithilfe eines Reportergen-Assays näher charakterisiert (Abbildung 1B). P_{s6} zeigte im Vergleich zu P_{Q2148} zwar eine geringere maximale Expressionsstärke, zugleich aber eine sehr starke Repression der Transkription in Abwesenheit des Induktors. Zudem ließ sich die Expressionsstärke von P_{s6} über die Menge der Induktorzugabe einstellen. Der hier vorgestellte neue Promotor ist aufgrund seiner Eigenschaften besonders geeignet für die kontrollierte Expression von Genen mit potenziell toxischen Produkten in *M. extorquens*.

Insgesamt belegt die vorliegende Arbeit die Eignung von *M. extorquens* als methylotrophe Zellfabrik. In den vorgestellten Anwendungen wird dabei die biotechnologische Produktion von wirtschaftlich und industriell vielversprechenden, chiralen Molekülen mit der Verwendung eines zukunftsfähigen, alternativen Substrats verbunden. Zudem werden neue Entwicklungen und Ansatzpunkte vorgestellt, die die Herstellung und Optimierung zukünftiger Produktionsstämme vereinfachen.

Abstract

In view of a growing world population and the finite nature of fossil resources, the development of eco-friendly production processes is essential for the transition towards a sustainable industry. Methanol, which can be produced both petrochemically and from renewable resources, offers itself as bridging technology and attractive alternative raw material for biotechnological processes. This work describes developments for the progress of the well-studied methylotrophic α-proteobacterium *Methylorubrum extorquens* AM1 (formerly *Methylobacterium extorquens* AM1) towards an efficient methylotrophic cell factory. Although many homologous and heterologous production routes have already been described and realized for *M. extorquens* in a laboratory scale, no industrial process has yet been realized. Three major reasons can be identified for this: (1) A relatively limited choice of tools for genetic modifications, (2) a lack of understanding of carbon fluxes and side reactions occurring in modified strains, such as product reimports, and (3) the lack of tailored production strains for profitable target products and the respective optimized bioprocessing protocols. The aim of the present work was to achieve developments for the three mentioned areas. As a model application, the high-level production of chiral dicarboxylic acids from the substrate methanol was chosen. Enantiomerically pure chiral compounds are of great interest, e.g., as building blocks for chiral drugs. The ethylmalonyl-CoA metabolic pathway (EMCP) which is part of the primary metabolism of *M. extorquens*, harbors unique chiral CoA-ester intermediates. Their acid derivatives can be released by cleavage of the CoA-moiety using heterologous enzymes. The dicarboxylic acids 2-methylsuccinic acid and mesaconic acid were produced in a previous study by introducing the heterologous thioesterase YciA into *M. extorquens*[1)]. In the said study, a combined 2-methylsuccinic acid and mesaconic acid titer of 0.65 g/L was obtained in shake flask experiments. These results serve as the basis for the developments in the present work.

First, the previously described reuptake of mesaconic acid and 2-methylsuccinic acid was thoroughly investigated and *dctA2*, a gene probably encoding for an acid transporter, was identified as target for reducing the product reuptake. In addition, reuptake of mesaconic acid was prevented by converting it to (*S*)-citramalic acid, a product not metabolizable by *M. extorquens*, by the introduction of a heterologous mesaconase. Together with 2-methylsuccinic acid, for which a high enantiomeric excess of (*S*)-2-methylsuccinic acid was determined, a second chiral molecule was

1) Sonntag F, Müller JEN, Kiefer P, Vorholt JA, Schrader J, Buchhaupt M (2015) High-level production of ethylmalonyl-CoA pathway-derived dicarboxylic acids by *Methylobacterium extorquens* under cobalt-deficient conditions and by polyhydroxybutyrate negative strains. Appl Microbiol Biotechnol 99:3407–3419. https://doi.org/10.1007/s00253-015-6418-3

thus added to the product spectrum. For the release of dicarboxylic acid products, YciA, a broad-range thioesterase that accepts a variety of CoA-esters with different chain lengths as substrates, was chosen. The enzyme should theoretically be able to hydrolyze all CoA-esters of interest present in the EMCP. However, in culture supernatants of *M. extorquens* strains that were overexpressing the corresponding *yciA* gene, only mesaconic acid and 2-methylsuccinic acid could be detected. To expand the substrate spectrum of YciA thioesterase with respect to other EMCP intermediates, semi-rational enzyme engineering was attempted. Screening of the corresponding strains carrying the respective YciA variants did not result in strains capable of producing new dicarboxylic acid products. However, the experiments revealed an amino acid position that strongly affected the production of mesaconic acid and 2-methylsuccinic acid *in vivo*. By substituting the according amino acid in YciA, the maximum titers of mesaconic acid and 2-methylsuccinic acid could be increased substantially. Application of an improved thioesterase variant in a second *E. coli*-based process confirmed the enhanced activity of the enzyme. The desired extension of the product spectrum by another chiral molecule (2-hydroxy-3-methylsuccinic acid, presumably the (2*S*,3*R*)-form) was finally achieved by using an alternative thioesterase. Tailored fermentation strategies were developed for the high-level production of the above-mentioned products. A particular challenge was the precise control of the methanol feeding, since high concentrations of methanol have a negative impact on the growth of *M. extorquens* AM1 cultures, while very low concentrations promote reimport of dicarboxylic acid products. With the developed process, titers of several g/L were achieved for all target compounds.

As second part of the work, two novel genetic tools for *M. extorquens* were developed and characterized. The pBBR1-derived plasmid pMis1_1B was shown to be stably maintained in *M. extorquens* cells. In addition, its suitability for co-transformations with other plasmids was demonstrated. The second tool, the cumate-inducible promoter P_{s6}, is tailored for expression of pathways with toxic products, as the transcription of genes controlled by P_{s6} is strongly repressed in the absence of an inducer.

Overall, the present work demonstrates the enormous potential of using *M. extorquens* as a methylotrophic cell factory. In the applications shown, the biotechnological production of high-priced chiral molecules is combined with the use of an attractive alternative substrate. In addition, new achievements and approaches are presented to facilitate the development of future *M. extorquens* production strains.

Table of Contents

List of Abbreviations

A	absorption
a.u. / A.U.	arbitrary unit
ACOT	acyl-CoA thioesterase
AM1	airborne methylamine or airborne methylotroph (specifier for *M. extorquens* isolate)
atm	standard atmospheric pressure
BLAST	Basic Local Alignment Search Tool
bp	base pair(s)
C_1	compounds containing no carbon-carbon bond
C_2	compounds containing only one carbon-carbon bond
ca.	circa
CAS	Chemical Abstracts Service (part of American Chemical Society)
CIP	Cahn-Ingold-Prelog (convention for naming a stereoisomer with an *R*- or *S*- descriptor)
CoA	coenzyme A
C-terminus	carboxyl-terminus or COOH-terminus (end of a protein or polypeptide)
CDW	cell dry weight
CRI	Carbon Recycling International
DAC	direct air capture
DNA	deoxyribonucleic acid
DO	dissolved oxygen
DOI	digital object identifier
DTNB	5,5′-dithiobis-(2-nitrobenzoic acid) (Ellman's reagent)
EDTA	ethylenediaminetetraacetic acid
e.g.	for example (lat. *exempli gratia*)
EMCP	ethylmalonyl-CoA pathway
Eq.	equation
et al.	and others (lat. *et alii*)
Fig.	figure
fw	forward primer
g	gram
GC/FID	gas chromatography with flame ionization detector

GFP	green fluorescent protein
h	hour(s)
ddH_2O	ultrapure water
HEPES	4-(2-hydroxyethyl)-1-piperazineethanesulfonic acid
his6	polyhistidine-tag consisting of six histidine residues
HPLC	high-performance liquid chromatography
IncP	incompatibility group P (classification for plasmids based on their (in)compatibility with other plasmids)
IPTG	isopropyl-β-D-thiogalactopyranoside
IS	insertion sequence
IUPAC	International Union of Pure and Applied Chemistry
Kan	kanamycin
Kan^R	kanamycin resistance gene/cassette or kanamycin-resistant
kDa	kilodalton (1 kDa = 1 000 Da)
L	liter
LB	lysogeny broth medium
LC-MS	Liquid chromatography–mass spectrometry
LC-MS/MS	Liquid chromatography–tandem mass spectrometry
LNG	liquefied natural gas
log	logarithm or logarithmic
M	molar (mol/L)
Mbp	Mega base pair(s)
MDH	methanol dehydrogenase
MeCF	methylotrophic cell factory
mg	milligram
min	minute(s)
MS	mass spectrometer or mass spectrometry
MS/MS	tandem mass spectrometer or tandem mass spectrometry
N/A	not applicable
n.d.	no data
NCBI	National Center for Biotechnology Information
ng	nanogram (1 ng = 10^{-9} g)
nm	nanometer (1 nm = 10^{-9} m)
nos	numbers

NO_X	nitrogen oxides, mixture of NO and NO_2
N-terminus	amino-terminus or NH_2-terminus (start of a protein or polypeptide)
OD_{600}	optical density, measured at 600 nm
PA1	phyllosphere of *Arabidopsis* (specifier for *M. extorquens* isolate)
PCN	plasmid copy number
PCR	polymerase chain reaction
PDB	protein data base
PHA	polyhydroxyalkanoate
PHB	polyhydroxybutyrate
PID	proportional–integral–derivative (controller), a special control loop mechanism using feedback signals
PPQ	pyrroloquinoline quinone
qPCR	quantitative PCR
RBS	ribosome binding site or ribosomal binding site
RNA	ribonucleic acid
rpm	revolutions per minute
rev	reverse primer
s	second(s)
SCP	single cell protein
SDS-PAGE	sodium dodecyl sulfate polyacrylamide gel electrophoresis
SNP	single nucleotide polymorphism
sp.	species
t	time
Tab.	table
Tc	tetracycline
TCA	tricarboxylic acid
Tc^R or Tet^R	tetracycline resistance gene/cassette or tetracycline-resistant
USD	US Dollar
UV	ultraviolet
v/v	volume per volume
vis	visible
w/v	weight per volume
WT	wild type

x *g*	unit of relative centrifugal force (RCF), measured in multiples of gravity
Y	Yield
µL	microliter (1 µL = 10^{-6} L)
µM	micromolar (1 µM = 10^{-6} M = 10^{-6} mol/L)
Z	atomic number
3HB	(*R*)-3-hydroxybutyric acid
5'- / 3'-end	chemical convention for directionality of single-stranded DNA or RNA molecules according to the carbon atom numbers in the nucleotide-pentose-sugar ring
%	percent
°C	degree Celsius
Δ	gene deletion
[ ]	concentration
xx/xx/xxxx	Date in format day/month/year

List of Figures - Chapters 1-3

List of Tables - Chapters 1-3

1. Introduction

1.1 Methanol production and methanol-based processes

Methanol is a basic chemical that has been used all over the world for thousands of years. A historical name for methanol is wood spirit or wood alcohol. This old name refers to an early methanol generation process using thermal destructive distillation of wood. This process was rather inefficient, yielding only 10-20 L of methanol per metric ton of wood (Olah et al. 2018). The first industrial process for methanol synthesis from coal derived syngas (a mixture of carbon monoxide and hydrogen) was developed and implemented by BASF scientists M. Pier and A. Mittasch in the 1920s (Offermanns 2014). The synthesis of methanol from syngas with a catalyst comprises two exothermic methanol generation reactions (Eq. 1 and Eq. 2) and an endothermic reverse water gas shift reaction (Eq. 3, Goeppert et al. 2014).

$CO + 2H_2 \leftrightharpoons CH_3OH$	ΔH_{298K} = - 21.7 kCal/mol	**Eq. 1**
$CO_2 + 3H_2 \leftrightharpoons CH_3OH + H_2O$	ΔH_{298K} = -11.9 kCal/mol	**Eq. 2**
$CO_2 + H_2 \leftrightharpoons CO + H_2O$	ΔH_{298K} = 9.8 kCal/mol	**Eq. 3**

The original BASF process used a $ZnO\text{-}Cr_2O_3$ catalyst and harsh conditions of 250-300 atm and 300 to 400 °C (BASF, German Patent nos. 415686, 441433 and 462837, 1923). The development of new, copper-based catalysts (e.g. $Cu\text{-}ZnO/Al_2O_3$) and advances in syngas purification enabled mid- and low-pressure processes (da Silva 2016). The syngas used today is predominantly produced from either coal (especially in China and South-Africa) or from natural gas (Olah et al. 2018). Natural gas predominantly consists of methane, which is reformed to CO_2, CO and hydrogen (Goeppert et al. 2018). The global methanol production has exceeded 98 million metric tons per year in 2021 and is growing rapidly (IRENA and Methanol Institute 2021). Methanol is an important building block for the chemical industry and serves as starting material for various other basic chemicals such as formaldehyde, dimethyl ether, acetic acid, polymers and specialty chemicals used in paints, adhesives and pharmaceuticals (Sonthalia et al. 2021).

1.1.1 Methanol as a universal sustainable feedstock of the future

Along with hydrogen, methanol is being envisioned as a future replacement for fossil fuels. Its high octane number makes methanol a good fuel itself and an excellent blend for gasoline, while emitting almost no harmful byproducts like NO_X (Wang et al. 2019). As a liquid raw material, methanol offers advantages over the highly volatile, gaseous H_2 in handling, transport and storage (Olah 2005). Although hydrogen has some excellent properties as potential fuel and its combustion produces only water as a byproduct, its universal and exclusive usage would require the installation of a whole new hydrogen infrastructure (Sonthalia et al. 2021). For methanol, such infrastructure is already in place as it has been used as a prevailing basic chemical for decades. Furthermore, the infrastructure for fossil fuels can be easily adapted for methanol. Due to this sophisticated infrastructure, methanol can also be readily used for energy storage. Converting methane to methanol for shipping and storage is a promising alternative to liquefied natural gas (LNG) (Olah et al. 2018). Moreover, the two largest sources of renewable energy, wind and solar, are intermittent and their availability fluctuates throughout the day and year. Long-term storage of energy in form of chemical bonds may be a feasible solution for this problem.

As already mentioned, methanol is still produced mainly from cheap fossil resources (syngas from natural gas or coal). Nevertheless, both syngas and methanol can be obtained from renewable sources, e.g. by modern gasification processes for wood and the production of biogas followed by reforming to syngas. In the last three decades, the methanol production from municipal waste and biomass has become more relevant with leading methanol production companies like OCI/BioMCN (Amsterdam, Netherlands), Chemrec (Stockholm, Sweden) and Enerkem (Montreal, Canada) opening large commercial production plants for so called bio-methanol.

In recent years, more and more attention has been drawn to “green” hydrogen production by electrolysis of water using energy from renewable sources. This is opening the possibility of producing regenerative methanol directly from CO_2 emissions and hydrogen with a homogenous or heterogenous catalyst (Eq. 2, Kar et al. 2018; Din et al. 2019). Considering the high energy demand for hydrogen generation in a water splitting reaction (Eq. 4), it is particularly crucial that the energy required is obtained from renewable sources (e.g. solar, wind or thermal energy) so that the subsequent methanol production is sustainable overall (Goeppert et al. 2018).

$$2H_2O \leftrightharpoons 2H_2 + O_2 \qquad \Delta H_{298K} = 285.83 \text{ kCal/mol} \qquad \textbf{Eq. 4}$$

In the last decade, fourteen new industrial projects have been launched worldwide aimed at recycling of CO_2 to so called e-methanol (IRENA and Methanol Institute 2021). The CO_2 is captured from the emissions of various production facilities such as power, steel or cement plants. These emissions contain over 10 % of CO_2, which can be captured by various techniques (Wang et al. 2017). The first demonstration plant for direct conversion of CO_2 emissions was established in Iceland by Carbon Recycling International in 2011. The hydrogen needed is produced with readily available cheap geothermal energy (Álvarez et al. 2017). Based on the technology used at the CRI site in Iceland, the first commercial ETL (emissions-to-liquid) plant with a production capacity of 110 000 tons of methanol per year was commissioned in 2022 (https://www.carbonrecycling.is/projects-shunli, accessed 21/05/2023). The direct air capture (DAC) of atmospheric CO_2 is not feasible yet, but the developments in this research area are progressing rapidly (Sanz-Pérez et al. 2016; Keith et al. 2018; Shi et al. 2020). With an efficient DAC, the CO_2 which is ultimately released by combustion of biomethanol, e-methanol or fossil-derived methanol can be captured and recycled again to methanol, resulting in a complete “methanol economy” (Olah et al. 2018).

A widely discussed alternative to conventional fuels are so-called biofuels. First-generation biofuels were processed from food crops such as corn, sugar cane or palm oil. A solution to the ethical “food vs. fuel” controversy was delivered by next-generation biofuels derived from non-food materials and byproducts such as algae, lignocellulose or rice straw (Zinoviev et al. 2010). The intensive research going on in this field will make these biofuels a competitive alternative to conventional fuels in the near future. However, the raw materials needed may not necessarily be ubiquitously available due to soil, climate or space constraints. Considering this, a parallel development of both e-methanol-based fuels and biomass-based biofuels (which also include bio-methanol) should be pursued for the diversification of sustainable fuel production.

Summed up, methanol has the potential to serve not only as a basic chemical, but also for energy storage and as fuel of the future. Due to the variety of methanol generation options, methanol-based processes can serve as bridging technologies. In combination with “green” hydrogen, methanol has the potential to be produced sustainably and to lower the dependency on fossil resources. The success of the introduction of a "methanol economy" will depend on the development of more efficient catalysts and carbon capture processes, but also on political will and environmental-ethical decisions.

1.1.2 Methanol-based biotechnology using methylotrophic bacteria

Besides methanol being one of the dominant basic chemicals for the chemical industry, using methanol as carbon feedstock for biotechnological applications has drawn huge interest in the recent years. As described in chapter 1.1.1, methanol has the potential to be entirely generated in a renewable or even regenerative manner. Its generation can be diversified and does not compete with food production, as is the case with many conventional carbon sources for biotechnological processes. Most industrial biotechnological processes are based on sugars, molasses, oils or protein hydrolysates (Chmiel et al. 2018). In addition to the benefits already mentioned, methanol also has process-related advantages over these traditional substrates. Methanol is more reduced than most sugars, making it an excellent substrate for achieving high product yields (Whitaker et al. 2015). Since methanol is cytotoxic for most organisms, its use reduces the risk of contaminations. Furthermore, methanol as highly pure, non-complex substrate can be used in well-defined synthetic media, which facilitates the downstream processing of products (Ochsner et al. 2015).

Organisms that use methanol as sole source of carbon and energy are called methylotrophs. Methylotrophy can be divided in three modular parts: (1) oxidation of the C_1-compound to formaldehyde followed by (2) the oxidation of formaldehyde and (3) the assimilation into biomass (Chistoserdova 2011). For the latter, two pathways are known in bacteria. *Methylobacillus glycogenes*, *Bacillus methanolicus* and *Methylophilus methylotrophus* are examples for organisms using the ribulose monophosphate (RuMP) cycle, in which C_1 assimilation takes place at the level of formaldehyde. Other methylotrophic bacteria, such as *Methyloligella halotolerans* and the widely studied *Methylorubrum extorquens*, utilize the serine cycle for C_1 assimilation, in which formaldehyde enters the assimilation route through methylene-H_4F (a detailed description of serine cycle methylotrophy is given in chapter 1.2.2). In either of the modes of methylotrophy described above, the strongly reduced character of methanol leads to a high oxygen demand in fermentations and a substantial heat generation (Schrader et al. 2009). To cope with the resulting increased heat output in competitive industrial processes, either thermophilic organisms may be used or the costs of cooling the bioreactor must be compensated by efficient production strains and high-value products. In the following, the enormous potential of methanol-based biotechnology and the possible applications of the respective products are demonstrated by various examples (summarized in Figure 2). The bacterium

M. extorquens is particularly interesting as a platform organism for the production of value-added compounds from its three interlocked metabolic pathways (EMCP, serine cycle and PHB cycle), but other bacterial methylotrophic production hosts are also presented in the following chapters. An exciting new area of research is the development of synthetic methylotrophs, which would allow streamlined applications of well-studied organisms such as *Escherichia coli* or *Corynebacterium glutamicum* for methanol-based biotechnology. Since the RuMP cycle is more efficient than the serine cycle in terms of generating NADH, ATP and biomass, most approaches in this field focus on implementing a synthetic RuMP cycle (Klein et al. 2022). The challenges here are manifold, ranging from DNA-protein crosslinking caused by formaldehyde and poor kinetics of heterologous methylotrophic enzymes to improper gene regulation (Gregory et al. 2022). Autonomous methylotrophy has only been reported for one *E. coli* strain with a doubling time of 8.5 hours and a final optical density of 2 (Chen et al. 2020). Although this is a very promising starting point for synthetic methylotrophy, further research is required to make it practical for biotechnological applications. Anaerobic acetogens or eukaryotic platforms, such as methylotrophic yeasts, are beyond the scope of this work and will not be discussed.

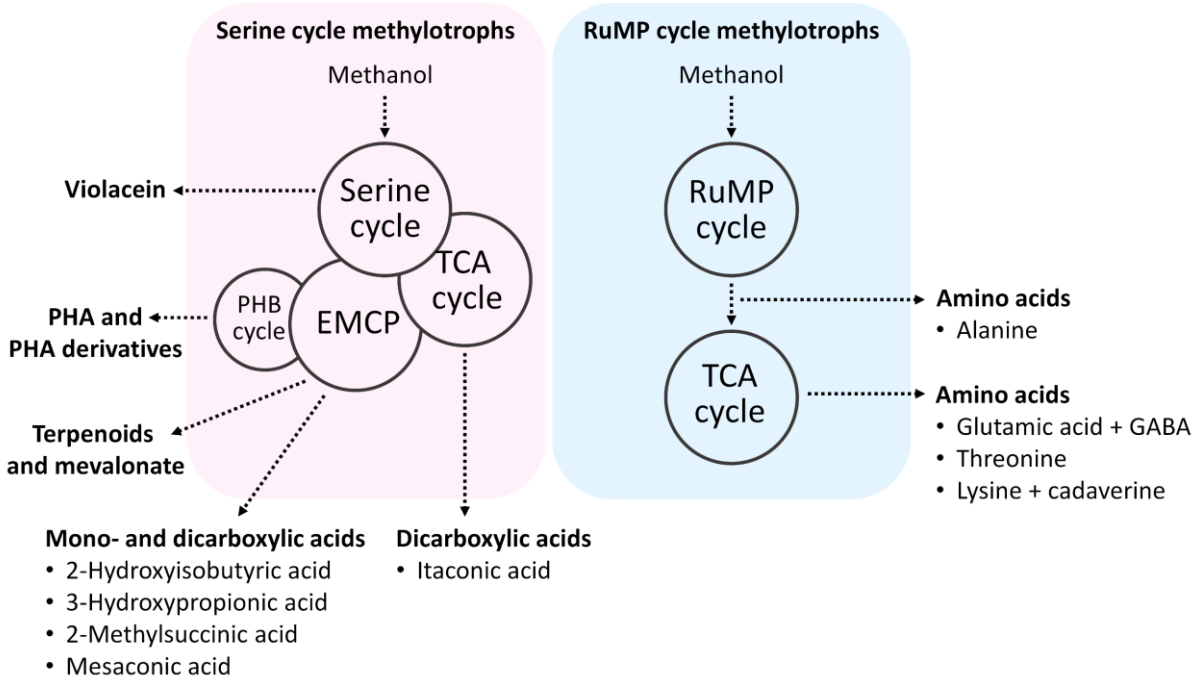

Figure 2 Schematic representation of natural and heterologous bacterial production routes of value-added chemicals from methanol as reported in the past. The target products are either generated by serine cycle methylotrophs or RuMP cycle methylotrophs and are derived from their respective metabolic pathways. Dotted arrows represent multi-step reactions.

1.1.2.1 Amino acids and amino acid derivatives

The first methanol-based industrial-scale bioprocesses with methylotrophic bacteria were established in the 1970s and 1980s for the production of single cell protein (SCP) (Litchfield 1983; Westlake 1986). With a production capacity of 50 000 tons of SCP per year, these processes demonstrated that methylotrophic bacteria are excellent platforms for biomass production from alternative substrates (Schrader et al. 2009). In the following years, processes for the production of single amino acids were developed. Titers of up to 69 g/L of L-glutamate, 65 g/L of L-lysine, 12 g/L of L-alanine and 16 g/L of L-threonine were achieved with different engineered methanol-grown strains of *Methylobacillus glycogenes* or *Bacillus methanolicus* (Motoyama et al. 1993; Motoyama et al. 1994; Brautaset et al. 2003; Brautaset et al. 2010). Stoichiometrically, the yields of L-lysine generation from methanol (*B. methanolicus*) and from glucose (*C. glutamicum*) are similar, proving that *B. methanolicus* is a valid alternative to conventional L-lysine production hosts (Brautaset et al. 2007). Overexpression of heterologous L-lysine decarboxylase gene *cadA* from *E. coli* in *B. methanolicus* led to the production of 6.5 g/L cadaverine, a molecule which is used as platform chemical for polyamides (Nærdal et al. 2015; Nærdal et al. 2019). Accordingly, (γ)-aminobutyric acid (GABA), a non-proteinogenic amino acid which can be used as precursor for biodegradable plastics and as food additive, was produced with *B. methanolicus* by heterologous expression of glutamate decarboxylase gene *gad* from *Sulfobacillus thermosulfidooxidans* or *E. coli* (Irla et al. 2017). Utilizing freeze-thawed cells of serine cycle methylotrophs *Methylorubrum extorquens* or *Methylobacterium sp.* and glycine as co-substrate, 54 g/L or 65 g/L of L-serine were produced, respectively (Sirirote et al. 1986; Hagishita et al. 1996). Recently, an *M. extorquens* strain for the production of violacein, a bioactive pigment derived from tryptophan, was developed by strain engineering and directed evolution (Quynh Le et al. 2022). In the mentioned study, a titer of 118 mg/L of violacein was achieved from the co-substrates methanol and acetate.

1.1.2.2 Polyhydroxyalkanoates

Polyhydroxyalkanoates (PHAs) are accumulated naturally by various microorganisms as energy and carbon storage molecule under growth limiting conditions (Khosravi-Darani et al. 2013). PHAs are not only promoted as future replacement for conventional non-degradable plastics, but, due to their biocompatibility, also as advanced material

e.g. for wound dressing, tissue engineering, implants and drug delivery (Kumar et al. 2020). However, the main issue with the production of PHAs from microorganisms is the comparatively high cost associated with bioprocessing and especially downstream processing, resulting in a price that is 5-10 times higher than that of conventionally produced plastic such as polyethylene (Raza et al. 2018). The higher costs may be mitigated by the benefit of using methanol as an alternative renewable carbon source in synthetic growth media. PHB synthesis in *M. extorquens* occurs through successive reactions of native ß-ketothiolase, NADPH-linked acetoacetyl-CoA reductase and PHB synthase starting from 3-hydroxybutyryl-CoA (Korotkova and Lidstrom 2001; Anthony 2011). Various studies have described the production of PHB and PHB derivatives with *M. extorquens* from methanol (Suzuki et al. 1986; Bourque et al. 1992; Bourque et al. 1995; Mokhtari-Hosseini et al. 2009; Orita et al. 2014). The reported production outcomes are in the same range as for non-methanol-based processes using classical platforms as *Cupriavidus necator* (Ochsner et al. 2015). The applicability of pure PHB is constrained because it is highly crystalline and has poor elastic properties (Khosravi-Darani et al. 2013). Therefore, the production of higher molecular weight PHB with improved mechanical characteristics is desirable. Such PHB species could be obtained with *M. extorquens* by limiting methanol and ammonium availability during the cultivation process (Bourque et al. 1995; Ezhov et al. 2017). Higher toughness and lower brittleness were also achieved by producing functionalized PHB or co- and terpolymers by addition of auxiliary carbon sources or strain engineering (Bourque et al. 1992; Yezza et al. 2006; Höfer et al. 2010; Orita et al. 2014).

1.1.2.3 Organic acids

Mono- and dicarboxylic acids serve as synthons for the food, cosmetic, pharmaceutical and chemical industry (Panda et al. 2019). Bulk organic acids have been produced biotechnologically at industrial scale from conventional carbon sources with various platforms as *Aspergillus niger* (citric acid), *Basfia succiniciproducens* (succinic acid), *Lactobacillus* sp. (lactic acid), *Aspergillus terreus* (itaconic acid) and *Rhisopus* sp. (fumaric acid) (Di Lorenzo et al. 2022). These biotechnological processes are not always competitive with petrochemical-based synthesis, as shown by the example of succinic acid, for which the market share of the biotechnological product is very low (Pleissner et al. 2017). Developing new processes based on alternative and cheap carbon sources as methanol might overcome this obstacle in the future. In the last

decade, some novel methanol-derived production routes for C_3-C_5 organic acids (Figure 3) with *M. extorquens* AM1 have been developed.

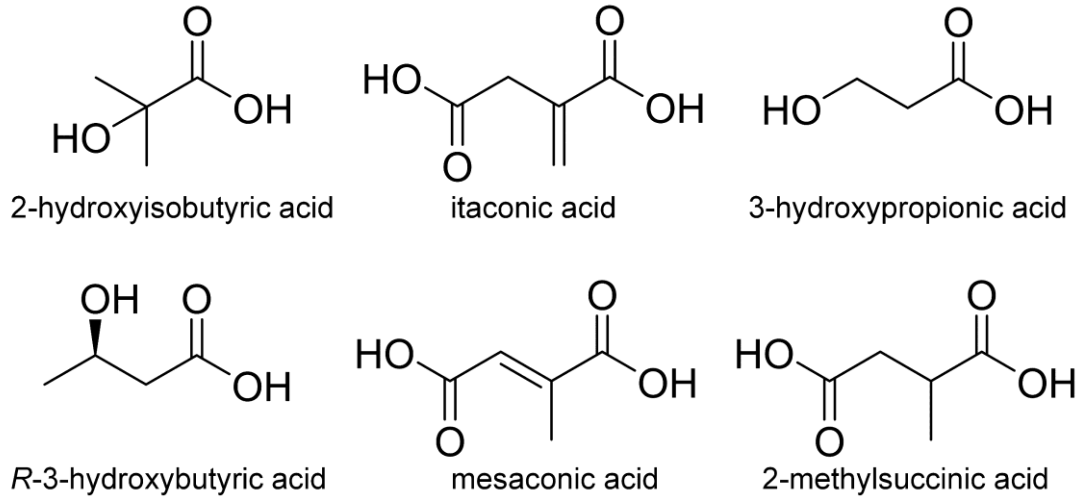

Figure 3 C_3-C_5 organic acids that have been produced biotechnologically from methanol. 2-hydrocyisobutyric acid, itaconic acid, 3-hydroxypropionic acid, mesaconic acid and 2-methylsuccinic acid were produced with genetically engineered *M. extorquens* AM1 strains, *R*-3-hydroxybutyric acid was produced with a genetically engineered *M. rhodesanium* strain.

Itaconic acid is a high-value building block for various biopolymers with applications in food packaging, hydrogels, drug carriers and supersorbents and can be derived from TCA-cycle intermediate *cis*-aconitate (Teleky and Vodnar 2021). It was generated from methanol with an *M. extorquens* AM1 strain heterologously expressing a gene encoding *cis*-aconitic acid decarboxylase from *A. terreus* (Lim et al. 2019). Although the production titers in the study with 31.6 ± 5.5 mg/L were rather low compared to published titers for the native producer of up to 150 g/L (Krull et al. 2017), it was the first demonstration of methanol-derived biotechnological production of itaconic acid.

As described in 1.1.2.2, members of the *Methylorubrum* genus produce high amounts of PHB for energy and carbon storage at growth limiting conditions. Under growth-promoting conditions, the stored polymer is degraded by PHB depolymerases to *R*-3-hydroxybutyric acid monomers (Korotkova and Lidstrom 2001). By deletion of the native *R*-3-hydroxybutyrate dehydrogenase gene *hbd* and lipoic acid synthase gene *lipA*, 2.8 g/L of *R*-3-hydroxybutyric acid could be produced in a fed-batch process with methanol-grown *Methylorubrum rhodesianum* (Hölscher et al. 2010).

The other products shown in Figure 3 are derived directly from intermediates of the ethylmalonyl-CoA pathway (EMCP), which provides a high carbon flux during methanol-dependent growth (Peyraud et al. 2009). One of these products is

3-hydroxybutyryl-CoA-derived 2-hydroxyisobutyric acid (2-HIBA), which can serve as precursor for acrylic glass and coatings (Rohwerder and Müller 2010). Titers of up to 2.1 g/L 2-HIBA were achieved by introduction of a B_{12}-dependent 2-hydroxyisobutyryl CoA mutase from *Bacillus massiliosenegalensis* JC6 into *M. extorquens* AM1 (Rohde et al. 2017). 2-Hydroxyisobutyryl CoA is thereby directly generated from EMCP intermediate 3-hydroxybutyryl-CoA and successively cleaved by a native thioesterase. Another closely related product, 3-hydroxypropionic acid, can also be produced from methanol with *M. extorquens* AM1. It serves as precursor for widely used chemicals such as 1,3-propanediol, acrylic acid and acrylamide (Matsakas et al. 2018). For production of 3-hydroxypropionic acid in *M. extorquens* AM1, a heterologous malonyl-CoA pathway was introduced by the overexpression of the *mcr* gene from *Chloroflexus aurantiacus* DSM 635 (Yang et al. 2017). The highest titer from the named study of 69.8 mg/L was later enhanced to 857 mg/L by using an *M. extorquens* AM1 strain with an artificial synergistic RuMP cycle for improved methanol assimilation and acetyl-CoA supply (Yuan et al. 2021).

In 2011, Birgit Alber evaluated the potential of the uncommon intermediates in the central part of the EMCP for the production of biotechnologically relevant products (Alber 2011). She suggested to cleave these partially chiral C_4 and C_5 CoA-ester intermediates to obtain valuable (chiral) dicarboxylic acids. Following this idea, mesaconic acid and 2-methylsuccinic acid were successfully produced by heterologous overexpression of thioesterase gene *yciA* originating from *E. coli* in *M. extorquens* AM1 (Sonntag et al. 2014). The combined product titer of mesaconic acid and 2-methylsuccinic acid could be increased to 650 mg/L under cobalt-limited growth conditions (Sonntag et al. 2015b). This enhancement is based on the accumulation of EMCP intermediates due to the lower activity of two cobalamin-dependent mutases (Kiefer et al. 2009). Although the authors stated the generation of enantiomerically pure (*S*)-2-methylsuccinic acid based on the premise of a pure (*S*)-2-methylsuccinyl-CoA precursor, the enantiopurity of the acid product was not tested. For more information on the enantiomeric purity of the products, refer to chapter 3.2.1.

1.1.2.4 Terpenoids

Terpenoids represent a large, structurally diverse class of natural products with a wide application as flavors, fragrances and drugs. Terpenoids are synthesized in nature either via the methylerythritol 4-phosphate pathway (which is the predominant pathway in bacteria) or via the mevalonate (MVA) pathway (Kuzuyama and Seto 2012). *M. extorquens* is a promising platform organism for terpenoid synthesis from methanol via a heterologous MVA route, since it harbors acetoacetyl-CoA, the starting molecule for this pathway, within the EMCP (Sonntag et al. 2015a). *M. extorquens* strains producing high amounts of mevalonate, which is a universal precursor for isoprenoid synthesis, have a tremendous potential for broadening the methanol derived product spectrum.

In the past, different approaches have been developed for the implementation of a heterologous MVA pathway in *M. extorquens.* Expression of the *hmgcs1* gene from *Blattella germanica* and the *tchmgr* gene from *Trypanosoma cruzi* in combination with *phaA* from *Ralstonia eutropha* yielded a mevalonate production of 180 mg/L (Zhu et al. 2016). With additional optimization of *phaA* expression by modification of the ribosome binding site (RBS), a strain was obtained that produced 2.22 g/L of mevalonate from methanol in a fed-batch process (Zhu et al. 2016). The same artificial MVA pathway was later used in a study for biosensor-assisted regulator engineering (Liang et al. 2017). In the mentioned study, a mevalonate biosensor was used for a high-throughput screening of a QscR (transcriptional regulator of the serine cycle) mutant library and isolation of a strain with increased acetyl-CoA supply and subsequent mevalonate synthesis. In a fed-batch process, a titer of 2.67 g/L mevalonate could be achieved (Liang et al. 2017). Re-distribution of the metabolic flux and increasement of acetyl-CoA supply might be the first step towards a competitive biotechnological production of terpenoids from methanol with *M. extorquens.*

Simultaneously to mevalonate production, another research group has demonstrated the production of a monocyclic sesquiterpenoid with *M. extorquens* from methanol (Sonntag et al. 2015a). α-Humulene and its isomers have raised attention as anti-tumor, anti-inflammatory and anti-microbial compounds (Fernandes et al. 2007; Mendes de Lacerda Leite et al. 2021). In the study of Sonntag and coworkers, the production was enabled by the introduction of farnesyl pyrophosphate (FPP) synthase from *Saccharomyces cerevisiae* in combination with α-humulene synthase from *Zingiber zerumbet* (Sonntag et al. 2015a). The combination of using a carotenoid

synthesis deficient strain, optimization of the RBS and heterologous expression of mevalonate pathway genes from *Myxococcus xanthus* for improved isopentenyl pyrophosphate (IPP) and dimethylallyl pyrophosphate (DMAPP) supply, further improved the production to a final titer of 1.65 g/L of α-humulene in a methanol-limited fed-batch process (Sonntag et al. 2015a).

1.1.2.5 Other products

In addition to the low molecular weight products described above, *M. extorquens* has also been used for the production of several proteins. For the widely used model protein GFP, a product titer of 4 g/L (16 % of total cell protein) was achieved in a high cell density fermentation using the strong native P_{mxaF} promoter (Bélanger et al. 2004). This suggests that *M. extorquens* may be a suitable alternative platform for recombinant production of industrial enzymes and proteins, keeping in mind the comparatively low cost of downstream processing of products from a defined synthetic growth medium. Consequently, the production of other recombinant proteins has been demonstrated. For example, bioactive enterocin P (EntP), which has antimicrobial properties, was produced in titers of up to 155 ng/L, exceeding the titers of an *E. coli* production strain by 25-fold (Gutiérrez et al. 2005). Further examples for recombinant protein production with *M. extorquens* are insecticidal protein Cry1Aa (4.5 % of total cell protein, Choi et al. 2008) and haloalkane dehalogenase DhlA (10 % of total cell protein, Fitzgerald and Lidstrom 2003).

Promising heterologous production pathways for 1-butanol and butadiene have been demonstrated for *M. extorquens*, but they are either limited by a poorly efficient enzymatic production cascade or can currently only use carbon sources other than methanol as a substrate (Hu and Lidstrom 2014; Yang et al. 2018). Further research might close these gaps in the near future.

Another interesting biotechnological application of methylotrophic bacteria is the production of a high viscosity polysaccharide called methylan, which can be used as an alternative polysaccharide to stabilize foods, medicines, and industrial products. A maximum titer of 20.7 g/L was produced in a high shear bioreactor with *Methylobacterium organophilum* (Oh et al. 1997).

1.2 *Methylorubrum extorquens*

As demonstrated in chapter 1.1.2, *M. extorquens* has enormous potential as platform for the production of various bulk and value-added fine chemicals from methanol. The following chapters provide an overview of the taxonomy and methylotrophic metabolism of *M. extorquens*, as well as available strains and genetic tools.

1.2.1 Taxonomy of *M. extorquens*

The genus *Methylorubrum* was reclassified from the widespread genus of *Methylobacterium* based on 16S rRNA analysis (Green and Ardley 2018). Recently, a phylogenomic study suggested that the genus *Methylorubrum* should be abandoned and reincorporated into *Methylobacterium* (Leducq et al. 2022). Since the scientific discussion is still ongoing, this work follows the taxonomy currently used by NCBI (accessed 06/05/2023). The genus of *Methylorubrum* currently comprises ten species of pink pigmented facultative methylotrophs (NCBI taxonomy ID 2282523, accessed 06/05/2023), including the intensively studied *Methylorubrum extorquens*. In addition to its characteristic ability to grow on methanol and methylamine as sole source of carbon and energy, *M. extorquens* is also capable of metabolizing multi-carbon compounds such as succinate, ethanol, acetate, and oxalate. Up to date, the complete genomes of eight *M. extorquens* strains have been reported, including three recently submitted genome sequences, so far without referring primary literature (Table 1). In addition to the previously mentioned substrates, strain CM4 is able to metabolize chloromethane and strain DM4 is able to metabolize dichloromethane. Interestingly, both strains were isolated from contaminated soils (Gälli and Leisinger 1985; Doronina 1996) and are closely related to strain AM1 (Lee et al. 2022). The strain *M. extorquens* AM1 (formerly *Pseudomonas* AM1) was originally isolated as airborne contaminant in a methylamine-containing growth medium (Peel and Quayle 1961). This strain was the first *M. extorquens* strain isolated and has been the subject of numerous studies (Anthony 2011). Over the long history of this strain, which has been passed through various laboratories, it has undergone significant changes from the original isolate first described in 1961 (Peel and Quayle 1961; Carroll et al. 2014). The genome of the nowadays used AM1 lineage harbors 32 partial and 142 intact highly diverse insertion sequence (IS) elements that confers to genome plasticity (Vuilleumier et al. 2009). In addition to the high GC content of *M. extorquens* genomes, this further impedes classical cloning and strain engineering procedures.

Table 1 List of *M. extorquens* genome sequences currently available at NCBI. There is no primary literature available for the genomes of strains PSBB040, NBC_00404, and NBC_00036 to date (06/05/2023).

Strain	Isolation	Genome size and replicons	GC content	References
AM1	Airborne contaminant (methylamine)	6.9 Mbp, 1 chromosome 1 megaplasmid 3 plasmids	68 %	Peel and Quayle 1961; Vuilleumier et al. 2009
CM4	Contaminated soil of a petrochemical factory	6.2 Mbp, 1 chromosome 2 plasmids	68.2 %	Doronina 1996; Marx et al. 2012
DM4	Contaminated soil from a treatment plant for halogenated hydrocarbon waste	6.1 Mbp, 1 chromosome 2 plasmids	67.5 %	Kohler-Staub et al. 1986; Vuilleumier et al. 2009
TK 0001	Soil	5.7 Mbp, 1 chromosome	68.2%	Urakami and Komagata 1984; Belkhelfa et al. 2018
ATCC 55366	Oil-contaminated soil	6 Mbp, 1 chromosome 1 plasmid	68 %	Bourque et al. 1992; Lee et al. 2022
PA1	*Arabidopsis thaliana* phyllosphere	5.5 Mbp, 1 chromosome	68.2 %	Knief et al. 2010; Marx et al. 2012
PSBB040	Freshwater Pond	5.7 Mbp, 1 chromosome	68 %	NCBI Assembly ASM197166v1[1)]
NBC_00404	n.d.	5.9 Mbp, 1 chromosome	68 %	NCBI Assembly ASM2612259v1[2)]
NBC_00036	n.d.	5.7 Mbp, 1 chromosome	68 %	NCBI Assembly ASM2612261v1[2)]

1) submitted to NCBI by Barney, B.M. (2017)
2) submitted to NCBI by Faurdal,D., Joergsen,T.S., Arevalo,M.A., Mourched,A.-S., Vuksanovic,O., Sterndorff,E.B. and Weber,T. (2022)

1.2.2 Methylotrophy in *M. extorquens*

“Methylotrophy” describes the ability to utilize compounds which do not contain carbon-carbon bonds (Chistoserdova and Kalyuzhnaya 2018). Methylotrophic bacteria are found to use three types of assimilation pathways, namely the Calvin-Benson-Bassham (CBB) cycle, the ribulose monophosphate (RuMP) cycle or the serine cycle. While in autotrophic methylotrophs the substrates are oxidized to CO_2 and assimilated via the CBB cycle (Anthony 1982), organisms lacking the CBB cycle are assimilating carbon in a more reduced state (formaldehyde) via the RuMP or serine cycle. The latter is used by *M. extorquens*, which has been a model organism for studying

methylotrophy for the past sixty years (Anthony 2011). As a facultative methylotroph, *M. extorquens* offers the possibility of constructing mutants with non-lethal deletions of methylotrophy genes and thus study the metabolic network. This rather classical approach for metabolic pathway elucidation has been complemented by state-of-the-art omics technologies in the last decades (for a summary of these studies, see Ochsner et al. (2015)).

The methylotrophic metabolism of *M. extorquens* for the generation of cell carbon and energy can be divided in three parts (Figure 4), namely the oxidation of methanol or other C_1 substrates to formaldehyde, further oxidation of formaldehyde to CO_2 and assimilation in the serine cycle (Chistoserdova 2011).

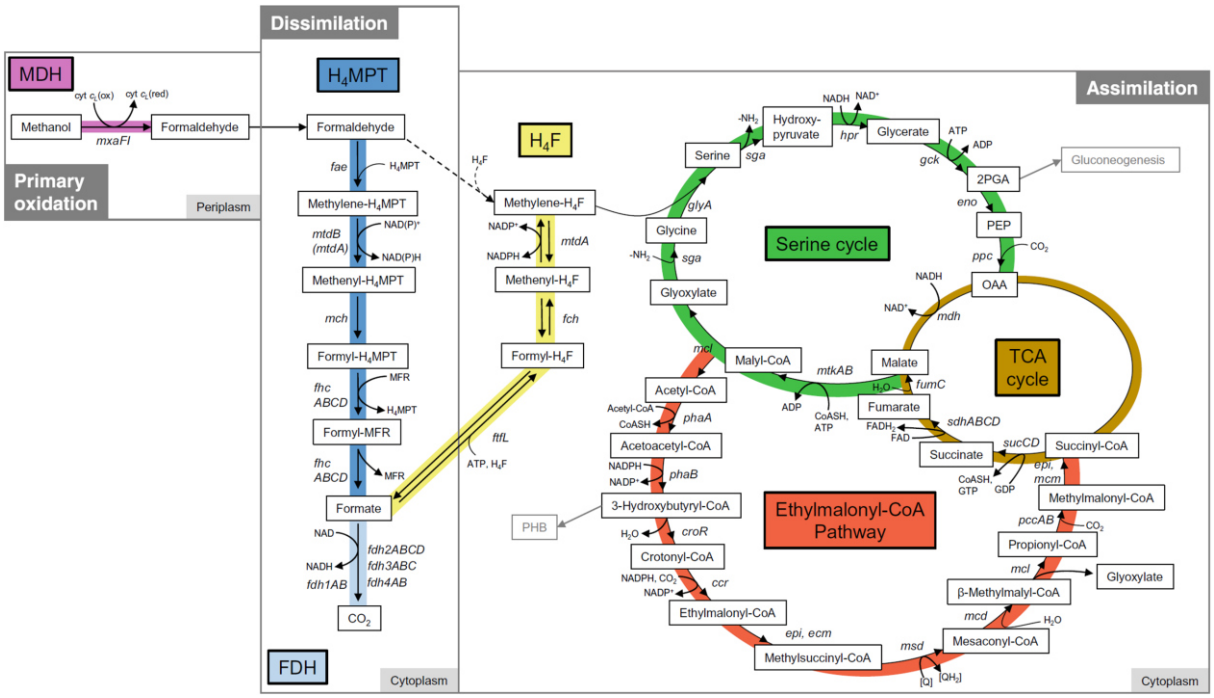

Figure 4 From Ochsner et al. (2015): Methanol metabolism of *M. extorquens* AM1. Genes encoding for the corresponding enzymes are shown in italics: *mxaFI* = methanol dehydrogenase; *fae* = formaldehyde activating enzyme; *mtdB* = methylene-H_4MPT dehydrogenase, *mch* = methenyl-H_4MPT cyclohydrolase, *fhcABCD* = formyltransferase/ hydrolase, *fdhABCD* = formate dehydrogenase, *mtdA* = methylene-H_4MPT/methylene-H_4F dehydrogenase, *fch* = methenyl-H_4F cyclohydrolase, *ftfL* = formyl-H_4F ligase, *sga* = serine glyoxylate aminotransferase; *hpr* = hydroxypyruvate reductase; *glyA* = serine hydroxymethyltransferase; *gck* = glycerate kinase; *eno* = enolase; *ppc* = phosphoenol pyruvate carboxylase; *mdh* = malate dehydrogenase; *mtkAB*= malate thiokinase complex, *mcl* = malyl-CoA lyase; *phaA* = β-ketothiolase; *phaB* = acetoacetyl-CoA reductase; *croR* = *R*-specific enoyl-CoA hydratase; *ccr* = crotonyl-CoA carboxylase/reductase; *epi* = ethylmalonyl-CoA/methylmalonyl-CoA epimerase; *ecm* = ethylmalonyl-CoA mutase; *msd* = methylsuccinyl-CoA dehydrogenase; *mcd* = mesaconyl-CoA hydratase; *pccAB* = propionyl-CoA carboxylase; *mcm* = methylmalonyl-CoA mutase; *sucCD* = succinyl-CoA synthetase, *sdhABCD* = succinate dehydrogenase; *fumC* = fumarase.

The primary oxidation of methanol in the periplasm is catalyzed by methanol dehydrogenases (MDH) using pyrroloquinoline quinone (PQQ) as electron acceptor. The intensively studied MxaF heterotetramer (two α-subunits and two β-subunits, encoded by *mxaF* and *mxaI*, respectively), requires a cytochrome c as terminal electron acceptor (encoded by *mxaG*) (Anthony 1982; Lidstrom et al. 1994). While the MxaF-type proteins additionally incorporate Ca^{2+} in the active site of the α-subunits, the more recently discovered XoxF-type MDH enzymes require lanthanides (Ln^{3+}) as cofactors (Chistoserdova and Kalyuzhnaya 2018). Ln^{3+} inversely regulates the expression of *mxa* and *xoxF* genes (Skovran et al. 2019). The coexistence of the two redundant systems and their evolutionary background is not yet fully understood and is subject to current research.

After the primary oxidation step, the resulting formaldehyde is condensed with tetrahydromethanopterin (H_4MPT). The resulting methylene derivative is further oxidized to CO_2 (Figure 4). The dissimilation of formaldehyde in the pterin pathway is needed for both energy generation and detoxification of the formaldehyde after entering the cytoplasm (Marx et al. 2003a). The assimilation of C_1 substrates takes place in the serine cycle, where methylene-tetrahydrofolate (methylene-H_4F) is condensing with glycine to serine (Figure 4). Methylene-H_4F is either derived from the H_4MPT-dependent pathway (see above) or generated by spontaneous condensation of formaldehyde with H_4F (Marx et al. 2003b). The serine obtained is further converted in the serine pathway (interlocked with the TCA and gluconeogenesis) to glyoxylate and acetyl-CoA. The serine cycle was elucidated in *M. extorquens* over 60 years ago, but at that time, the fate of acetyl-CoA could not be explained (Large et al. 1961; Large et al. 1962). Assimilation of carbon by the serine cycle requires continuous regeneration of glyoxylate (Kornberg and Krebs 1957). It was clear that unlike other bacteria that use the glyoxylate cycle to regenerate glyoxylate from acetyl-CoA, glyoxylate regeneration in isocitrate lyase-negative *M. extorquens* must proceed differently (Anthony 2011). In contrast to the serine cycle, for which most genes are clustered together in the genome and thus could easily be identified (Chistoserdova et al. 2003), the mode of glyoxylate regeneration in *M. extorquens* and other icl$^-$ methylotrophs was an unresolved mystery for a long time. A pathway harboring unusual intermediates was proposed based on studies with *Rhodobacter* (Meister et al. 2005; Alber et al. 2006; Erb et al. 2007) and was finally demonstrated in *M. extorquens* by using ^{13}C metabolomics (Peyraud et al. 2009). This pathway was

named ethylmalonyl-CoA pathway (EMCP) after the product of the key enzyme crotonyl-CoA carboxylase/reductase (Erb et al. 2007). In the first step of the pathway, two molecules of acetyl-CoA are condensed to acetoacetyl-CoA and further reduced to 3-hydroxybutyryl-CoA. At this point, the EMCP is interlocked with the PHB cycle, which is used for carbon storage under harsh conditions (Korotkova and Lidstrom 2001; Anthony 2011). Within the EMCP, 3-hydroxybutyryl-CoA is further converted to succinyl-CoA via a series of uncommon CoA esters, generating one molecule of glyoxylate (Figure 4).

1.2.3 The ethylmalonyl-CoA pathway in *M. extorquens* as source of value-added dicarboxylic acids

The EMCP as glyoxylate regeneration pathway is essential for the methylotrophic growth of *M. extorquens* as well as for the growth on C_2 compounds (Schneider et al. 2012). The EMCP is also interesting from a biotechnological point of view as it harbors uncommon saturated and unsaturated C_4- and C_5-acyl-CoA-esters (Figure 4). These CoA-esters rarely seen in nature include (2*S*)-ethylmalonyl-CoA, (2*R*)-ethylmalonyl-CoA, (2*S*)-methylsuccinyl-CoA and (2*R*,3*S*)-methylmalyl-CoA (Alber 2011). These chiral intermediates offer the possibility of producing valuable stereochemically defined dicarboxylic acids directly from a primary metabolic pathway, promising high yields. As described in chapter 1.1.2.3, a combined product titer of 0.65 g/L of mesaconic acid and 2-methylsuccinic acid could be achieved in shake flask cultivations by the introduction of the thioesterase YciA from *E. coli* (Sonntag et al. 2014; Sonntag et al. 2015b). Although YciA is a broad-range thioesterase (Zhuang et al. 2008), of all possible EMCP-derived mono- and dicarboxylic acid products, only mesaconic acid and 2-methylsuccinic acid were released into the culture medium by the modified *M. extorquens* AM1 strain (Sonntag et al. 2015b). The authors pointed out a possible limitation due to substrate selectivity or unfavorable CoA-ester pool sizes. Since its essential glyoxylate regeneration function for growth on C_1 and C_2 substrates, the EMCP cannot easily be interrupted to accumulate specific intermediates. In the run-up of the present work, a strain with an interrupted EMCP at the stage of crotonyl-CoA (Δ*ccr* strain) was rescued for growth in acetate medium by the introduction of a heterologous glyoxylate shunt, and by additionally expressing *yciA* heterologously, it produced low amounts of crotonic acid (Schada von Borzyskowski et al. 2018). Since the MDH and FDH activities were strongly decreased in the newly designed strain, the

methylotrophic growth could not be restored (Schada von Borzyskowski et al. 2018). Although these experiments were consequently performed with acetate as the sole carbon source, it was a proof of concept for the specific production of a previously inaccessible EMCP-derived acid, awaiting the development of a more effective EMCP bypass to also restore methylotrophic growth.

In the work of Sonntag and colleagues, the titers of the produced dicarboxylic acids were rapidly decreasing after the cultures reached the stationary growth phase (Sonntag et al. 2014; Sonntag et al. 2015b). Similar observations were also made for strains designed for 3-hydroxypropionic acid production (Yang et al. 2017), indicating a reimport of the products and metabolization over the EMCP route. Further efforts in decreasing the product reimport will be needed to ensure efficient production of EMCP derivatives.

1.2.4 Genetic tools for *M. extorquens*

A broad palette of tools for strain modifications, including gene expression, gene knockout, gene integration and mutagenesis, is a prerequisite for applicability of a bacterial platform as cell factory. Although *M. extorquens* AM1 has been used as a workhorse for studying methylotrophy for decades, for a long time only a basic set of genetic tools was available. Many well-established genetic tools such as commonly used plasmids or promoters like λPL or P_{lac} are not suitable for use in *M. extorquens* (Marx and Lidstrom 2001; Choi et al. 2006). A relatively high GC content of the strain's genome of 68.5 % (Vuilleumier et al. 2009) further complicates DNA cloning procedures and strain engineering. The genetic toolbox tailored to *M. extorquens* has only recently begun to expand. To date, only one broad-host-range plasmid system has been shown to be applicable without causing severe growth defects (Marx and Lidstrom 2001). A set of mini chromosomes that are stably inherited at single copy number were demonstrated as an alternative (Carrillo et al. 2019). Constitutive promotors with different strengths have been described for homo- and heterologous gene expression (Marx and Lidstrom 2001; Schada von Borzyskowski et al. 2015). In addition, several research groups have developed synthetic inducible promoters that allow for a range of expression levels (Choi et al. 2006; Chubiz et al. 2013; Kaczmarczyk et al. 2013; Carrillo et al. 2019; Sathesh-Prabu et al. 2021). A list of available genetic tools is given in Table 2.

Table 2 Available genetic tools for *M. extorquens* AM1.

Tool	Description	Reference
Promoters		
P_{mxaF}	Constitutive strong expression	Marx and Lidstrom 2001
P_{fumC}, P_{coxB}, P_{tuf}	Constitutive expression, Methylobricks	Schada von Borzyskowski et al. 2015
P_{mxaF} (inducible)	Cumate inducible expression, hybrid system based on P_{mxaF} and *cym*/*cmt* from *P. putida* F1	Choi et al. 2006
$P_{R/cmtO}$ and $P_{R/tetO}$	Cumate or anhydrotetracycline inducible expression, hybrid system based on P_R promoter from rhizobial phage 16-3	Chubiz et al. 2013
P_{Q2148}	Cumate inducible expression, hybrid system based on P_{syn2} and *cym*/*cmt* from *P. putida* F1	Kaczmarczyk et al. 2013
$P_{A1/O4/O3}$, $P_{L/O4}$, $P_{L/O4/O3}$, $P_{L/O4/A1}$, $P_{A1/O5/O4}$, $P_{A1con/O5/O4}$, $P_{A1/O4}$, $P_{A1/O4s}$, $P_{A1/O4s}$, $P_{T5s/A1}$	IPTG inducible expression, set of *lacO*-controlled promoters	Carrillo et al. 2019
P_{hpdH}	Levulinic acid inducible expression, hybrid system based on P_{hpdH} and *hpdR*	Sathesh-Prabu et al. 2021
Expression vectors		
pCM80, pCM160	Expression vector (IncP) with Tc^R or Kan^R resistance cassette, respectively	Marx and Lidstrom 2001
pABC variants	Mini chromosomes that can be shuttled between *M. extorquens* and *E. coli*	Carrillo et al. 2019
Plasmids for chromosomal deletion / insertion		
pCM184/pCM157	Allelic exchange vector with *loxP*-flanked Kan^R resistance cassette and Cre recombinase expression plasmid	Marx and Lidstrom 2002
pCM433	Allelic exchange vector based on *sacB*	Marx 2008
pCM168/pCM172	Insertional cloning and expression vectors	Marx and Lidstrom 2004
Plasmids for transposon mutagenesis		
pAlmar3	Plasmid carrying *himar*-1 mariner transposon	Lampe et al. 1999; Metzger et al. 2013
pCM639	Plasmid carrying IS*phoA*/hah transposon	D'Argenio et al. 2001; Marx et al. 2003c

1.2.5 Developments for the improved applicability of *M. extorquens* as a platform for methanol-derived production of value-added products

In addition to the genetic tools presented in the previous chapter, this chapter summarizes further achievements that will facilitate the future development of efficient *M. extorquens* production strains for various products. One development is the removal of the cellulose synthase genes *celA*, *celB* and *celC* to prevent biofilm formation (Delaney et al. 2013). Engineered *M. extorquens* strains developed today almost exclusively carry *celABC* deletions, as this facilitates cultivation in both microtiter plates and bioreactors and yields more efficient and homogenous processes. In the same study of Delaney and coworkers, an optimized medium for the cultivation of *M. extorquens* was presented, the use of which leads to more consistent growth compared to previously used media (Delaney et al. 2013). The composition of trace elements in the culture medium has been shown to strongly influence the output of *M. extorquens* production strains. For example, cobalt limitation in the culture medium reduces the metabolic flux through the EMCP due to the cobalt dependency of two mutases (Erb et al. 2008; Peyraud et al. 2009; Kiefer et al. 2009). This metabolic flux redistribution and the accumulation of EMCP intermediates was used for enhanced production of EMCP and PHB cycle-derived products (Orita et al. 2014; Sonntag et al. 2015b). Liang and colleagues described a strategy for targeted metabolic flux re-distribution (Liang et al. 2017). The authors succeeded in increasing the metabolic flux in *M. extorquens* cells towards acetyl-CoA by applying biosensor-assisted transcriptional regulator engineering. This achievement is particularly noteworthy given the difficulty of altering metabolic fluxes in interconnected cyclic pathways. This development might vastly improve the production of other acetyl-CoA-derived products with *M. extorquens* and the presented method might also be used for other flux adjustments.

Lately, efforts have been made to evolve *M. extorquens* to be more tolerant towards higher methanol concentrations. While the wild type strains can tolerate a methanol concentration of up to 1 % (v/v) without growth impairment, a lab evolution study succeeded in constructing a strain that tolerates up to 10 % (v/v) of methanol (Belkhelfa et al. 2019). All investigated “high-tolerance” strains showed *metY* as common target of mutation, a gene encoding *O*-acetyl-L-homoserine sulfhydrylase. This enzyme contributes to methanol toxicity as it uses methanol as substrate at higher concentrations, producing methoxine (*O*-methyl-L-homoserine), a toxic methionine

analog, leading to dysfunctional polypeptides (Leßmeier and Wendisch 2015). This finding might help to construct even more efficient methylotrophic platforms.
The cultivation of methylotrophic cell factories generally poses the challenge of avoiding methanol concentrations at toxic levels. Especially in fed-batch and continuous fermentation systems, a reliable control strategy is required. Several protocols have been developed in the past for the bioprocessing of methylotrophic organisms that can be adapted for the production of novel value-added compounds using *M. extorquens* strains (Suzuki et al. 1986; Sirirote et al. 1986; Bourque et al. 1995; Wagner et al. 1997; Bélanger et al. 2004; Mokhtari-Hosseini et al. 2009; Sonntag et al. 2015a; Rohde et al. 2016; Ezhov et al. 2017; Lim et al. 2019; Arenas et al. 2023).

1.3 Chiral compounds

Chirality is defined as the potential of a molecule to occur in two different, non-superimposable mirror-image forms while having the same atomic composition and bond order (Brooks et al. 2011). A prerequisite for chirality is the presence of four different substituents attached to a central atom (often carbon). The stereoisomers of chiral molecules are referred to as enantiomers or optical isomers, as they interact differently with plane polarized light (Nguyen et al. 2006). The basic concept of chirality and the convention for naming enantiomers according to the Cahn-Ingold-Prelog (CIP) convention are presented in Figure 5. A composition of both enantiomers is referred to as racemic mixture. While enantiomers are identical in most physical properties such as melting point, boiling point, pK_a and solubility, the behavior in chiral environments and thus bioactivity can differ significantly. Enantiomers and chirality per se are currently a focus of drug discovery for multiple reasons. Drug-receptor mechanisms are often based on stereo-discriminatory interactions and enantiomeric counterparts of active pharmaceutical ingredients may have no or even a detrimental effect (Brooks et al. 2011). In addition, enantiomers may have different pharmacokinetic properties such as absorption, distribution, bioavailability, etc. (Alkadi and Jbeily 2018). Many pharmaceutical companies are switching formerly racemic drugs to enantiomerically pure compounds in order to meet regulatory requirements or to extend their patents (Calcaterra and D'Acquarica 2018).
Enantiomerically pure molecules can be prepared either by isolation of a single enantiomer from a racemic mixture or by asymmetric synthesis. The latter can be achieved by using stereoselective catalysts and/or chiral precursor molecules. Since

both can be found in microorganisms, the biotechnological production of enantiomerically pure building blocks is very promising. It has to be mentioned that some chiral molecules undergo spontaneous or enzyme-catalyzed racemization or chiral inversion *in vivo*. In these cases, the synthesis of enantiomerically pure drugs is pointless.

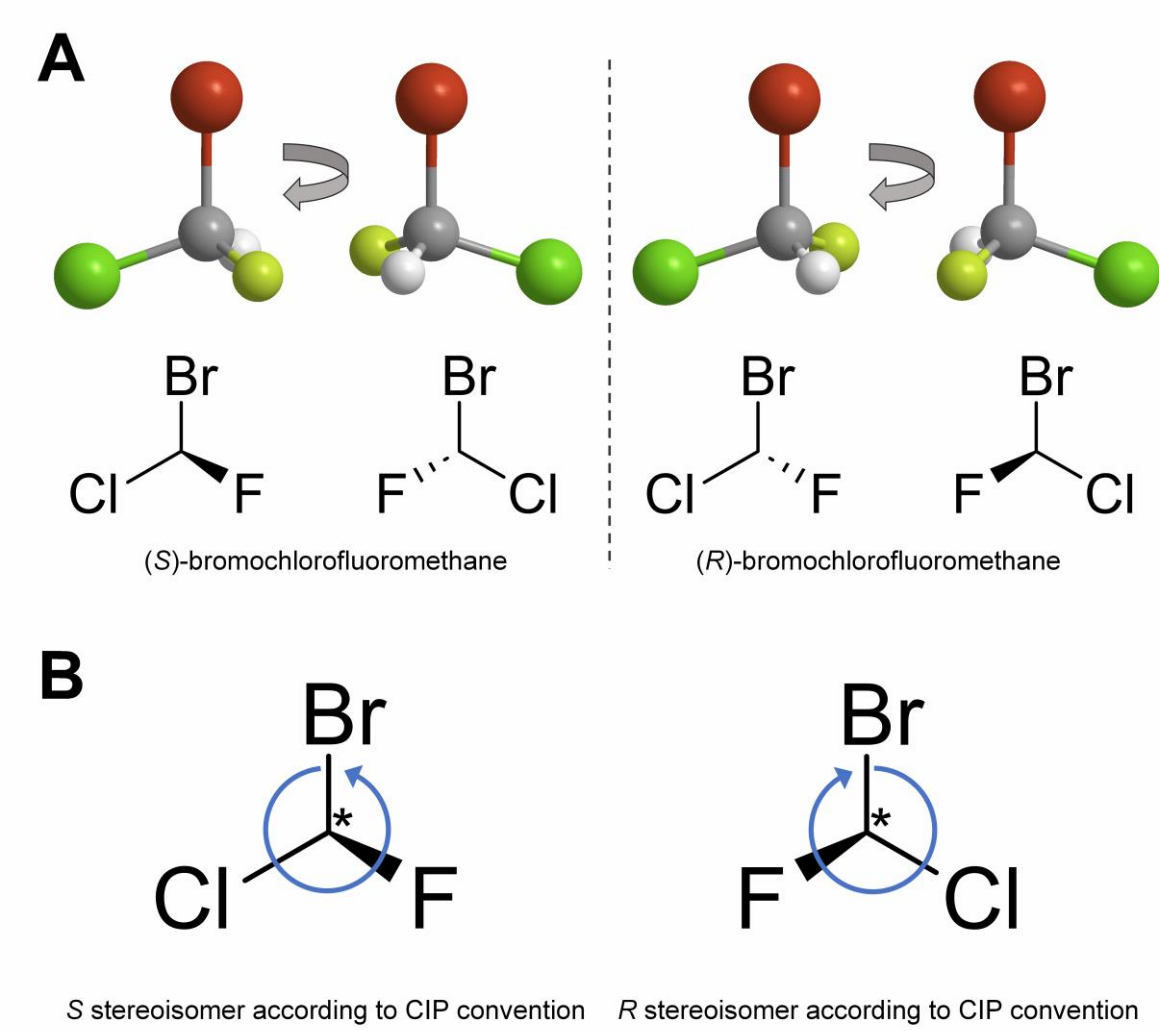

Figure 5 Representation of the basic concept of chirality. **A** The *S* and *R* enantiomers of bromochlorofluoromethane consist of the same atoms and bonds but cannot be superimposed or converted into each other by rotation. They relate to each other like image and mirror image. The atoms in the 3D representation are colored as follows: carbon = grey, bromine = red, chlorine = green, fluorine = yellow, hydrogen = white. **B** The *S* and *R* notations are assigned according to the CIP convention. Atoms attached to the stereocenter (central carbon marked with a star) are assigned a prioritization according to their atomic number (Z). The molecule is then rotated so the atom with the lowest atomic number faces away from the viewer, as done for hydrogen (Z = 1). In the next step, the rotation of the remaining groups attached to the stereocenter is determined in the order from the highest to the lowest atom number. Clockwise rotation assigns the *R* form and counterclockwise rotation assigns the *S* form. For bromochlorofluoromethane the prioritization is bromine (Z = 35) > chlorine (Z = 17) > fluorine (Z = 9), assigning the *S*-form to the left and the *R*-form to the right structure.

1.4 Aim of thesis

In view of the global climate crisis, it has become absolutely vital to develop more sustainable ways to produce bulk and fine chemicals. The sustainability of biotechnological production is largely determined by the substrates used. Methanol, an important building block in the chemical industry, has emerged not only as a promising candidate for a sustainably produced basic chemical, but also as an excellent alternative substrate for biotechnological processes. The methylotrophic organism *M. extorquens* is a well-studied organism, but an application as methylotrophic cell factory (MeCF) for large scale industrial processes has not been realized yet, either because of technical issues in strain development or for being economically infeasible. Due to their high commercial value, chiral building blocks represent ideal target products for viable methanol-based biotechnological processes. *M. extorquens* provides unique conditions for the production of value-added chiral products from methanol. One of the central pathways, the EMCP, harbors some chiral molecules that are rarely seen in nature. Moreover, as part of the primary energy and carbon network, a high metabolic flux is occurring in the EMCP, promising high yields for derived products.

In the present work, further developments were to be made for enhancing the applicability of *M. extorquens* as a future MeCF. For demonstrating the applicability of *M. extorquens* AM1 as efficient MeCF for value-added products, the previously published process for production of two dicarboxylic acids, mesaconic acid and (*S*)-2-methylsuccinic acid with a heterologous thioesterase (Sonntag et al. 2014; Sonntag et al. 2015b), was to be improved. To this end, it was aimed to reduce the resumption of the described products. Therefore, genomic factors involved in product import should be identified using novel screening methods and eventually be eliminated. As an alternative approach, an additional conversion step should be introduced to prevent metabolization of the products. The thioesterase used to release the CoA-bound intermediates was to be modified by semi-rational variant design, but also new thioesterase candidates should be tested for expansion of the *M. extorquens* AM1 product spectrum. Finally, using the previously constructed *M. extorquens* strains, a fermentation strategy was to be developed for the production of dicarboxylic acids in a g/L scale.

For the quantification of product levels, it was aimed to develop a new analytical method that enables fast screening of mutant libraries for the production of dicarboxylic acids. Also, the enantiopurity of the products was to be determined.

The second part of the work aimed at developing new genetic tools to expand the toolbox for *M. extorquens* AM1 for facilitating future strain developments. Therefore, plasmids were to be screened for their compatibility with the predominantly used pCM plasmid system and a novel P_{Q2148} promoter variant was to be characterized.

The overall aim of the thesis was to demonstrate that the methylotrophic organism *M. extorquens* is perfectly suited to be engineered and used for the synthesis of high-value specialty chemicals from the (potentially sustainably produced) carbon source methanol. The construction of production strains for a selection of chiral or achiral (but isomerically pure) dicarboxylic acids derived from the EMCP will serve as an example of application. Together with the novel genetic tools, these applications will support the progression of *M. extorquens* towards an efficient future MeCF.

2. Overview of manuscripts, publications and additional result section

This chapter briefly summarizes the key findings of the additional results section (chapter 5) and the manuscripts and publications listed in chapter 6.

2.1 Summary of "Development of fermentation strategies for EMCP-derived dicarboxylic acid production with *M. extorquens* AM1" (chapter 5)

This chapter demonstrates the development of a fermentation strategy tailored to dicarboxylic acid production with *M. extorquens*. The particular challenge here was the precise control of methanol feeding. Concentrations above 1 % (v/v) methanol have negative impacts on *M. extorquens* AM1 growth, while low concentrations may enhance the re-uptake of dicarboxylic acid products. Therefore, a tailored setup for dicarboxylic acid production, using a script-controlled fed-batch procedure that depends solely on DO-measurements, was tested for different dicarboxylic acid products. Titers reaching from 3.8 g/L to 5.8 g/L were obtained for the target compounds mesaconic acid, 2-methylsuccinic acid, citramalic acid and 2-hydroxy-3-methylsuccinic acid and represent the highest titers for methanol-based microbial production of these products.

2.2 Summary of "Improvement of dicarboxylic acid production with *Methylorubrum extorquens* by reduction of product reuptake" (chapter 6.1)

This publication focuses on the improvement of the previously described process for production of 2-methylsuccinic acid and mesaconic acid with *M. extorquens* AM1 by heterologous overexpression of thioesterase gene *yciA* from *E. coli* (Sonntag et al. 2014; Sonntag et al. 2015b). The two mentioned publications describe a decreased yield due to product reuptake. In the current study, *dctA2* was identified as a target for the reduction of dicarboxylic acid reuptake and confirmed experimentally with deletion strains. Additionally, a second way of preventing product reuptake was demonstrated by converting mesaconic acid to (*S*)-citramalic acid by the introduction of an *in vivo* mesaconase/fumarate hydratase reaction step.

2.3 Summary of "Engineering of thioesterase YciA from *Haemophilus influenzae* for production of carboxylic acids" (chapter 6.2)

This manuscript describes the modification of thioesterase YciA from *H. influenzae* (YciAHI) for the improved production of dicarboxylic acids with *M. extorquens* AM1.

Screening of a semi-rational mutant library of YciAHI revealed that position F35 has a major impact on the amount of dicarboxylic acid products released. Application of F35N and F35L YciAHI variants in *M. extorquens* AM1 resulted in a substantially increased release of 2-methylsuccinic acid and mesaconic acid, while the ratios of the two products slightly changed. An alternative *in vivo* application in an *E. coli* strain designed for 3-hydroxybutyric acid production finally confirmed the impact of the F35 position. In the discussion section of the publication, a hypothesis regarding the influence of the F35 position is presented based on comparisons with closely related thioesterases.

2.4 Summary of "A pBBR1-based vector with IncP group plasmid compatibility for *Methylorubrum extorquens*" (chapter 6.3)

This publication characterizes a novel plasmid for *M. extorquens* AM1. Currently, almost all *M. extorquens* expression vectors are based on the pCM plasmid system. Also, a compatible plasmid co-transformations with pCM was missing in the genetic toolbox for *M. extorquens*. In the present work, *M. extorquens* AM1 was transformed with a pBBR1-based plasmid, resulting in a strong growth defect. The plasmid variant pMis1_1B with a single point mutation in the *rep* gene region was isolated from a suppressor mutant. The plasmid was subsequently characterized for transformation rates, reporter gene expression and relative plasmid copy number, both alone and in co-transformation with pCM80. Despite the slight metabolic burden caused by pMis1_1B, this new plasmid can be readily used in *M. extorquens*.

2.5 Summary of "Expression of toxic genes in *Methylorubrum extorquens* with a tightly repressed, cumate-inducible promoter" (chapter 6.4)

This manuscript describes the expansion of the genetic toolbox of *M. extorquens* with a tightly repressed, cumate-inducible promoter. The promoter variant was identified during testing of terpene production strains harboring a recombinant mevalonate pathway. Controlling the expression of the heterologous terpene synthesis gene cluster with promotor P_{Q2148} led to strong growth defects even before induction. This led to the conclusion that P_{Q2148} repression was not strong enough for this use case. A screening of suppressor mutants resulted in the identification of P_{s6}, a P_{Q2148} variant. This P_{s6} promoter was further characterized with reporter gene experiments. The new promoter is a powerful tool for controlled expression of pathways with toxic intermediates or products with *M. extorquens*.

3. Discussion

This chapter discusses additional aspects of the manuscripts, publications and additional results section (chapters 5 and 6) in an expanded context that goes beyond the discussions in the individual chapters. It also includes an outlook for further improvements and a general conclusion for this thesis.

3.1 Potential and limitations of thioesterase YciA for dicarboxylic acid production in *M. extorquens* AM1

In chapter 5, the production of a novel product, namely 2-hydroxy-3-methylsuccinic acid, was achieved by overexpressing a *citE* like thioesterase gene from *Corynebacterium glutamicum.* Since no other EMCP-derived product could be detected in the respective culture medium, a high specificity of the *citE* enzyme can be assumed. While this is very beneficial for the production of 2-hydroxy-3-methylsuccinic acid and eventual down-stream processing, the thioesterase seems not be suitable for the release of other products. Therefore, for the majority of the experiments presented in this thesis, broad-range thioesterase YciA originating from either *E. coli* (YciAEc) or *Haemophilus influenzae* (YciAHI) was chosen for the production of different dicarboxylic acids. YciA thioesterases are promising candidates for catalyzing the hydrolysis of all EMCP CoA-esters of interest. The previously described process for the production of mesaconic acid and 2-methylsuccinic acid with YciAEc (Sonntag et al. 2014; Sonntag et al. 2015b) was used as the basis for the developments in this work. In the study of Sonntag et al. (2015b), the heterologous overexpression of the *yciAEc* gene in *M. extorquens* AM1 yielded a simultaneous release of both products with a combined titer of up to 0.65 g/L in shake flask experiments.

3.1.1 Modification of YciA thioesterase

The present work aimed at expanding the dicarboxylic acid product spectrum of *M. extorquens*. Rational enzyme engineering of YciA for changing the substrate specificity would have been very challenging as potential substrates found in the EMCP show high structural similarity. A second challenge arose from the fact that rapid *in vitro* assays are not suitable for screening YciA variants. The sizes of the in-cell EMCP-CoA-ester pools are a critical factor and cannot be replicated *in vitro*. Another rationale against extended *in vitro* screenings is that the required enantiomerically pure CoA-

esters are either very expensive or not commercially available at all. For the mentioned reasons, a semi-rational design of an enzyme variant library and a subsequent *in vivo* screening approach was chosen and performed directly in *M. extorquens* cells.

To be able to perform semi-rational engineering, the key enzyme YciAEc from *E. coli*, that was used in the previous studies, was switched to the YciAHI enzyme from *H. influenzae*. For the latter, a crystal structure (PDB entry 1YLI) and studies examining its function have been published (Willis et al. 2008; Zhuang et al. 2008). As in the case of the *E. coli* enzyme, YciAHI introduction into *M. extorquens* AM1 resulted in the release of only two dicarboxylic acids into the growth medium, namely mesaconic acid and 2-methylsuccinic acid (see chapter 6.1). This suggests that in *M. extorquens* cells, mesaconyl-CoA and methylsuccinyl-CoA are the main substrates for heterologous YciA thioesterases *in vivo*, although steady state kinetic measurements show high activities of the isolated enzyme also with other potential EMCP CoA-substrates (Zhuang et al. 2008). The hydrolysis products of the other EMCP-CoA-esters could not be detected in the supernatant of *yciAHI* expressing cells, despite the LC-MS/MS based analytical method being designed to detect and quantify a plethora of dicarboxylic acids including crotonic acid, 2-hydroxy-3-methylsuccinic acid, ethylmalonic acid and methylmalonic acid (see chapter 6.1). In chapter 6.2, the objective was to identify potential targets for broadening the substrate spectrum of YciAHI. Although the two thioesterases YciAEc and YciAHI have a moderate overall amino acid sequence identity of 69 % (Willis et al. 2008), the region surrounding the catalytic amino acid D44 is highly conserved (Figure 6). This high similarity could explain the apparent equivalent substrate selectivity. Therefore, this region was targeted for modifications aiming at increasing the substrate spectrum of YciAHI.

Figure 6 Alignment of the central part of YciAHI (WP_005655643.1, Willis et al. 2008) and YciAEc (WP_032198773.1, Willis et al. 2008) amino acid sequences. Colors are assigned to physicochemical properties: red marks small and hydrophobic amino acids, blue marks acidic amino acids, pink marks basic amino acids and green marks the rest. Catalytic D44 is additionally marked with a blue star. The alignment and illustration was made with the Clustal Omega (v1.2.4) multiple sequence alignment tool (McWilliam et al. 2013).

The original experimental plan was to randomly exchange selected hydrophobic amino acids likely to be involved in substrate binding and subsequently perform a comprehensive screening. Unfortunately, none of the companies specializing in DNA synthesis was able to construct a high-quality plasmid library for the expression of the corresponding gene variants due to the high GC content and uncommon codon usage of the *M. extorquens* genome. Therefore, a more streamlined approach was attempted by creating a semi-rational library with targeted replacements of hydrophobic amino acids of interest (see chapter 6.2). In the following *in vivo* screening, none of the strains showed a diversified product spectrum, but the modification of the F35 position of YciA had a considerable effect on mesaconic acid and 2-methylsuccinic acid production. Especially the F35L variant yielded a substantially higher production than the unmodified enzyme. Although the variant enzymes were too unstable for *in vitro* analysis, tests in an independent *in vivo* environment confirmed the results. This shows that the decision to screen the enzyme variants *in vivo* was strategically sound, as the variant would not have been detected in *in vitro* assays due to the apparent low activity. In the following experiment, the F35 position was substituted with sixteen other amino acids. Unexpectedly, it was not the physicochemical side-chain properties of the substituting amino acids that seemed to be the decisive factor for difference in productivity, but the side-chain length (Figure 7). This led to the conclusion that the F35 position, which is located at the N-terminus of an α-helix, may sterically modulate the size of the binding channel or the architecture of other regions involved in substrate binding. Surprisingly, a comparison with other related hot dog fold thioesterases revealed that this position at the start of the α-helix is conserved by the presence of either a phenylalanine or a histidine. Amino acids with aromatic rings are known to stabilize the structure of proteins through aromatic-aromatic interactions, and phenylalanine in particular is known to play an important role in the scaffold stability of helical bundle proteins (Makwana and Mahalakshmi 2015). Further studies are needed to gain more understanding of the effect of F35 on the architecture and substrate binding properties of YciA and related thioesterases. Similar observations for the change in substrate binding and turnover number due to the replacement of an α-helix embedded aromatic amino acid have been made in the past for thioesterase I/protease I/lysophospholipase L_1 from *E. coli* (Lee et al. 2009). However, a thorough search of the relevant literature did not reveal any similar observations for hot dog fold

thioesterases, suggesting that a new target for beneficial modification of these enzymes has been identified here.

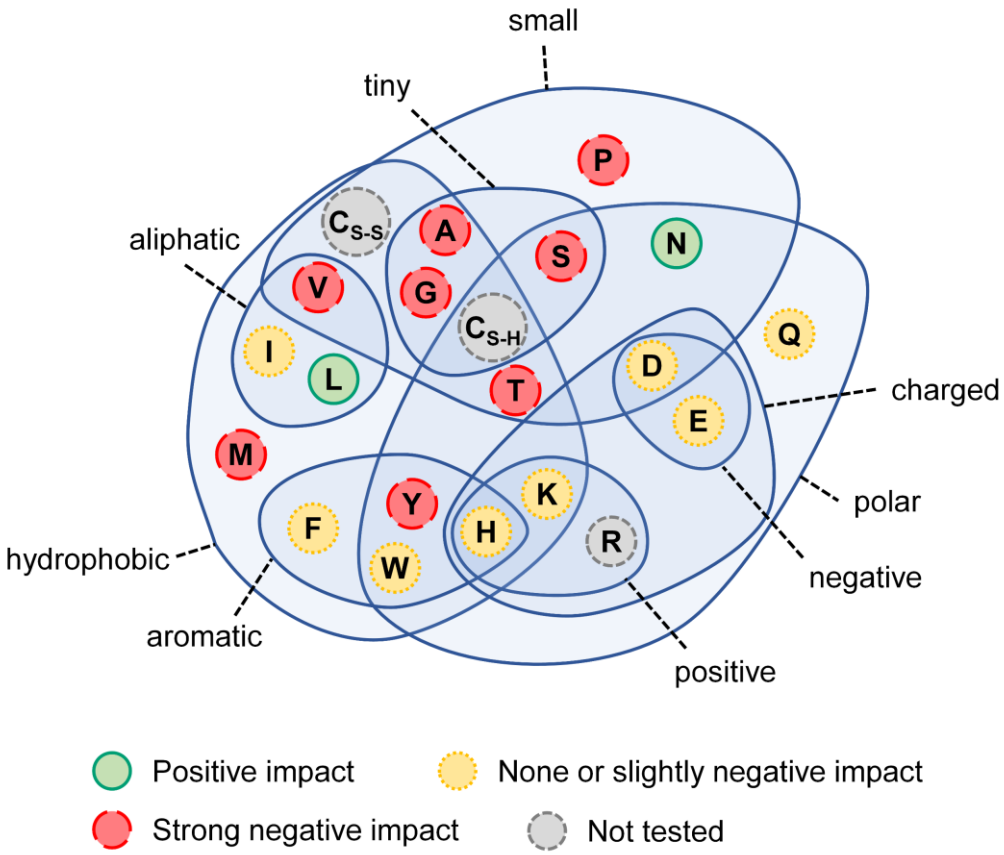

Figure 7 Influence of amino acid substitution at position F35 of YciAHI on the *in vivo* production of 2-methylsuccinic acid and mesaconic acid with *M. extorquens* AM1. Venn diagram grouping amino acids according to their properties was adapted from Taylor (1986).

3.1.2 Substrate selectivity and CoA inhibition may restrict the applicability of YciA in *M. extorquens* MeCFs

Although the productivity of strains with YciAHI modified at position F35 could be improved for mesaconic acid and 2-methylsuccinic acid, none of the approaches succeeded in creating enzyme variants with a diversified substrate or product spectrum. This restricts the applicability of YciA as a universal thioesterase for yielding different EMCP-derived products. Changing the size of CoA-ester pools could provide a direct solution without need of further enzyme engineering. Targeted modulation of the activity of specific EMCP enzymes could increase CoA-ester pools sizes, as shown for the reduction of B_{12}-dependent mutase activities by cobalt limitation (Kiefer et al. 2009; Sonntag et al. 2015b). Since the EMCP is essential for growth on methanol and other C_1 substrates, the activity would need to be tuned very carefully. Implementation of an alternative glyoxylate regeneration mechanism may provide the needed flexibility

by making the EMCP a facultative pathway. Thus, it would also be possible to interrupt the EMCP at any point (e.g. by gene deletion) and drain the desired intermediates with YciA or an alternative enzyme. Although attempts have been made in this regard, the recovery of methylotrophic growth of strains with interrupted EMCP has not yet been successful (Schada von Borzyskowski et al. 2018).

In addition to the challenge of changing the product spectrum, there is another major limitation in using YciAHI as a key catalyst for CoA cleavage in highly efficient production strains. To better understand this limitation, a more detailed look at the structure of YciAHI and related thioesterases is necessary. The catalytic site of YciAHI is embedded in a hot dog fold (see chapter 6.2). A variety of hot dog fold thioesterases with different structural compositions are described in literature. A high similarity in tertiary protein structure or substrate specificity is thereby not necessarily synonymous to sequence homology or the same architecture of the catalytic machinery as shown by the 4-hydroxybenzoyl-CoA thioesterases from *Arthrobacter* sp. and *Pseudomonas* sp. (Song et al. 2012). A more systematic way to group thioesterases was presented with the ThYme database (https://thyme.engr.unr.edu/v2.0/). This database classifies thioesterases based on a combination of the similarity of the primary and tertiary structures and the position and identity of catalytic residues. The database was originally published with 23 families and recently updated to 35 families (Cantu et al. 2010; Caswell et al. 2022). YciAHI belongs to the TE6 family acyl-CoA thioesterases (ACOTs) that are acting on short- to long-chain acyl-CoA-esters (C_4 - C_{18} acid groups). A dozen of crystal structures for TE6 thioesterases have been elucidated so far (see Caswell et al. 2022). While showing a high topologic similarity, prokaryotic and eukaryotic TE6 family members differ in domain organization. The functional units of prokaryotic TE6 thioesterases are assembled from two identical monomers, whereas the functional units of eukaryotic TE6 thioesterases contain a fused domain of double hot dogs (Swarbrick et al. 2020, chapter 6.2). For eukaryotic TE6 thioesterases such as ACOT7 and ACOT12, activity was shown for only one of the two potential active sites, indicating a half-of-sites activity (Forwood et al. 2007; Swarbrick et al. 2014). For procaryotic TE6 members, a half-of-sites activity has also been reported despite their symmetrical architecture. A CoA-binding induced conformation change of the second binding site was described in detail for the *Alkalihalobacillus halodurans* TE6 thioesterase by a comparison of the apoenzyme and a destabilized CoA-bound structure (Marfori et al. 2011). A similar observation was made for CoA-bound YciAHI

and an inactive mutant variant (Willis et al. 2008). Many purified TE6 thioesterases were found to be co-crystallized with a bound CoA molecule at one of the two potential active sites (Willis et al. 2008; Swarbrick et al. 2014). These observations, in combination with the steady-state inhibition data with desulfoCoA, led to the assumption that CoA is a strong feedback inhibitor of YciAHI (Zhuang et al. 2008). As a cytoplasmic enzyme, this feedback inhibition may have evolved from the need to prevent YciA from uncontrolled cleavage of acyl-CoAs. In a biotechnological application, this strong feedback inhibition might hinder the achievement of even higher product yields. This problem should be addressed in the future either through further enzyme engineering or by testing alternative thioesterases for their inhibition constants with CoA.

3.2 Characterization of dicarboxylic acid products

In the present work, *M. extorquens* AM1 production strains for four dicarboxylic acid products were constructed, namely citramalic acid, mesaconic acid, 2-methylsuccinic acid and 2-hydroxy-3-methylsuccinic acid. In the following, an evaluation is given with regard to the purity and possible applications of the products.

3.2.1 (Enantio-)purity of dicarboxylic acid products

A high product purity is a prerequisite for the potential application of the developed dicarboxylic acid production processes. Therefore, the purity of the dicarboxylic acid products was evaluated in scientific cooperation with Chiracon GmbH (Luckenwalde, Germany), a company specialized in the production, development and distribution of chiral molecules and APIs. The values presented in the following were reported by Chiracon GmbH (Zuhse et al. 2021), the scientific evaluation was done by the doctoral candidate.

All target chiral molecules, namely citramalic acid, 2-methylsuccinic acid and 2-hydroxy-3-methylsuccinic acid, could be extracted at a scale of 2-3 g with high purity from 0.6-0.9 L of respective culture broths from chapter 5 by Chiracon GmbH (Zuhse et al. 2021). The enantiomeric purity of the extracts was analyzed by Chiracon GmbH by chiral GC/FID analysis. For 2-methylsuccinic acid purified from the culture broth, an enantiomeric excess of 95 - 97.8 % of the *S*-enantiomer was reported (Zuhse et al. 2021). The remaining *R*-portion of the product is possibly due to a small amount of (2*R*)-methylsuccinyl-CoA present in the cell that could be formed during the reaction

of ethylmalonyl-CoA mutase in the EMCP. Although the mutase is stereoselective for its substrate (2*R*)-ethylmalonyl-CoA (Erb et al. 2008; Good et al. 2015), the possibility of epimerization during the reaction was reported for the closely related methylmalonyl-CoA mutase (Hull et al. 1988). A small amount of (2*R*)-methylsuccinyl-CoA could be therefore produced by erroneous reactions of ethylmalonyl-CoA mutase itself or by the methylmalonyl-CoA mutase, that may accept ethylmalonyl-CoA as a substrate analogue (Rétey et al. 1978, personal communication Tobias J. Erb). Since the hydrolysis reaction catalyzed by YciA is not stereoselective, (2*R*)-methylsuccinic acid would be released as a consequence by the engineered *M. extorquens* strain.

It was not possible for Chiracon GmbH to develop GC/FID methods for the chiral analysis of citramalic acid and 2-hydroxy-3-methylsuccinic acid since the molecules appear to decompose in the inlet of the GC before entering the gas phase (Zuhse et al. 2021). A possible alternative would be the derivatization of the carboxylic acids to corresponding esters, for which a higher stability in GC could be expected.

The presence of diastereomers in the workup was excluded by Chiracon GmbH using ^{1}H-NMR-spectroscopy (Zuhse et al. 2021). The identity of the enantiomers (or the pair of enantiomers) could not be determined. However, the stereoselective mechanisms of the enzymes used (see chapters 5 and 6.1) suggest that the obtained products are (*S*)-citramalic acid and (2*S*,3*R*)-2-hydroxy-3-methylsuccinic acid of high purity.

As shown in chapter 6.1, the production of 2-methylsuccinic acid by *yciA*-expressing *M. extorquens* AM1 strains is coupled with the release of achiral mesaconic acid. Although mesaconic acid itself could be an interesting building block and is isomerically pure, it is desirable to remove it from the mixture if 2-methylsuccinic acid is the target product. Semi-rational engineering of the thioesterase could only marginally influence the ratio of the two products (see chapter 6.2). In the work-up, the mesaconic acid content was successfully reduced to a ratio of 1:0.13 for 2-methylsuccinic acid:mesaconic acid by a crystallization process carried out by Chiracon GmbH (Zuhse et al. 2021).

3.2.2 Possible applications and economic potential of dicarboxylic acids produced with *M. extorquens* AM1

The chiral products targeted in this work, namely (*S*)-2-methylsuccinic acid, (*S*)-citramalic acid and (2*S*,3*R*)-2-hydroxy-3-methylsuccinic acid, were analyzed by Chiracon GmbH for their possible application. The company conducted extensive

market, literature and patent research, which led to the conclusion that these chiral building blocks may be used to produce highly effective cancer therapeutics (prostate, bicalutamide), statins (cholesterol-lowering agents), antihypertensive agents (treprostinil) or pheromones (Zuhse et al. 2021). A potential application for (*S*)-2-methylsuccinic acid was also practically demonstrated by conversion to its anhydride and the subsequent reaction with benzylamine to *N*-benzyl-methylsuccinimide as a potential intermediate step in the drug synthesis of novel antibiotics (Zuhse et al. 2021). Starting from (*S*)-citramalic acid, an intermediate for the preparation of bicalutamide was obtained, a drug used to treat prostate cancer (Zuhse et al. 2021). These derivatization reactions show the potential of using the produced chiral dicarboxylic acids as building blocks for APIs. The current market prizes for the fully chemically synthesized dicarboxylic acid products and the (*S*)-2-methylsuccinic anhydride are shown in Table 3. Since their synthesis is challenging, high prices can be achieved. For the achiral (but isomerically pure) mesaconic acid, an isomerization to itaconic acid, which is a valuable platform chemical for various applications (Teleky and Vodnar 2021), would be a conceivable scenario.

Table 3 Market prices for commercially available chemically synthesized dicarboxylic acids and derivatives targeted in this work. Data was retrieved from CAS SciFinder^{n} (CAS, Columbus, USA) for products synthesized in a 1 g scale. Accessed on 06/05/2023.

Molecule	IUPAC name	CAS	Price per g of product
(*S*)-2-Methylsuccinic acid	(2*S*)-2-Methylbutanedioic acid	2174-58-5	Starting from 25 USD
(*S*)-2-Methylsuccinic anhydride	(3*S*)-3-Methyloxolane-2,5-dione	6973-20-2	Starting from 675 USD
(*S*)-Citramalic acid	(2*S*)-2-Hydroxy-2-methylbutanedioic acid	6236-09-5	Starting from 2900 USD
(2*S*,3*R*)-2-Hydroxy-3-methylsuccinic acid	(2*S*,3*R*)-2-Hydroxy-3-methylbutanedioic acid	85026-06-8	Starting from 1600 USD

3.3 Further steps and aspects for the development of *M. extorquens* towards an efficient MeCF

The enormous potential of *M. extorquens* to serve as production platform for methanol-based production has been demonstrated in various applications (see chapter 1.1.2). Many heterologous metabolic pathways and genes have been successfully

implemented in *M. extorquens* to produce a variety of value-added products. Nonetheless, none of these products have been manufactured in an industrial process to date. In the 1970s and 1980s, methanol-based production of single-cell protein for animal feed with *Methylophilus methylotrophus* was employed by Imperial Chemical Industries (ICI) at a scale of 1500 m³ and with a production capacity of 50 000 tons per year (Windass et al. 1980; Westlake 1986). Despite this enormously high production capacity and a high process robustness, the process was discontinued after a few years because the rising methanol prices and low prices for soy protein made it no longer profitable (Bungard 1992). This example demonstrates that the feasibility of a biotechnological process also depends on manifold extrinsic factors. The process itself must be efficient and profitable enough to compensate for uncertainties, especially if the implementation means a conversion of conventional and already established processes, which entails enormous investment costs. Especially for bulk chemical products, which are usually sold at low prices, a highly efficient production strain and manufacturing process is absolutely crucial. Therefore, the strategy of producing fine chemicals with high market value, whose chemical synthesis is very challenging and costly, may be more advantageous for early biotechnological processes in a just emerging methanol economy. This chapter discusses further ways to improve future *M. extorquens* production strains and, in particular, strains for the production of chiral dicarboxylic acids.

3.3.1 General considerations for development of *M. extorquens* strains for biotechnological production

Chapter 1.2.5 summarizes the developments made in the past to improve the applicability of *M. extorquens* as a production platform. The genome structure of *M. extorquens* AM1 is far from ideal for genetic engineering approaches. In addition to the high GC content, strain AM1 exhibits high genomic plasticity due to transposable elements and has a complex genome structure with five replicons (Vuilleumier et al. 2009; Green and Ardley 2018). It was shown that *M. extorquens* AM1 laboratory strains have diverged over the long period of domestication from the archival strain, which has undergone only a small number of growth cycles since its isolation (Carroll et al. 2014). Also during the work on this thesis, differences were found between the genome sequence of the strains used and sequences found in the databases. Table S2 of chapter 6.1 lists mutations in the analyzed strains revealed by genome sequencing.

This unwanted strain divergence over time may be limited by the use of strain PA1, which was isolated almost fifty years after strain AM1 (Knief et al. 2010; Marx et al. 2012). PA1 contains a streamlined genome with a single replicon and a low number of IS elements (Nayak and Marx 2014). It also shows faster growth on C_1 and multicarbon substrates in synthetic media compared to strain AM1 (Nayak and Marx 2014). These aspects make strain PA1 an even more promising candidate for a further development towards an MeCF (Lee et al. 2022). Since the genomes of AM1 and PA1 strains show high similarity, especially with respect to central metabolism pathway genes, many production processes already developed for AM1 should be readily transferable to strain PA1.

3.3.2 Prospects for further developments to improve the production of chiral dicarboxylic acids

In cooperation with Insilico Biotechnology AG (Stuttgart, Germany), a metabolic network model for *M. extorquens* AM1 was developed, which includes the thioesterase reaction of heterologous YciA (Schmid et al. 2021). This model was based on the model of Peyraud and colleagues (Peyraud et al. 2011), but reactions have been added or removed according to the current state of knowledge. The model predicted theoretical product/substrate yields ($Y_{P/S}$) of roughly 0.5-0.75 $g_P/g_{methanol}$ for the target products 2-methylsuccinic acid, mesaconic acid and 2-hydroxy-3-methylsuccinic acid (Schmid et al. 2021). In chapter 5, the maximum $Y_{P/S}$ achieved were 0.08 for 2-hydroxy-3-methylsuccinic acid, 0.1 for mesaconic acid, 0.09 for 2-methylsuccinic acid and 0.1 for citramalic acid. For the latter, the metabolic model does not provide any theoretical maximum yield, as the mesaconase reaction is not represented in the network model. The gaps between the achieved yields and the predicted maximum theoretical yields leave room for further improvements of dicarboxylic acid production. A combination of metabolic network model predictions and analysis of transcriptome data from chapter 6.1 for differential gene expression revealed the following options to increase product formation (see Schmid et al. 2021):

(1) avoiding the formation of by-products (e.g. by reducing the PHB formation)
(2) reducing the degradation or consumption of the product(s)
(3) the adjustment of feeding to ensure an adequate respiratory chain and to prevent down-regulation due to growth or stress

(4) separating biomass production and product synthesis. Induction and/or overexpression of the genes *mqo* (TCA + energy metabolism) *metK* (methionine, activated C_1 building blocks), *fbpA* (iron transport) and *cysH* (sulfate reduction, assimilation) represent potential switches to switch from biomass formation to product synthesis

In addition to the mainly respiratory chain and TCA related gene targets, a functional analysis of the metabolic network model further revealed two potential target reactions for applying a higher metabolic flux towards the products, namely methanol oxidation (*mxaFI1*) and malyl-CoA synthetase (*mtkAB2*) reaction (Schmid et al. 2021).
Some of the strategies mentioned above, as reduction of consumption of the products or reduction of PHB formation, were already tested (chapter 6.1, Sonntag et al. 2015b). Both showed positive effects on production, although knockout of the polyhydroxyalkanoate synthase *phaC* was antagonized by suppressor mutations (Sonntag et al. 2015b). A more recent study tested the effect of deletion of gene *phaR*, a regulator for PHB synthesis (Korotkova and Lidstrom 2001; Van Dien et al. 2003), in a dicarboxylic acid production strain (Lim et al. 2019). Surprisingly, application of the *phaR* mutant strain even resulted in less product formation despite only minimal PHB accumulation. A subsequent transcriptome analysis revealed a rewiring of gene transcription (Lim et al. 2019). A more fundamental understanding of the network of PHB synthesis genes and interconnected reactions with other metabolic pathways in *M. extorquens* is needed to construct more efficient strains for EMCP-derived production. The other potential targets for strain improvement that emerge from the metabolic network model analysis remain to be confirmed experimentally.

3.4 Novel genetic tools for *M. extorquens*

The new genetic tools described in 6.3 and 6.4 are valuable additions to the toolset for *M. extorquens* (see 1.2.4). The novel plasmid pMis1_1B can be used in co-transformations together with plasmids of the IncP group. The Inc group classification is based on origins of replication and partitioning systems (Novick 1987; del Solar et al. 1998). Plasmids of the same Inc group are not recognized as different genetic units by the microbial cell and therefore cannot be reliably replicated. The IncP group compatibility of pMis1_1B is particularly important as this group includes the pCM plasmids that are predominantly employed for *M. extorquens* (Marx and Lidstrom

2001). The possibility of introducing two stably contained plasmids at once facilitates screening and engineering approaches and provides experimental flexibility.

The pMis1_1B plasmid developed in 6.3 imposes a fitness cost on the cell, which is manifested by slower growth, especially when it is present in combination with pCM plasmids. The reasons for plasmid burdens are not yet fully understood. A part of the plasmid-imposed fitness costs are implied through the necessity to apply cellular resources as nucleotides and the machinery for replication, gene transcription and translation (San Millan and Craig MacLean 2017). In addition to these “basic costs” of plasmid carriage, fitness costs can also derive from plasmid specific genes (e.g. genes conferring resistance to antibiotics) or from genes interfering with the hosts metabolism (Carroll and Wong 2018; Hall et al. 2021). When *M. extorquens* was co-transformed with pMis1_1B and pCM80, a substantially higher plasmid copy number and plasmid-borne gene expression was observed for pMis1_1B compared to the single transformants. The reason for this might be some kind of positive epistasis as reported before for plasmid co-transformations (San Millan et al. 2014). The increased copy number could in turn imply a higher plasmid burden for the cell, e.g., due to high expression of the kanamycin resistance gene. Similar effects have been reported for the pBR332 plasmid and an enhanced expression of the tetracycline resistance gene in *E. coli* (Valenzuela et al. 1996). Further laboratory evolution of pMis1_1B might help optimize plasmid-host interaction with *M. extorquens*. An indication that this approach may be promising is found in the nature of the genesis of pMis1_1B, which was derived from pMis1 by a single point mutation.

The development of a second new genetic tool for *M. extorquens* is described in 6.4. Deletion of 28 nucleotides in the promoter region of P_{Q2148} (Kaczmarczyk et al. 2013) resulted in the P_{s6} promoter that exhibited an extremely low background expression level and allowed expression of the toxic *cis*-abienol synthesis operon. The application of this novel promoter will likely be limited for cases where a very strong repression is required, as the maximal expression strength is considerably lower than for other artificial inducible promoters used in *M. extorquens* (Choi et al. 2006; Chubiz et al. 2013; Kaczmarczyk et al. 2013; Carrillo et al. 2019; Sathesh-Prabu et al. 2021). Nevertheless, a promoter that is tight and tunable to lower-range expression levels is a valuable addition to the *M. extorquens* genetic toolbox.

3.5 Conclusion

A major advantage of using *M. extorquens* as a platform organism for the production of value-added products is the use of methanol as a substrate, which could be obtained in a renewable or even regenerative manner in the future (see 1.1.1) and brings many advantages for biotechnological processes (see 1.1.2). However, the introduction of methanol-based bioprocesses and the introduction of a so-called methanol economy is only just beginning. Two factors are thereby decisive for success: On the one hand, the political will to invest in sustainable processes, especially in the production of e-methanol and bio-methanol, and on the other hand, scientists and engineers developing highly efficient processes to replace conventional fully chemical, petroleum- or sugar-based ones. In this work, the ongoing development of the model organism *M. extorquens* AM1 towards a MeCF was further advanced, aiming for the efficient and sustainable production of the target products in the future.

4. References of chapters 1-3

Alber BE (2011) Biotechnological potential of the ethylmalonyl-CoA pathway. Appl Microbiol Biotechnol 89:17–25. https://doi.org/10.1007/s00253-010-2873-z

Alber BE, Spanheimer R, Ebenau-Jehle C, Fuchs G (2006) Study of an alternate glyoxylate cycle for acetate assimilation by *Rhodobacter sphaeroides*. Mol Microbiol 61:297–309. https://doi.org/10.1111/j.1365-2958.2006.05238.x

Alkadi H, Jbeily R (2018) Role of Chirality in Drugs: An Overview. Infect Disord - Drug Targets 18:88–95. https://doi.org/10.2174/1871526517666170329123845

Álvarez A, Bansode A, Urakawa A, Bavykina A V., Wezendonk TA, Makkee M, Gascon J, Kapteijn F (2017) Challenges in the Greener Production of Formates/Formic Acid, Methanol, and DME by Heterogeneously Catalyzed CO_2 Hydrogenation Processes. Chem Rev 117:9804–9838. https://doi.org/10.1021/acs.chemrev.6b00816

Anthony C (2011) How half a century of research was required to understand bacterial growth on C_1 and C_2 compounds; the story of the serine cycle and the ethylmalonyl-CoA pathway. Sci Prog 94:109–137. https://doi.org/10.3184/003685011X13044430633960

Anthony C (1982) The biochemistry of methylotrophs. Academic Press, London, England

Arenas AMZ, De Wever H, Brendolise L, Keil A, Van Hecke W (2023) Polyhydroxybutyrate/valerate production from methanol by *Methylorubrum extorquens*: Process limiting factors and polymer characterisation. Bioresour Technol Reports 21:101309. https://doi.org/10.1016/j.biteb.2022.101309

Bélanger L, Figueira M., Bourque D, Morel L, Béland M, Laramée L, Groleau D, Míguez C. (2004) Production of heterologous protein by *Methylobacterium extorquens* in high cell density fermentation. FEMS Microbiol Lett 231:197–204. https://doi.org/10.1016/S0378-1097(03)00956-X

Belkhelfa S, Labadie K, Cruaud C, Aury J-M, Roche D, Bouzon M, Salanoubat M, Döring V (2018) Complete Genome Sequence of the Facultative Methylotroph *Methylobacterium extorquens* TK 0001 Isolated from Soil in Poland. Genome Announc 6:1–2. https://doi.org/10.1128/genomeA.00018-18

Belkhelfa S, Roche D, Dubois I, Berger A, Delmas VA, Cattolico L, Perret A, Labadie K, Perdereau AC, Darii E, Pateau E, de Berardinis V, Salanoubat M, Bouzon M, Döring V (2019) Continuous Culture Adaptation of *Methylobacterium extorquens* AM1 and TK 0001 to Very High Methanol Concentrations. Front Microbiol 10:1–17. https://doi.org/10.3389/fmicb.2019.01313

Bourque D, Ouellette B, Andre G, Groleau D (1992) Production of poly-*ß*-hydroxybutyratehydroxybutyrate from methanol: characterization of a new isolate of *Methylobacterium extorquens*. 7–12. https://doi.org/https://doi.org/10.1007/BF00174194

Bourque D, Pomerleau Y, Groleau D (1995) High-cell-density production of poly-*β*-hydroxybutyrate (PHB) from methanol by *Methylobacterium extorquens*: production of high-molecular-mass PHB. Appl Microbiol Biotechnol 44:367–376. https://doi.org/10.1007/BF00169931

Brautaset T, Jakobsen ØM, Degnes KF, Netzer R, Nærdal I, Krog A, Dillingham R, Flickinger MC, Ellingsen TE (2010) *Bacillus methanolicus* pyruvate carboxylase and homoserine dehydrogenase I and II and their roles for L-lysine production from methanol at 50°C. Appl Microbiol Biotechnol 87:951–964. https://doi.org/10.1007/s00253-010-2559-6

Brautaset T, Jakobsen ØM, Josefsen KD, Flickinger MC, Ellingsen TE (2007) *Bacillus methanolicus*: a candidate for industrial production of amino acids from methanol at 50°C. Appl Microbiol Biotechnol 74:22–34. https://doi.org/10.1007/s00253-006-0757-z

Brautaset T, Williams MD, Dillingham RD, Kaufmann C, Bennaars A, Crabbe E, Flickinger MC (2003) Role of the *Bacillus methanolicus* Citrate Synthase II Gene, *citY*, in Regulating the Secretion of Glutamate in L-Lysine-Secreting Mutants. Appl Environ Microbiol 69:3986–3995. https://doi.org/10.1128/AEM.69.7.3986-3995.2003

Brooks WH, Guida WC, Daniel KG (2011) The Significance of Chirality in Drug Design and Development. Curr Top Med Chem 11:760–770. https://doi.org/10.2174/156802611795165098

Bungard SJ (1992) Bugs in the works—biology at ICI Billingham. J Biol Educ 26:252–256. https://doi.org/10.1080/00219266.1992.9655282

Calcaterra A, D'Acquarica I (2018) The market of chiral drugs: Chiral switches versus *de novo* enantiomerically pure compounds. J Pharm Biomed Anal 147:323–340. https://doi.org/10.1016/j.jpba.2017.07.008

Cantu DC, Chen Y, Reilly PJ (2010) Thioesterases: A new perspective based on their primary and tertiary structures. Protein Sci 19:1281–1295. https://doi.org/10.1002/pro.417

Carrillo M, Wagner M, Petit F, Dransfeld A, Becker A, Erb TJ (2019) Design and Control of Extrachromosomal Elements in *Methylorubrum extorquens* AM1. ACS Synth Biol 8:2451–2456. https://doi.org/10.1021/acssynbio.9b00220

Carroll AC, Wong A (2018) Plasmid persistence: costs, benefits, and the plasmid paradox. Can J Microbiol 64:293–304. https://doi.org/10.1139/cjm-2017-0609

Carroll SM, Xue KS, Marx CJ (2014) Laboratory divergence of *Methylobacterium extorquens* AM1 through unintended domestication and past selection for antibiotic resistance. BMC Microbiol 14:2. https://doi.org/10.1186/1471-2180-14-2

Caswell BT, Carvalho CC, Nguyen H, Roy M, Nguyen T, Cantu DC (2022) Thioesterase enzyme families: Functions, structures, and mechanisms. Protein Sci 31:652–676. https://doi.org/10.1002/pro.4263

Chen FYH, Jung H-W, Tsuei C-Y, Liao JC (2020) Converting *Escherichia coli* to a Synthetic Methylotroph Growing Solely on Methanol. Cell 182:933-946.e14. https://doi.org/10.1016/j.cell.2020.07.010

Chistoserdova L (2011) Modularity of methylotrophy, revisited. Environ Microbiol 13:2603–2622. https://doi.org/10.1111/j.1462-2920.2011.02464.x

Chistoserdova L, Chen S, Lapidus A, Lidstrom ME (2003) Methylotrophy in *Methylobacterium extorquens* AM1 from a Genomic Point of View. J Bacteriol 185:2980–2987. https://doi.org/10.1128/JB.185.10.2980-2987.2003

Chistoserdova L, Kalyuzhnaya MG (2018) Current Trends in Methylotrophy. Trends Microbiol 26:1–12. https://doi.org/10.1016/j.tim.2018.01.011

Chmiel H, Takors R, Weuster-Botz D (2018) Bioprozesstechnik, 4th edn. Springer Berlin Heidelberg, Berlin

Choi YJ, Gringorten JL, Bélanger L, Morel L, Bourque D, Masson L, Groleau D, Míguez CB (2008) Production of an Insecticidal Crystal Protein from *Bacillus thuringiensis*

by the Methylotroph *Methylobacterium extorquens*. Appl Environ Microbiol 74:5178–5182. https://doi.org/10.1128/AEM.00598-08

Choi YJ, Morel L, Bourque D, Mullick A, Massie B, Míguez CB (2006) Bestowing Inducibility on the Cloned Methanol Dehydrogenase Promoter (P_{mxaF}) of *Methylobacterium extorquens* by Applying Regulatory Elements of *Pseudomonas putida* F1. Appl Environ Microbiol 72:7723–7729. https://doi.org/10.1128/AEM.02002-06

Chubiz LM, Purswani J, Carroll SM, Marx CJ (2013) A novel pair of inducible expression vectors for use in *Methylobacterium extorquens*. BMC Res Notes 6:1–8. https://doi.org/10.1186/1756-0500-6-183

D'Argenio DA, Gallagher LA, Berg CA, Manoil C (2001) Drosophila as a Model Host for *Pseudomonas aeruginosa* Infection. J Bacteriol 183:1466–1471. https://doi.org/10.1128/JB.183.4.1466-1471.2001

da Silva MJ (2016) Synthesis of methanol from methane: Challenges and advances on the multi-step (syngas) and one-step routes (DMTM). Fuel Process Technol 145:42–61. https://doi.org/10.1016/j.fuproc.2016.01.023

del Solar G, Giraldo R, Ruiz-Echevarría MJ, Espinosa M, Díaz-Orejas R (1998) Replication and Control of Circular Bacterial Plasmids. Microbiol Mol Biol Rev 62:434–464. https://doi.org/10.1128/MMBR.62.2.434-464.1998

Delaney NF, Kaczmarek ME, Ward LM, Swanson PK, Lee M-C, Marx CJ (2013) Development of an Optimized Medium, Strain and High-Throughput Culturing Methods for *Methylobacterium extorquens*. PLOS ONE 8:e62957. https://doi.org/10.1371/journal.pone.0062957

Di Lorenzo RD, Serra I, Porro D, Branduardi P (2022) State of the Art on the Microbial Production of Industrially Relevant Organic Acids. Catalysts 12:234. https://doi.org/10.3390/catal12020234

Din IU, Shaharun MS, Alotaibi MA, Alharthi AI, Naeem A (2019) Recent developments on heterogeneous catalytic CO_2 reduction to methanol. J CO_2 Util 34:20–33. https://doi.org/10.1016/j.jcou.2019.05.036

Doronina N (1996) Isolation and initial characterization of aerobic chloromethane-utilizing bacteria. FEMS Microbiol Lett 142:179–183. https://doi.org/10.1016/0378-1097(96)00262-5

Erb TJ, Berg IA, Brecht V, Müller M, Fuchs G, Alber BE (2007) Synthesis of C_5-dicarboxylic acids from C_2-units involving crotonyl-CoA carboxylase/reductase: the ethylmalonyl-CoA pathway. Proc Natl Acad Sci USA 104:10631–10636. https://doi.org/10.1073/pnas.0702791104

Erb TJ, Rétey J, Fuchs G, Alber BE (2008) Ethylmalonyl-CoA mutase from *Rhodobacter sphaeroides* defines a new subclade of coenzyme B_{12}-dependent Acyl-CoA mutases. J Biol Chem 283:32283–32293. https://doi.org/10.1074/jbc.M805527200

Ezhov VA, Doronina N V, Shmareva MN, Trotsenko YA (2017) Synthesis of high-molecular-mass polyhydroxybutyrate from methanol in *Methyloligella halotolerans* C2. Appl Biochem Microbiol 53:47–51. https://doi.org/10.1134/S0003683817010112

Fernandes ES, Passos GF, Medeiros R, da Cunha FM, Ferreira J, Campos MM, Pianowski LF, Calixto JB (2007) Anti-inflammatory effects of compounds alpha-humulene and (−)-*trans*-caryophyllene isolated from the essential oil of *Cordia verbenacea*. Eur J Pharmacol 569:228–236. https://doi.org/10.1016/j.ejphar.2007.04.059

Fitzgerald KA, Lidstrom ME (2003) Overexpression of a heterologous protein, haloalkane dehalogenase, in a poly-ß-hydroxybutyrate-deficient strain of the facultative methylotroph *Methylobacterium extorquens* AM1. Biotechnol Bioeng 81:263–268. https://doi.org/10.1002/bit.10470

Forwood JK, Thakur AS, Guncar G, Marfori M, Mouradov D, Meng W, Robinson J, Huber T, Kellie S, Martin JL, Hume DA, Kobe B (2007) Structural basis for recruitment of tandem hotdog domains in acyl-CoA thioesterase 7 and its role in inflammation. Proc Natl Acad Sci USA 104:10382–10387. https://doi.org/10.1073/pnas.0700974104

Gälli R, Leisinger T (1985) Specialized bacterial strains for the removal of dichloromethane from industrial waste. Conserv Recycl 8:91–100. https://doi.org/10.1016/0361-3658(85)90028-1

Goeppert A, Czaun M, Jones J-P, Surya Prakash GK, Olah GA (2014) Recycling of carbon dioxide to methanol and derived products – closing the loop. Chem Soc Rev 43:7995–8048. https://doi.org/10.1039/C4CS00122B

Goeppert A, Olah GA, Surya Prakash GK (2018) Toward a Sustainable Carbon Cycle. In: Török B, Dransfield T (eds) Green Chemistry. Elsevier, Amsterdam, Netherlands, pp 919–962

Good NM, Martinez-Gomez NC, Beck DAC, Lidstrom ME (2015) Ethylmalonyl Coenzyme A Mutase Operates as a Metabolic Control Point in *Methylobacterium extorquens* AM1. J Bacteriol 197:727–735. https://doi.org/10.1128/JB.02478-14

Green PN, Ardley JK (2018) Review of the genus *Methylobacterium* and closely related organisms: a proposal that some *Methylobacterium* species be reclassified into a new genus, *Methylorubrum* gen. nov. Int J Syst Evol Microbiol 68:2727–2748. https://doi.org/10.1099/ijsem.0.002856

Gregory GJ, Bennett RK, Papoutsakis ET (2022) Recent advances toward the bioconversion of methane and methanol in synthetic methylotrophs. Metab Eng 71:99–116. https://doi.org/10.1016/j.ymben.2021.09.005

Gutiérrez J, Bourque D, Criado R, Choi YJ, Cintas LM, Hernández PE, Míguez CB (2005) Heterologous extracellular production of enterocin P from *Enterococcus faecium* P13 in the methylotrophic bacterium *Methylobacterium extorquens*. FEMS Microbiol Lett 248:125–131. https://doi.org/10.1016/j.femsle.2005.05.029

Hagishita T, Yoshida T, Izumi Y, Mitsunaga T (1996) Efficient L-Serine Production from Methanol and Glycine by Resting Cells of *Methylobacterium* sp. Strain MN43. Biosci Biotechnol Biochem 60:1604–1607. https://doi.org/10.1271/bbb.60.1604

Hall JPJ, Wright RCT, Harrison E, Muddiman KJ, Wood AJ, Paterson S, Brockhurst MA (2021) Plasmid fitness costs are caused by specific genetic conflicts enabling resolution by compensatory mutation. PLOS Biol 19:e3001225. https://doi.org/10.1371/journal.pbio.3001225

Höfer P, Choi YJ, Osborne MJ, Miguez CB, Vermette P, Groleau D (2010) Production of functionalized polyhydroxyalkanoates by genetically modified *Methylobacterium extorquens* strains. Microb Cell Factories 9:70. https://doi.org/10.1186/1475-2859-9-70

Hölscher T, Breuer U, Adrian L, Harms H, Maskow T (2010) Production of the Chiral Compound (*R*)-3-Hydroxybutyrate by a Genetically Engineered Methylotrophic Bacterium. Appl Environ Microbiol 76:5585–5591. https://doi.org/10.1128/AEM.01065-10

Hu B, Lidstrom ME (2014) Metabolic engineering of *Methylobacterium extorquens* AM1 for 1-butanol production. Biotechnol Biofuels 7:156. https://doi.org/10.1186/s13068-014-0156-0

Hull WE, Michenfelder M, Retey J (1988) The error in the cryptic stereospecificity of methylmalonyl-CoA mutase. The use of carba-(dethia)-coenzyme A substrate analogues gives new insight into the enzyme mechanism. Eur J Biochem 173:191–201. https://doi.org/10.1111/j.1432-1033.1988.tb13984.x

IRENA and Methanol Institute (2021) Innovation Outlook: Renewable Methanol. International Renewable Energy Agency, Abu Dhabi, Abu Dhabi

Irla M, Nærdal I, Brautaset T, Wendisch VF (2017) Methanol-based γ-aminobutyric acid (GABA) production by genetically engineered *Bacillus methanolicus* strains. Ind Crops Prod 106:12–20. https://doi.org/10.1016/j.indcrop.2016.11.050

Kaczmarczyk A, Vorholt JA, Francez-Charlot A (2013) Cumate-Inducible Gene Expression System for Sphingomonads and Other *Alphaproteobacteria*. Appl Environ Microbiol 79:6795–6802. https://doi.org/10.1128/AEM.02296-13

Kar S, Kothandaraman J, Goeppert A, Prakash GKS (2018) Advances in catalytic homogeneous hydrogenation of carbon dioxide to methanol. J CO_2 Util 23:212–218. https://doi.org/10.1016/j.jcou.2017.10.023

Keith DW, Holmes G, St. Angelo D, Heidel K (2018) A Process for Capturing CO_2 from the Atmosphere. Joule 2:1573–1594. https://doi.org/10.1016/j.joule.2018.05.006

Khosravi-Darani K, Mokhtari Z, Amai T, Tanaka K (2013) Microbial production of poly(hydroxybutyrate) from C_1 carbon sources. Appl Microbiol Biotechnol 97:1407–1424. https://doi.org/10.1007/s00253-012-4649-0

Kiefer P, Buchhaupt M, Christen P, Kaup B, Schrader J, Vorholt JA (2009) Metabolite Profiling Uncovers Plasmid-Induced Cobalt Limitation under Methylotrophic Growth Conditions. PLOS ONE 4:e7831. https://doi.org/10.1371/journal.pone.0007831

Klein VJ, Irla M, Gil López M, Brautaset T, Fernandes Brito L (2022) Unravelling Formaldehyde Metabolism in Bacteria: Road towards Synthetic Methylotrophy. Microorganisms 10:220. https://doi.org/10.3390/microorganisms10020220

Knief C, Frances L, Vorholt JA (2010) Competitiveness of Diverse *Methylobacterium*

Strains in the Phyllosphere of *Arabidopsis thaliana* and Identification of Representative Models, Including *M. extorquens* PA1. Microb Ecol 60:440–452. https://doi.org/10.1007/s00248-010-9725-3

Kohler-Staub D, Hartmans S, Galli R, Suter F, Leisinger T (1986) Evidence for Identical Dichloromethane Dehalogenases in Different Methylotrophic Bacteria. Microbiology 132:2837–2843. https://doi.org/10.1099/00221287-132-10-2837

Kornberg HL, Krebs HA (1957) Synthesis of cell constintuents from C_2-units by a modified tricarboxylic acid cycle. Nature 179:988–991. https://doi.org/10.1038/179988a0

Korotkova N, Lidstrom ME (2001) Connection between Poly-β-Hydroxybutyrate Biosynthesis and Growth on C_1 and C_2 Compounds in the *Methylotroph extorquens* AM1. J Bacteriol 183:1038–1046. https://doi.org/10.1128/JB.183.3.1038

Krull S, Hevekerl A, Kuenz A, Prüße U (2017) Process development of itaconic acid production by a natural wild type strain of *Aspergillus terreus* to reach industrially relevant final titers. Appl Microbiol Biotechnol 101:4063–4072. https://doi.org/10.1007/s00253-017-8192-x

Kumar M, Rathour R, Singh R, Sun Y, Pandey A, Gnansounou E, Andrew Lin K-Y, Tsang DCW, Thakur IS (2020) Bacterial polyhydroxyalkanoates: Opportunities, challenges, and prospects. J Clean Prod 263:121500. https://doi.org/10.1016/j.jclepro.2020.121500

Kuzuyama T, Seto H (2012) Two distinct pathways for essential metabolic precursors for isoprenoid biosynthesis. Proc Japan Acad Ser B 88:41–52. https://doi.org/10.2183/pjab.88.41

Lampe DJ, Akerley BJ, Rubin EJ, Mekalanos JJ, Robertson HM (1999) Hyperactive transposase mutants of the Himar1 mariner transposon. Proc Natl Acad Sci USA 96:11428–33. https://doi.org/10.1073/pnas.96.20.11428

Large P, Peel D, Quayle J (1961) Microbial growth on C_1 compounds. 2. Synthesis of cell constituents by methanol- and formate-grown *Pseudomonas* AM 1, and methanol-grown *Hyphomicrobium vulgare*. Biochem J 81:470–480. https://doi.org/10.1042/bj0810470

Large P, Peel D, Quayle J (1962) Microbial growth on C_1 compounds. 3. Distribution

of radioactivity in metabolites of methanol-grown *Pseudomonas* AM1 after incubation with [^{14}C]methanol and [^{14}C]bicarbonate. Biochem J 82:483–488. https://doi.org/10.1042/bj0820483

Leducq J-B, Sneddon D, Santos M, Condrain-Morel D, Bourret G, Martinez-Gomez NC, Lee JA, Foster JA, Stolyar S, Shapiro BJ, Kembel SW, Sullivan JM, Marx CJ (2022) Comprehensive Phylogenomics of *Methylobacterium* Reveals Four Evolutionary Distinct Groups and Underappreciated Phyllosphere Diversity. Genome Biol Evol 14:1–20. https://doi.org/10.1093/gbe/evac123

Lee GM, Scott-Nevros ZK, Lee S, Kim D (2022) Pan-genome Analysis Reveals Comparative Genomic Features of Central Metabolic Pathways in *Methylorubrum extorquens*. https://doi.org/10.1007/s12257-022-0154-1

Lee L-C, Chou Y-L, Chen H-H, Lee Y-L, Shaw J-F (2009) Functional role of a non-active site residue Trp^{23} on the enzyme activity of *Escherichia coli* thioesterase I/protease I/lysophospholipase L_1. Biochim Biophys Acta - Proteins Proteomics 1794:1467–1473. https://doi.org/10.1016/j.bbapap.2009.06.008

Leßmeier L, Wendisch VF (2015) Identification of two mutations increasing the methanol tolerance of *Corynebacterium glutamicum*. BMC Microbiol 15:1–11. https://doi.org/10.1186/s12866-015-0558-6

Liang WF, Cui LY, Cui JY, Yu KW, Yang S, Wang TM, Guan CG, Zhang C, Xing XH (2017) Biosensor-assisted transcriptional regulator engineering for *Methylobacterium extorquens* AM1 to improve mevalonate synthesis by increasing the acetyl-CoA supply. Metab Eng 39:159–168. https://doi.org/10.1016/j.ymben.2016.11.010

Lidstrom ME, Anthony C, Biville F, Gasser F, Goodwin P, Hanson RS, Harms N (1994) New unified nomenclature for genes involved in the oxidation of methanol in Gram-negative bacteria. FEMS Microbiol Lett 117:103–106. https://doi.org/10.1111/j.1574-6968.1994.tb06749.x

Lim CK, Villada JC, Chalifour A, Duran MF, Lu H, Lee PKH (2019) Designing and Engineering *Methylorubrum extorquens* AM1 for Itaconic Acid Production. Front Microbiol 10:1–14. https://doi.org/10.3389/fmicb.2019.01027

Litchfield JH (1983) Single-Cell Proteins. Science 219:740–746. https://doi.org/10.1126/science.219.4585.740

Makwana KM, Mahalakshmi R (2015) Implications of aromatic–aromatic interactions: From protein structures to peptide models. Protein Sci 24:1920–1933. https://doi.org/10.1002/pro.2814

Marfori M, Kobe B, Forwood JK (2011) Ligand-induced Conformational Changes within a Hexameric Acyl-CoA Thioesterase. J Biol Chem 286:35643–35649. https://doi.org/10.1074/jbc.M111.225953

Marx CJ (2008) Development of a broad-host-range *sacB*-based vector for unmarked allelic exchange. BMC Res Notes 1:1–8. https://doi.org/10.1186/1756-0500-1-1

Marx CJ, Bringel F, Chistoserdova L, Moulin L, Farhan Ul Haque M, Fleischman DE, Gruffaz C, Jourand P, Knief C, Lee M-C, Muller EEL, Nadalig T, Peyraud R, Roselli S, Russ L, Goodwin LA, Ivanova N, Kyrpides N, Lajus A, Land ML, Medigue C, Mikhailova N, Nolan M, Woyke T, Stolyar S, Vorholt JA, Vuilleumier S (2012) Complete Genome Sequences of Six Strains of the Genus *Methylobacterium*. J Bacteriol 194:4746–4748. https://doi.org/10.1128/JB.01009-12

Marx CJ, Chistoserdova L, Lidstrom ME (2003a) Formaldehyde-Detoxifying Role of the Tetrahydromethanopterin-Linked Pathway in *Methylobacterium extorquens* AM1. J Bacteriol 185:7160–7168. https://doi.org/10.1128/JB.185.23.7160-7168.2003

Marx CJ, Laukel M, Vorholt JA, Lidstrom ME (2003b) Purification of the Formate-Tetrahydrofolate Ligase from *Methylobacterium extorquens* AM1 and Demonstration of Its Requirement for Methylotrophic Growth. J Bacteriol 185:7169–7175. https://doi.org/10.1128/JB.185.24.7169-7175.2003

Marx CJ, Lidstrom ME (2001) Development of improved versatile broad-host-range vectors for use in methylotrophs and other Gram-negative bacteria. Microbiology 147:2065–2075. https://doi.org/10.1099/00221287-147-8-2065

Marx CJ, Lidstrom ME (2002) Broad-Host-Range *cre-lox* System for Antibiotic Marker Recycling in Gram-Negative Bacteria. Biotechniques 33:1062–1067. https://doi.org/10.2144/02335rr01

Marx CJ, Lidstrom ME (2004) Development of an insertional expression vector system for *Methylobacterium extorquens* AM1 and generation of null mutants lacking *mtdA* and/or *fch*. Microbiology 150:9–19. https://doi.org/10.1099/mic.0.26587-0

Marx CJ, O'Brien BN, Breezee J, Lidstrom ME (2003c) Novel methylotrophy genes of

Methylobacterium extorquens AM1 identified by using transposon mutagenesis including a putative dihydromethanopterin reductase. J Bacteriol 185:669–673. https://doi.org/10.1128/JB.185.2.669-673.2003

Matsakas L, Hrůzová K, Rova U, Christakopoulos P (2018) Biological Production of 3-Hydroxypropionic Acid: An Update on the Current Status. Fermentation 4:13. https://doi.org/10.3390/fermentation4010013

McWilliam H, Li W, Uludag M, Squizzato S, Park YM, Buso N, Cowley AP, Lopez R (2013) Analysis Tool Web Services from the EMBL-EBI. Nucleic Acids Res 41:W597–W600. https://doi.org/10.1093/nar/gkt376

Meister M, Saum S, Alber BE, Fuchs G (2005) L-Malyl-Coenzyme A/β-Methylmalyl-Coenzyme A Lyase Is Involved in Acetate Assimilation of the Isocitrate Lyase-Negative Bacterium *Rhodobacter capsulatus*. J Bacteriol 187:1415–1425. https://doi.org/10.1128/JB.187.4.1415-1425.2005

Mendes de Lacerda Leite G, de Oliveira Barbosa M, Pereira Lopes MJ, de Araújo Delmondes G, Bezerra DS, Araújo IM, Carvalho de Alencar CD, Melo Coutinho HD, Peixoto LR, Barbosa-Filho JM, Bezerra Felipe CF, Barbosa R, Alencar de Menezes IR, Kerntof MR (2021) Pharmacological and toxicological activities of α-humulene and its isomers: A systematic review. Trends Food Sci Technol 115:255–274. https://doi.org/10.1016/j.tifs.2021.06.049

Metzger LC, Francez-Charlot A, Vorholt JA (2013) Single-domain response regulator involved in the general stress response of *Methylobacterium extorquens*. Microbiology 159:1067–1076. https://doi.org/10.1099/mic.0.066068-0

Mokhtari-Hosseini ZB, Vasheghani-Farahani E, Shojaosadati SA, Karimzadeh R, Heidarzadeh-Vazifekhoran A (2009) Effect of feed composition on PHB production from methanol by HCDC of *Methylobacterium extorquens* (DSMZ 1340). J Chem Technol Biotechnol 84:1136–1139. https://doi.org/10.1002/jctb.2145

Motoyama H, Anazawa H, Katsumata R, Araki K, Teshiba S (1993) Amino Acid Production from Methanol by *Methylobacillus glycogenes* Mutants: Isolation of L-Glutamic Acid Hyper-producing Mutants from *M. glycogenes* Strains, and Derivation of L-Threonine and L-Lysine-producing Mutants from Them. Biosci Biotechnol Biochem 57:82–87. https://doi.org/10.1271/bbb.57.82

Motoyama H, Yano H, Ishino S, Anazawa H, Teshiba S (1994) Effects of the

amplification of the genes coding for the L-threonine biosynthetic enzymes on the L-threonine production from methanol by a gram-negative obligate methylotroph, *Methylobacillus glycogenes*. Appl Microbiol Biotechnol 42:67–72. https://doi.org/10.1007/BF00170226

Nærdal I, Pfeifenschneider J, Brautaset T, Wendisch VF (2019) Methanol-based cadaverine production by genetically engineered *Bacillus methanolicus* strains (Corrigendum). Microb Biotechnol 12:182–183. https://doi.org/10.1111/1751-7915.13352

Nærdal I, Pfeifenschneider J, Brautaset T, Wendisch VF (2015) Methanol-based cadaverine production by genetically engineered *Bacillus methanolicus* strains. Microb Biotechnol 8:342–350. https://doi.org/10.1111/1751-7915.12257

Nayak DD, Marx CJ (2014) Genetic and Phenotypic Comparison of Facultative Methylotrophy between *Methylobacterium extorquens* Strains PA1 and AM1. PLOS ONE 9:e107887. https://doi.org/10.1371/journal.pone.0107887

Nguyen LA, He H, Pham-Huy C (2006) Chiral drugs: an overview. Int J Biomed Sci 2:85–100. https://doi.org/10.1111/deci.12302

Novick RP (1987) Plasmid Incompatibility. Microbiol Rev 51:381–395. https://doi.org/10.1128/mr.51.4.381-395.1987

Ochsner AM, Sonntag F, Buchhaupt M, Schrader J, Vorholt JA (2015) *Methylobacterium extorquens*: methylotrophy and biotechnological applications. Appl Microbiol Biotechnol 99:517–534. https://doi.org/10.1007/s00253-014-6240-3

Offermanns H (2014) Methanol: The Basic Chemical and Energy Feedstock of the Future. In: Bertau M, Offermanns H, Plass L, Schmidt F, Wernicke H-J (eds) Methanol: The Basic Chemical and Energy Feedstock of the Future: Asinger's Vision Today, 1st edn. Springer-Verlag Berlin, Heidelberg, Germany, pp 10–13

Oh D, Kim J, Yoshida T (1997) Production of a high viscosity polysaccharide, methylan, in a novel bioreactor. Biotechnol Bioeng 54:115–121. https://doi.org/10.1002/(SICI)1097-0290(19970420)54:2<115::AID-BIT3>3.0.CO;2-O

Olah GA (2005) Beyond Oil and Gas: The Methanol Economy. Angew Chemie Int Ed 44:2636–2639. https://doi.org/10.1002/anie.200462121

Olah GA, Goeppert A, Surya Prakash GK (2018) Beyond Oil and Gas:The Methanol Economy: Third edition. Wiley-VCH, Weinheim, Germany

Orita I, Nishikawa K, Nakamura S, Fukui T (2014) Biosynthesis of polyhydroxyalkanoate copolymers from methanol by *Methylobacterium extorquens* AM1 and the engineered strains under cobalt-deficient conditions. Appl Microbiol Biotechnol 98:3715–3725. https://doi.org/10.1007/s00253-013-5490-9

Panda SK, Sahu L, Behera SK, Ray RC (2019) Research and Production of Organic Acids and Industrial Potential. In: Molina G, Gupta VK, Singh BN, Gathergood N (eds) Bioprocessing for Biomolecules Production. John Wiley & Sons, Ltd, Chichester, UK, pp 195–209

Peel D, Quayle JR (1961) Microbial growth on C_1 compounds. 1. Isolation and characterization of *Pseudomonas* AM 1. Biochem J 81:465–469. https://doi.org/10.1042/bj0810465

Peyraud R, Kiefer P, Christen P, Massou S, Portais J-C, Vorholt JA (2009) Demonstration of the ethylmalonyl-CoA pathway by using ^{13}C metabolomics. Proc Natl Acad Sci USA 106:4846–51. https://doi.org/10.1073/pnas.0810932106

Peyraud R, Schneider K, Kiefer P, Massou S, Vorholt JA, Portais JC (2011) Genome-scale reconstruction and system level investigation of the metabolic network of *Methylobacterium extorquens* AM1. BMC Syst Biol 5:189. https://doi.org/10.1186/1752-0509-5-189

Pleissner D, Dietz D, van Duuren JBJH, Wittmann C, Yang X, Lin CSK, Venus J (2017) Biotechnological Production of Organic Acids from Renewable Resources. In: Wagemann K, Tippkötter N (eds) Biorefineries. Advances in Biochemical Engineering/Biotechnology. Springer, Cham, Germany, pp 373–410

Quynh Le HT, Anh Mai DH, Na J-G, Lee EY (2022) Development of *Methylorubrum extorquens* AM1 as a promising platform strain for enhanced violacein production from co-utilization of methanol and acetate. Metab Eng 72:150–160. https://doi.org/10.1016/j.ymben.2022.03.008

Raza ZA, Abid S, Banat IM (2018) Polyhydroxyalkanoates: Characteristics, production, recent developments and applications. Int Biodeterior Biodegradation 126:45–56. https://doi.org/10.1016/j.ibiod.2017.10.001

Rétey J, Smith EH, Zagalak B (1978) Investigation of the Mechanism of the Methylmalonyl-CoA Mutase Reaction with the Substrate Analogue: Ethylmalonyl-CoA. Eur J Biochem 83:437–451. https://doi.org/10.1111/j.1432-1033.1978.tb12110.x

Rohde M-T, Paufler S, Harms H, Maskow T (2016) Calorespirometric feeding control enhances bioproduction from toxic feedstocks-Demonstration for biopolymer production out of methanol. Biotechnol Bioeng 113:2113–2121. https://doi.org/10.1002/bit.25986

Rohde M-T, Tischer S, Harms H, Rohwerder T (2017) Production of 2-Hydroxyisobutyric Acid from Methanol by *Methylobacterium extorquens* AM1 Expressing (*R*)-3-Hydroxybutyryl Coenzyme A-Isomerizing Enzymes. Appl Environ Microbiol 83:1–16. https://doi.org/10.1128/AEM.02622-16

Rohwerder T, Müller RH (2010) Biosynthesis of 2-hydroxyisobutyric acid (2-HIBA) from renewable carbon. Microb Cell Factories 9:13. https://doi.org/10.1186/1475-2859-9-13

San Millan A, Craig MacLean R (2017) Fitness Costs of Plasmids: A Limit to Plasmid Transmission. Microb Spectr 5:1–12. https://doi.org/doi:10.1128/microbiolspec.MTBP-0016-2017

San Millan A, Heilbron K, MacLean RC (2014) Positive epistasis between co-infecting plasmids promotes plasmid survival in bacterial populations. ISME J 8:601–612. https://doi.org/10.1038/ismej.2013.182

Sanz-Pérez ES, Murdock CR, Didas SA, Jones CW (2016) Direct Capture of CO_2 from Ambient Air. Chem Rev 116:11840–11876. https://doi.org/10.1021/acs.chemrev.6b00173

Sathesh-Prabu C, Ryu YS, Lee SK (2021) Levulinic Acid-Inducible and Tunable Gene Expression System for *Methylorubrum extorquens*. Front Bioeng Biotechnol 9:1–10. https://doi.org/10.3389/fbioe.2021.797020

Schada von Borzyskowski L, Remus-Emsermann M, Weishaupt R, Vorholt JA, Erb TJ (2015) A Set of Versatile Brick Vectors and Promoters for the Assembly, Expression, and Integration of Synthetic Operons in *Methylobacterium extorquens* AM1 and Other Alphaproteobacteria. ACS Synth Biol 4:430–443. https://doi.org/10.1021/sb500221v

Schada von Borzyskowski L, Sonntag F, Pöschel L, Vorholt JA, Schrader J, Erb TJ, Buchhaupt M (2018) Replacing the Ethylmalonyl-CoA Pathway with the Glyoxylate Shunt Provides Metabolic Flexibility in the Central Carbon Metabolism of *Methylobacterium extorquens* AM1. ACS Synth Biol 7:86–97. https://doi.org/10.1021/acssynbio.7b00229

Schmid J, Mauch K, Terfloth L, Insilico Biotechnology AG (2021) Maßgeschneiderte Inhaltsstoffe - Verbundvorhaben: Biotechnologische Synthese chiraler Substanzen aus dem Biomasse-Konversionsprodukt Methanol (Chiramet), Teilprojekt D : Schlussbericht zu Nr. 8.2 NKBF 98 : Berichtszeitraum: 01.07.2017-30.06.2020. Stuttgart, Germany. https://doi.org/10.2314/KXP:1805183796

Schneider K, Peyraud R, Kiefer P, Christen P, Delmotte N, Massou S, Portais JC, Vorholt JA (2012) The ethylmalonyl-CoA pathway is used in place of the glyoxylate cycle by *Methylobacterium extorquens* AM1 during growth on acetate. J Biol Chem 287:757–766. https://doi.org/10.1074/jbc.M111.305219

Schrader J, Schilling M, Holtmann D, Sell D, Filho MV, Marx A, Vorholt JA (2009) Methanol-based industrial biotechnology: current status and future perspectives of methylotrophic bacteria. Trends Biotechnol 27:107–115. https://doi.org/10.1016/j.tibtech.2008.10.009

Shi X, Xiao H, Azarabadi H, Song J, Wu X, Chen X, Lackner KS (2020) Sorbents for the Direct Capture of CO_2 from Ambient Air. Angew Chemie Int Ed 59:6984–7006. https://doi.org/10.1002/anie.201906756

Sirirote P, Yamane T, Shimizu S (1986) Production of L-serine from methanol and glycine by resting cells of a methylotroph under automatically controlled conditions. J Ferment Technol 64:389–396. https://doi.org/10.1016/0385-6380(86)90025-7

Skovran E, Raghuraman C, Martinez-Gomez NC (2019) Lanthanides in Methylotrophy. Curr Issues Mol Biol 33:101–116. https://doi.org/10.21775/cimb.033.101

Song F, Thoden JB, Zhuang Z, Latham J, Trujillo M, Holden HM, Dunaway-Mariano D (2012) The Catalytic Mechanism of the Hotdog-fold Enzyme Superfamily 4-Hydroxybenzoyl-CoA Thioesterase from *Arthrobacter* sp. Strain SU. Biochemistry 51:7000–7016. https://doi.org/10.1021/bi301059m

Sonntag F, Buchhaupt M, Schrader J (2014) Thioesterases for ethylmalonyl–CoA

pathway derived dicarboxylic acid production in *Methylobacterium extorquens* AM1. Appl Microbiol Biotechnol 98:4533–4544. https://doi.org/10.1007/s00253-013-5456-y

Sonntag F, Kroner C, Lubuta P, Peyraud R, Horst A, Buchhaupt M, Schrader J (2015a) Engineering *Methylobacterium extorquens* for de novo synthesis of the sesquiterpenoid α-humulene from methanol. Metab Eng 32:82–94. https://doi.org/10.1016/j.ymben.2015.09.004

Sonntag F, Müller JEN, Kiefer P, Vorholt JA, Schrader J, Buchhaupt M (2015b) High-level production of ethylmalonyl-CoA pathway-derived dicarboxylic acids by *Methylobacterium extorquens* under cobalt-deficient conditions and by polyhydroxybutyrate negative strains. Appl Microbiol Biotechnol 99:3407–3419. https://doi.org/10.1007/s00253-015-6418-3

Sonthalia A, Kumar N, Tomar M, Geo VE, Thiyagarajan S, Pugazhendhi A (2021) Moving ahead from hydrogen to methanol economy: scope and challenges. Clean Technol Environ Policy 25:551–575. https://doi.org/10.1007/s10098-021-02193-x

Suzuki T, Yamane T, Shimizu S (1986) Mass production of poly-*β*-hydroxybutyric acid by fully automatic fed-batch culture of methylotroph. Appl Microbiol Biotechnol 23:322–329. https://doi.org/10.1007/BF00257027

Swarbrick CMD, Nanson JD, Patterson EI, Forwood JK (2020) Structure, function, and regulation of thioesterases. Prog Lipid Res 79:101036. https://doi.org/10.1016/j.plipres.2020.101036

Swarbrick CMD, Roman N, Cowieson N, Patterson EI, Nanson J, Siponen MI, Berglund H, Lehtiö L, Forwood JK (2014) Structural Basis for Regulation of the Human Acetyl-CoA Thioesterase 12 and Interactions with the Steroidogenic Acute Regulatory Protein-related Lipid Transfer (START) Domain. J Biol Chem 289:24263–24274. https://doi.org/10.1074/jbc.M114.589408

Taylor WR (1986) The classification of amino acid conservation. J Theor Biol 119:205–218. https://doi.org/10.1016/S0022-5193(86)80075-3

Teleky B-E, Vodnar DC (2021) Recent Advances in Biotechnological Itaconic Acid Production, and Application for a Sustainable Approach. Polymers 13:3574. https://doi.org/10.3390/polym13203574

Urakami T, Komagata K (1984) *Protomonas*, a New Genus of Facultatively

Methylotrophic Bacteria. Int J Syst Bacteriol 34:188–201. https://doi.org/10.1099/00207713-34-2-188

Valenzuela MS, Ikpeazu E V, Siddiqui KAI (1996) *E. coli* Growth Inhibition by a High Copy Number Derivative of Plasmid pBR322. Biochem Biophys Res Commun 219:876–883. https://doi.org/10.1006/bbrc.1996.0339

Van Dien SJ, Okubo Y, Hough MT, Korotkova N, Taitano T, Lidstrom ME (2003) Reconstruction of C_3 and C_4 metabolism in *Methylobacterium extorquens* AM1 using transposon mutagenesis. Microbiology 149:601–609. https://doi.org/10.1099/mic.0.25955-0

Vuilleumier S, Chistoserdova L, Lee M-C, Bringel F, Lajus A, Zhou Y, Gourion B, Barbe V, Chang J, Cruveiller S, Dossat C, Gillett W, Gruffaz C, Haugen E, Hourcade E, Levy R, Mangenot S, Muller E, Nadalig T, Pagni M, Penny C, Peyraud R, Robinson DG, Roche D, Rouy Z, Saenampechek C, Salvignol G, Vallenet D, Wu Z, Marx CJ, Vorholt JA, Olson M V, Kaul R, Weissenbach J, Médigue C, Lidstrom ME (2009) *Methylobacterium* Genome Sequences: A Reference Blueprint to Investigate Microbial Metabolism of C1 Compounds from Natural and Industrial Sources. PLOS ONE 4:e5584. https://doi.org/10.1371/journal.pone.0005584

Wagner LW, Matheson NH, Heisey RF, Schneider K (1997) Use of a silicone tubing sensor to control methanol concentration during fed batch fermentation of *Pichia pastoris*. Biotechnol Tech 11:791–795. https://doi.org/10.1023/A:1018469007145

Wang C, Li Y, Xu C, Badawy T, Sahu A, Jiang C (2019) Methanol as an octane booster for gasoline fuels. Fuel 248:76–84. https://doi.org/10.1016/j.fuel.2019.02.128

Wang Y, Zhao L, Otto A, Robinius M, Stolten D (2017) A Review of Post-combustion CO_2 Capture Technologies from Coal-fired Power Plants. Energy Procedia 114:650–665. https://doi.org/10.1016/j.egypro.2017.03.1209

Westlake R (1986) Large-scale Continuous Production of Single Cell Protein. Chemie Ing Tech 58:934–937. https://doi.org/10.1002/cite.330581203

Whitaker WB, Sandoval NR, Bennett RK, Fast AG, Papoutsakis ET (2015) Synthetic methylotrophy: engineering the production of biofuels and chemicals based on the biology of aerobic methanol utilization. Curr Opin Biotechnol 33:165–175. https://doi.org/10.1016/j.copbio.2015.01.007

Willis MA, Zhuang Z, Song F, Howard A, Dunaway-Mariano D, Herzberg O (2008)

Structure of YciA from *Haemophilus influenzae* (HI0827), a Hexameric Broad Specificity Acyl-Coenzyme A Thioesterase. Biochemistry 47:2797–2805. https://doi.org/10.1021/bi702336d

Windass JD, Worsey MJ, Pioli EM, Pioli D, Barth PT, Atherton KT, Dart EC, Byrom D, Powell K, Senior PJ (1980) Improved conversion of methanol to single-cell protein by *Methylophilus methylotrophus*. Nature 287:396–401. https://doi.org/10.1038/287396a0

Yang J, Zhang C-T, Yuan X-J, Zhang M, Mo X-H, Tan L-L, Zhu L-P, Chen W-J, Yao M-D, Hu B, Yang S (2018) Metabolic engineering of *Methylobacterium extorquens* AM1 for the production of butadiene precursor. Microb Cell Factories 17:194. https://doi.org/10.1186/s12934-018-1042-4

Yang Y-M, Chen W-J, Yang J, Zhou Y-M, Hu B, Zhang M, Zhu L-P, Wang G-Y, Yang S (2017) Production of 3-hydroxypropionic acid in engineered *Methylobacterium extorquens* AM1 and its reassimilation through a reductive route. Microb Cell Factories 16:179. https://doi.org/10.1186/s12934-017-0798-2

Yezza A, Fournier D, Halasz A, Hawari J (2006) Production of polyhydroxyalkanoates from methanol by a new methylotrophic bacterium *Methylobacterium* sp. GW2. Appl Microbiol Biotechnol 73:211–218. https://doi.org/10.1007/s00253-006-0458-7

Yuan X-J, Chen W-J, Ma Z-X, Yuan Q-Q, Zhang M, He L, Mo X-H, Zhang C, Zhang C-T, Wang M-Y, Xing X-H, Yang S (2021) Rewiring the native methanol assimilation metabolism by incorporating the heterologous ribulose monophosphate cycle into *Methylorubrum extorquens*. Metab Eng 64:95–110. https://doi.org/10.1016/j.ymben.2021.01.009

Zhu W-L, Cui J-Y, Cui L-Y, Liang W-F, Yang S, Zhang C, Xing X-H (2016) Bioconversion of methanol to value-added mevalonate by engineered *Methylobacterium extorquens* AM1 containing an optimized mevalonate pathway. Appl Microbiol Biotechnol 100:2171–2182. https://doi.org/10.1007/s00253-015-7078-z

Zhuang Z, Song F, Zhao H, Li L, Cao J, Eisenstein E, Herzberg O, Dunaway-Mariano D (2008) Divergence of Function in the Hot Dog Fold Enzyme Superfamily: The Bacterial Thioesterase YciA. Biochemistry 47:2789–2796.

https://doi.org/10.1021/bi702334h

Zinoviev S, Müller-Langer F, Das P, Bertero N, Fornasiero P, Kaltschmitt M, Centi G, Miertus S (2010) Next-Generation Biofuels: Survey of Emerging Technologies and Sustainability Issues. ChemSusChem 3:1106–1133. https://doi.org/10.1002/cssc.201000052

Zuhse R, Kohlmann J, Chiracon GmbH (2021) “Maßgeschneiderte Inhaltsstoffe - Verbundvorhaben: Biotechnologische Synthese chiraler Substanzen aus dem Biomasse-Konversionsprodukt Methanol (Chiramet), Teilprojekt B” : Kurzbericht zur Veröffentlichung der Ergebnisse von Forschungsvorhaben im BMBF-Prog. ramm : Projektlaufzeit: 01.07.2017 bis 31.01.2021. Luckenwalde, Germany. https://doi.org/10.2314/KXP:1837312621

5. Additional results - Development of fermentation strategies for EMCP-derived dicarboxylic acid production with *M. extorquens* AM1

This chapter consists of additional results that are not currently published or submitted in manuscript form to a scientific journal. The chapter is formatted independently with its own numbering, results and discussion section, references and appendices.

Introduction

A variety of fed batch fermentation strategies were developed for engineered *M. extorquens* strains for the production of PHB, terpenes, amino acids, dicarboxylic acids or heterologous proteins (Suzuki et al. 1986; Sirirote et al. 1986; Bourque et al. 1995; Bélanger et al. 2004; Mokhtari-Hosseini et al. 2009; Sonntag et al. 2015a; Lim et al. 2019; Arenas et al. 2023). In these fermentation setups, the methanol feeding strategy per se, as well as the setpoint methanol concentration varied widely (between 0.01 g/L and 10 g/L). A methanol concentration above 1 % [v/v] in the culture medium results in reduced growth of *M. extorquens* AM1 and a concentration above 5 % [v/v] results in growth inhibition (Peel and Quayle 1961). However, limitations at the lower concentration limit must also be considered. A reuptake of dicarboxylic acid products has been described previously (Sonntag et al. 2014; Pöschel et al. 2022). Considering the possibility of re-metabolization, a very low methanol concentration in the cultivation medium could be unfavorable as it may lead to increased product uptake. These aspects must be taken into account when developing a new methanol feeding strategy for dicarboxylic acid production.

In the majority of the published fed batch processes for *M. extorquens*, the fermentation strategies are designed for high cell densities or two-stage fermentations in which growth and production phases are separated. This strategy is not feasible for the current methodology of dicarboxylic acid production, where the products are directly drawn from the anaplerotic EMCP (Sonntag et al. 2014). Furthermore, in many published studies, the methanol feed is either controlled using the OTR, which is calculated from the off-gas analysis (Suzuki et al. 1986; Sirirote et al. 1986; Bourque et al. 1995; Béland et al. 2004; Bélanger et al. 2004) or relies on an online measurement via a methanol sensor (Sonntag et al. 2015a; Arenas et al. 2023). These setups require additional highly sensitive analytical modules and calibration steps and are not necessarily feasible for all processes. In this chapter, a methanol feeding

strategy is described, which relies solely on dissolved oxygen (DO) measurement and is tailored to dicarboxylic acid production.

It was previously shown, that a reduction of the default cobalt concentration in the growth medium to 0.2 µM strongly improves the production of dicarboxylic acids by decreasing the activity of cobalt-dependend mutases, resulting in an accumulation of EMCP thioester intermediates (Kiefer et al. 2009; Sonntag et al. 2015b). The optimal amount of other trace elements for dicarboxylic acid production with *M. extorquens* has not yet been determined. Therefore, in the new fermentation setup, different feeding strategies for trace element solution were tested.

In addition to the previously reported EMCP-derived dicarboxylic acid products mesaconic acid, 2-methylsuccinic acid and citramalic acid (Sonntag et al. 2014; Sonntag et al. 2015b; Pöschel et al. 2022), the production of the new, presumably enantiomerically pure product 2-hydroxy-3-methylsuccinic acid (assumed (2*S*,3*R*)-form) is described in this chapter. Titers ranging from 3.8 g/L to 5.8 g/L were obtained for each of the compounds with the developed setup and represent the highest titers achieved for microbial production of these compounds.

Material and methods

Bacterial strains

Bacterial strains and plasmids used in this study are listed in Table 1.

Table 1 Bacterial strains and plasmids used in this work. Ribosomal binding site (RBS) sequences were optimized with RBS Calculator 2.1 (Salis 2011).

Name	Description/Genotype	Reference
Bacterial strains		
M. extorquens AM1 Δ*cel* (CM2720)	Cm^R, Gram-negative, facultative methylotrophic, obligate aerobic, α-proteobacterium with chromosomal deletion of cellulose biosynthesis genes	Delaney et al. (2013)
M. extorquens AM1 Δ*cel* Δ*dctA1* Δ*dctA2* Δ*dctA3*	*M. extorquens* AM1 Δ*cel* with chromosomal deletion of MEXAM1_RS15430, MEXAM1_RS10985 and MEXAM1_RS20450	(Pöschel et al. 2022)
Plasmids		
pCM160	Kan^R, pmxaF, oriT, pBR322ori	Marx and Lidstrom (2001)
pCM160_RBS_*yciA*HI	pCM160 containing for *M. extorquens* codon-optimized thioesterase gene *yciA* from *H. influenzae* with optimized RBS	Pöschel et al. (2022)
pCM160_RBS_*yciAEc*	pCM160 containing for *M. extorquens* codon-optimized thioesterase gene *yciA* from *E. coli* with optimized RBS	Sonntag et al. (2014)
pCM160_*yciAEc_mesaPx*	pCM160 containing for *M. extorquens* codon-optimized thioesterase gene *yciA* from *E. coli* and fumarate hydratase gene *bxe_A3136* from *Paraburkholderia xenovorans* with optimized RBS	Pöschel et al. (2022)
pCM160_RBS_*citECg*	pCM160 containing for *M. extorquens* codon-optimized *citE* thioesterase gene from *Corynebacterium glutamicum* (GenBank entry CAF19568) with optimized RBS	This work

Chemicals

All chemicals were purchased from Carl Roth (Karlsruhe, Germany), VWR International (Darmstadt, Germany) or Merck (Darmstadt, Germany). The water used was purified with an ELGA Purelab Ultra system (ELGA LabWater, Celle, Germany).

Plasmid construction and transformation

The plasmid pCM160_RBS_*citECg* was constructed by inserting a synthetic DNA fragment (Table 2) containing the codon-optimized *citE* gene from *Corynebacterium glutamicum* (GenBank entry CAF19568) into pCM160. The insert was synthesized by BioCat (Heidelberg, Germany). Transformations of *M. extorquens* AM1 strains were done by electroporation as described before (Toyama et al. 1998).

Table 2 Synthetic sequence used for plasmid construction. The restriction sites *Sph*I and *Nco*I used for subcloning into pCM160 are indicated by underlined letters. The RBS sequence was generated with RBS Calculator 2.1 (Salis 2011) and is given in italics.

Name of target construct	Sequence
pCM160_RBS_*citECg*	GCATGC*TACGTTAAACCCCGACAGGGGGGAAAGGAGGTTTTTTTT* ATGTCGGAGCTCATCTGCGGCCCGGCCATCCTCTTCGCCCCGGC CGGCCGCGCCGAGATCATCCCGAAGGCCGCCTCGAAGGCCGACA TGGTCATCATCGACCTCGAGGACGGCGCCGGCGAGGTCGACCGC GAGGTCGCCTACCGCAACATCCGCGAGTCGGGCCTCGACCCGAA GCGCACCATCGTCCGCACCGTCGGCCCGTCGGACCCGCACTTCC TCGCCGACGTCGAGATGGTCAAGTCGACCGACTTCACCCTCGTCA TGGTCCCGAAGCTCCTCGGCTCGGTCCCGGAGGAGCTCGACGGC CTCAACATCATCGCCATGATCGAGACCCCGCAGGCCGCCACCTCG ATCCCGCAGATCGCCGCCGACCCGAAGGTCGTCGGCATGTTCTG GGGCGCCGAGGACCTCACCCACCTCCTCGGCGGCACCCACTCGC GCTTCCTCGGCGACGAGTCGAACGAGGGCTCGTACCGCGACACC ATGCGCCTCACCCGCGCCCTCATGCACCTCCACGCCGCCGCCAA CGGCAAGTTCACCATCGACGCCATCCACGCCGACTTCCACGACGA GGAGGGCCTCTACCTCGAGGCCGTCGACGCCGCCCGCACCGGCT TCGCCGGCACCGCCTGCATCCACCCGAAGCAGATCGAGATCGTC CGCCGCGCCTACCGCCCGGAGGCCAACCAGCTCGAGTGGGCCAA GAAGGTCGTCGAGGAGGCCGAGAACCACCCGGGCGCCTTCAAGC TCGACGGCCAGATGATCGACGCCCCGCTCATCTCGCAGGCCCGC ATGGTCATCTCGCGCCAGCCGGCCTGACCATGG

Seed trains and growth medium for bioreactor cultivations

For each bioreactor cultivation, a distinct seed train starting from an individual transformant colony was used. A primary preculture of 5 mL was grown in a test tube in methanol minimal medium (Peyraud et al. 2009) containing 12.6 µM of $CoCl_2$ and 50 µg/mL kanamycin sulfate at 30 °C in a rotary shaker. Subsequently, the second preculture of 700 mL (same cultivation medium) was inoculated to OD_{600} = 0.1 and grown for 48 h at 30 °C in 3 L shake flasks. Cultures were harvested in the exponential growth phase (about 48 hours after inoculation) and the cells were washed twice in a Sorvall LYNX 4000 centrifuge (Thermo Scientific, Waltham, USA) with fresh and prewarmed methanol medium containing 0.2 µM of $CoCl_2$. Bioreactors with 700 mL of

fresh methanol minimal medium containing 0.2 µM of $CoCl_2$, 50 µg/mL kanamycin sulfate and 0.058 % [v/v] of XIAMETER™ ACP-1500 Antifoam Compound (DOW, Midland, USA) were inoculated with resuspended cells to an OD_{600} of 2.8 - 3.2. For cultivations in the BiostatB® system (Sartorius, Göttingen, Germany) with a starting volume of 4 L, 6 seed trains from a single transformant colony were grown in parallel, pooled and used to inoculate the bioreactor. In this second setup, instead of the previously described antifoaming agent, 0.005 % [v/v] Antifoam B (Merck, Darmstadt, Germany) was added to the bioreactor before starting the cultivation.

Bioprocessing setups and process control strategies

Two types of bioreactors were used in this study. For initial tests, a BiostatB® system (Sartorius, Göttingen, Germany) was used. A 5 L UniVessel® (Sartorius, Göttingen, Germany) was equipped with an EasyFerm sensor for pH measurement and a VisiFermDO 325 sensor for optical DO measurement (both from Hamilton, Bonaduz, Switzerland). The bioreactor vessels and probes were sterilized in an autoclave for 60 min at 120 °C. An ammonia solution of 15 % [v/v] was used to maintain the pH value at 7 (± 0.1). The temperature was kept at 30 °C during cultivation. For agitation, a stirrer with three superimposed Rushton impellers was installed. Excessive foam formation was detected with probe BB-8844463 from Sartorius (Göttingen, Germany) and inhibited by addition of Antifoam B (Merck, Darmstadt, Germany). The DO level was regulated near the set point of 30 % saturation. Therefore, two successive PID controllers were used in a cascade by first increasing the stirrer speed from 500 to 1500 rpm and second increasing the air flow rate from 1 sL/min to 7 sL/min. For both controllers, the XP-overlap was set to 90 % and TI to 100 s. The methanol concentration in the culture broth was tracked online using the ProcessTRACE 1.21 MT system equipped with an alcohol oxidase enzyme reactor (TRACE Analytics, Braunschweig, Germany). Methanol concentration in the reactor was measured every 30 minutes amperometrically with a dialysis probe. If the concentration dropped below 1 g/L, 2.3 mL of methanol was added into the reactor via a coupled Du505 pump (Watson-Marlow GmbH, Rommerskirchen, Germany). The feeding strategy for additional trace element solution during the course of cultivation was chosen individually for each experiment.

For parallel cultivation in a 700 mL scale, a DASGIP® parallel bioreactor system with 1 L glass vessels (Eppendorf, Hamburg, Germany) was used. The bioreactor vessels

and probes were sterilized in an autoclave at 120 °C for 45 min. DO level was regulated near the set point of 30 % saturation. For regulation, the following cascade was used. First, the stirrer speed was increased, then the oxygen content of the gassing mixture was raised and finally the gas flow rate was increased (equations 1-3). In all experiments shown in this chapter, increasing the stirrer speed was sufficient to maintain the target DO value.

$$f_N(x)\begin{cases} 20x + 400 & for\ 0 \leq x < 40 \\ 1200 & for\ 40 \leq x \leq 100 \end{cases} \quad \textbf{Eq. 1}$$

where x is the DO-value in percentage points and $f_N(x)$ is the stirrer speed in rpm.

$$f_{\%O_2}(x)\begin{cases} 1{,}4364x - 14{,}909 & for\ 25 \leq x < 80 \\ 100 & for\ 80 \leq x \leq 100 \end{cases} \quad \textbf{Eq. 2}$$

where x is the DO-value in percentage points and $f_{\%O_2}(x)$ is the oxygen content in %.

$$f_F(x)\begin{cases} 6 & for\ 0 \leq x < 80 \\ 0{,}95x\ -\ 70 & for\ 80 \leq x \leq 100 \end{cases} \quad \textbf{Eq. 3}$$

where x is the DO-value in percentage points and $f_F(x)$ is the gas flow rate in sL/h.

Each vessel was individually equipped with an amperometric InPro6800 sensor for DO measurement and an InPro3100 sensor for pH measurement (both Mettler-Toledo GmbH, Gießen, Germany). The feeding of methanol was controlled by a reactor script (Appendix 1), in which a low and a high DO value are defined as trigger values. After a deadband of 10 h starting from inoculation, a value exceeding the high DO-trigger value, indicating a depletion of methanol, initiated a rapid addition of 3.5 mL of methanol to the bioreactor. The upper trigger was deactivated until the lower trigger value was reached. Temperature and pH were controlled using the default settings of the bioreactor software (DASGIP Control V 4.5.230, Eppendorf, Hamburg, Germany). The temperature was kept at 30 °C (± 0.5 °C). An ammonia solution of 15 % [v/v] was used to maintain the pH value at 7 (± 0.1). Excess foaming was manually counteracted by adding 200 µL of XIAMETER™ ACP-1500 Antifoam Compound (DOW, Midland, USA) at the beginning of the process and dosing manually with 200 µL as needed during the fermentation run. The feeding strategy for trace element solution was chosen individually for each experiment. The starting trace element concentration in the cultivation medium previously described in Peyraud et al. (2009) was adapted for dicarboxylic acid production by reducing the $CoCl_2$ concentration from 1.2 µM to 0.2 µM (Sonntag et al. 2015b). For the feeding of trace element solution, a 1000-fold

concentrated stock solution containing 15 g/L $Na_2EDTA_2 \cdot H_2O$, 4.5 g/L $ZnSO_4 \cdot 7H_2O$, 1 g/L $MnCl_2 \cdot 4H_2O$, 1 g/L H_3BO_3, 0.4 g/L $Na_2MoO_4 \cdot 2H_2O$, 3 g/L $FeSO_4 \cdot 7H_2O$ and 0.3 g/L $CuSO_4 \cdot 5H_2O$ was prepared. If needed, $CoCl_2 \cdot 6H_2O$ was added to a concentration of 0.0476 g/L. The stock solution was freshly mixed in a 1:1 ratio with a 1.5 mg/L $CaCl_2 \cdot 2H_2O$ solution. The resulting 500-fold concentrated trace element feeding solution contained either 0 or 100 µM of $CoCl_2$. Culture samples were collected under sterile conditions and measured off-line to analyze dicarboxylic acid concentration and cell density. The cell dry weight (CDW) value is a product of the measured OD_{600} multiplied with 4.29 (previously determined).

Dicarboxylic acid analysis

Culture samples were centrifuged for 5 minutes at 16 000 g and the supernatants were passed through a 0.22 µm PDVF-syringe filter (Carl Roth, Karlsruhe, Germany). Analysis of the filtered supernatants was performed on a LC-MS/MS system (Nexera X2 UHPLC (Shimadzu, Duisburg, Germany) equipped with a 150 x 4.6 mm Luna Omega 3 µm PS C18 100 Å column (Phenomenex, Aschaffenburg, Germany) coupled with an LCMS-8045 system (Shimadzu, Duisburg, Germany)) as described before (Pöschel et al. 2022). Dicarboxylic acid concentration was determined by comparing the peak areas to calibration curves determined for corresponding standard solutions. Ethylmalonic acid, mesaconic acid, 2-methylsuccinic acid, methylmalonic acid and succinic acid were purchased from Merck (Darmstadt, Germany), crotonic acid was purchased from Carl Roth (Karlsruhe, Germany) and 2-hydroxy-3-methylsuccinic acid was purchased from Enamine (Riga, Latvia).

Results and discussion

Comparison of different trace element feeding strategies in a fed-batch process with methanol sensor

Initially, a previously published fermentation strategy with an online methanol sensor (Sonntag et al. 2015a) was adapted for a 4-liter fed-batch fermentation in a BiostatB® system (Sartorius, Göttingen, Germany) to test its feasibility for dicarboxylic acid production. The initial methanol concentration was set to 3.95 g/L and was later maintained at a set point of 1 g/L during fermentation with an external methanol sensor and pump. Figure 1 and Figure 2 show that this feeding strategy is indeed suitable for dicarboxylic acid production with *M. extorquens* AM1 strains overexpressing *yciAHI* (thioesterase gene from *Haemophilus influenzae*). By feeding a trace element solution containing 100 µM $CoCl_2$ after initially reaching an OD_{600} of 15 and then every 24 h, titers of up to 2.6 g/L mesaconic acid, 2.1 g/L 2-methylsuccinic acid and 0.1 g/L 2-hydroxy-3-methylsuccinic acid were achieved (Figure 1). Feeding a trace element solution without $CoCl_2$ every 12 h, increased the titer of mesaconic acid to 4.9 g/L, the titer of 2-methylsuccinic acid to 3.9 g/L and the titer of 2-hydroxy-3-methylsuccinic acid to 0.3 g/L (Figure 2). The ratios of product to CDW were 2.9-fold (± 0.3) higher with the second trace element feeding strategy (see Table 3 for P/CDW ratio values). No exponential cell growth was observed in either setup. The growth initially progressed in a linear fashion, followed by a plateau phase. As expected, the maximum CDW of the cultivation using the second strategy was substantially lower (5.8 g/L) than in the one using the first strategy (8.9 g/L), in which additional $CoCl_2$ was fed. Since the targeted dicarboxylic acid products are converted from intermediates of the EMCP, a negative correlation of maximal product titer and CDW is not surprising. By adjusting the $CoCl_2$ concentration in the bioreactor medium, the carbon flux in *yciAHI* expressing *M. extorquens* AM1 Δ*cel* cells can be impacted towards dicarboxylic acid production, as previously shown for shake flask experiments (Sonntag et al. 2015b). In neither of the fermentation setups, other potential EMPC-derived thioesterase hydrolysis products could be detected.

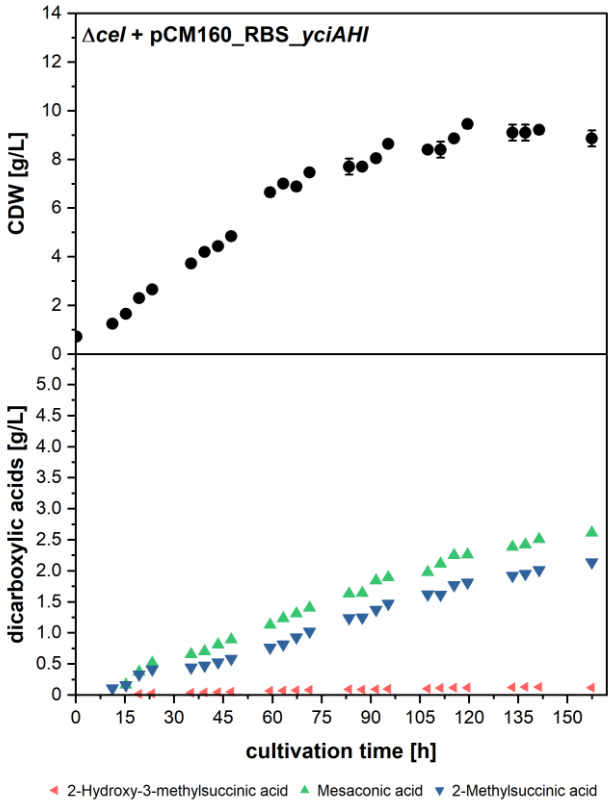

Figure 1 Growth and product formation during fermentation of *M. extorquens* AM1 Δ*cel* + pCM160_RBS_*yciAHI* in a BiostatB® bioreactor system (Sartorius, Göttingen, Germany) with 4-liter starting volume. Methanol concentration at the start was 3.95 g/L and was controlled close to a setpoint of 1 g/L via an online methanol sensor. 8 mL of trace element feeding solution containing 100 µM $CoCl_2$ was added after the OD_{600} reached a value of 15 (39.3 h after inoculation) and then every 24 h. The temperature was kept at 30 °C ± 0.01 °C and pH was kept at 7 ± 0.1. The DO setpoint was 30 %. Online parameters are shown in Appendix 2.

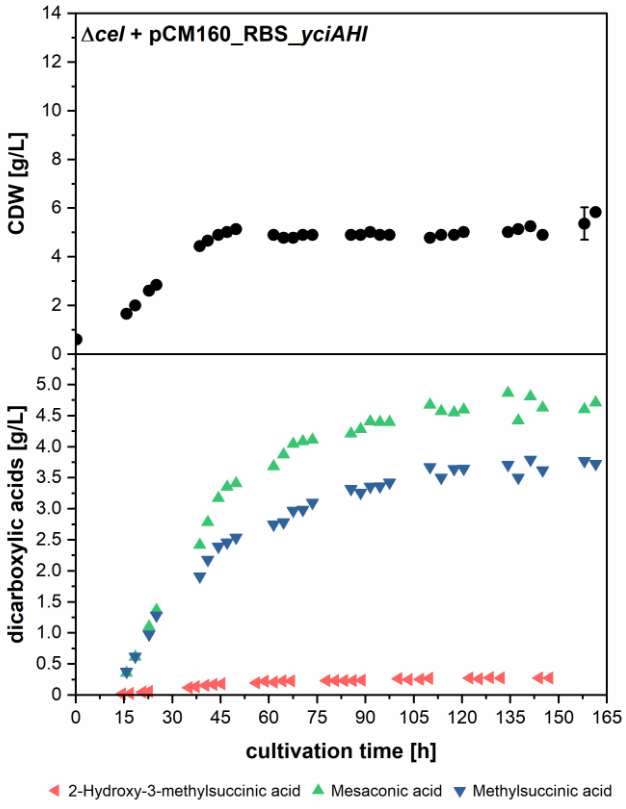

Figure 2 Growth and product formation during fermentation of *M. extorquens* AM1 Δ*cel* + pCM160_RBS_*yciAHI* in a BiostatB® bioreactor system (Sartorius, Göttingen, Germany) with 4-liter starting volume. Methanol concentration at the start was 3.95 g/L and was controlled close to a setpoint of 1 g/L via an online methanol sensor. 8 mL of trace element feeding solution without $CoCl_2$ was added every 12 h. The temperature was kept at 30 °C ± 0.01 °C and pH was kept at 7 ± 0.1. The DO setpoint was 30 %. Online parameters are shown in Appendix 3.

Establishment of a DO-based feeding strategy for *M. extorquens* AM1 Δ*cel*

Although the previously shown fermentations already yielded high product titers of up to 8.9 g/L of total product, a method which works independently from an online methanol measuring was to be developed. The following experiments were performed in a DASGIP® parallel bioreactor system in 1 L vessels (Eppendorf, Hamburg, Germany). The feeding of methanol was controlled by a reactor script (Appendix 1), wherein a low (31 %) and a high DO value (e.g., 60 %) are defined as trigger values. After a deadband of 10 h starting from inoculation, the pump is set to idle for rapidly pumping 3.5 mL into the vessel if the high DO trigger is reached, indicating a depletion of methanol. As a safety net, the pump was not turned back to idle until a DO value below 30 % was reached. This prevented overfeeding of methanol to an inhibitory concentration.

First, the setup was tested with a *M. extorquens* AM1 Δ*cel* strain harboring an empty vector control (pCM160) in four parallel fermentation runs (Figure 3). The feeding worked consistently for all four reactors (Appendix 4-7) and led to a total methanol consumption of 47.1 ± 3.9 g (in a total approximated culture volume of 700 mL) and a maximum CDW of 7.1 ± 0.3 g/L. Since the cultivations yielded robust results, the following laborious fermentations were performed in duplicate rather than in quadruplicate. Please note that the standard deviations reported for dicarboxylic acid production in the DASGIP® parallel bioreactor system were calculated using duplicates.

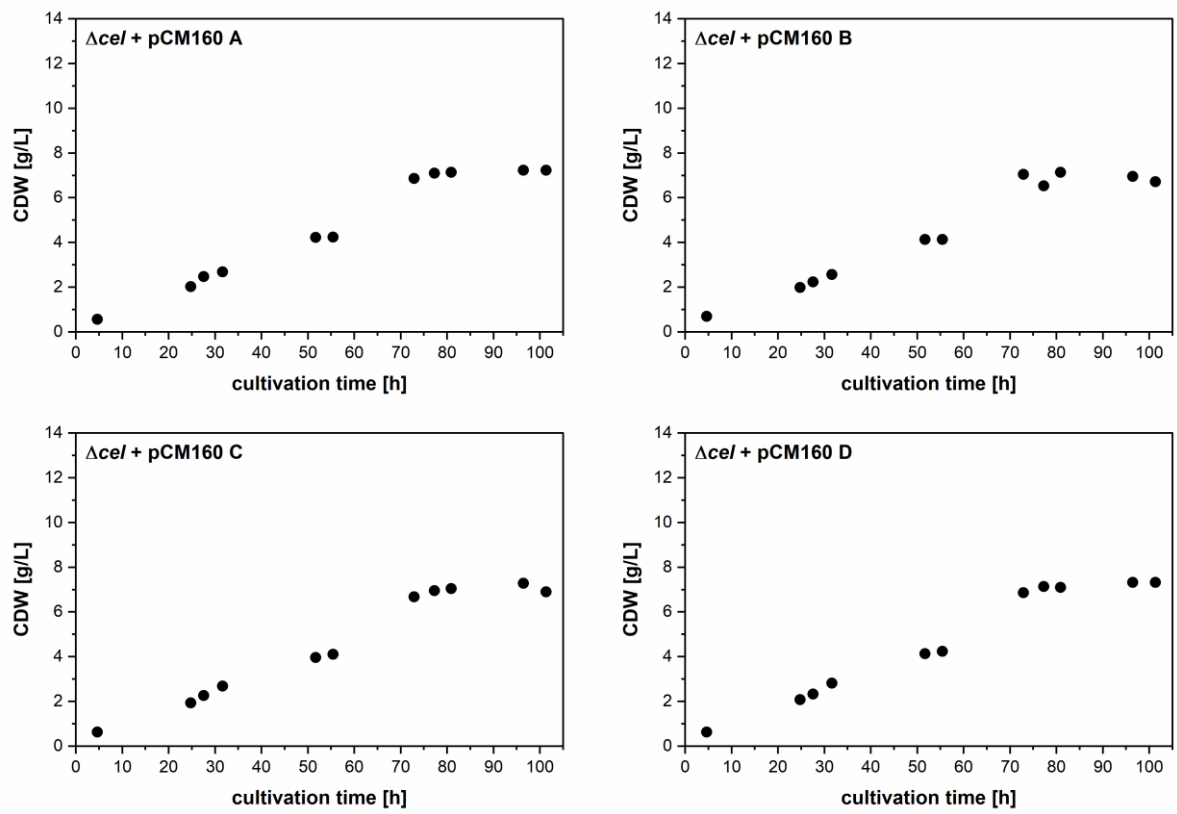

Figure 3 Growth during modified DO-stat cultivations of *M. extorquens* AM1 Δ*cel* + pCM160. Four replicate experiments were run in parallel (A-D) in a DASGIP® bioreactor system (Eppendorf, Hamburg, Germany). The temperature was kept at 30 °C ± 0.01 °C and pH was kept at 7 ± 0.1. Methanol concentration at the start was 3.95 g/L and was set back to 3.95 g/L immediately after depletion, which was indicated by a rapid DO-shift. The overall DO setpoint was 30 %. 1.4 mL of trace element feeding solution containing 100 µM of $CoCl_2$ was added after the OD_{600} reached a value of 15 (49.7 h after inoculation) and then every 24 h. Online parameters are shown in Appendices 4-7.

Testing of the DO-based feeding strategy for dicarboxylic acid production with heterologous thioesterase YciA in *M. extorquens* AM1 Δ*cel*

Next, the previously described fermentation setup was tested for dicarboxylic acid production. For this experiment, a *M. extorquens* AM1 Δ*cel* strain overexpressing *yciAHI* was used. Although reactor A showed some irregularities in measured CO_2 and DO values after 62 hours of cultivation (Appendix 8), the dicarboxylic acid production in the duplicates were found to be equivalent (Figure 4). A maximum titer of 2.8 ± 0.1 g for mesaconic acid and 2.5 ± 0.1 g for 2-methylsuccinic acid was reached. 2-Hydroxy-3-methylsuccinic acid could only be measured in small amounts in the late stage of the fermentations and other EMPC-derived dicarboxylic acids were not detectable at all.

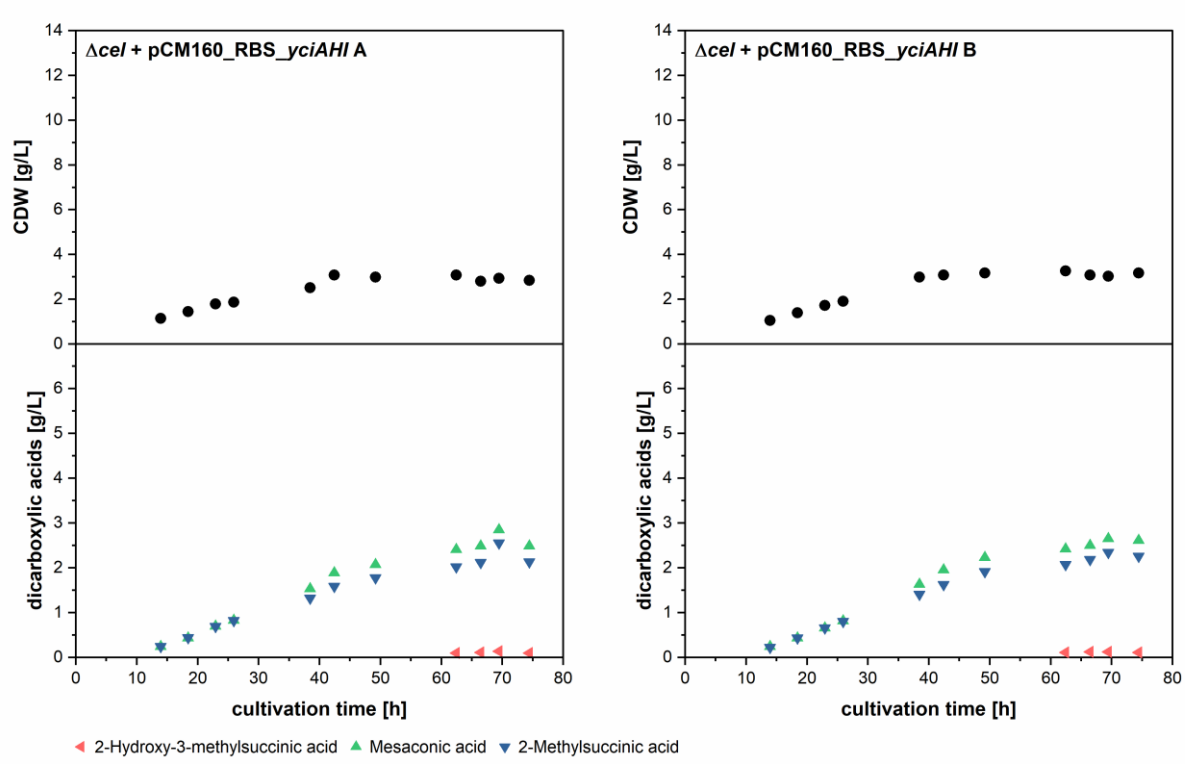

Figure 4 Growth and product formation during modified DO-stat cultivations of *M. extorquens* AM1 Δ*cel* + pCM160_RBS_*yciAHI*. Two replicate experiments were run in parallel (A and B) in a DASGIP® bioreactor system (Eppendorf, Hamburg, Germany). The temperature was kept at 30 °C ± 0.01 °C and pH was kept at 7 ± 0.1. Methanol concentration at the start was 3.95 g/L. After methanol depletion, indicated by a rapid DO shift, the concentration was rapidly set back to 3.95 g/L. The overall DO setpoint was 30 %. 1.4 mL of trace element feeding solution containing 100 µM $CoCl_2$ was added after the OD_{600} reached a value of 15 (40.4 h after inoculation) and then every 24 h. Online parameters are shown in Appendices 8 and 9.

The strategy of altering the trace element addition exhibited a remarkable effect on cell growth and dicarboxylic acid in the previously tested fermentation setup (Figure 1 and Figure 2). Therefore, this strategy was also tested for the new DO-based setup (Figure 5) by adding 0.7 mL of trace element feeding solution without $CoCl_2$ every 8 h to each of the bioreactors. Both, dicarboxylic acid and biomass production was enhanced compared to the previously tested feeding strategy (adding 1.4 mL trace element solution containing 100 µM $CoCl_2$ after the OD_{600} reached a value of 15 and then every 24 h (Figure 4)). This result can be accounted for by a combined effect of a low availability of cobalt and a higher availability of other trace elements. The latter seems to be beneficial for cell growth, indicating a limitation in the prior experiment. Therefore, the following fermentations were carried out with a higher supply of trace elements except for cobalt.

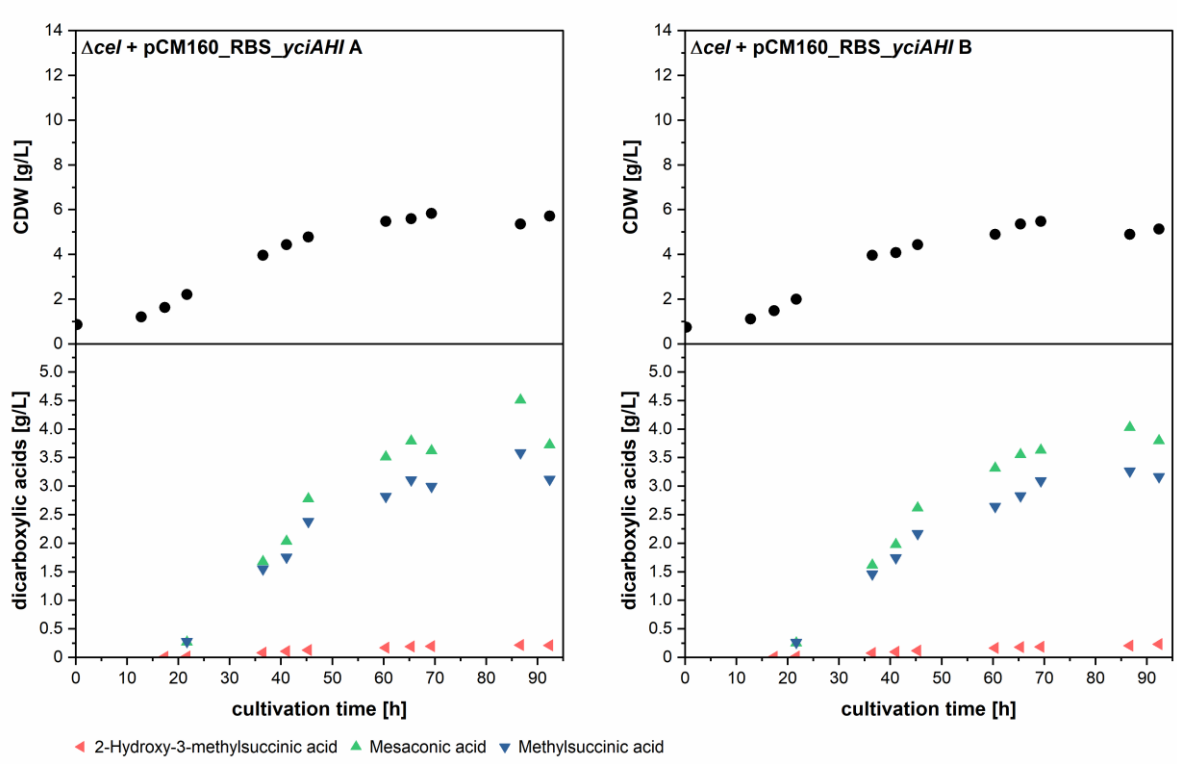

Figure 5 Growth and product formation during modified DO-stat cultivations of *M. extorquens* AM1 Δ*cel* + pCM160_RBS_*yciAHI*. Two replicate experiments were run in parallel (A and B) in a DASGIP® bioreactor system (Eppendorf, Hamburg, Germany). The temperature was kept at 30 °C ± 0.01 °C and pH was kept at 7 ± 0.1. Methanol concentration at the start was 3.95 g/L. After methanol depletion, indicated by a rapid DO shift, the concentration was rapidly set back to 3.95 g/L. The overall DO setpoint was 30 %. 0.7 mL of trace element feeding solution without $CoCl_2$ was added every 8 h. Online parameters are shown in Appendices 10 and 11.

In previous studies (Sonntag et al. 2014; Sonntag et al. 2015b; Pöschel et al. 2022), an alternative YciA thioesterase originating from *E. coli* (YciAEc) was used for the production of mesaconic acid and 2-methylsuccinic acid. To test, which enzyme is more favorable for high-level production, *M. extorquens* AM1 Δ*cel* overexpressing *yciAEc* was also tested in the DO-based reactor setup described above. The growth and production kinetics of the strains harboring YciAEc (Figure 6) differed substantially from the previous fermentations with strains harboring YciAHI (Figure 4 and Figure 5). A CDW of 13.4 ± 0.2 g/L was reached and the maximum mixed product titer did not exceed 2.7 ± 0.1 g/L. As for the experiments with YciAHI, 2-hydroxy-3-methylsuccinic acid could only be measured in small amounts and other EMPC-derived dicarboxylic acids were not detectable at all. Summarized, strains overexpressing the *H. influenzae yciA* variant were more suitable to produce high amounts of mesaconic acid and 2-methylsuccinic acid.

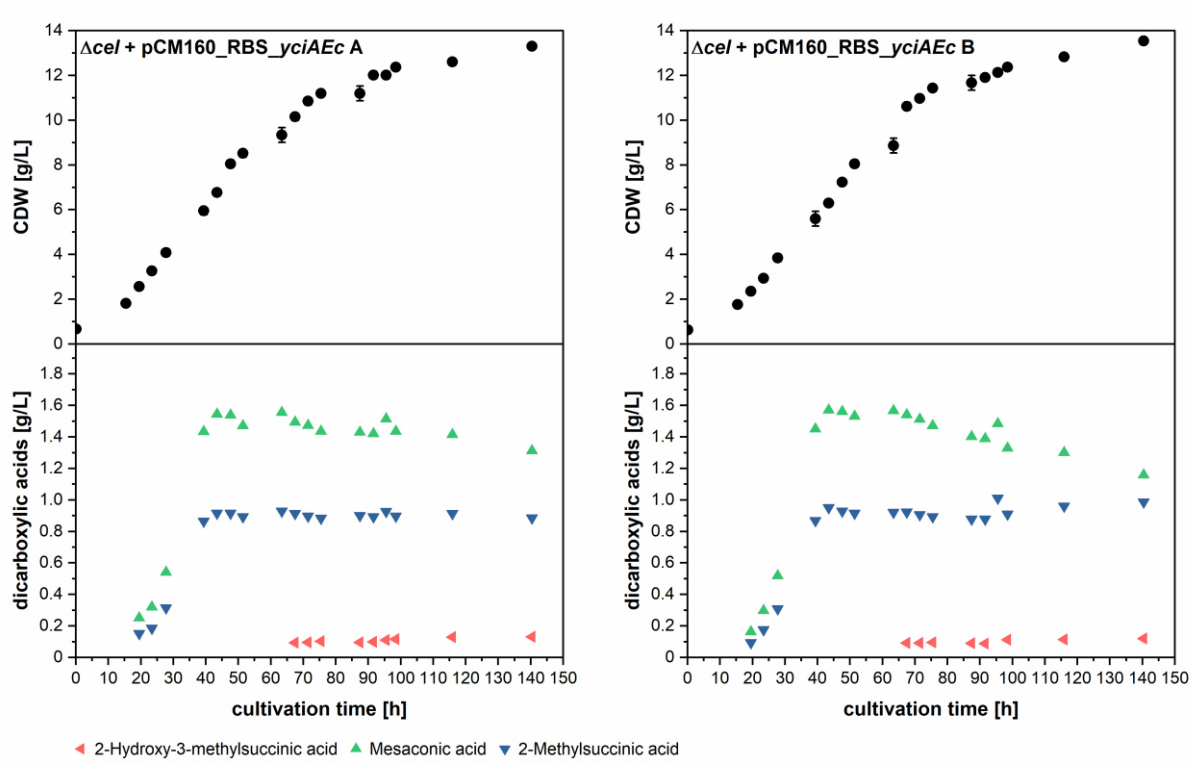

Figure 6 Growth and product formation during modified DO-stat cultivations of *M. extorquens* AM1 Δ*cel* + pCM160_RBS_*yciAEc*. Two replicate experiments were run in parallel (A and B) in a DASGIP® bioreactor system (Eppendorf, Hamburg, Germany). The temperature was kept at 30 °C ± 0.01 °C and pH was kept at 7 ± 0.1. Methanol concentration at the start was 3.95 g/L. After methanol depletion, indicated by a rapid DO shift, the concentration was rapidly set back to 3.95 g/L. The overall DO setpoint was 30 %. 0.7 mL of trace element feeding solution without $CoCl_2$ was added every 8 h. Online parameters are shown in Appendices 12 and 13.

Dicarboxylic acid production with *dctA* deletion mutants overexpressing *yciAHI*

In a study of Pöschel et al. (2022), the production of mesaconic acid and 2-methylsuccinic acid in optimized strains with deletions of the putative acid transporter genes *dctA1*, *dctA2* and *dctA3* was described. In these strains, the uptake of produced dicarboxylic acids that is typically observed in shake flask experiments shortly after the cultures reach the stationary growth phase, is substantially reduced (Pöschel et al. 2022). To investigate whether a masked uptake reduces the actual yield of the fermentations shown in this chapter, the triple deletion strain was tested in the new setup. Although it was shown that deletion of *dctA2* alone already suppressed product reuptake (Pöschel et al. 2022), strains with triple deletions of all *dctA* genes were used in the following to account for a possible upregulation of alternative DctA transporters in a bioreactor setup.

The fermentations of *M. extorquens* AM1 Δ*cel* Δ*dctA1* Δ*dctA2* Δ*dctA3* overexpressing *yciaHI* (Figure 7) yielded comparable CDW values and dicarboxylic acid titers as

fermentations of strains without genomic *dctA* deletions (Figure 5). Therefore, a masked product reuptake seems not to be an issue in this fermentation setup.

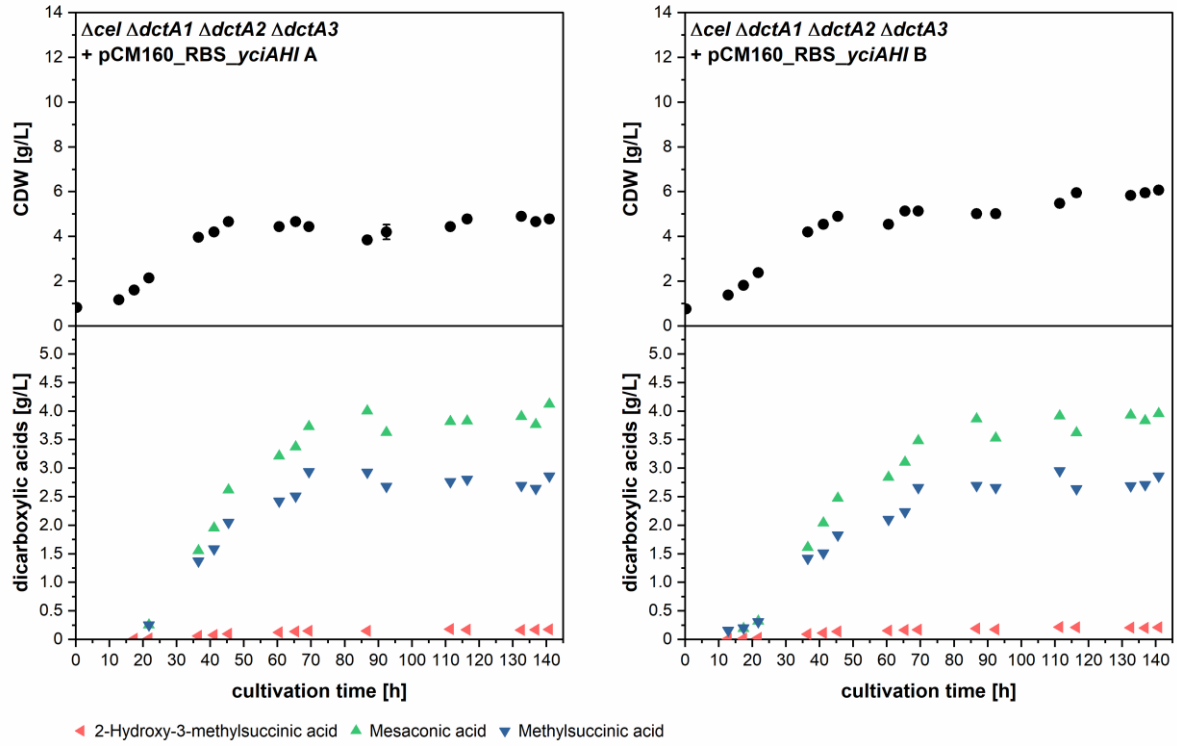

Figure 7 Growth and product formation during modified DO-stat cultivations of *M. extorquens* AM1 Δ*cel* Δ*dctA1* Δ*dctA2* Δ*dctA3* + pCM160_RBS_*yciAHI*. Two replicate experiments were run in parallel (A and B) in a DASGIP® bioreactor system (Eppendorf, Hamburg, Germany). The temperature was kept at 30 °C ± 0.01 °C and pH was kept at 7 ± 0.1. Methanol concentration at the start was 3.95 g/L. After methanol depletion, indicated by a rapid DO shift, the concentration was rapidly set back to 3.95 g/L. The overall DO setpoint was 30 %. 0.7 mL of trace element feeding solution without $CoCl_2$ was added every 8 h. Online parameters are shown in Appendices 14 and 15.

Production of presumably enantiomerically pure citramalic acid in a bioreactor scale

The previously mentioned study of Pöschel et al. (2022) also describes the production of citramalic acid with *M. extorquens* AM1 by expressing a mesaconase gene from *Paraburholderia xenovorans* (*mesaPx*) additionally to *yciAEc.* The promiscuous mesaconase/fumarase MesaPx converts mesaconic acid to enantiomerically pure (*S*)-citramalic acid by hydration (Kronen et al. 2015). For the experiments (and also in Pöschel et al. (2022)), the YciA enzyme originating from *E. coli* was used since the ratio of mesaconic acid to 2-methylsuccinic acid produced is slightly higher than for the *H. influenzae* YciA. Up to 4.3 ± 0.1 g/L of citramalic acid was produced with the new

modified DO-stat setup. Although no chiral analysis was performed, it can be concluded from the kinetic *in vitro* data of the mesaconase used (Kronen et al. 2015), that the enantiomerically pure (*S*)-form of citramalic acid is produced. Residual mesaconic acid titers of 0.1 g/L and 0.2 g/L were measured in reactor A and B, respectively. Furthermore, a 2-methylsuccinic acid titer of 1 ± 0.1 g/L was measured at the end of cultivations.

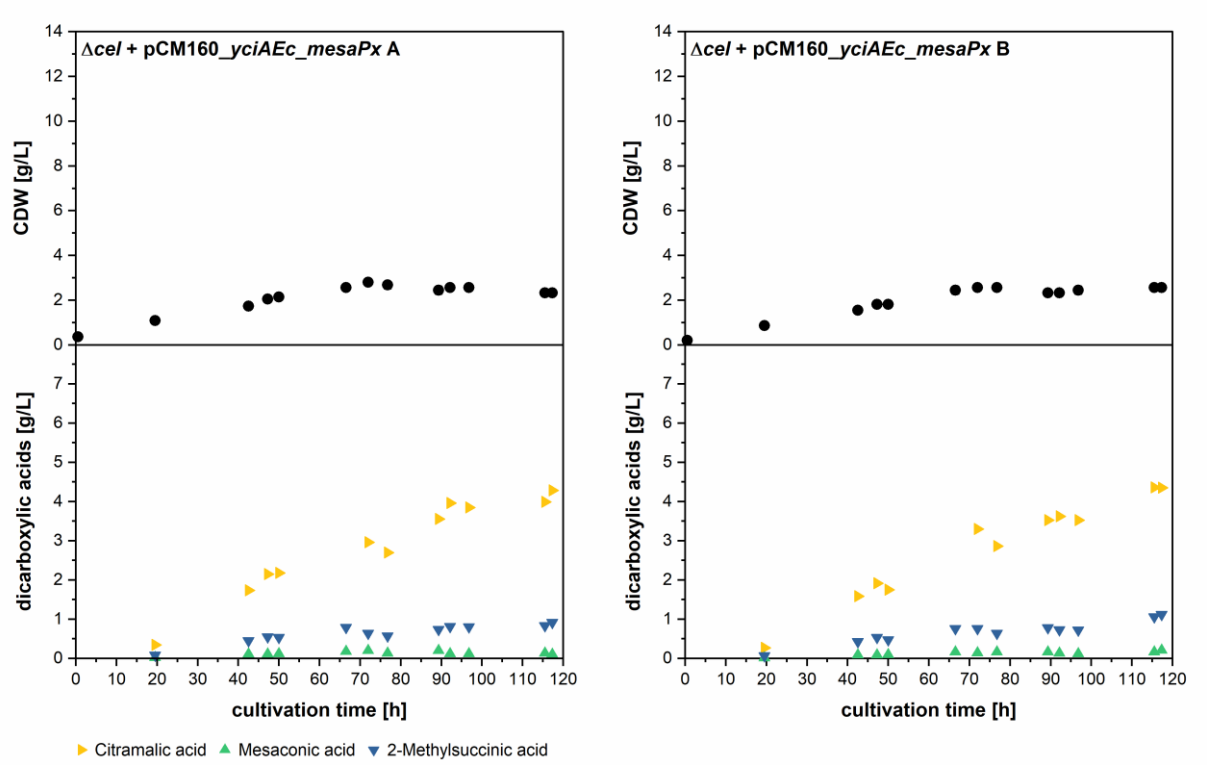

Figure 8 Growth and product formation during modified DO-stat cultivations of *M. extorquens* AM1 Δ*cel* + pCM160_RBS_*yciAEc_mesaPx*. Two replicate experiments were run in parallel (A and B) in a DASGIP® bioreactor system (Eppendorf, Hamburg, Germany). The temperature was kept at 30 °C ± 0.01 °C and pH was kept at 7 ± 0.1. Methanol concentration at the start was 3.95 g/L. After methanol depletion, indicated by a rapid DO shift, the concentration was rapidly set back to 3.95 g/L. The overall DO setpoint was 30 %. 1.4 mL of trace element feeding solution without $CoCl_2$ was added every 8 h. Online parameters are shown in Appendices 16 and 17.

Production of presumably enantiomerically pure 2-hydroxy-3-methylsuccinic acid in a bioreactor scale

From all potential EMCP-derived dicarboxylic acid products, only mesaconic acid, 2-methylsuccinic acid and citramalic acid were produced at a higher mg/L scale in the past (Sonntag et al. 2015b; Pöschel et al. 2022). Besides mesaconyl-CoA and 2-methylsuccinyl-CoA, the EMCP harbors further interesting thioester intermediates,

e.g. ß-methylmalyl-CoA (Alber 2011). As shown in the previous chapters and figures, overexpression of the *yciA* gene did not yield considereable amounts of the hydrolysis product 2-hydroxy-3-methylsuccinic acid, although the YciA enzyme showed *in vitro* acitivites for a plethora of closely related thioester substrates (Zhuang et al. 2008). Therefore, an alternative thioesterase was tested for the production of novel products such as (2*S*,3*R*)-2-hydroxy-3-methylsuccinic acid. The *citE* like thioesterase gene from *Corynebacterium glutamicum* was codon optimized for *M. extorquens* AM1 and cloned into pCM160 along with an optimized RBS. The resulting overexpression plasmid was introduced into *M. extorquens* AM1 and tested in the newly developed fermentation setup. For this new product, all three previously described trace element solution feeding strategies were tested: Feeding a solution without $CoCl_2$ every 8 hours (Figure 9) or feeding every 24 hours after OD_{600} reaches a value of 15, either with a solution without $CoCl_2$ (Figure 10) or with a solution containing 100 µM $CoCl_2$ (Figure 11). Also for the production of 2-hydroxy-3-methylsuccinic acid, feeding a trace element solution without $CoCl_2$ every 8 hours yielded the highest product titers. In the respective fermentations, a titer of 5.7 ± 0.1 g/L of 2-hydroxy-3-methylsuccinic acid was achieved (Figure 9). When the feeding period of the same trace element solution was prelonged to 24 h, only 2.0 ± 0.1 g/L of 2-hydroxy-3-methylsuccinic acid was produced (Figure 10). The same feeding strategy executed with a trace element solution containing 100 µM of $CoCl_2$ improved cell growth, but yielded lower maximum product titers (1.5 ± 0.4 g/L, Figure 11). Similar to the experiments with *yciA* overexpression, a low amount of $CoCl_2$ was favorable for higher product yields, but at least one of the other trace elements seems to be limiting in the prelonged trace element feeding strategy. The optimal concentration of each trace element may lead to even higher productivity. No other EMCP-derived dicarboxylic acid was detectable in the culture supernatants with LC-MS/MS analysis. This high product purity faciliates potential downstream processing of 2-hydroxy-3-methylsuccinic acid.

Although a chiral analysis for the produced 2-hydroxy-3-methylsuccinic acid is yet to be performed, it can be presumed that the enantiomerically pure (2*S*,3*R*)-form is obtained. The precursor (2*R*,3*S*)-ß-methylmalyl-CoA (Erb et al. 2009) is generated by hydration of mesaconyl-CoA, catalyzed by mesaconyl-CoA hydratase (Mch) (Zarzycki et al. 2008). The presumed reaction scheme from mesaconyl CoA to (2*S*,3*R*)-2-hydroxy-3-methylsuccinic acid is given in Figure 12.

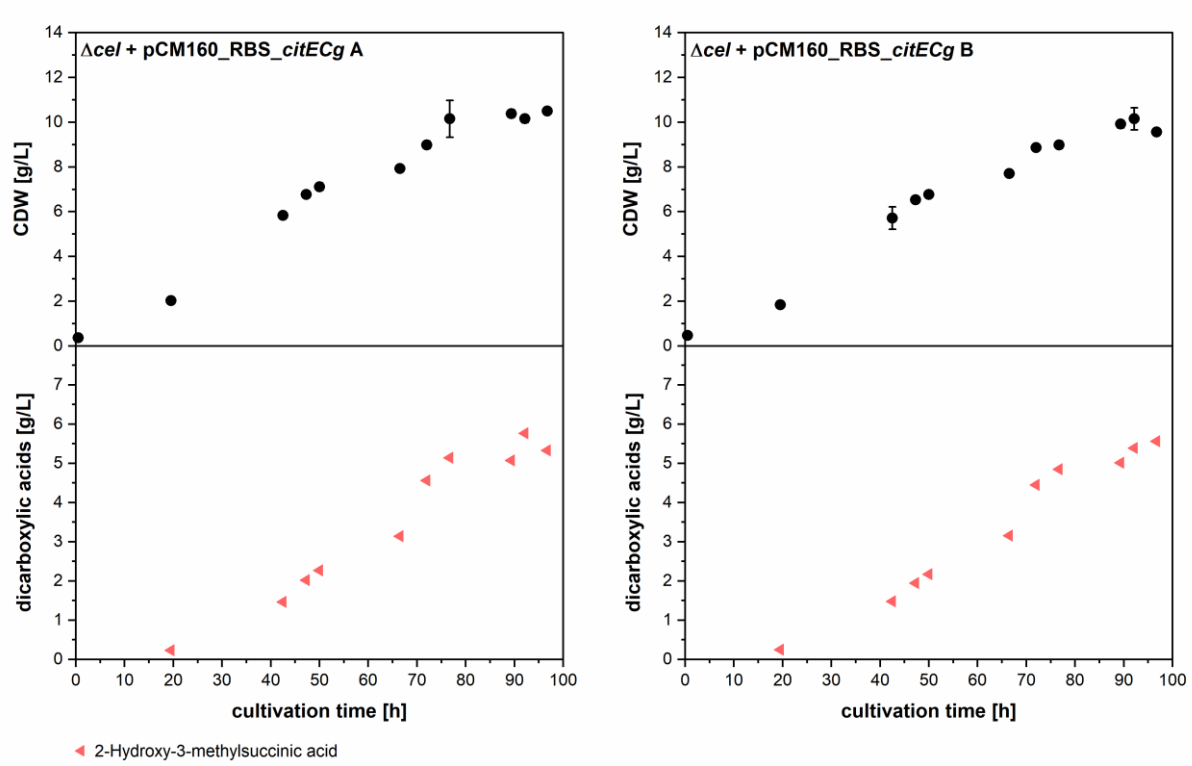

Figure 9 Growth and product formation during modified DO-stat cultivations of *M. extorquens* AM1 Δ*cel* + pCM160_RBS_*citECg*. Two replicate experiments were run in parallel (A and B) in a DASGIP® bioreactor system (Eppendorf, Hamburg, Germany). The temperature was kept at 30 °C ± 0.01 °C and pH was kept at 7 ± 0.1. Methanol concentration at the start was 3.95 g/L. After methanol depletion, indicated by a rapid DO shift, the concentration was rapidly set back to 3.95 g/L. The overall DO setpoint was 30 %. 1.4 mL of trace element feeding solution without $CoCl_2$ was added every 8 h. Online parameters are shown in Appendices 18 and 19.

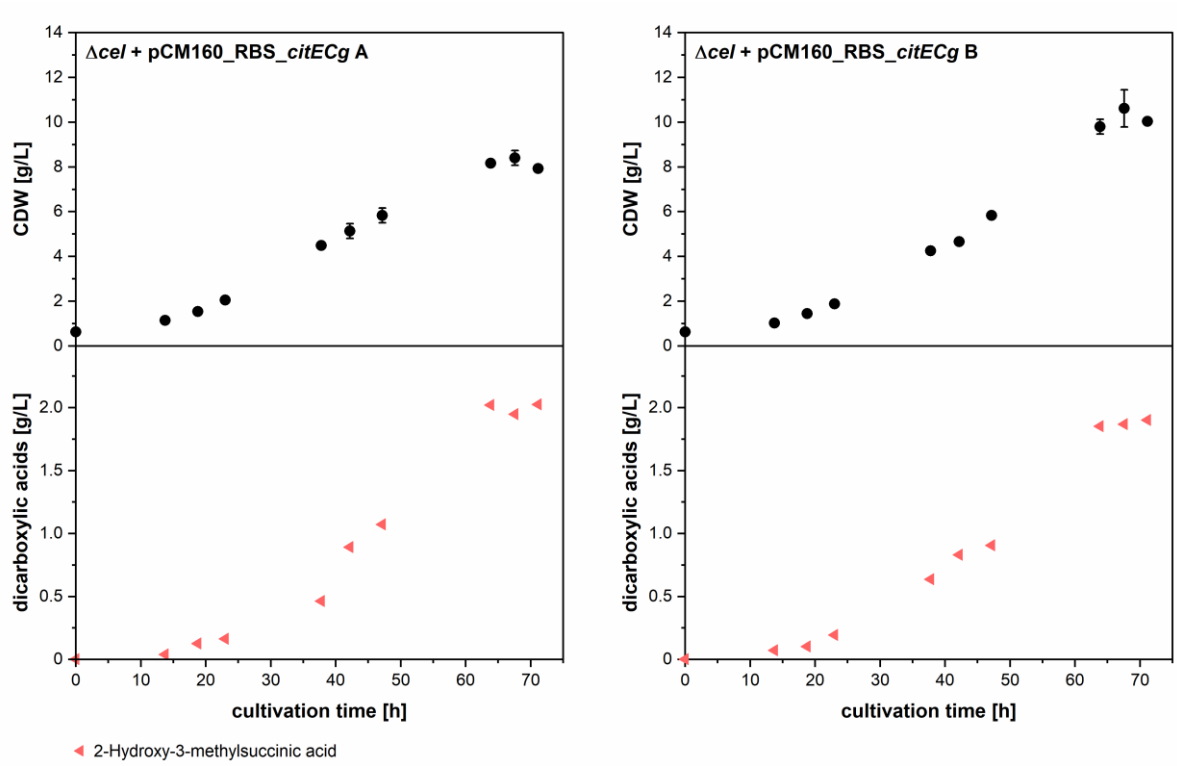

Figure 10 Growth and product formation during modified DO-stat cultivations of *M. extorquens* AM1 Δ*cel* + pCM160_RBS_*citECg*. Two replicate experiments were run in parallel (A and B) in a DASGIP® bioreactor system (Eppendorf, Hamburg, Germany). The temperature was kept at 30 °C ± 0.01 °C and pH was kept at 7 ± 0.1. Methanol concentration at the start was 3.95 g/L. After methanol depletion, indicated by a rapid DO shift, the concentration was rapidly set back to 3.95 g/L. The overall DO setpoint was 30 %. 1.4 mL of trace element feeding solution without $CoCl_2$ was added after the OD_{600} reached a value of 15 (31 h after inoculation) and then every 24 h. Online parameters are shown in Appendices 20 and 21.

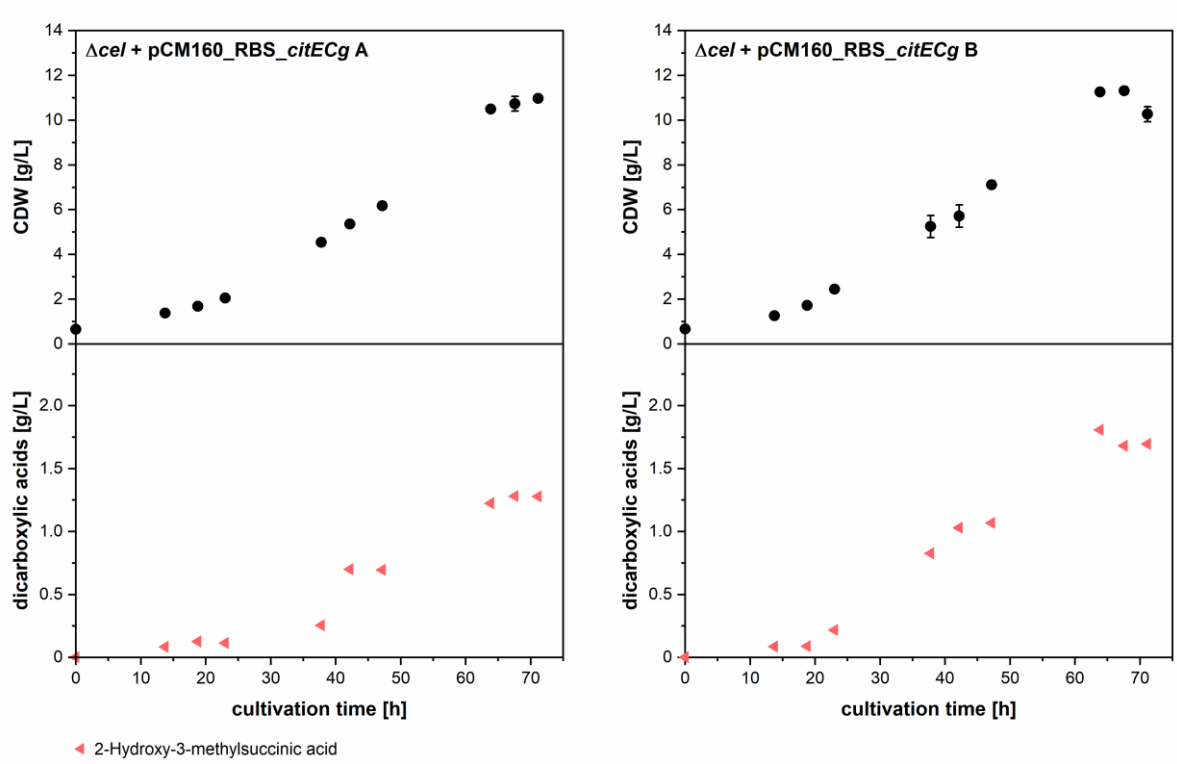

Figure 11 Growth and product formation during modified DO-stat cultivations of *M. extorquens* AM1 Δ*cel* + pCM160_RBS_*citECg*. Two replicate experiments were run in parallel (A and B) in a DASGIP® bioreactor system (Eppendorf, Hamburg, Germany). The temperature was kept at 30 °C ± 0.01 °C and pH was kept at 7 ± 0.1. Methanol concentration at the start was 3.95 g/L. After methanol depletion, indicated by a rapid DO shift, the concentration was rapidly set back to 3.95 g/L. The overall DO setpoint was 30 %. 1.4 mL of trace element feeding solution containing 100 µM $CoCl_2$ was added after the OD_{600} reached a value of 15 (31 h after inoculation) and then every 24 h. Online parameters are shown in Appendices 22 and 23.

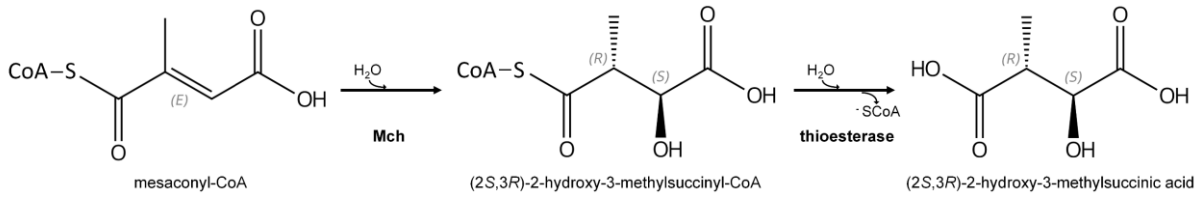

Figure 12 Reaction scheme for the hydration of EMCP intermediate mesaconyl-CoA to EMCP intermediate (2*S*,3*R*)-2-hydroxy-3-methylsuccinyl-CoA (alternative name (2*R*,3*S*)-ß-methylmalyl-CoA) catalyzed by mesaconyl-CoA hydratase (Mch). Subsequent cleavage of the CoA moiety to produce (2*S*,3*R*)-2-hydroxy-3-methylsuccinic acid can be realized with a thioesterase.

Summary and conclusion

This study presents a fermentation design tailored to the production of dicarboxylic acids with *M. extorquens* with a methanol feeding strategy solely based on DO measurements. By using the developed process, four dicarboxylic acid products could be produced in concentrations of 3.8 g/L to 5.8 g/L. Two of the compounds, namely 2-hydroxy-3-methylsuccinic acid and citramalic acid are presumably pure enantiomers, but confirmation by chiral analysis is still to be performed. The feeding strategies, maximum product titers and yields of all fermentations performed in this work are summarized in Table 3.

As shown in the experiments, different feeding strategies for trace elements strongly influenced the product yields. Various media compositions have been published for the cultivation of *M. extorquens* AM1, which differ from the methanol minimal medium used in this work in the concentrations of trace elements. In Bourque et al. (1995), the final medium optimized for growth contained multiple times higher concentrations of trace elements, whereas in the medium of Delaney et al. (2013) the concentrations varied in both directions and citrate was chosen as chelator instead of EDTA (Table 4). This indicates that concentrations of trace elements may be varied over a wide range for different applications. The use of EDTA as a chelator has been discussed critically and is presumably inhibiting the growth of *M. extorquens* by sequestering the metal cations, making them inaccessible for the cells (Chan 1992; Delaney et al. 2013). An experimental design to optimize the concentration of each trace element in the growth medium and exchanging the chelator for e.g. citrate, holds great potential to maximize the dicarboxylic acid yields obtained with the new fermentation setup.

Further improvements of the product yields may be obtained by using strains with separated growth and production phases. With this approach, high cell masses could be achieved in a first process phase and subsequently, conditions optimized for production could be applied in a second process phase. Such a procedure would require the construction of a genetic switch which can be triggered e.g. through induction. Another restriction is the previously reported downregulation of the expression of methanol dehydrogenase and acetoacetyl-CoA reductase genes after reaching exponential growth phase (Rohde et al. 2017). Before developing a two-phase fermentation setup, these questions must be addressed first.

Table 3 Yields and maximum product titers of fermentations described in this chapter.

2-Hydroxy-3-methylsuccinic acid

Figure	Strain	Trace element feeding strategy	Replicate	Maximum product titer (Pmax) [g/L]	t_Pmax [h]	Product Yield $Y(P)_{t\_Pmax} = P_{t\_Pmax}/S_{t\_Pmax}$ [g product/ g methanol]	Biomass Yield $Y(X)_{t\_Pmax} = X_{t\_Pmax}/S_{t\_Pmax}$ [g CDW / g methanol]	Ratio P/CDW [g product / g CDW]	Maximum product titer all products [g/L]
1	Δ*cel* + pCM160_RBS_*yciAHI*	1)	A	0.13	141.33	0.00	0.12	0.01	**4.88**
2	Δ*cel* + pCM160_RBS_*yciAHI*	2)	A	0.28	141.25	0.00	0.05	0.05	**8.94**
4	Δ*cel* + pCM160_RBS_*yciAHI*	1)	A	0.14	67.43	0.00	0.10	0.05	**5.54**
			B	0.13	67.43	0.00	0.09	0.04	**5.11**
5	Δ*cel* + pCM160_RBS_*yciAHI*	3)	A	0.26	111.38	0.00	0.11	0.04	**8.35**
			B	0.23	92.38	0.01	0.13	0.05	**7.52**
6	Δ*cel* + pCM160_RBS_*yciAEc*	3)	A	0.13	140.38	0.00	0.19	0.01	**2.62**
			B	0.12	140.38	0.00	0.19	0.01	**2.70**
7	Δ*cel* Δ*dctA1* Δ*dctA2* Δ*dctA3* + pCM160_RBS_*yciAH.*	3)	A	0.18	111.38	0.00	0.10	0.04	**7.24**
			B	0.22	111.38	0.00	0.12	0.04	**7.13**
8	Δ*cel* + pCM160_RBS_*yciAEc_mesaPx*	4)	A	/	/	/	/	/	**5.41**
			B	/	/	/	/	/	**5.69**
9	Δ*cel* + pCM160_RBS_*citECg*	4)	A	5.77	92.17	0.08	0.14	0.57	**5.77**
			B	5.56	96.75	0.08	0.14	0.58	**5.56**
10	Δ*cel* + pCM160_RBS_*citECg*	5)	A	2.03	71.17	0.05	0.20	0.26	**2.03**
			B	1.90	71.17	0.04	0.23	0.19	**1.90**
11	Δ*cel* + pCM160_RBS_*citECg*	1)	A	1.28	67.58	0.03	0.25	0.12	**1.28**
			B	1.81	63.83	0.04	0.27	0.16	**1.81**

Mesaconic acid

Figure	Strain	Trace element feeding strategy	Replicate	Maximum product titer (Pmax) [g/L]	t_Pmax [h]	Product Yield $Y(P)_{t\_Pmax} = P_{t\_Pmax}/S_{t\_Pmax}$ [g product/ g methanol]	Biomass Yield $Y(X)_{t\_Pmax} = X_{t\_Pmax}/S_{t\_Pmax}$ [g CDW / g methanol]	Ratio P/CDW [g product / g CDW]	Maximum product titer all products [g/L]
1	Δ*cel* + pCM160_RBS_*yciAHI*	1)	A	2.62	157.42	0.03	0.11	0.29	**4.88**
2	Δ*cel* + pCM160_RBS_*yciAHI*	2)	A	4.87	134.25	0.04	0.05	0.81	**8.94**
4	Δ*cel* + pCM160_RBS_*yciAHI*	1)	A	2.85	67.43	0.09	0.10	0.97	**5.54**
			B	2.65	72.43	0.08	0.09	0.82	**5.11**
5	Δ*cel* + pCM160_RBS_*yciAHI*	3)	A	4.51	86.72	0.10	0.11	0.84	**8.35**
			B	4.03	86.72	0.10	0.13	0.82	**7.52**
6	Δ*cel* + pCM160_RBS_*yciAEc*	3)	A	1.56	63.38	0.04	0.23	0.17	**2.62**
			B	1.57	43.47	0.06	0.24	0.25	**2.70**
7	Δ*cel* Δ*dctA1* Δ*dctA2* Δ*dctA3* + pCM160_RBS_*yciAH.*	3)	A	4.12	86.72	0.10	0.10	1.04	**7.24**
			B	3.96	132.58	0.08	0.12	0.67	**7.13**
8	Δ*cel* + pCM160_RBS_*yciAEc_mesaPx*	4)	A	0.20	89.33	0.01	0.11	0.08	**5.41**
			B	0.21	117.33	0.01	0.10	0.08	**5.69**
9	Δ*cel* + pCM160_RBS_*citECg*	4)	A	/	/	/	/	/	**5.77**
			B	/	/	/	/	/	**5.56**
10	Δ*cel* + pCM160_RBS_*citECg*	5)	A	/	/	/	/	/	**2.03**
			B	/	/	/	/	/	**1.90**
11	Δ*cel* + pCM160_RBS_*citECg*	1)	A	/	/	/	/	/	**1.28**
			B	/	/	/	/	/	**1.81**

Table 3 (continued)

2-Methylsuccinic acid

Figure	Strain	Trace element feeding strategy	Replicate	Maximum product titer (Pmax) [g/L]	t_Pmax [h]	Product Yield $Y(P)_{t\_Pmax} = P_{t\_Pmax}/S_{t\_Pmax}$ [g product/ g methanol]	Biomass Yield $Y(X)_{t\_Pmax} = X_{t\_Pmax}/S_{t\_Pmax}$ [g CDW / g methanol]	Ratio P/CDW [g product / g CDW]	Maximum product titer all products [g/L]
1	Δ*cel* + pCM160_RBS_*yciAHI*	1)	A	2.14	157.42	0.03	0.11	0.24	**4.88**
2	Δ*cel* + pCM160_RBS_*yciAHI*	2)	A	3.79	141.25	0.03	0.05	0.64	**8.94**
4	Δ*cel* + pCM160_RBS_*yciAHI*	1)	A	2.55	67.43	0.08	0.10	0.87	**5.54**
			B	2.34	72.43	0.06	0.09	0.71	**5.11**
5	Δ*cel* + pCM160_RBS_*yciAHI*	3)	A	3.58	86.72	0.08	0.11	0.67	**8.35**
			B	3.26	86.72	0.08	0.13	0.67	**7.52**
6	Δ*cel* + pCM160_RBS_*yciAEc*	3)	A	0.93	63.38	0.02	0.23	0.10	**2.62**
			B	1.01	95.47	0.02	0.22	0.08	**2.70**
7	Δ*cel* Δ*dctA1* Δ*dctA2* Δ*dctA3* + pCM160_RBS_*yciAH*	3)	A	2.94	69.38	0.09	0.13	0.66	**7.24**
			B	2.95	111.38	0.06	0.12	0.54	**7.13**
8	Δ*cel* + pCM160_RBS_*yciAEc_mesaPx*	4)	A	0.92	117.33	0.03	0.08	0.39	**5.41**
			B	1.12	117.33	0.05	0.10	0.44	**5.69**
9	Δ*cel* + pCM160_RBS_*citECg*	4)	A	/	/	/	/	/	**5.77**
			B	/	/	/	/	/	**5.56**
10	Δ*cel* + pCM160_RBS_*citECg*	5)	A	/	/	/	/	/	**2.03**
			B	/	/	/	/	/	**1.90**
11	Δ*cel* + pCM160_RBS_*citECg*	1)	A	/	/	/	/	/	**1.28**
			B	/	/	/	/	/	**1.81**

Citramalic acid

Figure	Strain	Trace element feeding strategy	Replicate	Maximum product titer (Pmax) [g/L]	t_Pmax [h]	Product Yield $Y(P)_{t\_Pmax} = P_{t\_Pmax}/S_{t\_Pmax}$ [g product/ g methanol]	Biomass Yield $Y(X)_{t\_Pmax} = X_{t\_Pmax}/S_{t\_Pmax}$ [g CDW / g methanol]	Ratio P/CDW [g product / g CDW]	Maximum product titer all products [g/L]
1	Δ*cel* + pCM160_RBS_*yciAHI*	1)	A	/	/	/	/	/	**4.88**
2	Δ*cel* + pCM160_RBS_*yciAHI*	2)	A	/	/	/	/	/	**8.94**
4	Δ*cel* + pCM160_RBS_*yciAHI*	1)	A	/	/	/	/	/	**5.54**
			B	/	/	/	/	/	**5.11**
5	Δ*cel* + pCM160_RBS_*yciAHI*	3)	A	/	/	/	/	/	**8.35**
			B	/	/	/	/	/	**7.52**
6	Δ*cel* + pCM160_RBS_*yciAEc*	3)	A	/	/	/	/	/	**2.62**
			B	/	/	/	/	/	**2.70**
7	Δ*cel* Δ*dctA1* Δ*dctA2* Δ*dctA3* + pCM160_RBS_*yciAH*	3)	A	/	/	/	/	/	**7.24**
			B	/	/	/	/	/	**7.13**
8	Δ*cel* + pCM160_RBS_*yciAEc_mesaPx*	4)	A	4.29	117.33	0.16	0.08	1.84	**5.41**
			B	4.36	115.50	0.18	0.10	1.70	**5.69**
9	Δ*cel* + pCM160_RBS_*citECg*	4)	A	/	/	/	/	/	**5.77**
			B	/	/	/	/	/	**5.56**
10	Δ*cel* + pCM160_RBS_*citECg*	5)	A	/	/	/	/	/	**2.03**
			B	/	/	/	/	/	**1.90**
11	Δ*cel* + pCM160_RBS_*citECg*	1)	A	/	/	/	/	/	**1.28**
			B	/	/	/	/	/	**1.81**

1) 1/500 reactor volume of trace element feeding solution containing 100 µM $CoCl_2$ was added after the OD_{600} reached a value of 15 and then every 24 h

2) 1/500 reactor volume of trace element feeding solution without $CoCl_2$ was added every 12 h

3) 1/1000 reactor volume of trace element feeding solution without $CoCl_2$ was added every 8 h

4) 1/500 reactor volume of trace element feeding solution without $CoCl_2$ was added every 8 h

5) 1/500 reactor volume of trace element feeding solution without $CoCl_2$ was added after the OD_{600} reached a value of 15 and then every 24 h

Table 4 Starting concentrations of trace elements and chelators in the methanol minimal medium used in the present work and in media from literature.

Compound	Methanol minimal medium[1)]	Medium 4[2)]	MP Medium[3)]
$Na_2EDTA_2 \cdot H_2O$	15 mg/L	-	-
$ZnSO_4 \cdot 7H_2O$	4.5 mg/L	7.8 mg/L	0.35 mg/L
$MnCl_2 \cdot 4H_2O$	1 mg/L	-	0.2 mg/L
$MnSO_4 \cdot H_2O$	-	14.7 mg/L	-
H_3BO_3	1 mg/L	1.8 mg/L	-
$Na_2MoO_4 \cdot 2H_2O$	0.4 mg/L	2.4 mg/L	-
$(NH_4)_6Mo_7O_{24} \cdot 4H_2O$	-	-	2.47 mg/L
$FeSO_4 \cdot 7H_2O$	3 mg/L	60 mg/L	5 mg/L
$CuSO_4 \cdot 5H_2O$	0.3 mg/L	2.4 mg/L	0.25 mg/L
$CoCl_2 \cdot 6H_2O$	0.0476 mg/L	2.4 mg/L	0.48 mg/L
$CaCl_2 \cdot 2H_2O$	1.5 mg/L	60 mg/L	
$(Na_3C_6H_5O_7 \cdot 2H_2O)$	-	-	13.41 mg/L
$Na_2WO_4 \cdot 2H_2O$	-	-	0.11 mg/L

1) used in this work, modified from Peyraud et al. (2009) and Sonntag et al. (2015b)
2) Bourque et al. (1995)
3) Delaney et al. (2013)

Reference list

Alber BE (2011) Biotechnological potential of the ethylmalonyl-CoA pathway. Appl Microbiol Biotechnol 89:17–25. https://doi.org/10.1007/s00253-010-2873-z

Arenas AMZ, De Wever H, Brendolise L, Keil A, Van Hecke W (2023) Polyhydroxybutyrate/valerate production from methanol by *Methylorubrum extorquens*: Process limiting factors and polymer characterisation. Bioresour Technol Reports 21:101309. https://doi.org/10.1016/j.biteb.2022.101309

Béland M, Bourque D, Perrier M, Miguez CB (2004) ON-LINE ESTIMATION OF STOICHIOMETRIC GROWTH PARAMETERS FOR *METHYLOBACTERIUM EXTORQUENS*. IFAC Proc Vol 37:49–54. https://doi.org/10.1016/s1474-6670(17)32558-2

Bélanger L, Figueira M., Bourque D, Morel L, Béland M, Laramée L, Groleau D, Míguez C. (2004) Production of heterologous protein by *Methylobacterium extorquens* in high cell density fermentation. FEMS Microbiol Lett 231:197–204. https://doi.org/10.1016/S0378-1097(03)00956-X

Bourque D, Pomerleau Y, Groleau D (1995) High-cell-density production of poly-*β*-hydroxybutyrate (PHB) from methanol by *Methylobacterium extorquens*: production of high-molecular-mass PHB. Appl Microbiol Biotechnol 44:367–376. https://doi.org/10.1007/BF00169931

Chan HTC (1992) The mechanism of inhibition by EDTA and EGTA of methanol oxidation by methylotrophic bacteria. FEMS Microbiol Lett 96:231–234. https://doi.org/10.1016/0378-1097(92)90409-H

Delaney NF, Kaczmarek ME, Ward LM, Swanson PK, Lee M-C, Marx CJ (2013) Development of an Optimized Medium, Strain and High-Throughput Culturing Methods for *Methylobacterium extorquens*. PLOS ONE 8:e62957. https://doi.org/10.1371/journal.pone.0062957

Erb TJ, Fuchs G, Alber BE (2009) (2*S*)-Methylsuccinyl-CoA dehydrogenase closes the ethylmalonyl-CoA pathway for acetyl-CoA assimilation. Mol Microbiol 73:992–1008. https://doi.org/10.1111/j.1365-2958.2009.06837.x

Kiefer P, Buchhaupt M, Christen P, Kaup B, Schrader J, Vorholt JA (2009) Metabolite Profiling Uncovers Plasmid-Induced Cobalt Limitation under Methylotrophic Growth Conditions. PLOS ONE 4:e7831. https://doi.org/10.1371/journal.pone.0007831

Kronen M, Sasikaran J, Berg IA (2015) Mesaconase Activity of Class I Fumarase Contributes to Mesaconate Utilization by *Burkholderia xenovorans*. Appl Environ Microbiol 81:5632–5638. https://doi.org/10.1128/AEM.00822-15

Lim CK, Villada JC, Chalifour A, Duran MF, Lu H, Lee PKH (2019) Designing and Engineering *Methylorubrum extorquens* AM1 for Itaconic Acid Production. Front Microbiol 10:1–14. https://doi.org/10.3389/fmicb.2019.01027

Marx CJ, Lidstrom ME (2001) Development of improved versatile broad-host-range vectors for use in methylotrophs and other Gram-negative bacteria. Microbiology

147:2065–2075. https://doi.org/10.1099/00221287-147-8-2065

Mokhtari-Hosseini ZB, Vasheghani-Farahani E, Shojaosadati SA, Karimzadeh R, Heidarzadeh-Vazifekhoran A (2009) Effect of feed composition on PHB production from methanol by HCDC of *Methylobacterium extorquens* (DSMZ 1340). J Chem Technol Biotechnol 84:1136–1139. https://doi.org/10.1002/jctb.2145

Peel D, Quayle JR (1961) Microbial growth on C_1 compounds. 1. Isolation and characterization of *Pseudomonas* AM 1. Biochem J 81:465–469. https://doi.org/10.1042/bj0810465

Peyraud R, Kiefer P, Christen P, Massou S, Portais J-C, Vorholt JA (2009) Demonstration of the ethylmalonyl-CoA pathway by using ^{13}C metabolomics. Proc Natl Acad Sci U S A 106:4846–51. https://doi.org/10.1073/pnas.0810932106

Pöschel L, Gehr E, Buchhaupt M (2022) Improvement of dicarboxylic acid production with *Methylorubrum extorquens* by reduction of product reuptake. Appl Microbiol Biotechnol 106:6713–6731. https://doi.org/10.1007/s00253-022-12161-0

Rohde M-T, Tischer S, Harms H, Rohwerder T (2017) Production of 2-Hydroxyisobutyric Acid from Methanol by *Methylobacterium extorquens* AM1 Expressing (*R*)-3-Hydroxybutyryl Coenzyme A-Isomerizing Enzymes. Appl Environ Microbiol 83:1–16. https://doi.org/10.1128/AEM.02622-16

Salis HM (2011) The Ribosome Binding Site Calculator. Methods Enzymol 498:19–42. https://doi.org/10.1016/B978-0-12-385120-8.00002-4

Sirirote P, Yamane T, Shimizu S (1986) Production of L-serine from methanol and glycine by resting cells of a methylotroph under automatically controlled conditions. J Ferment Technol 64:389–396. https://doi.org/10.1016/0385-6380(86)90025-7

Sonntag F, Buchhaupt M, Schrader J (2014) Thioesterases for ethylmalonyl–CoA pathway derived dicarboxylic acid production in *Methylobacterium extorquens* AM1. Appl Microbiol Biotechnol 98:4533–4544. https://doi.org/10.1007/s00253-013-5456-y

Sonntag F, Kroner C, Lubuta P, Peyraud R, Horst A, Buchhaupt M, Schrader J (2015a) Engineering *Methylobacterium extorquens* for de novo synthesis of the sesquiterpenoid α-humulene from methanol. Metab Eng 32:82–94. https://doi.org/10.1016/j.ymben.2015.09.004

Sonntag F, Müller JEN, Kiefer P, Vorholt JA, Schrader J, Buchhaupt M (2015b) High-level production of ethylmalonyl-CoA pathway-derived dicarboxylic acids by *Methylobacterium extorquens* under cobalt-deficient conditions and by polyhydroxybutyrate negative strains. Appl Microbiol Biotechnol 99:3407–3419. https://doi.org/10.1007/s00253-015-6418-3

Suzuki T, Yamane T, Shimizu S (1986) Mass production of poly-*β*-hydroxybutyric acid by fully automatic fed-batch culture of methylotroph. Appl Microbiol Biotechnol 23:322–329. https://doi.org/10.1007/BF00257027

Toyama H, Anthony C, Lidstrom ME (1998) Construction of insertion and deletion *mxa* mutants of *Methylobacterium extorquens* AM1 by electroporation. FEMS Microbiol Lett 166:1–7. https://doi.org/10.1111/j.1574-6968.1998.tb13175.x

Zarzycki J, Schlichting A, Strychalsky N, Müller M, Alber BE, Fuchs G (2008) Mesaconyl-Coenzyme A Hydratase, a New Enzyme of Two Central Carbon Metabolic Pathways in Bacteria. J Bacteriol 190:1366–1374. https://doi.org/10.1128/JB.01621-07

Zhuang Z, Song F, Zhao H, Li L, Cao J, Eisenstein E, Herzberg O, Dunaway-Mariano D (2008) Divergence of Function in the Hot Dog Fold Enzyme Superfamily: The Bacterial Thioesterase YciA. Biochemistry 47:2789–2796. https://doi.org/10.1021/bi702334h

Appendices

Appendix 1 Vessel script in Visual Basic for DO-based methanol feeding developed in cooperation with DASGIP GmbH (Hamburg, Germany).

```
'Vessel Script
'Script parameters
Dim StartDelay_h As Double = 10 '[h] delay after inoculation
Dim lowDOTrg As Double = 31 'DOPV < lowDOTrg start waiting DO peak Trigger
Dim peakDOTrg As Double = 60 'DOPV > peakDOTrg DO peak Trigger
Dim DOBasedFeedLevelStop As Double = 31 'DOPV < DOBasedFeedingLevelStop stop Feed
Dim maxFeedFlowRate As Double = 30 ' [ml/h] Feed flow rate [ml/h]
dim ShotFeedFlowRate as double = 30 ' [ml/h]
dim ShotVolumn as double = 3.5 '[ml] short volume
dim StopFeedFlowRate as double = 0 ' [ml/h]
'internal variables
Dim Feed As Double = 0
if P isNot Nothing Then
   with P
   select case .phase
   case 0
     .phase = .phase + 1
     .LogMessage("Entering phase " & .phase & ": Waiting for InoculationTime > " & StartDelay_h & " [h]")
   case 1
     if .InoculationTime_H > StartDelay_h then
       .phase = .phase + 1
       .LogMessage("Entering phase " & .phase & ": Waiting for DO < " & lowDOTrg)
     end if
   case 2
     if .DOPV < lowDOTrg then
       .phase = .phase + 1
       .LogMessage("Entering phase " & .phase & ": Waiting for DO > " & peakDOTrg)
     end if
   case 3
     if .DOPV > peakDOTrg then
       .phase = p.phase + 1
       .LogMessage("Entering phase " & .phase & ": shot ")
     end if
   case 4 ' add shot
     Feed = ShotFeedFlowRate
     if .runtime_h - .phasestart_h > (ShotVolumn / ShotFeedFlowRate) then
       .phase = .phase + 1
```

Appendix 1 (continued)

```
      .LogMessage("Entering phase " & .phase & ": stop DO based feeding ")
    end if
  case 5 'Feed stop
    Feed = StopFeedFlowRate
    if .DOPV < DOBasedFeedLevelStop then
      .phase = .phase - 3
    end if
  end select
  'Select medium pump
  .FCSP = Feed
 end with
end if
```

Appendix 2 Parameters of fermentation of *M. extorquens* AM1 Δ*cel* + pCM160_RBS_*yciAHI* in a BiostatB® bioreactor system (Sartorius, Göttingen, Germany) with 4-liter starting volume. Methanol concentration at the start was 3.95 g/L and was controlled close to a setpoint of 1 g/L measured via an online methanol sensor. The temperature was kept at 30 °C (± 0.01 °C) and pH was kept at 7.0 (± 0.1) with base feeding (15 % [v/v] ammonium hydroxide). The DO setpoint was 30 %.

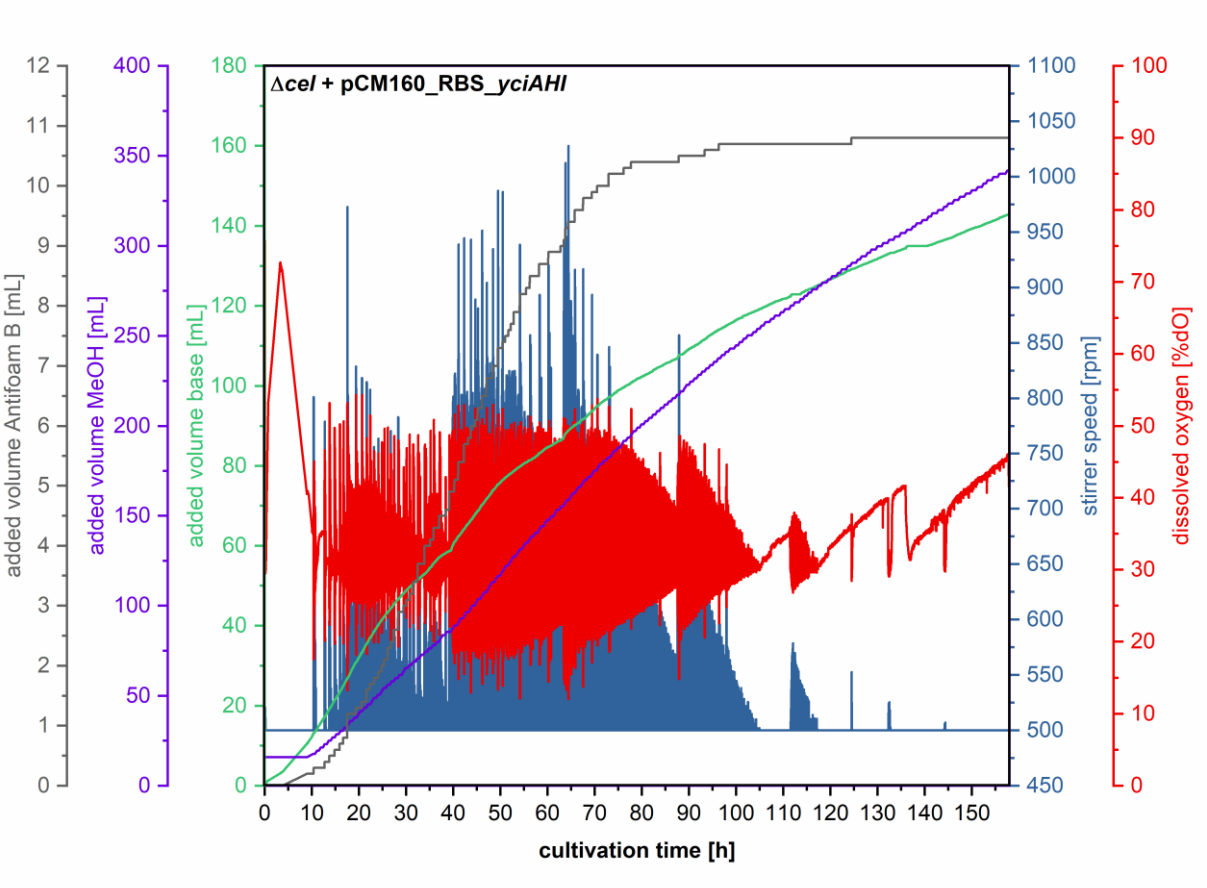

Appendix 3 Parameters of fermentation of *M. extorquens* AM1 Δ*cel* + pCM160_RBS_*yciAHI* in a BiostatB® bioreactor system (Sartorius, Göttingen, Germany) with 4-liter starting volume. Methanol concentration at the start was 3.95 g/L and was controlled close to a setpoint of 1 g/L measured via an online methanol sensor. Due to a failure of the data tracker, methanol feeding was not recorded between 17.8 and 76.3 h of cultivation time, indicated by a dashed line. The overall methanol feeding could be reconstructed by determination of the start and end methanol volume in the sealed feeding bottle and the recorded feeding events. The temperature was kept at 30 °C (± 0.01 °C) and pH was kept at 7.0 (± 0.1) with base feeding (15 % [v/v] ammonium hydroxide). The DO setpoint was 30 %.

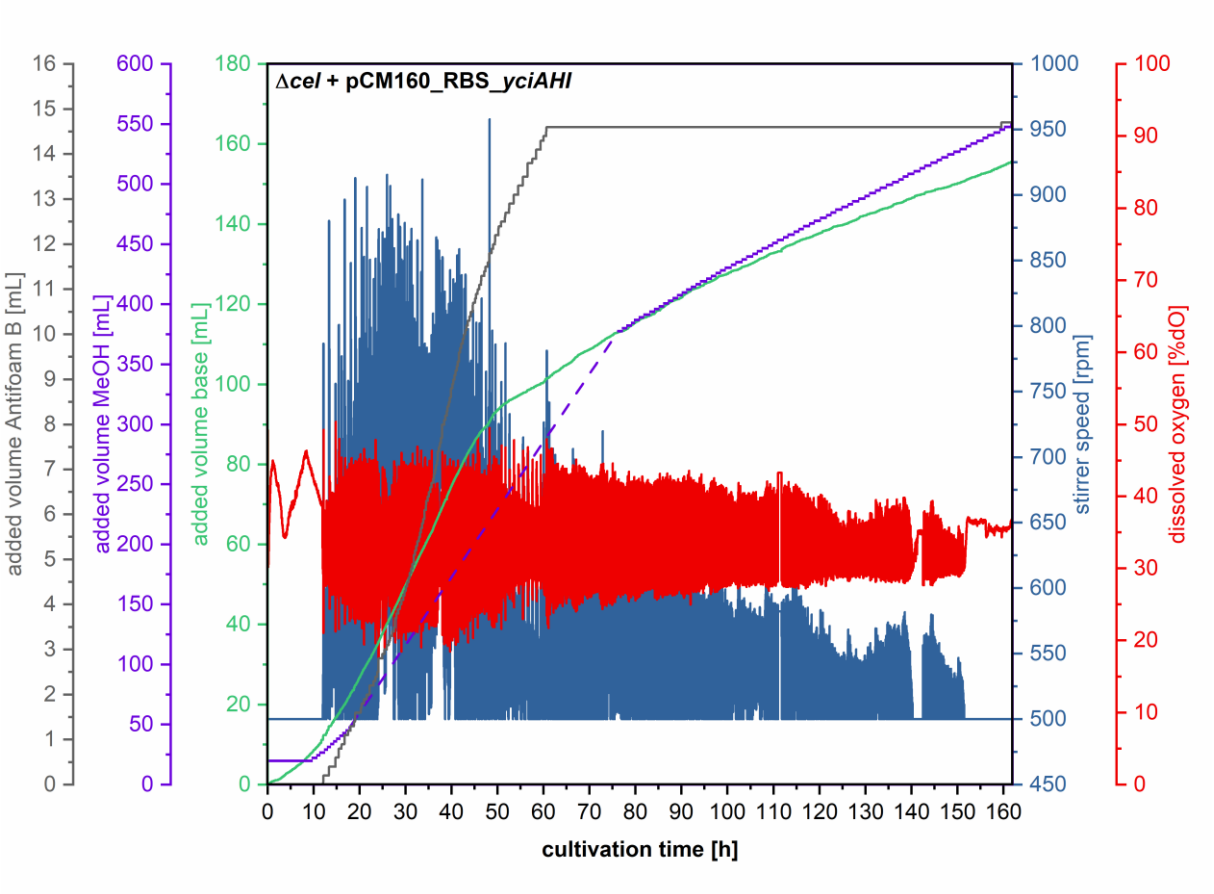

Appendix 4 Parameters of fermentation of *M. extorquens* AM1 Δ*cel* + pCM160 A in a DASGIP® parallel bioreactor system (Eppendorf, Hamburg, Germany) with 700 mL starting volume. Methanol concentration at the start was 3.95 g/L and set back to 3.95 g/L immediately after depletion, which was indicated by a rapid DO-shift. The overall DO setpoint was 30 %. The temperature was kept at 30 °C (± 0.01 °C) and pH was kept at 7.0 (± 0.1) with base feeding (15 % [v/v] ammonium hydroxide). 200 µL of XIAMETER™ ACP-1500 Antifoam Compound (DOW, Midland, USA) was added 52.8 h after inoculation.

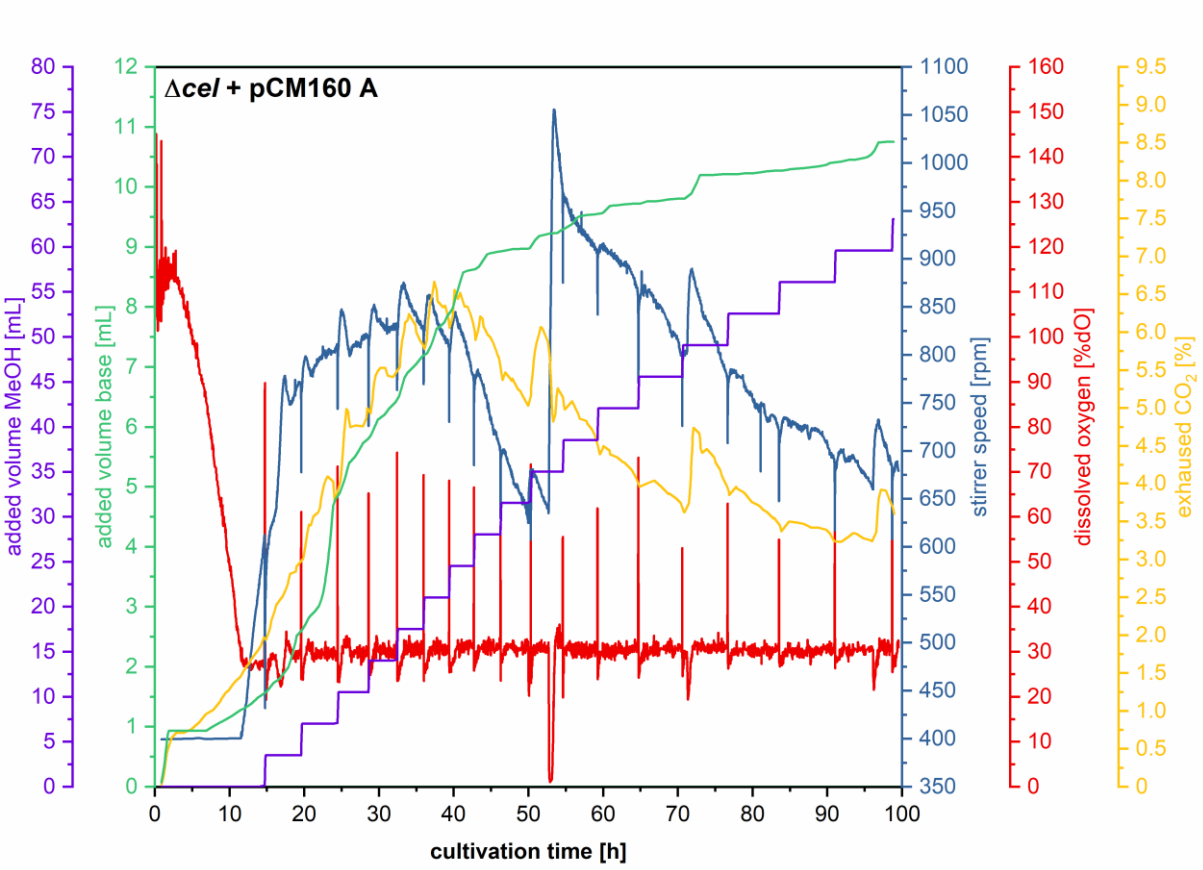

Appendix 5 Parameters of fermentation of *M. extorquens* AM1 Δ*cel* + pCM160 B in a DASGIP® parallel bioreactor system (Eppendorf, Hamburg, Germany) with 700 mL starting volume. Methanol concentration at the start was 3.95 g/L and was set back to 3.95 g/L immediately after depletion, which was indicated by a rapid DO-shift. The overall DO setpoint was 30 %. The temperature was kept at 30 °C (± 0.01 °C) and pH was kept at 7.0 (± 0.1) with base feeding (15 % [v/v] ammonium hydroxide). 200 µL of XIAMETER™ ACP-1500 Antifoam Compound (DOW, Midland, USA) was added 52.8 h after inoculation.

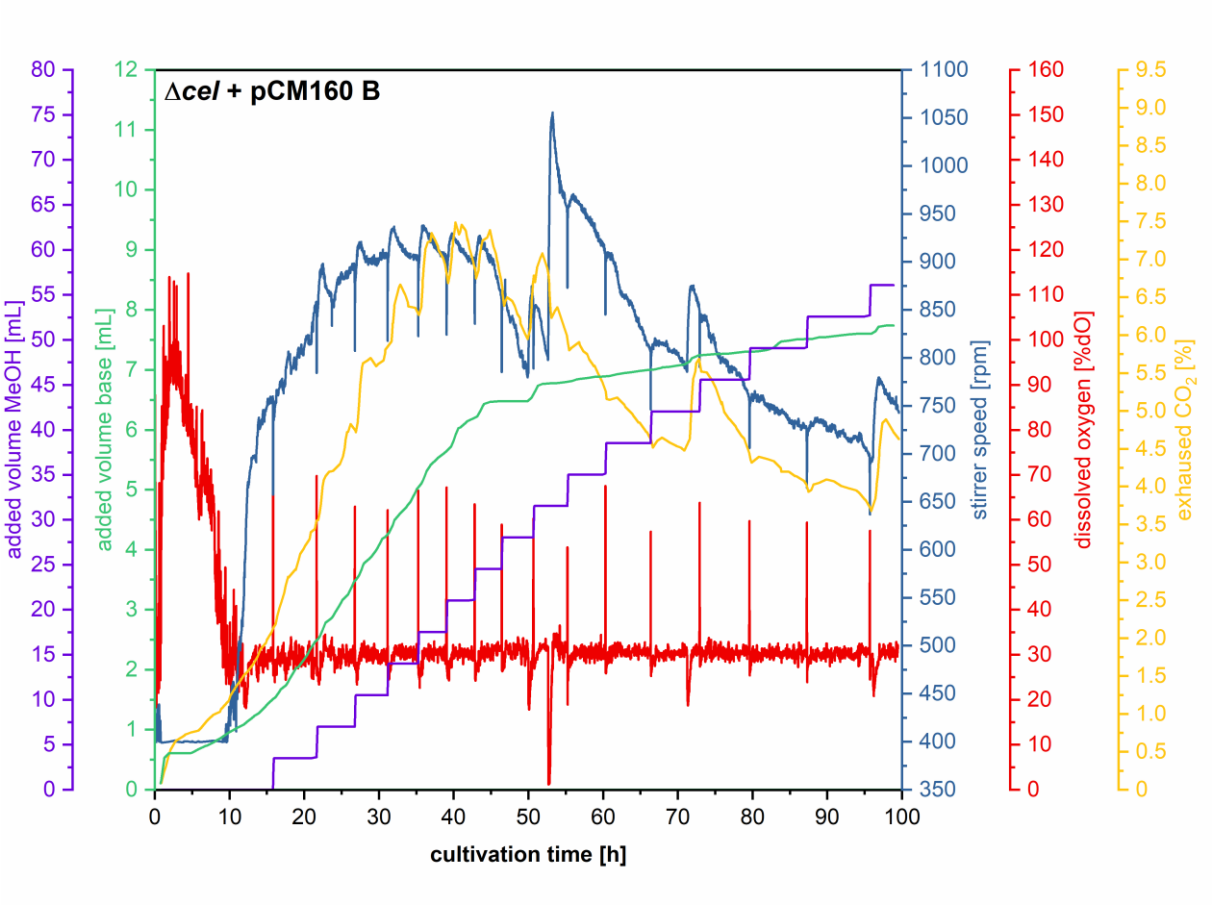

Appendix 6 Parameters of fermentation of *M. extorquens* AM1 Δ*cel* + pCM160 C in a DASGIP® parallel bioreactor system (Eppendorf, Hamburg, Germany) with 700 mL starting volume. Methanol concentration at the start was 3.95 g/L and was set back to 3.95 g/L immediately after depletion, which was indicated by a rapid DO-shift. The overall DO setpoint was 30 %. The temperature was kept at 30 °C (± 0.01 °C) and pH was kept at 7.0 (± 0.1) with base feeding (15 % [v/v] ammonium hydroxide). 200 µL of XIAMETER™ ACP-1500 Antifoam Compound (DOW, Midland, USA) was added 52.8 h after inoculation.

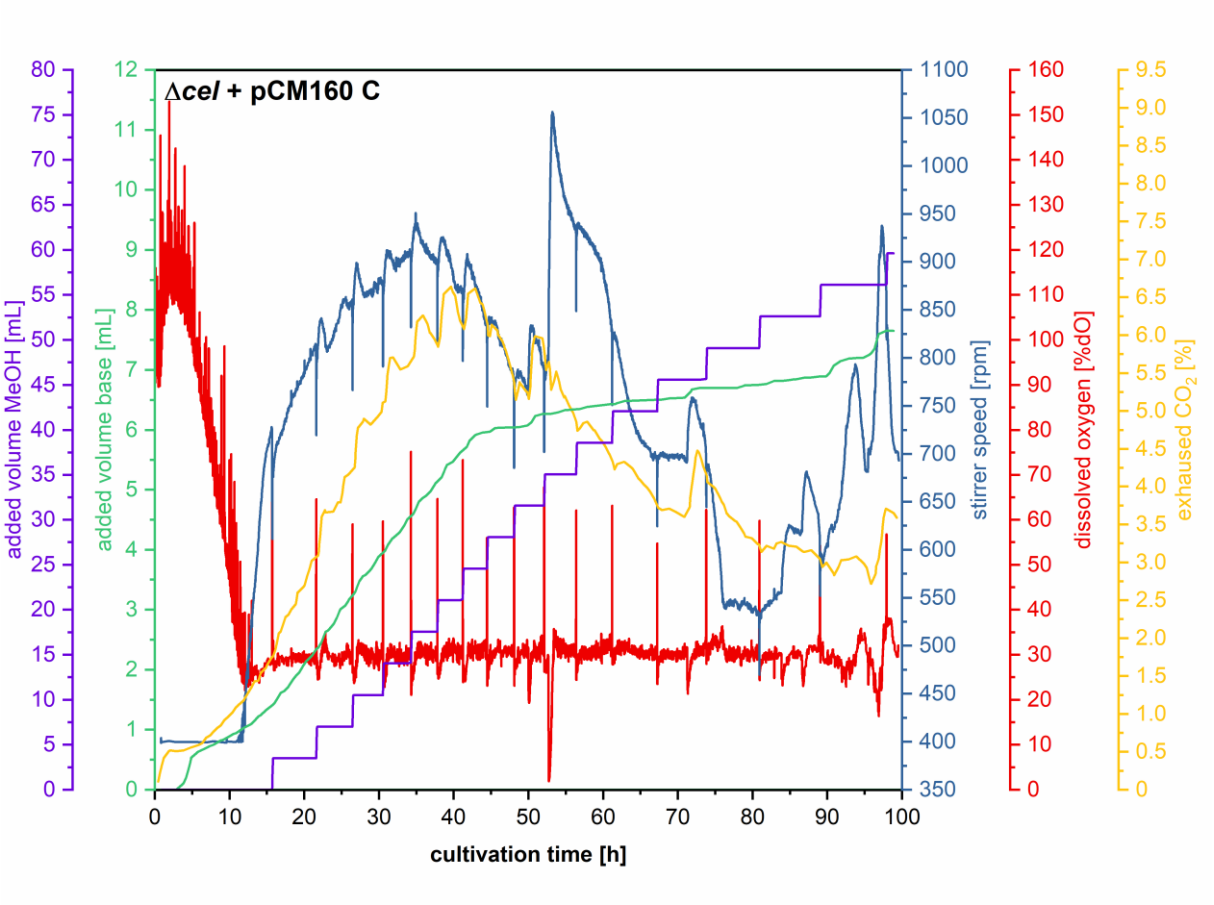

Appendix 7 Parameters of fermentation of *M. extorquens* AM1 Δ*cel* + pCM160 D in a DASGIP® parallel bioreactor system (Eppendorf, Hamburg, Germany) with 700 mL starting volume. Methanol concentration at the start was 3.95 g/L and was set back to 3.95 g/L immediately after depletion, which was indicated by a rapid DO-shift. The overall DO setpoint was 30 %. The temperature was kept at 30 °C (± 0.01 °C) and pH was kept at 7.0 (± 0.1) with base feeding (15 % [v/v] ammonium hydroxide). 200 µL of XIAMETER™ ACP-1500 Antifoam Compound (DOW, Midland, USA) was added 52.8 h after inoculation.

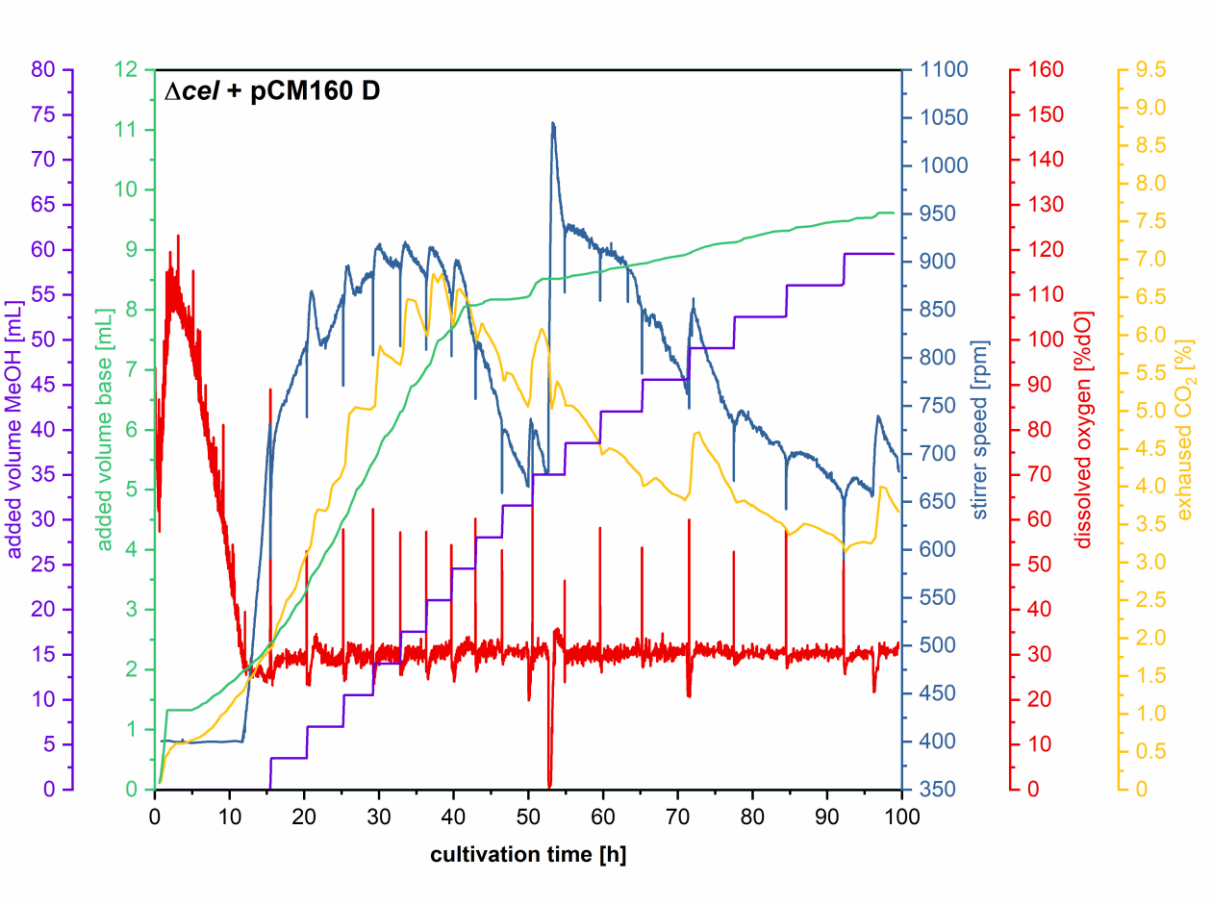

Appendix 8 Parameters of fermentation of *M. extorquens* AM1 Δ*cel* + pCM160_RBS_*yciAHI* A in a DASGIP® parallel bioreactor system (Eppendorf, Hamburg, Germany) with 700 mL starting volume. Methanol concentration at the start was 3.95 g/L and was set back to 3.95 g/L immediately after depletion, which was indicated by a rapid DO-shift. The overall DO setpoint was 30 %. The temperature was kept at 30 °C (± 0.01 °C) and pH was kept at 7.0 (± 0.1) with base feeding (15 % [v/v] ammonium hydroxide). 200 µL of XIAMETER™ ACP-1500 Antifoam Compound (DOW, Midland, USA) was added 21.5, 22.9 and 60.7 h after inoculation.

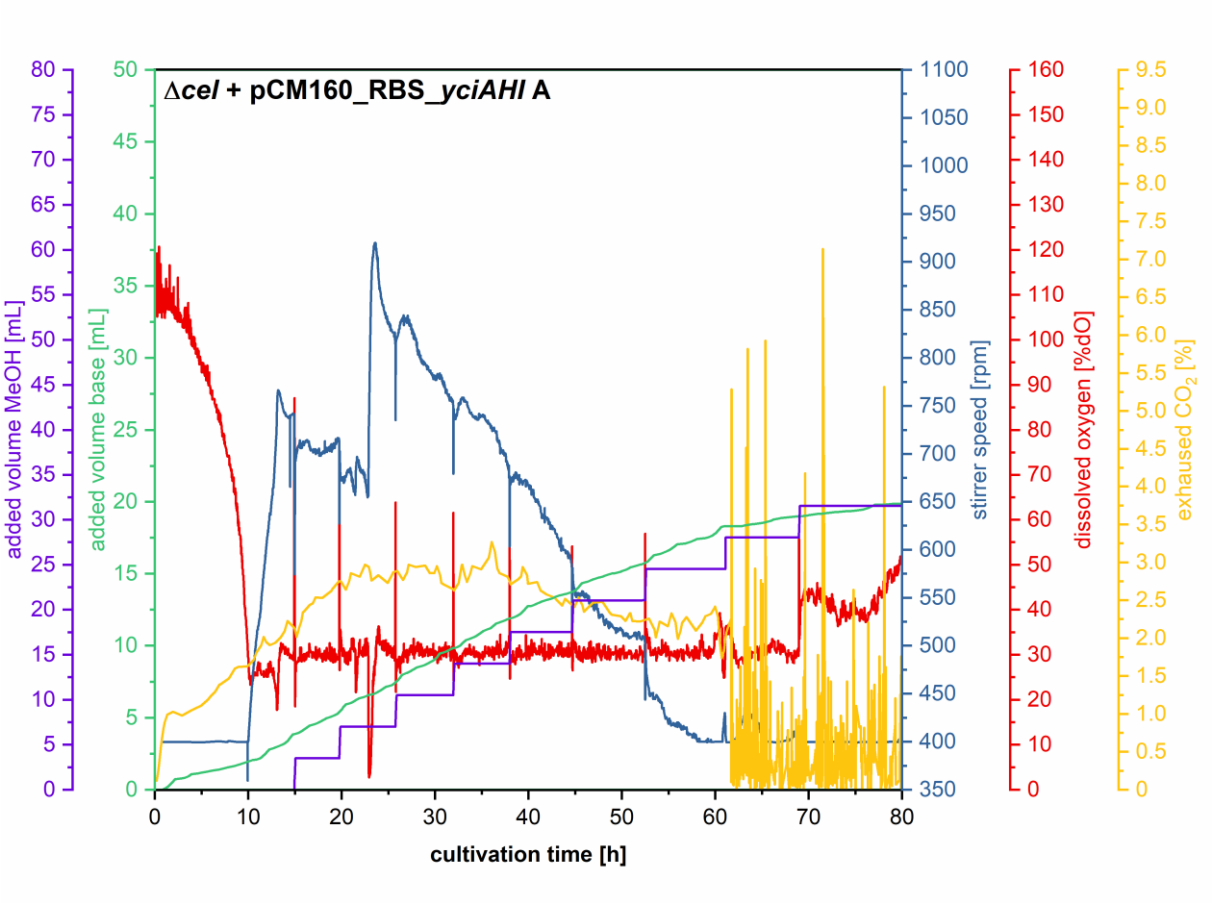

Appendix 9 Parameters of fermentation of *M. extorquens* AM1 Δ*cel* + pCM160_RBS_*yciAHI* B in a DASGIP® parallel bioreactor system (Eppendorf, Hamburg, Germany) with 700 mL starting volume. Methanol concentration at the start was 3.95 g/L and was set back to 3.95 g/L immediately after depletion, which was indicated by a rapid DO-shift. The overall DO setpoint was 30 %. The temperature was kept at 30 °C (± 0.01 °C) and pH was kept at 7.0 (± 0.1) with base feeding (15 % [v/v] ammonium hydroxide). 200 µL of XIAMETER™ ACP-1500 Antifoam Compound (DOW, Midland, USA) was added 21.5, 22.9 and 60.7 h after inoculation.

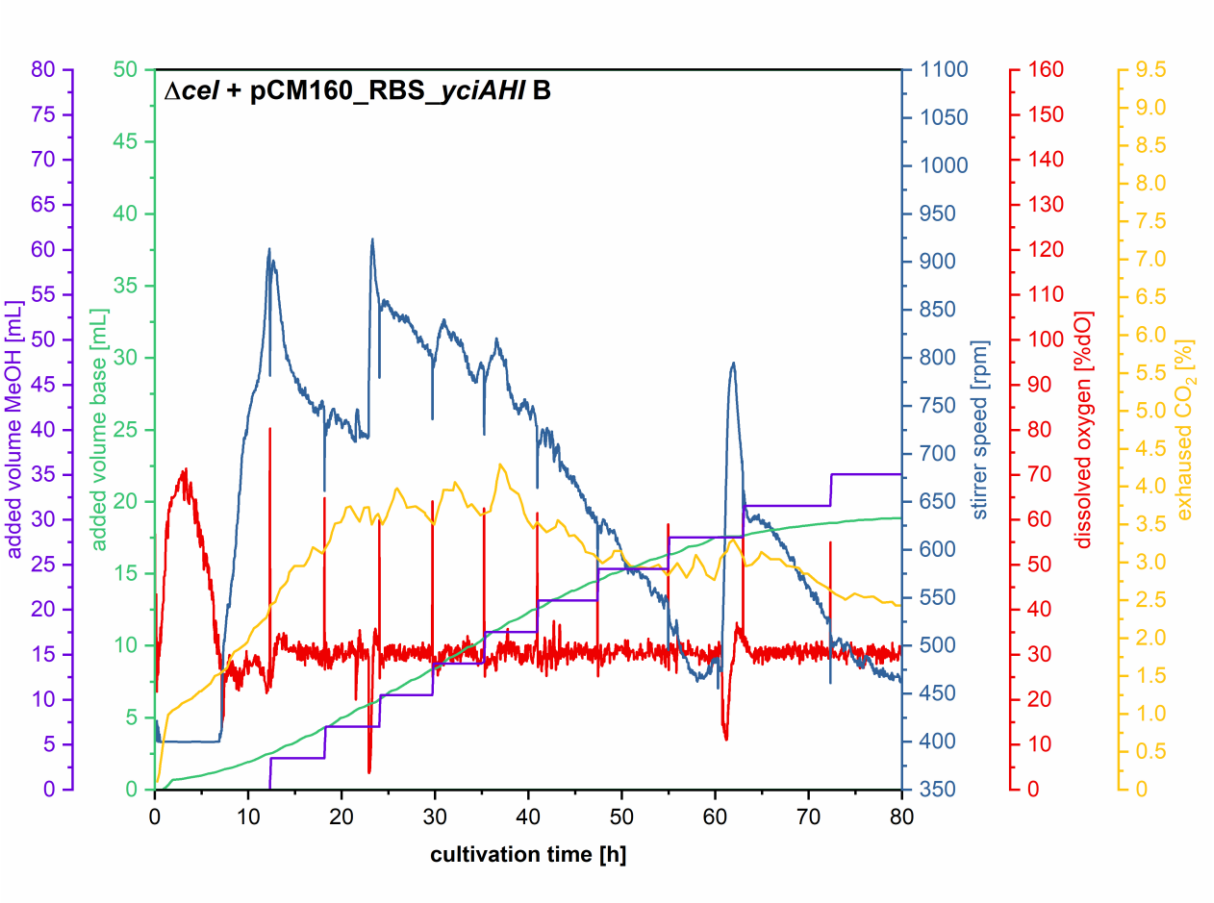

Appendix 10 Parameters of fermentation of *M. extorquens* AM1 Δ*cel* + pCM160_RBS_*yciAHI* B in a DASGIP® parallel bioreactor system (Eppendorf, Hamburg, Germany) with 700 mL starting volume. Methanol concentration at the start was 3.95 g/L and was set back to 3.95 g/L immediately after depletion, which was indicated by a rapid DO-shift. The overall DO setpoint was 30 %. The temperature was kept at 30 °C (± 0.01 °C) and pH was kept at 7.0 (± 0.1) with base feeding (15 % [v/v] ammonium hydroxide). 200 µL of XIAMETER™ ACP-1500 Antifoam Compound (DOW, Midland, USA) was added 60.3 h after inoculation.

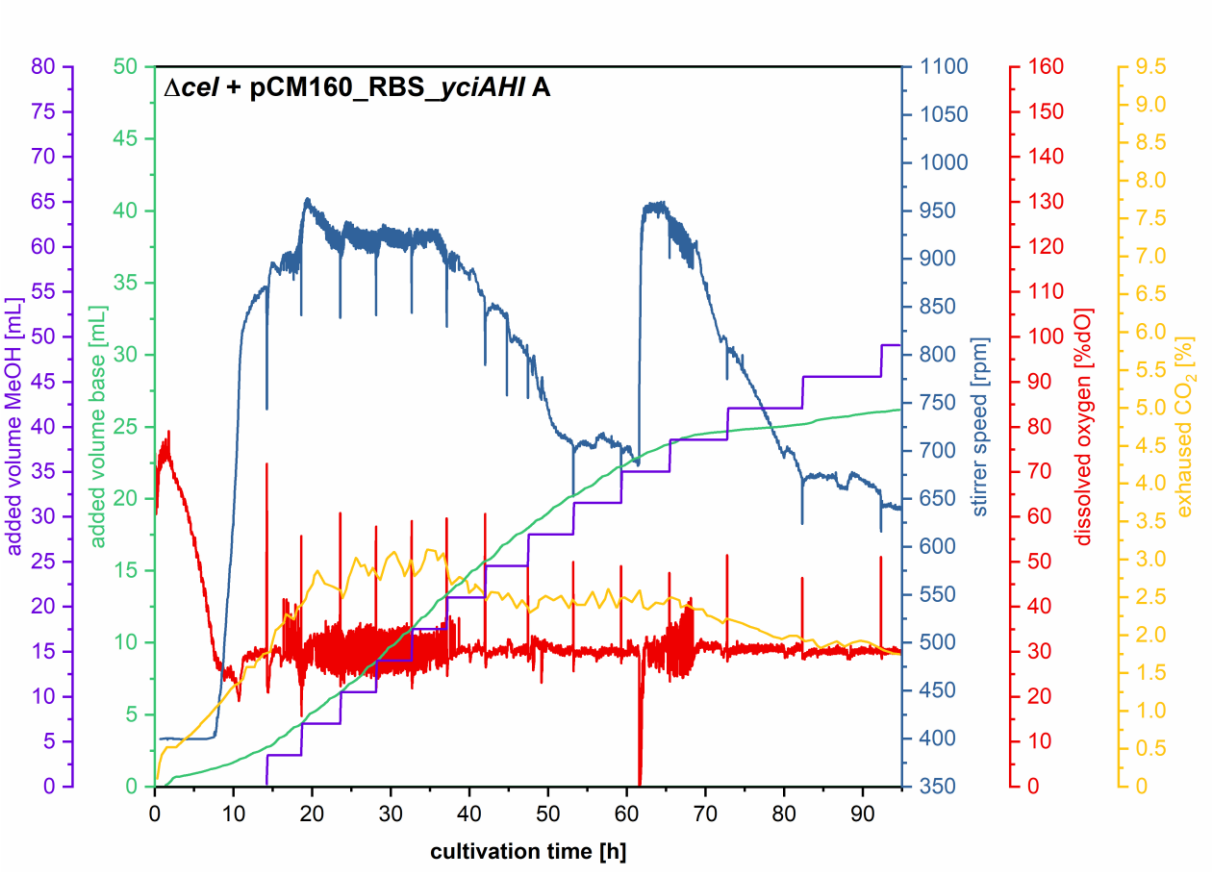

Appendix 11 Parameters of fermentation of *M. extorquens* AM1 Δ*cel* + pCM160_RBS_*yciAHI* B in a DASGIP® parallel bioreactor system (Eppendorf, Hamburg, Germany) with 700 mL starting volume. Methanol concentration at the start was 3.95 g/L and was set back to 3.95 g/L immediately after depletion, which was indicated by a rapid DO-shift. The overall DO setpoint was 30 %. The temperature was kept at 30 °C (± 0.01 °C) and pH was kept at 7.0 (± 0.1) with base feeding (15 % [v/v] ammonium hydroxide). 200 µL of XIAMETER™ ACP-1500 Antifoam Compound (DOW, Midland, USA) was added 60.3 h after inoculation.

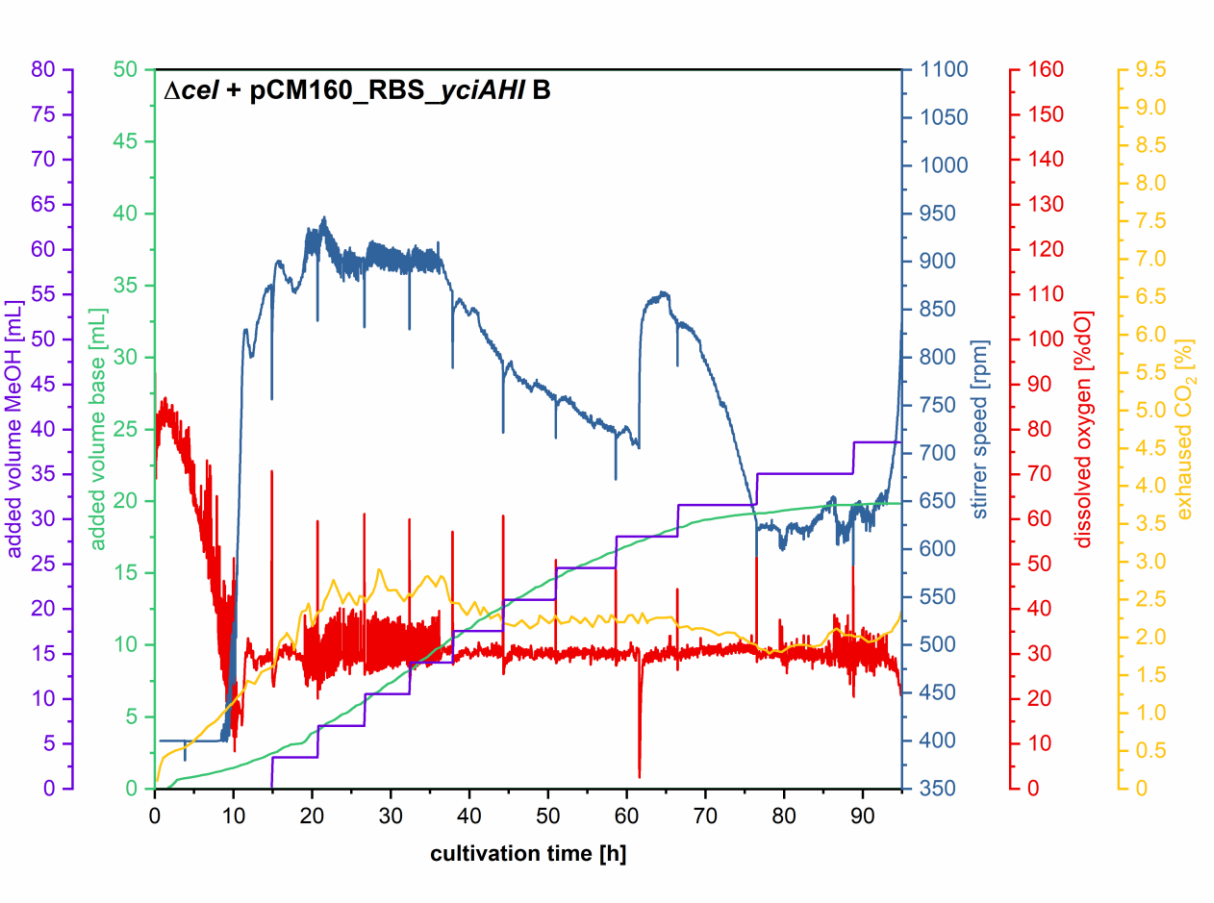

Appendix 12 Parameters of fermentation of *M. extorquens* AM1 Δ*cel* + pCM160_RBS_*yciAEc* A in a DASGIP® parallel bioreactor system (Eppendorf, Hamburg, Germany) with 700 mL starting volume. Methanol concentration at the start was 3.95 g/L and was set back to 3.95 g/L immediately after depletion, which was indicated by a rapid DO-shift. The overall DO setpoint was 30 %. The temperature was kept at 30 °C (± 0.01 °C) and pH was kept at 7.0 (± 0.1) with base feeding (15 % [v/v] ammonium hydroxide). 200 µL of XIAMETER™ ACP-1500 Antifoam Compound (DOW, Midland, USA) was added 43.5 h, 67.5 h and 98.5 h after inoculation.

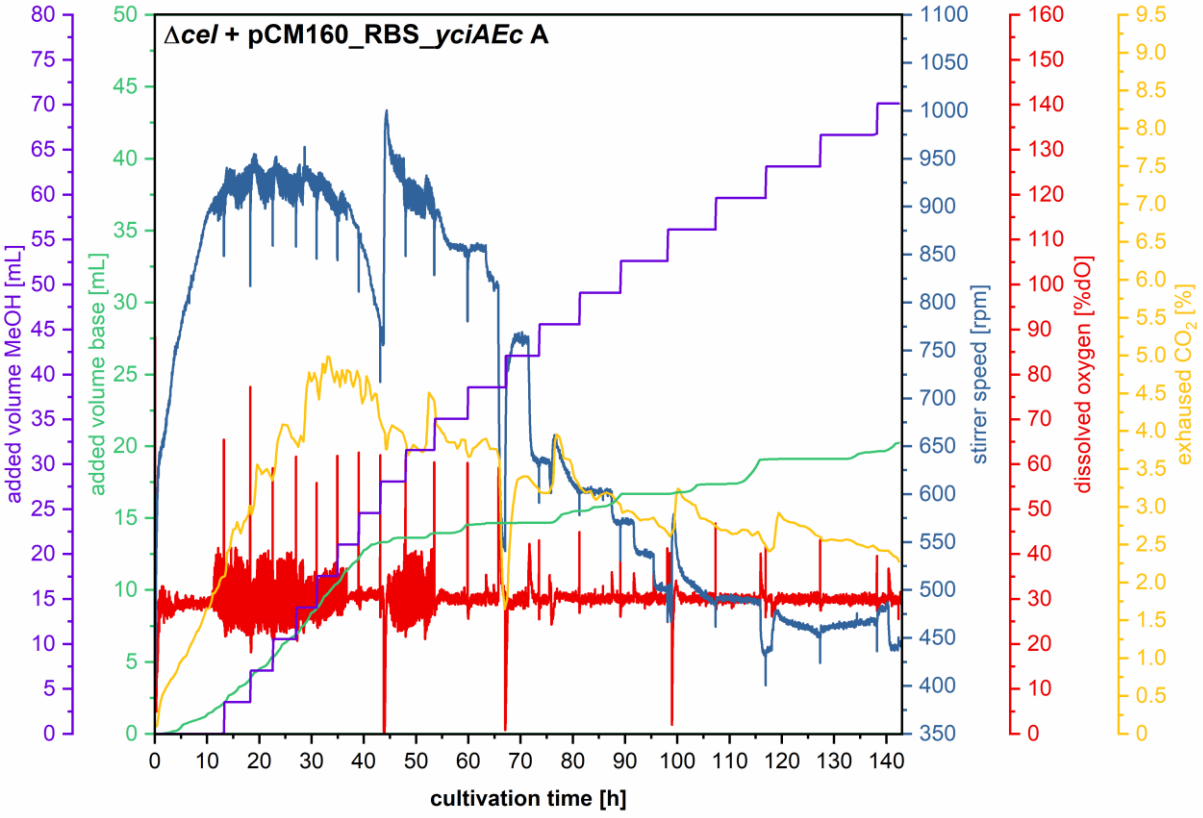

Appendix 13 Parameters of fermentation of *M. extorquens* AM1 Δ*cel* + pCM160_RBS_*yciAEc* B in a DASGIP® parallel bioreactor system (Eppendorf, Hamburg, Germany) with 700 mL starting volume. Methanol concentration at the start was 3.95 g/L and was set back to 3.95 g/L immediately after depletion, which was indicated by a rapid DO-shift. The overall DO setpoint was 30 %. The temperature was kept at 30 °C (± 0.01 °C) and pH was kept at 7.0 (± 0.1) with base feeding (15 % [v/v] ammonium hydroxide). 200 µL of XIAMETER™ ACP-1500 Antifoam Compound (DOW, Midland, USA) was added 43.5 h, 67.5 h and 98.5 h after inoculation.

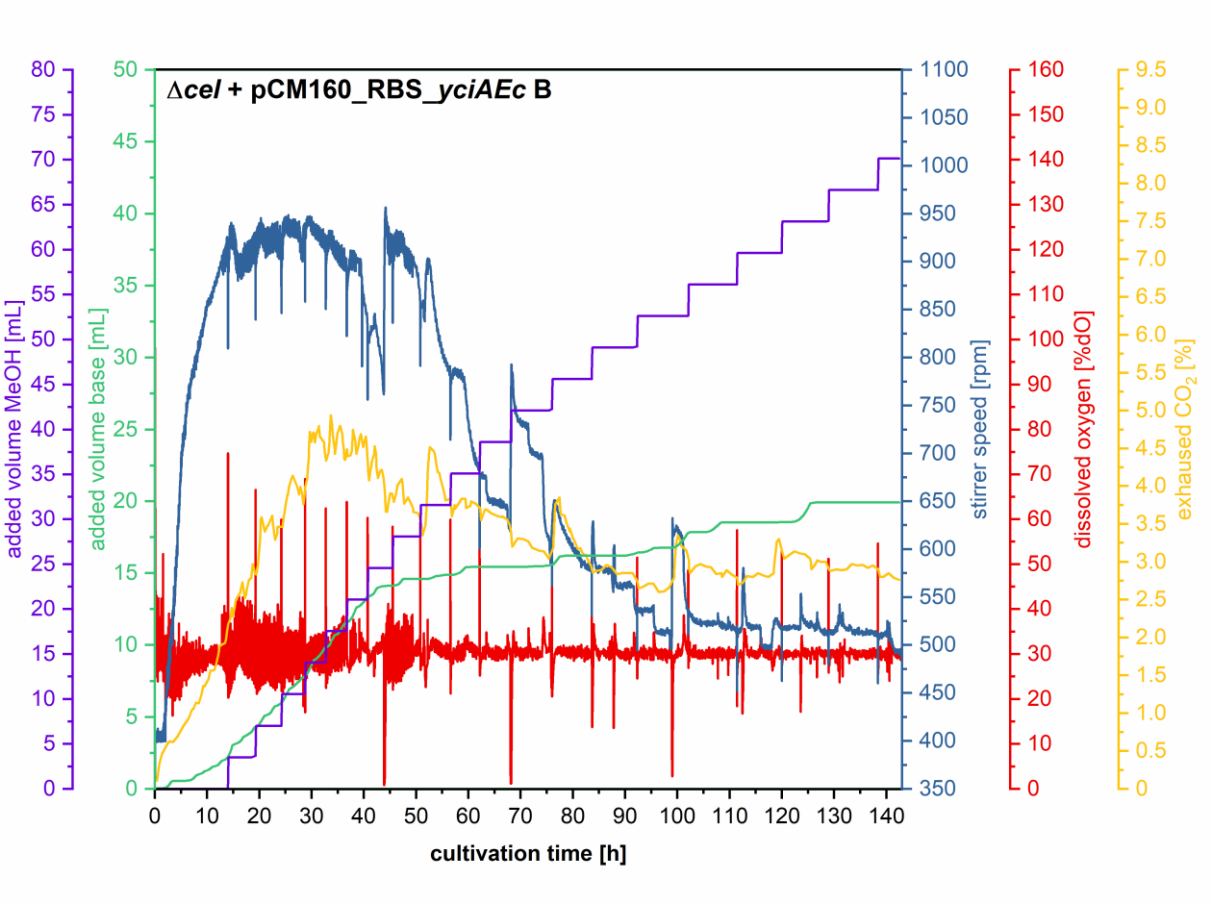

Appendix 14 Parameters of fermentation of *M. extorquens* AM1 Δ*cel* Δ*dctA1* Δ*dctA2* Δ*dctA3* + pCM160_RBS_*yciAHI* A in a DASGIP® parallel bioreactor system (Eppendorf, Hamburg, Germany) with 700 mL starting volume. Methanol concentration at the start was 3.95 g/L and was set back to 3.95 g/L immediately after depletion, which was indicated by a rapid DO-shift. The overall DO setpoint was 30 %. The temperature was kept at 30 °C (± 0.01 °C) and pH was kept at 7.0 (± 0.1) with base feeding (15 % [v/v] ammonium hydroxide). 200 µL of XIAMETER™ ACP-1500 Antifoam Compound (DOW, Midland, USA) was added 60.5 h after inoculation.

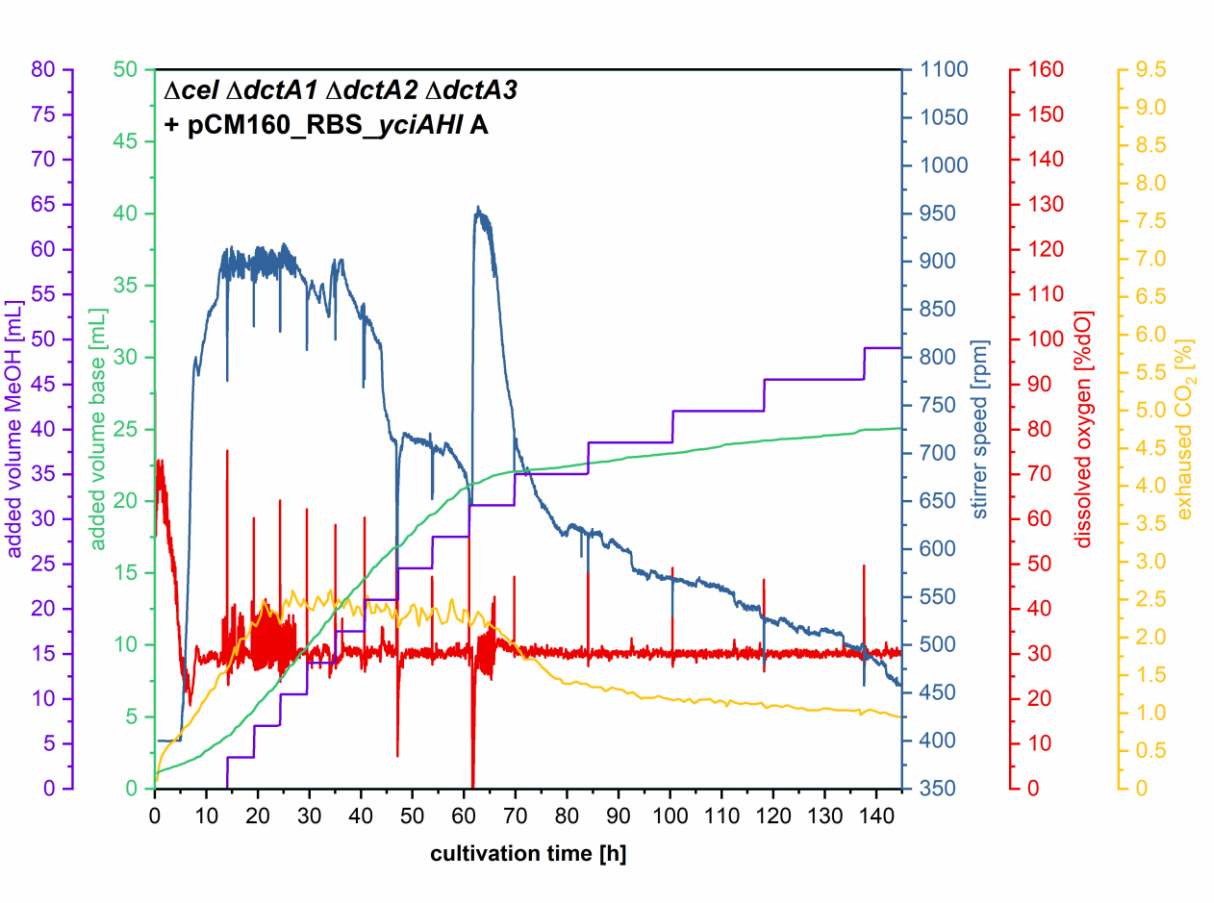

Appendix 15 Parameters of fermentation of *M. extorquens* AM1 Δ*cel* Δ*dctA1* Δ*dctA2* Δ*dctA3* + pCM160_RBS_*yciAHI* B in a DASGIP® parallel bioreactor system (Eppendorf, Hamburg, Germany) with 700 mL starting volume. Methanol concentration at the start was 3.95 g/L and was set back to 3.95 g/L immediately after depletion, which was indicated by a rapid DO-shift. The overall DO setpoint was 30 %. The temperature was kept at 30 °C (± 0.01 °C) and pH was kept at 7.0 (± 0.1) with base feeding (15 % [v/v] ammonium hydroxide). 200 µL of XIAMETER™ ACP-1500 Antifoam Compound (DOW, Midland, USA) was added 60.5 h after inoculation.

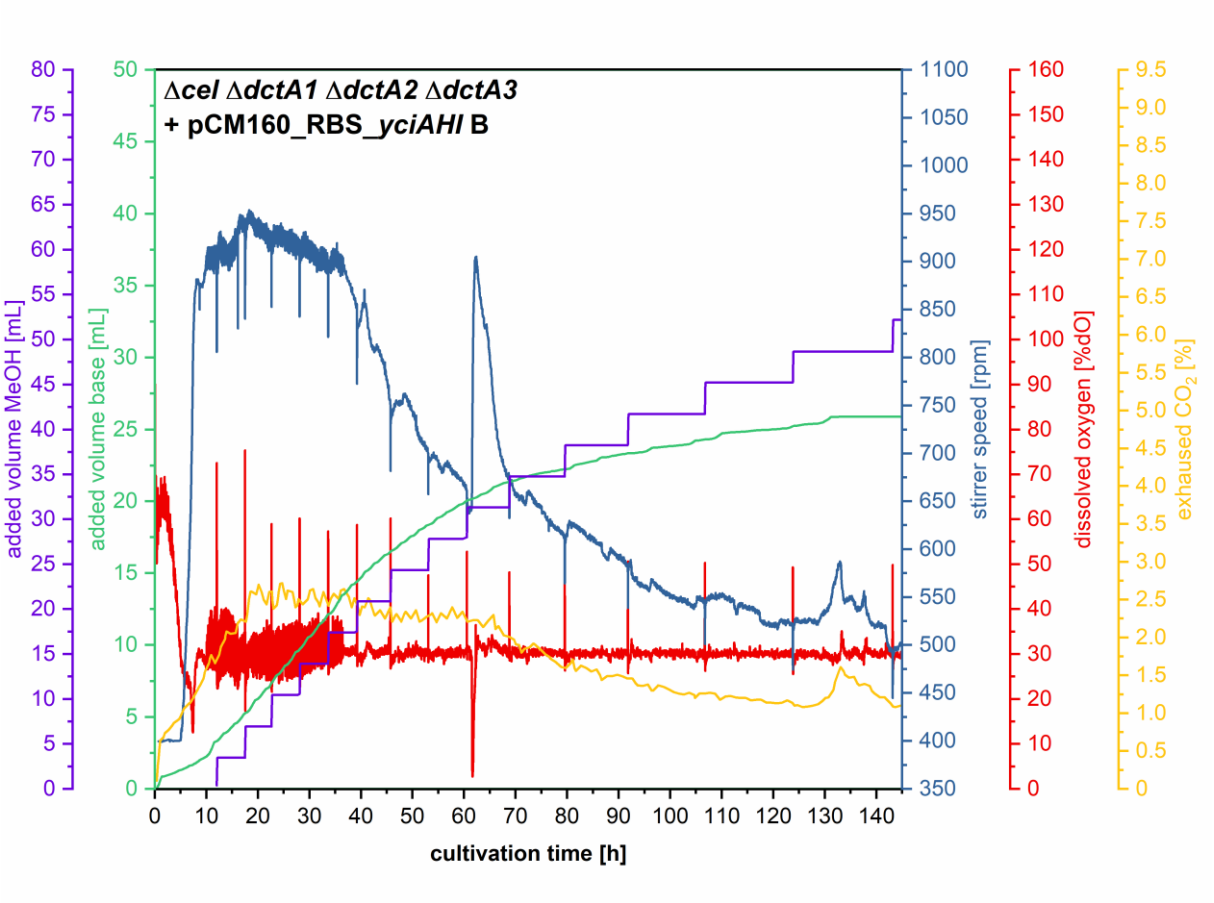

Appendix 16 Parameters of fermentation of *M. extorquens* AM1 Δ*cel* + pCM160_RBS_*yciAEc_mesaPx* A in a DASGIP® parallel bioreactor system (Eppendorf, Hamburg, Germany) with 700 mL starting volume. Methanol concentration at the start was 3.95 g/L and was set back to 3.95 g/L immediately after depletion, which was indicated by a rapid DO-shift. The overall DO setpoint was 30 %. The temperature was kept at 30 °C (± 0.01 °C) and pH was kept at 7.0 (± 0.1) with base feeding (15 % [v/v] ammonium hydroxide).

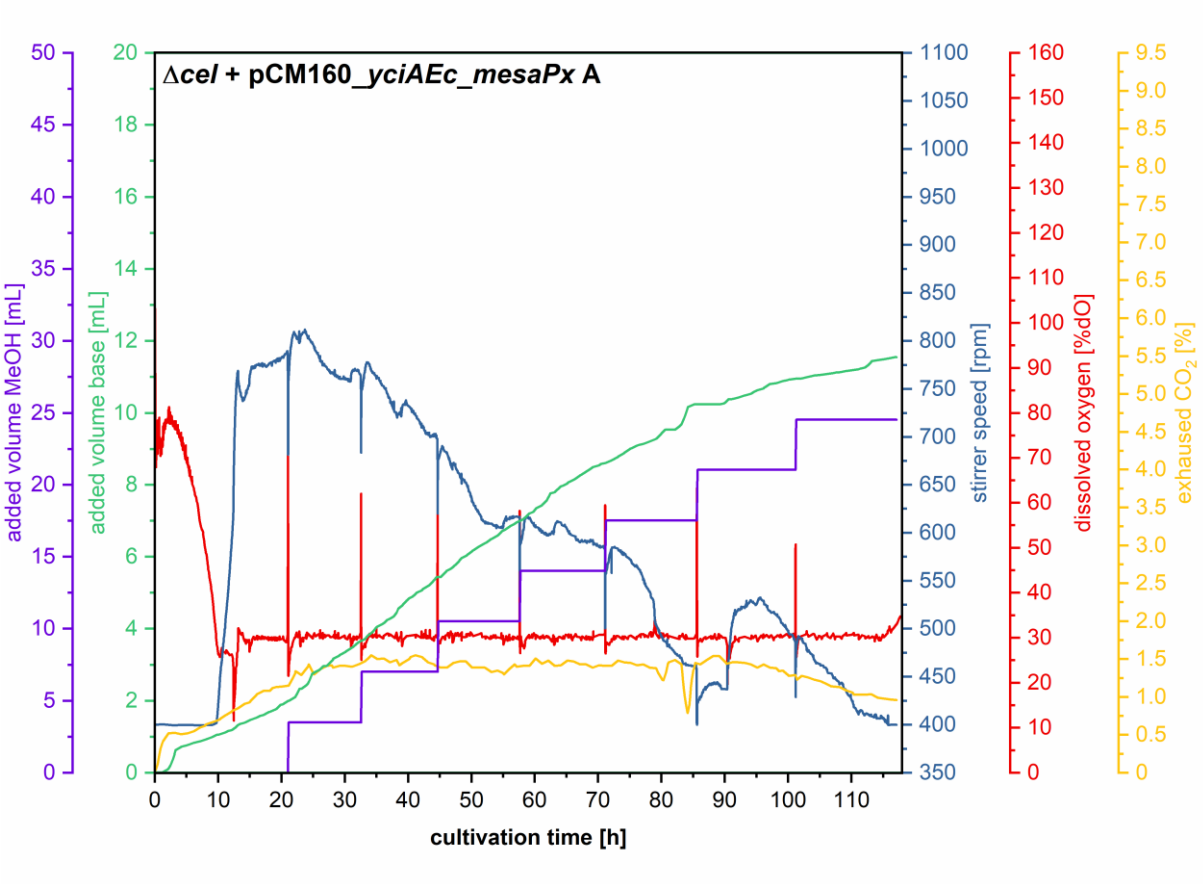

Appendix 17 Parameters of fermentation of *M. extorquens* AM1 Δ*cel* + pCM160_RBS_*yciAEc_mesaPx* B in a DASGIP® parallel bioreactor system (Eppendorf, Hamburg, Germany) with 700 mL starting volume. Methanol concentration at the start was 3.95 g/L and was set back to 3.95 g/L immediately after depletion, which was indicated by a rapid DO-shift. The overall DO setpoint was 30 %. The temperature was kept at 30 °C (± 0.01 °C) and pH was kept at 7.0 (± 0.1) with base feeding (15 % [v/v] ammonium hydroxide).

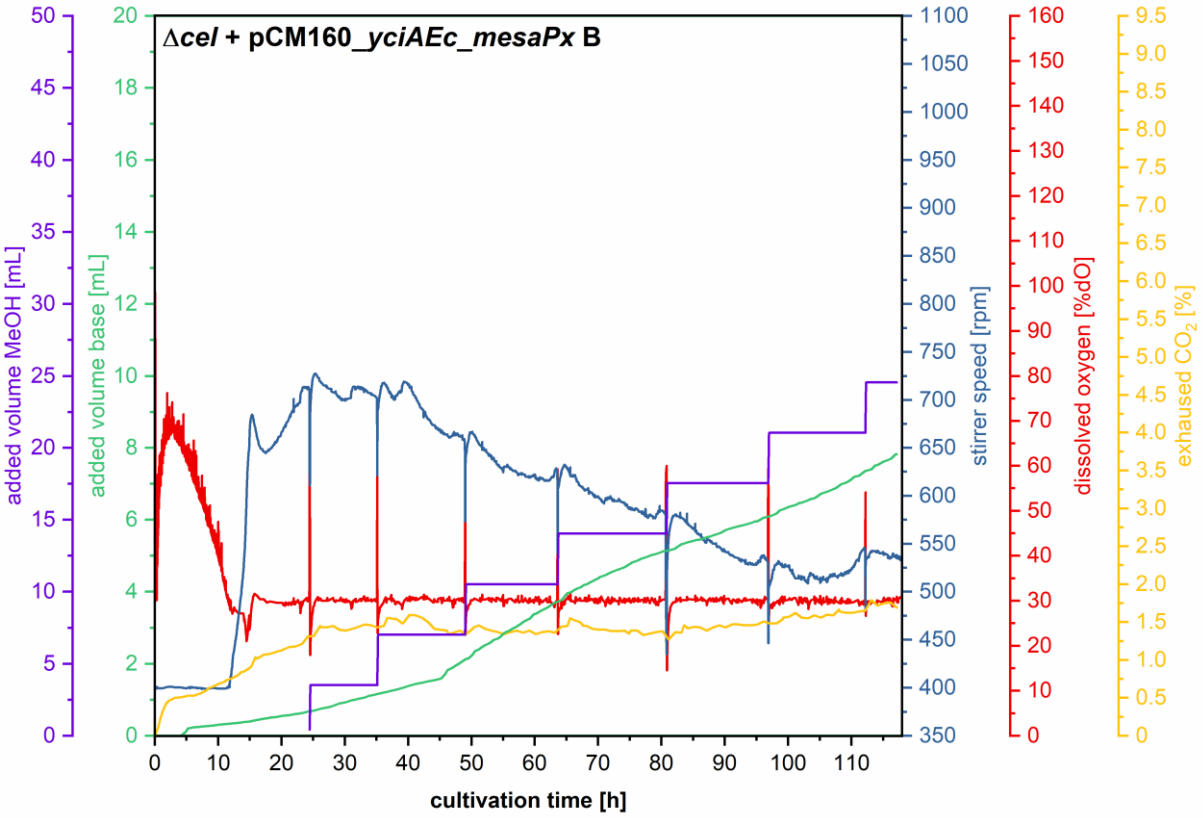

Appendix 18 Parameters of fermentation of *M. extorquens* AM1 Δ*cel* + pCM160_RBS_*CitECg* A in a DASGIP® parallel bioreactor system (Eppendorf, Hamburg, Germany) with 700 mL starting volume. Methanol concentration at the start was 3.95 g/L and was set back to 3.95 g/L immediately after depletion, which was indicated by a rapid DO-shift. The overall DO setpoint was 30 %. The temperature was kept at 30 °C (± 0.01 °C) and pH was kept at 7.0 (± 0.1) with base feeding (15 % [v/v] ammonium hydroxide).

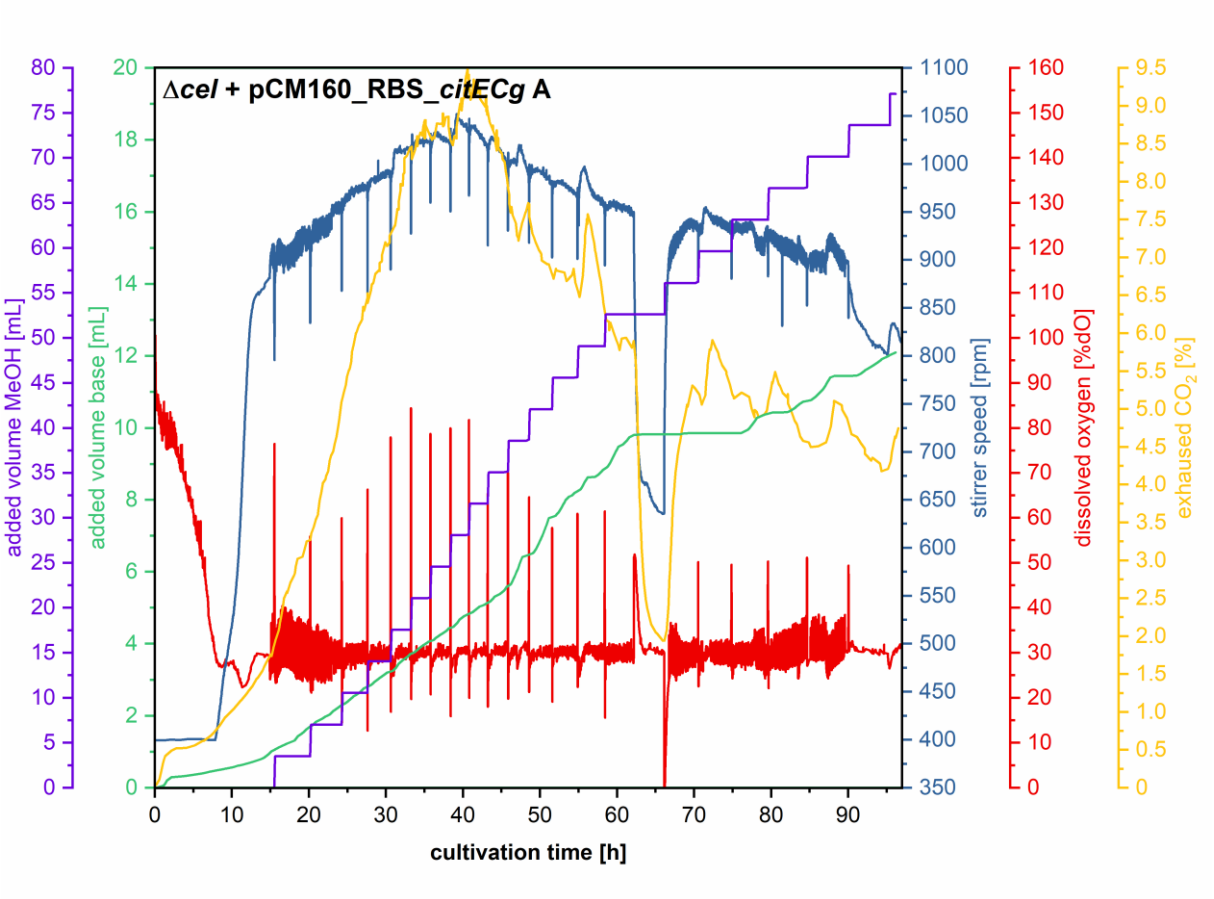

Appendix 19 Parameters of fermentation of *M. extorquens* AM1 Δ*cel* + pCM160_RBS_*CitECg* B in a DASGIP® parallel bioreactor system (Eppendorf, Hamburg, Germany) with 700 mL starting volume. Methanol concentration at the start was 3.95 g/L and was set back to 3.95 g/L immediately after depletion, which was indicated by a rapid DO-shift. The overall DO setpoint was 30 %. The temperature was kept at 30 °C (± 0.01 °C) and pH was kept at 7.0 (± 0.1) with base feeding (15 % [v/v] ammonium hydroxide).

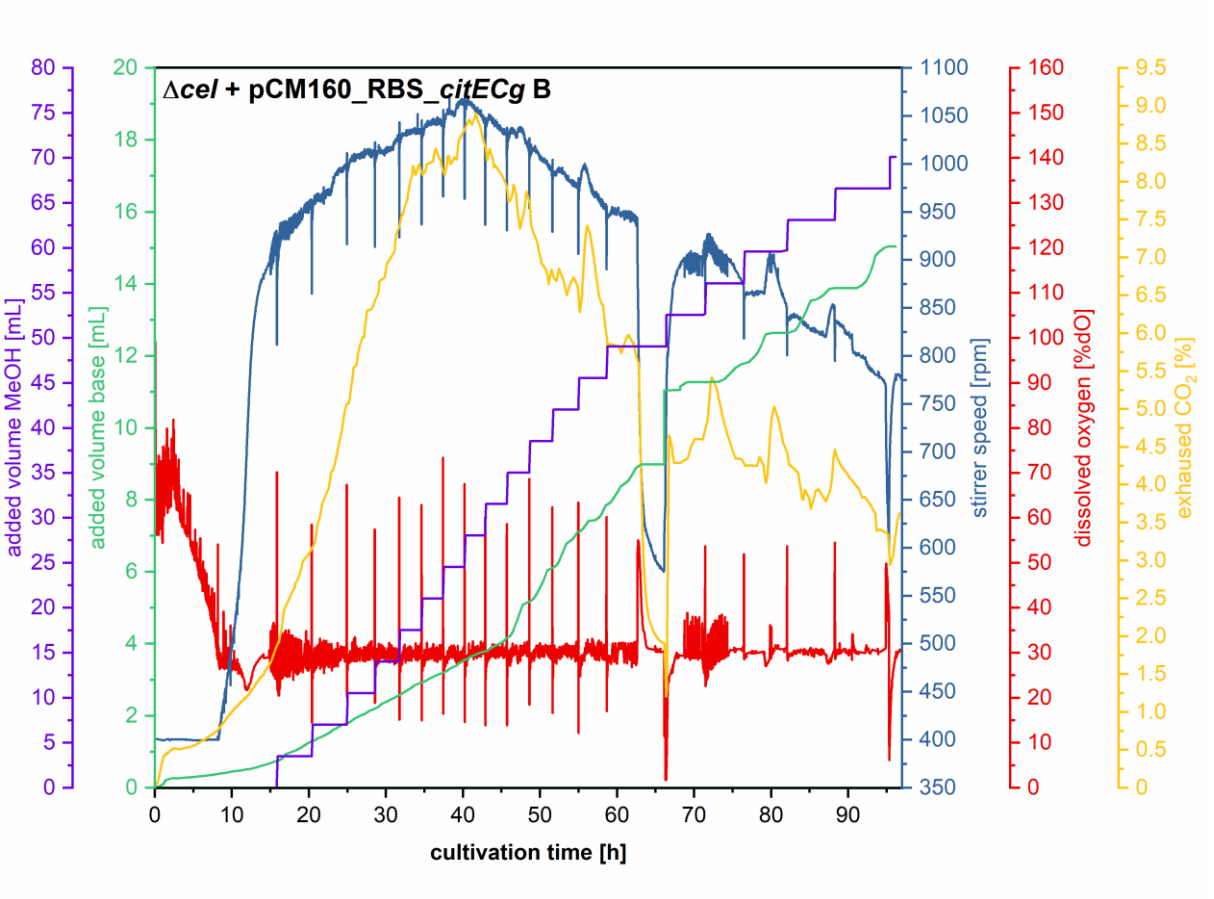

Appendix 20 Parameters of fermentation of *M. extorquens* AM1 Δ*cel* + pCM160_RBS_*CitECg* A in a DASGIP® parallel bioreactor system (Eppendorf, Hamburg, Germany) with 700 mL starting volume. Methanol concentration at the start was 3.95 g/L and was set back to 3.95 g/L immediately after depletion, which was indicated by a rapid DO-shift. The overall DO setpoint was 30 %. The temperature was kept at 30 °C (± 0.01 °C) and pH was kept at 7.0 (± 0.1) with base feeding (15 % [v/v] ammonium hydroxide).

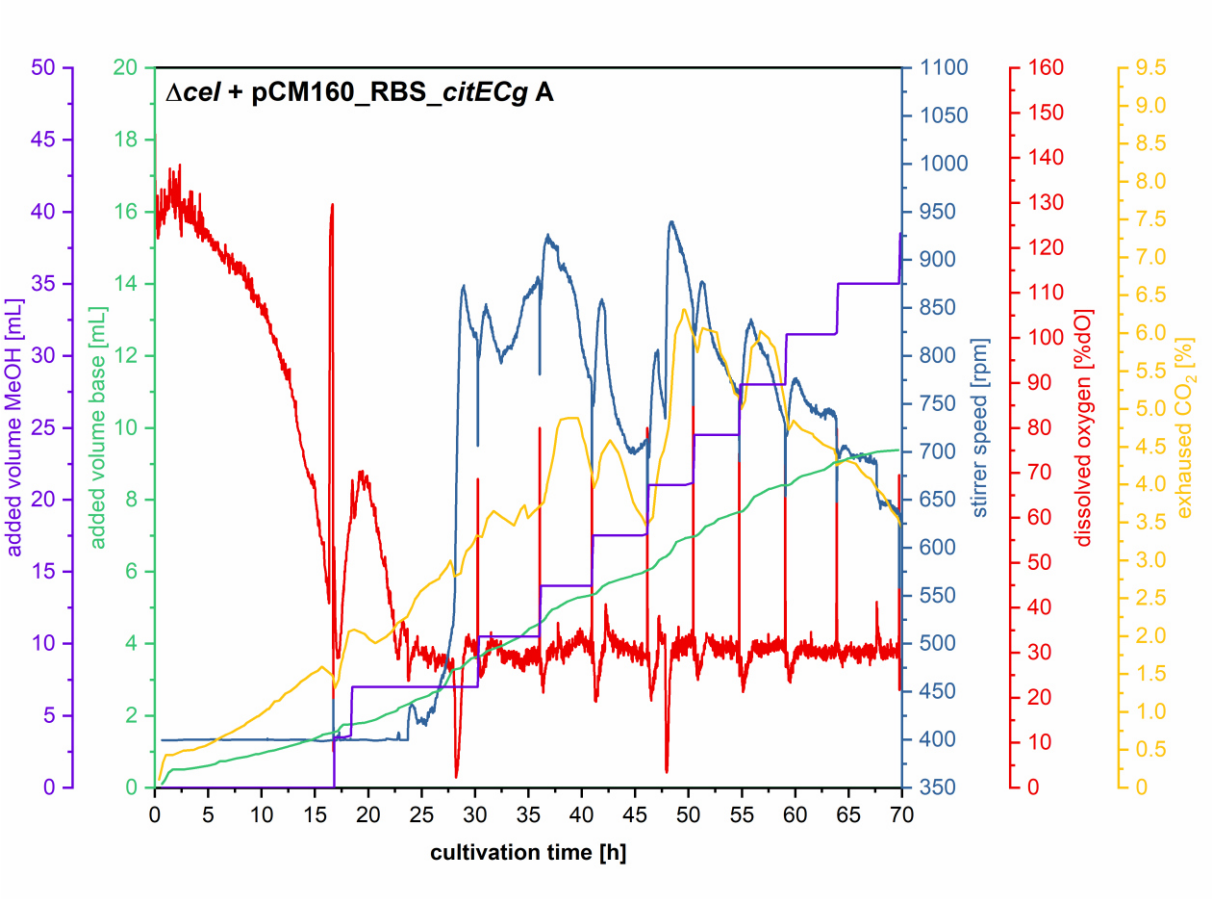

Appendix 21 Parameters of fermentation of *M. extorquens* AM1 Δ*cel* + pCM160_RBS_*CitECg* B in a DASGIP® parallel bioreactor system (Eppendorf, Hamburg, Germany) with 700 mL starting volume. Methanol concentration at the start was 3.95 g/L and was set back to 3.95 g/L immediately after depletion, which was indicated by a rapid DO-shift. The overall DO setpoint was 30 %. The temperature was kept at 30 °C (± 0.01 °C) and pH was kept at 7.0 (± 0.1) with base feeding (15 % [v/v] ammonium hydroxide).

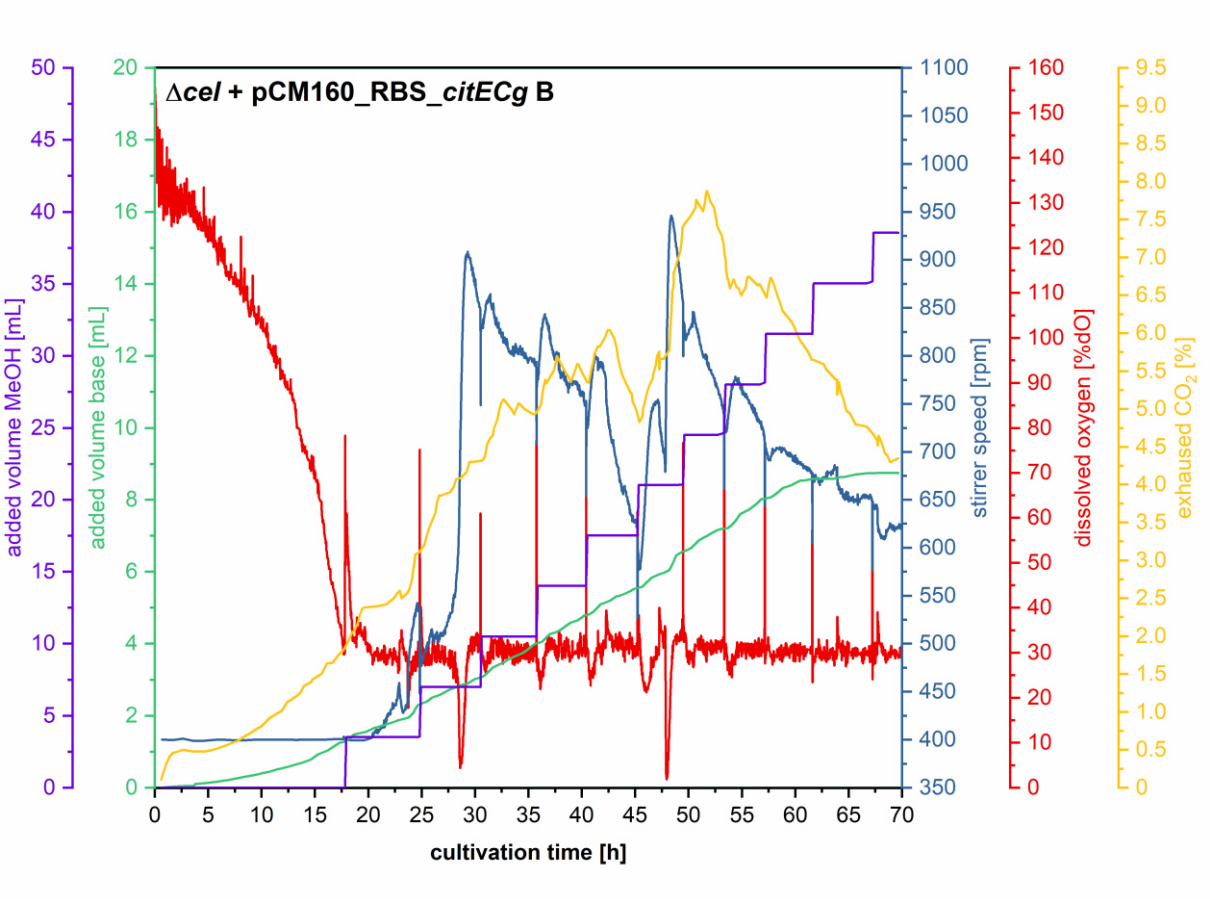

Appendix 22 Parameters of fermentation of *M. extorquens* AM1 Δ*cel* + pCM160_RBS_*CitECg* C in a DASGIP® parallel bioreactor system (Eppendorf, Hamburg, Germany) with 700 mL starting volume. Methanol concentration at the start was 3.95 g/L and was set back to 3.95 g/L immediately after depletion, which was indicated by a rapid DO-shift. The overall DO setpoint was 30 %. The temperature was kept at 30 °C (± 0.01 °C) and pH was kept at 7.0 (± 0.1) with base feeding (15 % [v/v] ammonium hydroxide).

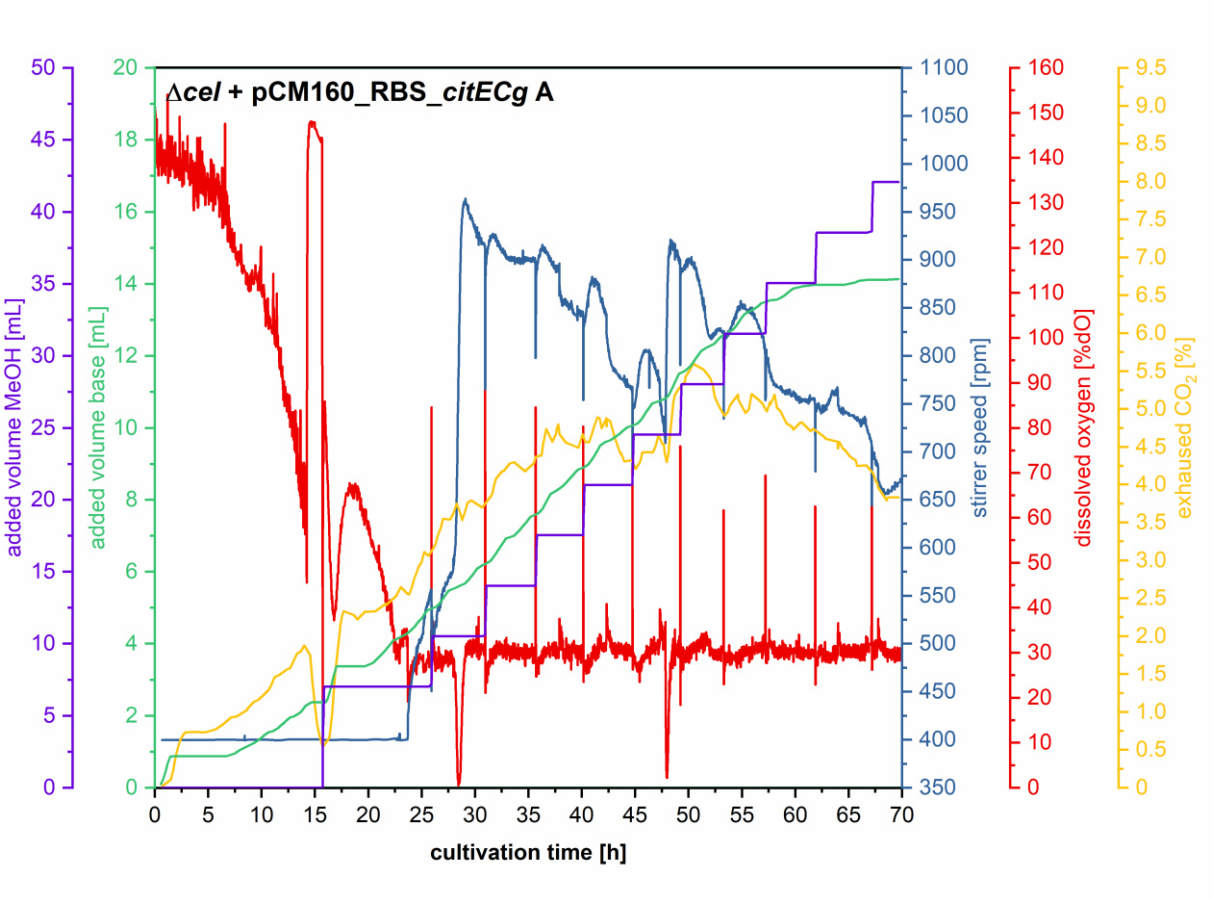

Appendix 23 Parameters of fermentation of *M. extorquens* AM1 Δ*cel* + pCM160_RBS_*CitECg* D in a DASGIP® parallel bioreactor system (Eppendorf, Hamburg, Germany) with 700 mL starting volume. Methanol concentration at the start was 3.95 g/L and was set back to 3.95 g/L immediately after depletion, which was indicated by a rapid DO-shift. The overall DO setpoint was 30 %. The temperature was kept at 30 °C (± 0.01 °C) and pH was kept at 7.0 (± 0.1) with base feeding (15 % [v/v] ammonium hydroxide).

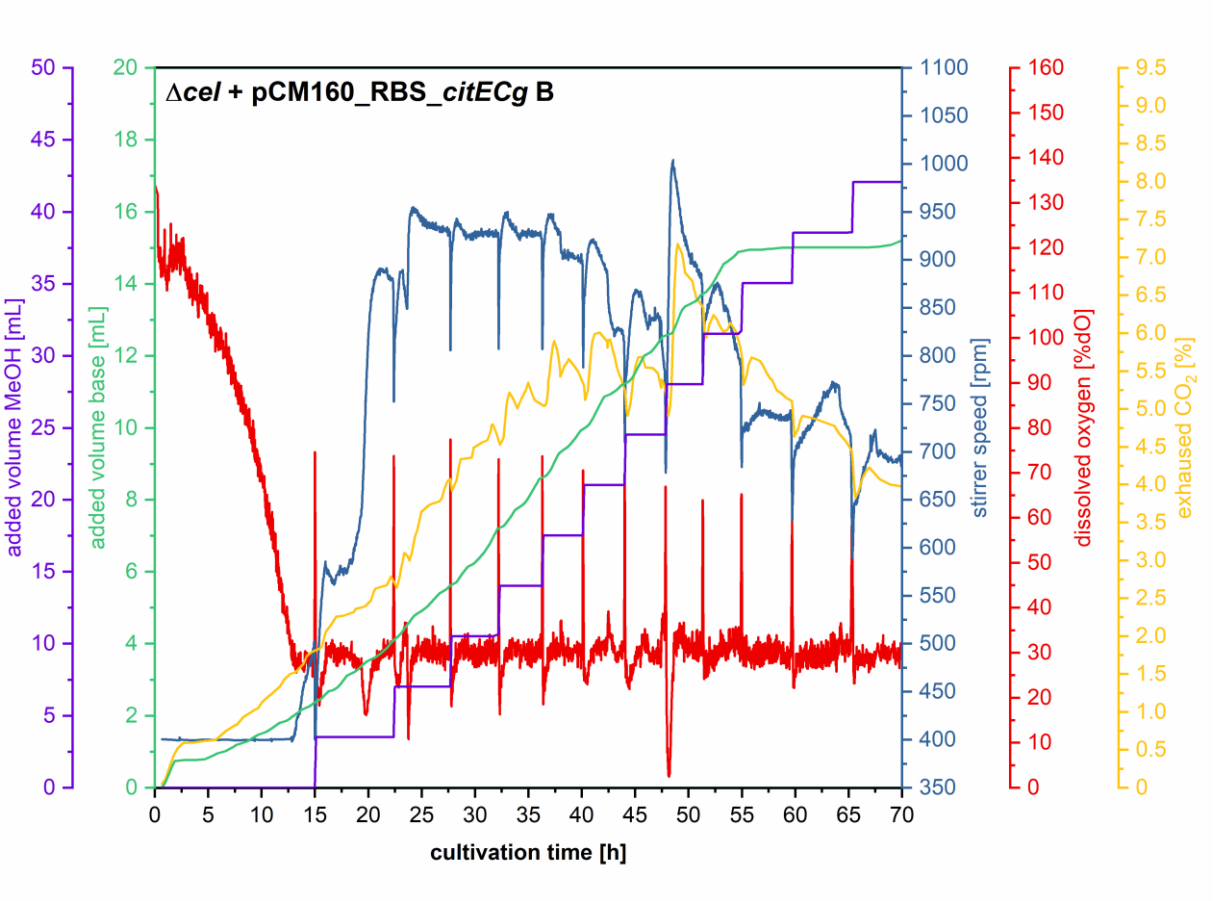

6. Manuscripts and publications

This chapter contains the manuscripts and publications on which this thesis is based. The manuscripts and publications are presented in the form specified by the respective journal.

6.1 Improvement of dicarboxylic acid production *with Methylorubrum extorquens* by reduction of product reuptake

Declaration of author contributions to the publication:

Improvement of dicarboxylic acid production with *Methylorubrum extorquens* by reduction of product reuptake

Status: published

Name of journal: Applied Microbiology and Biotechnology

Contributing authors: Laura Pöschel (LP), Elisabeth Gehr (EG), Markus Buchhaupt (MB)

What are the contributions of the doctoral candidate and his co-authors?

(1) Concept and design

Doctoral candidate:	50 %	
Co-author MB:	50 %	

(2) Conducting tests and experiments

Doctoral candidate:	95 %	All experiments except construction of plasmid pCM160_RBS_*yciAHI*
Co-author EG:	5 %	Construction of plasmid pCM160_RBS_yciAHI

(3) Compilation of data sets and figures

Doctoral candidate:	100 %	Data collection, preparation of figures and tables

(4) Analysis and interpretation of data

Doctoral candidate:	70 %	Analysis and interpretation of data
Co-author MB:	30 %	Interpretation of data

(5) Drafting of manuscript

Doctoral candidate:	90 %
Co-author MB:	10 %

Applied Microbiology and Biotechnology
https://doi.org/10.1007/s00253-022-12161-0

APPLIED MICROBIAL AND CELL PHYSIOLOGY

Improvement of dicarboxylic acid production with *Methylorubrum extorquens* by reduction of product reuptake

Laura Pöschel[1,2] · **Elisabeth Gehr**[1] · **Markus Buchhaupt**[1]

Received: 23 March 2022 / Revised: 29 August 2022 / Accepted: 30 August 2022

Abstract
The methylotrophic bacterium *Methylorubrum extorquens* AM1 has the potential to become a platform organism for methanol-driven biotechnology. Its ethylmalonyl-CoA pathway (EMCP) is essential during growth on C1 compounds and harbors several CoA-activated dicarboxylic acids. Those acids could serve as precursor molecules for various polymers. In the past, two dicarboxylic acid products, namely mesaconic acid and 2-methylsuccinic acid, were successfully produced with heterologous thioesterase YciA from *Escherichia coli*, but the yield was reduced by product reuptake. In our study, we conducted extensive research on the uptake mechanism of those dicarboxylic acid products. By using 2,2-difluorosuccinic acid as a selection agent, we isolated a dicarboxylic acid import mutant. Analysis of the genome of this strain revealed a deletion in gene *dctA2*, which probably encodes an acid transporter. By testing additional single, double, and triple deletions, we were able to rule out the involvement of the two other DctA transporter homologs and the ketoglutarate transporter KgtP. Uptake of 2-methylsuccinic acid was significantly reduced in *dctA2* mutants, while the uptake of mesaconic acid was completely prevented. Moreover, we demonstrated *M. extorquens*-based synthesis of citramalic acid and a further 1.4-fold increase in product yield using a transport-deficient strain. This work represents an important step towards the development of robust *M. extorquens* AM1 production strains for dicarboxylic acids.

Key points
- *2,2-Difluorosuccinic acid is used to select for dicarboxylic acid uptake mutations.*
- *Deletion of dctA2 leads to reduction of dicarboxylic acid uptake.*
- *Transporter-deficient strains show improved production of citramalic acid.*

Keywords Dicarboxylic acids · *Methylorubrum extorquens* · Product reuptake · Acid transporters · Ethylmalonyl-CoA pathway · Methylotroph

Introduction

Given the limited availability and global concern about the sustainability of fossil resources, the development of sustainable production processes for prevalent chemicals is indispensable. Currently, a new field of biotechnological processes is emerging that focuses on the use of alternative carbon sources. To be sustainable, these carbon sources must be derivable from renewable sources and must not compete with food production. Methanol, whose production share from renewable sources and waste streams starts to increase (Roode-Gutzmer et al. 2019), offers itself as an alternative raw material for biotechnological processes of the future. Moreover, its use as feedstock minimizes the risk of contamination during biotechnological applications and reduces the cost of downstream processing by using a defined minimal medium.

A group of widely used chemicals that are currently mainly produced from fossil raw materials are polyamides and polyesters. Biotechnologically produced dicarboxylic acids can serve as sustainable platform chemicals for the production of those polymers (Jang et al. 2012). Although

✉ Markus Buchhaupt
markus.buchhaupt@dechema.de

[1] DECHEMA-Forschungsinstitut, Microbial Biotechnology, Theodor-Heuss-Allee 25, 60486 Frankfurt am Main, Germany

[2] Department of Life Sciences of the Goethe University Frankfurt am Main, Max-von-Laue-Str. 9, 60438 Frankfurt am Main, Germany

Published online: 15 September 2022

pathways for microbiological production of dicarboxylic acids from classical feedstocks have been known for many years (Lee et al. 2011; Alonso et al. 2014), methanol-based routes for carboxylic acid production have been described only recently for the methylotrophic bacterium *Methylorubrum extorquens* AM1 (DSM 1338), e.g., for itaconic acid, 3-hydroxypropionic acid, mesaconic acid, and 2-methylsuccinic acid (Sonntag et al. 2014; Yang et al. 2017; Lim et al. 2019). The latter two are directly derived from the ethylmalonyl-CoA pathway (EMCP) by enzymatic hydrolysis (Fig. 1). The EMCP as an anaplerotic pathway is essential for methylotrophic growth of *M. extorquens*. It regenerates glyoxylate, which is needed for replenishment of the serine cycle and includes two CO_2-fixing steps (Erb et al. 2007; Peyraud et al. 2009). The pathway is also essential for the assimilation of C2 compounds during growth on e.g. acetate in microorganisms having no glyoxylate pathway as *M. extorquens* (Erb et al. 2010; Okubo et al. 2010). The EMCP consists of 11 enzymes and includes several CoA-bound dicarboxylic acid intermediates with high biotechnological potential (Alber 2011). Mixtures of mesaconic acid and 2-methylsuccinic acid were produced from respective CoA-precursors by introducing the thioesterase YciA

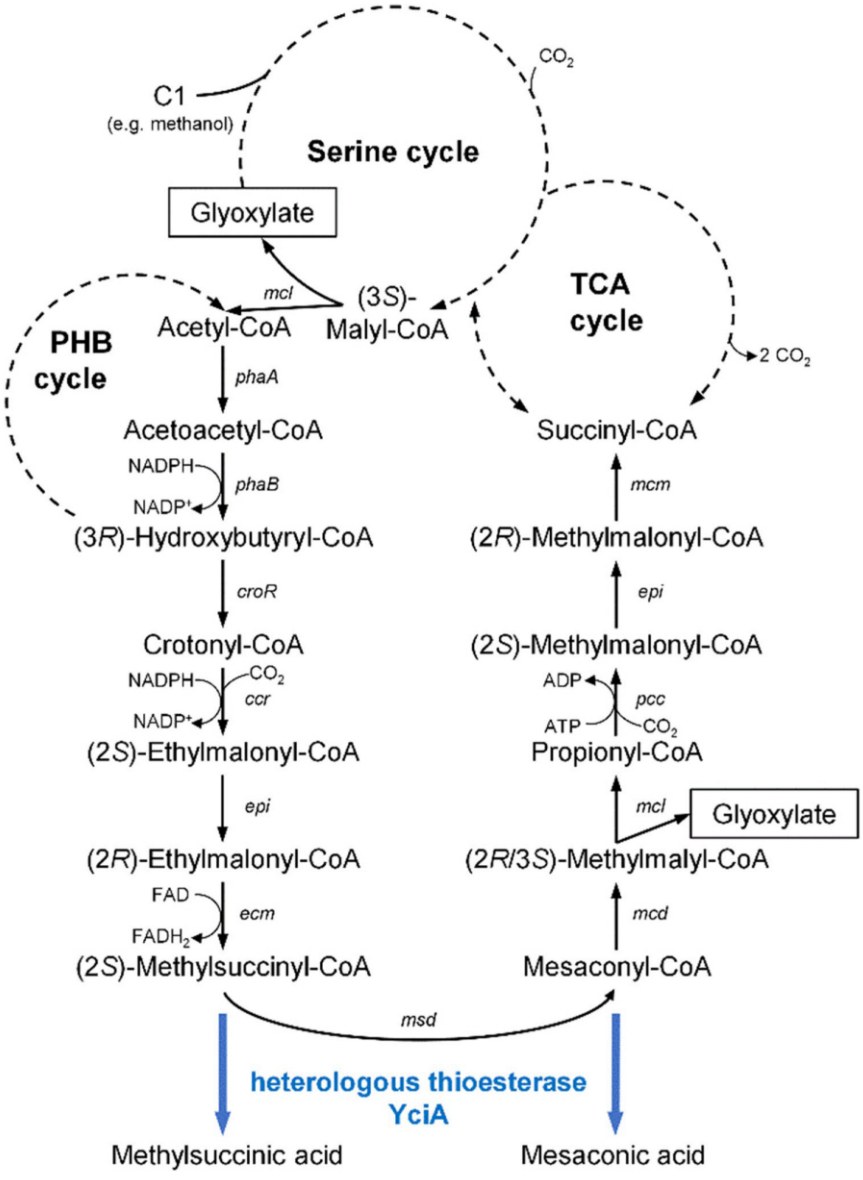

Fig. 1 Overview of ethylmalonyl-CoA pathway (EMCP) *in M. extorquens* AM1. The EMCP is interlaced with the serine cycle, the PHB cycle, and the tricarboxylic acid cycle. Cleavage of (2*R*/3*S*)-methylmalyl-CoA by malyl-CoA/beta-methylmalyl-CoA lyase (*mcl*) releases glyoxylate, which replenishes the serine cycle (indicated by boxes). Further genes of EMCP are: β-ketothiolase (*phaA*); acetoacetyl-CoA reductase (*phaB*); crotonase (*croR*); crotonyl-CoA carboxylase/reductase (*ccr*); ethylmalonyl-CoA epimerase (*epi*); ethylmalonyl-CoA mutase (*ecm*); methylsuccinyl-CoA dehydrogenase (*msd*); mesaconyl-CoA dehydratase (*mcd*); propionyl-CoA carboxylase (*pcc*); methylmalonyl-CoA mutase (*mcm*). Expression of heterologous thioesterase-encoding gene *yciA* leads to hydrolysis of (2*S*)-methylsuccinyl-CoA and mesaconyl-CoA (bold blue arrows). The corresponding products, namely 2-methylsuccinic acid and mesaconic acid, are released into the supernatant

originating from *Escherichia coli* (Sonntag et al. 2014). The high carbon flux via the EMCP enabled remarkable product titers to be achieved without further modification of metabolic pathways. In both studies of Sonntag and colleagues (2014; 2015), the concentration of dicarboxylic acid products in supernatant was reduced remarkably (i.e., 45% or 60% over a period of 20 h, respectively) as soon as the cells were reaching the stationary growth phase. This behavior is probably attributable to product reuptake. An adjustment of the cobalt concentration in the growth medium from 12.6 µM to 0.2 µM did not only lead to a sixfold increase in product yield due to biomass formation-limiting inhibition of certain EMCP enzymes, but also decreased the reuptake of products in stationary growth phase (Sonntag et al. 2015). Despite the lack of obvious product reuptake under these low-cobalt conditions in the late cultivation phase, it remains unclear whether product uptake continuously proceeds during the acid production phase. This would resemble a partial futile cycle, leading to loss of resources and therefore decreased product yield. The phenomenon of product reuptake was also described for 3-hydroxypropionic acid, another EMCP-derived product from *M. extorquens* AM1, even when using a low cobalt concentration of 1.26 µM in the medium (Yang et al. 2017). These observations make it worth to investigate the product uptake mechanism and to prevent it on a molecular level.

The main targets for prevention of product uptake are the dicarboxylic acid import proteins. It has been observed that a 30-fold reduction in sodium concentration in the growth medium resulted in ceasing of product uptake (Sonntag et al. 2015), suggesting that carriers of the DctA family may be involved, which are known to be sodium-dependent (Janausch et al. 2002). A transposon mutant study by Van Dien and coworkers identified a mutant with a disrupted *dctA* homolog that was no longer able to use succinate as sole carbon source (Van Dien et al. 2003). The affected protein was referred to as GenBank entry A33597. Since this mutant strain was promising for dicarboxylic acid production, the gene encoding the protein with the highest similarity to A33597 was deleted by Sonntag et al. (2015). Surprisingly, the strain did not show the phenotype previously described. Sonntag et al. (2015) speculated that the deleted gene might not be identical to the gene mutated in the Van Dien study, as the GenBank entry A33597 in question represents a *Sinorhizobium meliloti* protein sequence and therefore cannot be unambiguously assigned.

Another possibility of preventing the reuptake of products is to convert them to non-metabolizable molecules. For example, the hydration product of mesaconic acid, namely (*S*)-citramalic acid, would not only fulfill this criterion, but would also extend the product spectrum of *M. extorquens* AM1 by a chiral, enantiopure product. The mesaconase/fumarate hydratase from *Paraburkholderia xenovorans* (Kronen et al. 2015) seems promising for heterologous expression for this purpose.

In our study, we aimed at reducing reuptake of dicarboxylic acids at the molecular level. Using a simple and straightforward selection approach, we identified a mutant (partial deletion of *dctA2*) with reduced uptake of mesaconic acid and 2-methylsuccinic acid. We confirmed our results by construction of deletion mutants and were able to rule out the involvement of other DctA transporters. In addition, we have successfully implemented the production of a new dicarboxylic acid product from *M. extorquens* AM1, whose production also benefits from the transport deficiency. These new insights into dicarboxylic acid transport contribute to the development of *M. extorquens* AM1 towards a comprehensive production platform for methanol-based biotechnology.

Material and methods

Bacterial strains and growth conditions

Escherichia coli DH5α (Hanahan 1985; Grant et al. 1990) cultures were grown in LB medium (Bertani 1951) at 37 °C. For cultivation of *M. extorquens* AM1 (DSM 1338, Peel and Quayle 1961), minimal medium was prepared as described before (Peyraud et al. 2009), containing 123 mM methanol, 31 mM sodium succinate or 5 mM sodium acetate as carbon source, respectively. $CoCl_2$ concentration in the medium was set to 12.6 µM (Kiefer et al. 2009; Sonntag et al. 2014). For solid medium, agar–agar at 15 g/L was added. For cultivation of *M. extorquens* AM1 in liquid medium, 5 mL precultures in methanol minimal medium were grown in test tubes for 48 h at 30 °C and 180 rpm on a rotary shaker. Main cultures of 20 mL were subsequently inoculated to an OD_{600} of 0.1 in 100 mL shake flasks and incubated under the same conditions and in the same medium as the precultures. If required, tetracycline-hydrochloride at 10 µg/mL, kanamycin sulfate at 30 µg/mL (for *E. coli*), or kanamycin sulfate at 50 µg/mL (for *M. extorquens* AM1) was added to the medium. For high-resolution measurements of growth curves, 1 ml of main cultures were incubated in a BioLector® microbioreactor system in 48-well Flowerplates® (m2p-labs GmbH, Baesweiler, Germany) at 30 °C and 1000 rpm. For complementation experiments, glyoxylate was added to a final concentration of 370 mg/L (5 mM). Depending on the specific production experiment, heterologously expressed genes encoding thioesterase YciA from either *E. coli* (YciAEc) or *H. influenza* (YciAHI) and a gene encoding a fumarate hydratase (mesaconase) from *Paraburkholderia xenovorans* (MesaPx) was used. The two thioesterases produce similar amounts of products with

slightly different ratios. For YciAHI, a crystal structure is available (3BJK, Willis et al. 2008).

Chemicals

All chemicals were purchased from Carl Roth (Karlsruhe, Germany), VWR International (Darmstadt, Germany), or Merck (Darmstadt, Germany). Solvents for chromatography were purchased in LC–MS grade quality.

Genome sequencing

DNA of *M. extorquens* AM1 wild type and mutant strains was sequenced by Illumina sequencing (MiSeq; 2×250 bp; 1–2 million PE-Reads; GenXPro, Frankfurt, Germany). Paired and cleaned Illumina reads were trimmed with BBDuk Trimmer (JGI, Berkeley, USA) to a quality cut-off of 20. Mapping to the reference genome (NCBI NC_012807–NC_012811, annotation date 04/11/2021) and calling for SNPs was done with Geneious Prime (Biomatters, Auckland, New Zealand). Assembling qualities and base coverages are listed in Online Resource Table S1.

DNA cloning and plasmid construction

All standard plasmid cloning procedures were performed in *E. coli* DH5α. Plasmid DNA was purified with GeneJET Plasmid Miniprep Kit from Thermo Scientific (Waltham, USA). Polymerase chain reactions (PCR) were performed with Q5 Polymerase from New England Biolabs (Frankfurt, Germany) according to the manufacturer's protocol. Subsequently, PCR products were purified using the DNA Clean & Concentrator Kit from Zymo Research Europe (Freiburg, Germany). Oligonucleotides were purchased from Merck (Darmstadt, Germany), restriction enzymes and T4 ligase from NEB. All genetic constructs were confirmed by Sanger sequencing at Eurofins Scientific (Luxembourg, Luxembourg). Transformation of *M. extorquens* AM1 was done as described before (Toyama et al. 1998). Genomic DNA of *M. extorquens* AM1 was purified with GenElute™ Bacterial Genomic DNA Kit from Merck (Darmstadt, Germany).

Generation of dicarboxylic acid transporter deletion mutants

Knockout of the genes encoding potential carboxylic acid importers (*dctA1*: MEXAM1_RS15430, *dctA2*: MEXAM1_RS10985 and *dctA3*: MEXAM1_RS20450) and the ketoglutarate permease KgtP (*kgtP*: MEXAM1_RS24315) were carried out with allelic exchange vector pCM184 carrying a kan^R antibiotic resistance cassette (Marx and Lidstrom 2002). Vector pCM184_Δ*dctA1* was constructed as described in the publication by Sonntag et al. (2015), in which *dctA1* is referred to as *dctA*. The deletion vectors pCM184_Δ*dctA2*, pCM184_Δ*dctA3* and pCM184_Δ*kgtP* were designed accordingly in two constitutive cloning steps. First, 500 bp of genomic upstream flanking region of the respective gene of interest was amplified while introducing restriction sites at both ends of the PCR product. The resulting fragment was digested with according restriction enzymes and ligated to equally digested pCM184 (Table 1). The resulting vectors carrying the upstream fragment were subsequently treated in the same manner to introduce the previously digested downstream fragment to result in the final allelic exchange vectors. After restreaking *M. extorquens* AM1 transformants on solid methanol medium containing kanamycin, the correct integration of resistance marker was verified with respective primer pairs, binding inside and outside of the cassette. Screening for single recombination mutants and removal of the resistance marker with *cre*-expression vector pCM157 was achieved on solid methanol medium containing tetracycline as described by Marx and Lidstrom (2002). Elimination of pCM157 was performed by cultivating strains overnight in medium without antibiotics and screening single colonies for tetracycline sensitivity. Deletion of the complete ORF was double checked by PCR of genomic DNA. All used oligonucleotides are listed in Table 1. For multiple gene deletions, the described procedure was performed several times in succession. Single, double and triple deletion mutants were simultaneously created in *M. extorquens* AM1 wild type as well as in the Δ*cel* strain (Delaney et al. 2013).

Dicarboxylic acid analysis

For quantification of dicarboxylic acid products, the supernatant of *M. extorquens* AM1 cultures was centrifuged for 5 min at 16.000 g and passed through a 0.22 µm PDVF-syringe filter (Carl Roth, Karlsruhe, Germany). For the quantification of mesaconic acid and 2-methylsuccinic acid, 10 µL of the cell free supernatant was chromatographed on a 150×4.6 mm Rezex™ ROA-Organic Acid H + (8%) column (Phenomenex, Aschaffenburg, Germany) at 30 °C oven temperature in a SLC10-A HPLC system (Shimadzu, Duisburg, Germany). 5 mM H_2SO_4 in MilliQ water was used as mobile phase. Samples were analyzed with a SPD20A UV–Vis detector at 205 nm as described in Sonntag et al. (2014). Retention times of the analytes are listed in Table 2. For the quantification of samples containing additional dicarboxylic acid products (e.g., citramalic acid), which all have similar retention times, an alternative LC–MS/MS setup was used. Chromatography of 1 µL of the respective samples was done on a 150×4.6 mm Luna Omega 3 µm PS C18 100 Å column (Phenomenex, Aschaffenburg, Germany) in a Nexera X2 UHPLC system (Shimadzu, Duisburg, Germany). Separation was performed isocratically at 12% [v/v] acetonitrile and

Table 1 Oligonucleotides, plasmids, and strains used in this work. Capital letters in DNA sequences indicate restriction sites. Restriction enzymes used for subcloning into pCM184 are indicated in brackets. Optimization of RBS sequences was done with RBS Calculator 2.1 (Salis 2011)

Name	Sequence/genotype	Description/application	Reference
Bacterial strains			
E. coli DH5α	F^- φ80*lac*ZΔM15 Δ(*lac*ZYA-*arg*F)U169 *rec*A1 *end*A1 *hsd*R17(r_K^-, m_K^+) *pho*A *sup*E44 λ^-*thi*-1 *gyr*A96 *rel*A1	Standard cloning applications	Hanahan (1985); Grant et al. (1990)
M. extorquens AM1	Cm^R, Gram-negative, facultative methylotrophic, obligate aerobic, α-proteobacterium		Peel and Quayle (1961)
M. extorquens AM1 DFS mutant 1	*M. extorquens* AM1 with chromosomal 12 bp deletion within MEXAM1_RS10985 (*dctA2*)	Mutants isolated by selection with DFS	This work
M. extorquens AM1 DFS mutant 2	*M. extorquens* AM1 with chromosomal mutation of MEXAM1_RS18205 (SLC13 family transporter gene)		This work
Wild type Δ*dctA3*	*M. extorquens* AM1 with chromosomal deletion of MEXAM1_RS20450	Dicarboxylic acid transporter deletion strains	This work
Wild type Δ*dctA1* Δ*dctA3*	*M. extorquens* AM1 with chromosomal deletion of MEXAM1_RS15430 and MEXAM1_RS20450		This work
Wild type Δ*dctA1* Δ*dctA2* Δ*dctA3*	*M. extorquens* AM1 with chromosomal deletion of MEXAM1_RS15430, MEXAM1_RS10985 and MEXAM1_RS20450		This work
M. extorquens AM1 Δ*cel* (CM2720)	*M. extorquens* AM1 with chromosomal deletion of cellulose biosynthesis genes	Reduced biofilm formation without loss of fitness	Delaney et al. (2013)
Δ*cel* Δ*dctA1*	*M. extorquens* AM1 Δ*cel* with chromosomal deletion of MEXAM1_RS15430	Dicarboxylic acid transporter deletion strains in Δ*cel* strain background	This work
Δ*cel* Δ*dctA2*	*M. extorquens* AM1 Δ*cel* with chromosomal deletion of MEXAM1_RS10985		This work
Δ*cel* Δ*kgtP*	*M. extorquens* AM1 Δ*cel* with chromosomal deletion of MEXAM1_RS24315		This work
Δ*cel* Δ*dctA1* Δ*dctA2*	*M. extorquens* AM1 Δ*cel* with chromosomal deletion of MEXAM1_RS15430 and MEXAM1_RS10985		This work
Δ*cel* Δ*dctA2* Δ*dctA3*	*M. extorquens* AM1 Δ*cel* with chromosomal deletion of MEXAM1_RS10985 and MEXAM1_RS20450		This work
Δ*cel* Δ*dctA1* Δ*dctA2* Δ*dctA3*	*M. extorquens* AM1 Δ*cel* with chromosomal deletion of MEXAM1_RS15430, MEXAM1_RS10985 and MEXAM1_RS20450		This work
Plasmids			
pCM184	Kan^R, Tc^R, Amp^R oriT, pBR322ori	Allelic exchange vector for gene deletion in *M. extorquens*	Marx and Lidstrom (2002)
pCM157	Tc^R, oriT, pBR322ori	Cre recombinase expression plasmid	Marx and Lidstrom (2002)
pCM184_Δ*dctA1*	pCM184 containing ~ 500 bp flanking sites of *dctA1*	Allelic exchange vector for *dctA1*	Sonntag et al. (2015)
pCM184_Δ*dctA2*	pCM184 containing ~ 500 bp flanking sites of *dctA2*	Allelic exchange vector for *dctA2*	This work
pCM184_Δ*dctA3*	pCM184 containing ~ 500 bp flanking sites of *dctA3*	Allelic exchange vector for *dctA3*	This work

Table 1 (continued)

Name	Sequence/genotype	Description/application	Reference
pCM184_Δ*kgtP*	pCM184 containing ~ 500 bp flanking sites of *kgtP*	Allelic exchange vector for *kgtP*	This work
pCM160	Kan^R, pmxaF, oriT, pBR322ori	Constitutive expression vector for *M. extorquens*	(Marx and Lidstrom 2001)
pCM160_RBS_*yciA*Ec	pCM160 containing codon-optimized thioesterase gene *yciA* from *E. coli*, optimized RBS	Constitutive expression of *yciA*Ec	Sonntag et al. (2014)
pCM160_RBS_*yciA*HI	pCM160 containing codon-optimized thioesterase gene *yciA* from *Haemophilus influenzae*, optimized RBS	Constitutive expression of *yciA*HI	This work (GenBank ON109394)
pCM160_RBS_*yciA*Ec_MesaPx	pCM160 containing codon-optimized thioesterase gene *yciA* from *E. coli*, codon-optimized fumarate hydratase gene *bxe_A3136* from *P. xenovorans*, optimized RBS	Constitutive expression of *yciA*Ec *and* fumarate hydratase/ mesaconase (WP_038456612, (Kronen et al. 2015))	this work (GenBank ON109395)
Oligonucleotides			
dctA1_up_fw	actaGACGTCagcggaagcgaactctgcg (AatII)	Amplification of up- and downstream fragments	Sonntag et al. (2015)
dctA1_up_rev	actaCATATGgggcgtttctccctgtcgga (NdeI)		
dctA1_down_fw	actaTACGTAtccggtcaggagggcgcac (SnaBI)		
dctA1_down_rev	actaGAGCTCagggcttcgggcgtatcgag (SacI)		
dctA2_up_fw	ccGACGTCtcggtctggtcgctcatgg (AatII)		This work
dctA2_up_rev	actaCCATGGtcctcaccgataccgtgttgc (NcoI)		This work
dctA2_down_fw	actaTACGTAatgagcctgccaccgctc (SnaBI)		This work
dctA2_down_rev	actaGAGCTCaaccgcgatgcccgaacc (SacI)		This work
dctA3_up_fw	ccGACGTCtgcacgctccacgagaagc (AatII)		This work
dctA3_up_rev	ggaattcCATATGcaccgccgtttagggcgaat (NdeI)		This work
dctA3_down_fw	actaTACGTAaacgggcttccgcttcgg (SnaBI)		This work
dctA3_down_rev	actaGAGCTCaacaccgccaccgagtacg (SacI)		This work
kgtP_up_fw	actaCCATGGactcacatccacaacgcgc (NcoI)		This work
kgtP_up_rev	actaGCGGCCGCcgctgggacgcaagacga (NotI)		This work
kgtP_down_fw	actaCCGCGGtgagcccttatcagaggccg (SacII)		This work
kgtP_down_rev	actaTACGTAacatcagaattgcggccgtc (SnaBI)		This work
kan_up_dctA1_check_fw	aactcgatcttcacgacgac	Verification of integration site of kanamycin resistance marker	This work
kan_up_dctA2_check_fw	tttcgtagaggccgatgtc		This work
kan_up_dctA3_check_fw	ttgaaggcctcgttatgc		This work
kan_up_kgtP_check_fw	agatcgaagtgttcgacctc		This work
kan_up_check_rev	agacgtttcccgttgaatatg		Sonntag et al. (2015)
kan_down_check_fw	agtttcatttgatgctcgatgag		
kan_down_dctA1_check_rev	atacagcttggtatcaaccg		This work
kan_down_dctA2_check_rev	tcgaggatgttgaccacc		This work
kan_down_dctA3_check_rev	ctccttcttcaagaccgac		This work
kan_down_kgtP_check_rev	cacgatctcgtaggtgtc		This work

Table 1 (continued)

Name	Sequence/genotype	Description/application	Reference
check_del_dctA1_fw	agccatgactgaactgcag	Verification of complete gene deletion	This work
check_del_dctA1_rev	aatcgcgaagcagcaatg		This work
check_del_dctA2_fw	aatacgcggctaggtcg		This work
check_del_dctA2_rev	tcttgatcaggccggtg		This work
check_del_dctA3_fw	atcaatgccgtacccgc		This work
check_del_dctA3_rev	gaccgeatgggtctaagga		This work
check_del_kgtP_fw	tctcgaaggagcggctc		This work
check_del_kgtP_rev	tctccggcatctgtcatgg		This work

88% [v/v] ddH_2O, both containing 0.2% [v/v] formic acid at 40 °C oven temperature. The column was washed after every run by raising the acetonitrile content in the mobile phase to 95%. Mesaconic acid, 2-methylsuccinic acid, citramalic acid as well as other potential EMCP-derived carboxylic acid products (Table 2) were analyzed on a LCMS-8045 system (Shimadzu). The analytes were negatively ionized with APCI or ESI ion source, fragmented and finally quantified by comparing the results to calibration curves of corresponding standards. Quantification was performed with the LabSolutions software (Shimadzu). The retention times and the manufacturers of the standard substances are listed in Table 2. Fragmentation of (2*S*,3*R*)-2-hydroxy-3-methylsuccinic acid and (*S*)-citramalic acid for unambiguous identification is shown in Online Resource Fig. S1.

Transcriptome analysis

A whole transcriptome analysis was done for *M. extorquens* AM1 harboring pCM160_RBS_*yciAHI* or pCM160, respectively. Samples were taken after 22.75, 31.75, 47, 51.25 and 70.5 h of cultivation. For stabilization of RNA, one volume of growing bacterial culture (> 10^6 cells) was mixed with two volumes of RNAprotect Bacteria Reagent from QIAGEN (Hilden, Germany) and incubated for 5 min. Cells were centrifuged for 10 min at 5000 g to remove supernatant and stored pelleted at − 80 °C. RNA was isolated and analyzed by GenXPro (Frankfurt, Germany) via Illumina sequencing (2–5 million reads; 2 × 75 bp). Raw read counts were normalized by CPM (counts per million) method to compensate for varying sample sequencing depth. For graphical representation, transcript levels were scaled to the count of the respective gene in the control strain at the first sampling point. The transcriptome dataset was deposited at NCBI (accession number GSE199961).

Results

Search for dicarboxylic acid transporter candidates by transcriptome analysis

M. extorquens AM1 naturally produces small amounts of dicarboxylic acids derived from the EMCP pathway. Sonntag and colleagues succeeded in increasing the amounts of released 2-methylsuccinic acid and mesaconic acid to a combined titer of 0.13 g/L by expressing the thioesterase encoding gene *yciA* from *E. coli* heterologously in a methanol minimal medium containing 12.6 µM $CoCl_2$ (Sonntag et al. 2014, 2015). However, at the end of the exponential growth phase, the acid concentrations started to decrease again, which is probably caused by product-reuptake and metabolization. It is unclear whether product uptake also

Table 2 Analytical standards and retention times used for the quantification of carboxylic acids produced by *M. extorquens* AM1

Standard substance	Manufacturer	Retention times [min] in HPLC measurements	Retention times [min] in LC–MS/MS measurements
Crotonic acid	Carl Roth (Karlsruhe, Germany)	n.d	1.06
(2*S*,3*R*)-2-Hydroxy-3-methylsuccinic acid	Enamine (Riga, Latvia)	n.d	1.08
(*S*)-Citramalic acid	Merck (Darmstadt, Germany)	n.d	1.08
Ethylmalonic acid		n.d	1.58
Mesaconic acid		12.88	1.38
2-Methylsuccinic acid		8.10	1.32
Methylmalonic acid		n.d	1.20
Succinic acid		n.d	1.02

occurs during the exponential growth phase, which could reduce the overall yield. To address this question, we investigated the dicarboxylic acid importers of *M. extorquens* AM1. A number of candidates with homology to the multispecies dicarboxylic acid transporter DctA (Janausch et al. 2002) were identified by BLAST analysis by Sonntag et al. (2014). In the referred study (Sonntag et al. 2014), unexpectedly and in contrast to other publications (Van Dien et al. 2003), a *dctA* knockout mutant (MEXAM1_RS15430) was still able to grow on succinate. Therefore, it was questioned whether *dctA* (hereinafter referred to as *dctA1*) from both studies was in fact the identical ORF. Sonntag et al. also identified two other *dctA* homologs (MEXAM1_RS10985 and MEXAM1_RS20450, referred to as *dctA2* and *dctA3* in our study) and an additional dicarboxylic acid transporter encoding gene (*kgtP* MEXAM1_RS24315, Seol and Shatkin 1991) in the genome sequence, but these were not further investigated (Sonntag et al. 2014). To monitor expression levels of the homolog candidates and to potentially identify additional dicarboxylic acid importers in our study, *M. extorquens* AM1 cells expressing an alternative thioesterase gene from *Haemophilus influenzae* (*yci*AHI) were analyzed on a whole transcriptome level together with an empty vector control strain. Additionally, product titers were determined. Small amounts of the EMCP derived carboxylic acids (2*S*,3*R*)-2-hydroxy-3-methylsuccinic acid, crotonic acid, ethylmalonic acid, methylmalonic acid and succinic acid were detected, but their titers were irrelevant and insufficient for quantification (< 5 mg/L, also present in the empty vector control culture). *M. extorquens* AM1 cells harboring plasmid pCM160_RBS_*yci*AHI released up to 104 ± 8 mg/L 2-methylsuccinic acid and up to 85 ± 9 mg/L mesaconic acid in the production phase, followed by clear decreases of 2-methylsuccinic acid and mesaconic acid titers (Fig. 2a).

The relative expression levels of dicarboxylic acid transporter candidates identified by Sonntag and colleagues (2014) were analyzed in the production strain as well as in cells harboring an empty control vector. Hydrolysis of EMCP-esters by a heterologous thioesterase is a strong intervention in the primary carbon metabolism of the cell. This is reflected by the different growth kinetics of production and control strain (Fig. 2a,b). Therefore, we decided not to perform an analysis of differential gene expression. Instead, relative gene expression was determined for each strain separately, before comparing the kinetic patterns of both strains. The gene *dctA1*, which has been already deleted in the work of Sonntag et al. (2015), showed a higher relative gene expression rate compared to control strains (Fig. 2c,d). This effect is particularly noticeable in the early sampling points, whereas expression was comparably strong during the main acid production phase (e.g., equivalent timepoints 47 h in production strains vs. 23 h or 32 h in control strains). Furthermore, moderately increased expression levels at later time points in the production strain were observed for *dctA2*, *dctA3*, and *kgtP* but at least for *dctA2* and *kgtP* a similar pattern was found in the non-producing reference strain.

We could not identify any additional genes with acid transporter annotation within the transcriptome data that were significantly higher expressed in cells sampled at the late stages of cultivation (51 h or 71 h) compared to the earlier sampling time points in the data set. Therefore, the transcriptome analysis of *M. extorquens* AM1 harboring pCM160_RBS_*yci*AHI yielded no candidates for potential dicarboxylic acid uptake factors.

Investigation of 2,2-difluorosuccinic acid as potential selection agent for dicarboxylic acid transport mutants

Since the transcriptome analysis did not provide clear hints for genes with clear upregulation before the phase of product reuptake, a more direct approach was considered to identify cells incapable of dicarboxylic acid uptake. For selection for respective *M. extorquens* cells with an uptake defect, 2,2-difluorosuccinic acid (DFS), a presumably cytotoxic

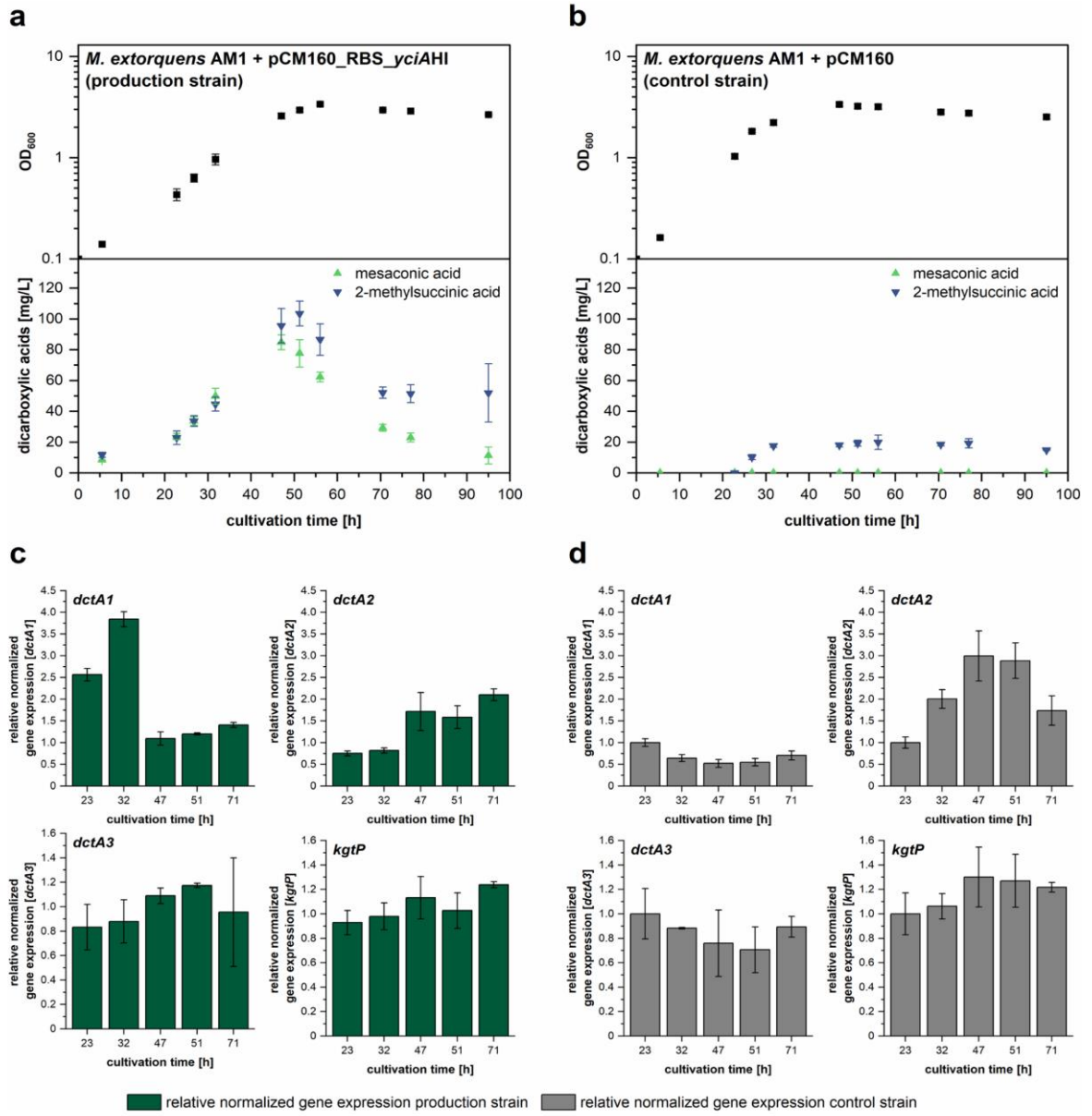

Fig. 2 Transcriptome analysis of dicarboxylic acid production strain to identify candidates for product uptake factors. **a**–**b** Growth kinetics and time-dependent concentration of mesaconic acid and 2-methylsuccinic acid in supernatant of *M. extorquens* AM1 + pCM160_RBS_*yciAHI* (**a**) or *M. extorquens* AM1 + pCM160 (**b**) growing in methanol minimal medium. Other EMCP-derived carboxylic acid products with titers insufficient for quantification (< 5 mg/L) are not displayed. **c** Normalized relative gene expression of *dctA1*, *dctA2*, *dctA3*, and *kgtP* for *M. extorquens* AM1 + pCM160_RBS_*yciAHI*. **d** Normalized relative gene expression of *dctA1*, *dctA2*, *dctA3*, and *kgtP* for *M. extorquens* AM1 + pCM160. The transcript levels are scaled to the transcript count of the respective gene in the control strain *M. extorquens* AM1 + pCM160 at 23 h of cultivation. Error bars represent standard deviations from three independent replicates. An additional visualization of the data in form of products per OD_{600} can be found in Online Resource Fig. S2

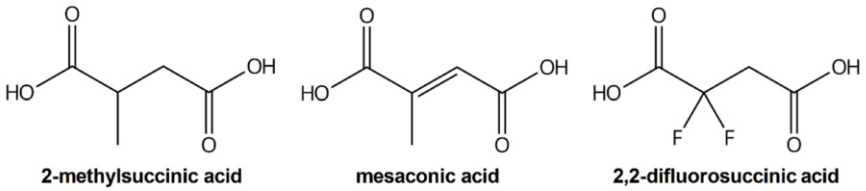

Fig. 3 Chemical structures of 2-methylsuccinic acid, mesaconic acid, and 2,2-difluorosuccinic acid

dicarboxylic acid with structural similarity to the target products, was used (Fig. 3).

To investigate the effect of DFS, the growth of *M. extorquens* AM1 in minimal medium containing different carbon sources and different concentrations of DFS was monitored in a microbioreactor system. Although the differences between replicates growing on succinate medium were quite high, the results showed, that the addition of 2, 5, or 10 mg/L DFS had no significant effect on growth (Fig. 4a). In contrast, the addition of DFS to acetate or methanol containing cultures resulted in suppression of growth and prolonged lag phases (Fig. 4b,c). The addition of 2 mg/L DFS to the methanol medium resulted only in a slight delay in growth. In turn, the addition of 5 mg/L resulted in a greater delay and a reduction of the maximum cell density, and the addition of 10 mg/L DFS completely inhibited growth (Fig. 4c). Although maximum cell densities were lower, similar effects were observed when cells were cultured in acetate medium (Fig. 4b). Since an active EMCP in *M. extorquens* AM1 is required for the use of methanol

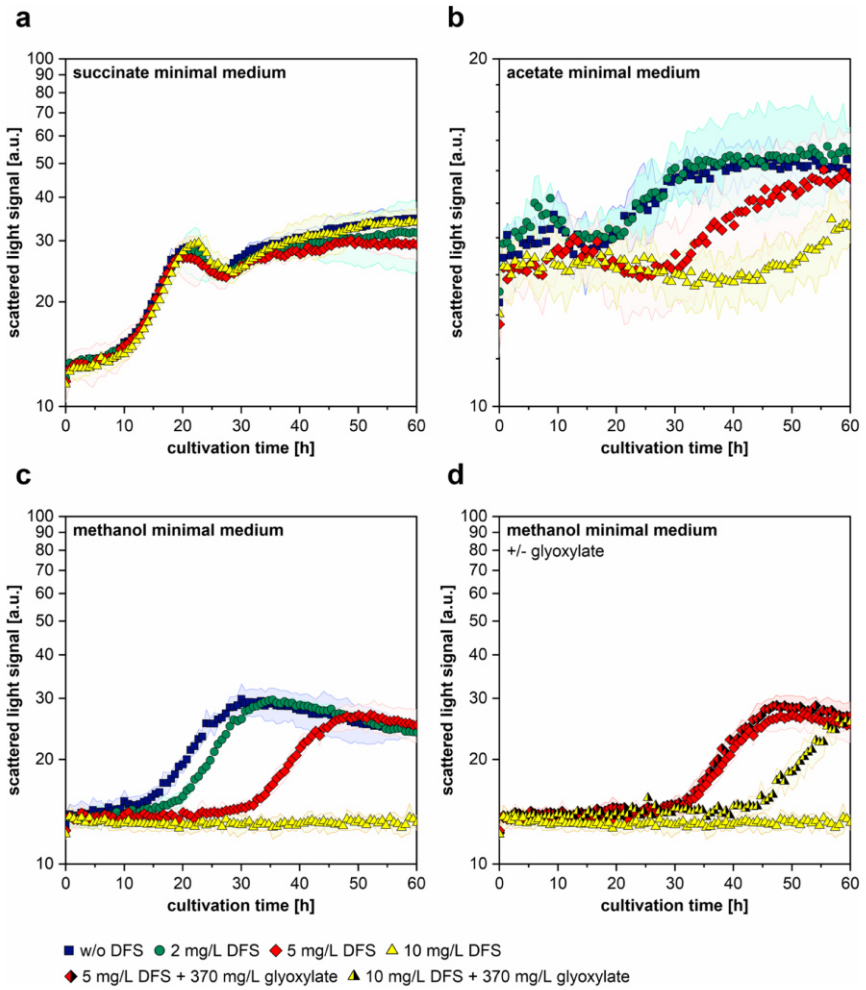

Fig. 4 Investigation of toxic effects of DFS on *M. extorquens* AM1. **a–c** Growth of *M. extorquens* AM1 in succinate, acetate, or methanol minimal medium with different additives. Cultures were grown in a microbioreactor. Growth was monitored by scattered light signal. 2,2-Difluorosuccinic acid (DFS) was added at the start of cultivation in concentrations of 2 mg/L, 5 mg/L, or 10 mg/L. *M. extorquens* AM1 culture without DFS was used as a negative control. For better readability, figure part **b** is scaled differently. **d** Complementation experiment, in which 370 mg/L of glyoxylate was added to cultures containing 5 mg/L or 10 mg/L of DFS, respectively. Colored areas represent standard deviations from three independent replicates

or acetate as sole carbon source (Peyraud et al. 2009), we assumed that DFS might target the EMCP. This assumption was reinforced by the fact, that the DFS-mediated growth defect in methanol medium could be partially compensated by the addition of glyoxylate (Fig. 4d). The provision of glyoxylate is the essential function of the EMCP during growth on C1 or C2 compounds (Fig. 1, Peyraud et al. 2009) and the rescue of EMCP mutants by glyoxylate addition was already demonstrated many years ago (Salem and Quayle 1971; Chistoserdova and Lidstrom 1996).

When DFS was added to an *M. extorquens* AM1 culture expressing the *E. coli yciA* gene, we observed a growth delay but at the same time the production of 2-methylsuccinic acid and mesaconic acid was raised to a maximum measured combined product titer of 153 mg/L ± 2 mg/L (Fig. 5). Even though the measured time points can only give an indication of the complete production kinetics, the product titers were clearly increased compared to the control experiment without DFS addition. This experiment provided further indication of an EMCP inhibitory effect, as EMCP flux limitation leads to increased dicarboxylic acid production in thioesterase expression strains (Sonntag et al. 2015).

Altogether, our investigations showed DFS to be a suitable selection agent for dicarboxylic acid uptake mutants. However, the mutant selection has to be performed under conditions, which require a functional EMCP, as this pathway seems to contain the molecular target for the compound.

Identification of potential dicarboxylic acid uptake transporters by using DFS

To isolate DFS-resistant strains, an *M. extorquens* AM1 culture was transferred to solid minimal medium containing acetate or methanol as carbon source and additional 5 mg/L DFS. After 18 days of incubation, a small number of colonies could be observed (one colony on methanol medium, 20 colonies on acetate medium). One strain from each medium was isolated. Restreaking the cells on solid succinate, methanol, or acetate minimal medium resulted in wild-type-like growth behavior. Isolated *M. extorquens* DFS mutant 1 (isolated from acetate-DFS minimal medium) and DFS mutant 2 (isolated on methanol-DFS minimal medium) were transformed with plasmid pCM160_RBS_*yciA*Ec and tested for dicarboxylic acid production along with an *M. extorquens*

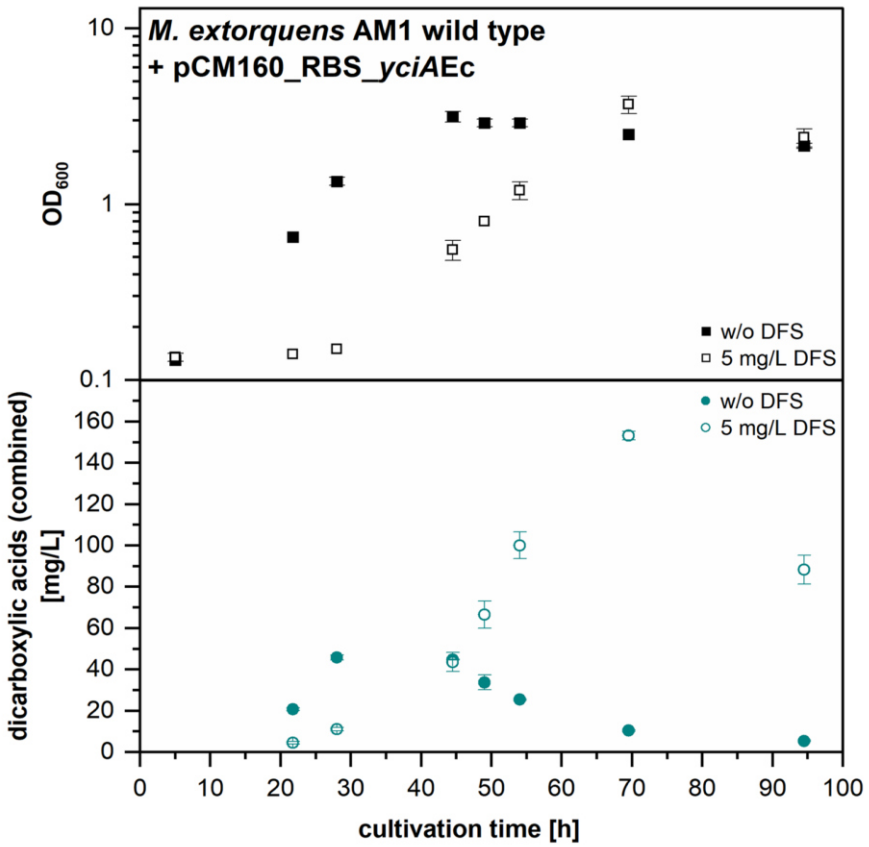

Fig. 5 Growth kinetics and time-dependent combined concentration of dicarboxylic acid products (mesaconic acid and 2-methylsuccinic acid) in supernatant of *M. extorquens* AM1 harboring pCM160_RBS_*yciA*Ec in methanol minimal medium (*filled symbols*) and in methanol minimal medium with addition of 5 mg/L 2,2-difluorosuccinic acid (DFS) after 5 h of cultivation (*empty symbols*). Other EMCP-derived carboxylic acid products with titers insufficient for quantification (< 5 mg/L) are not displayed. Error bars represent standard deviations from two independent replicates. An additional visualization of the data in form of products per OD_{600} can be found in Online Resource Fig. S3

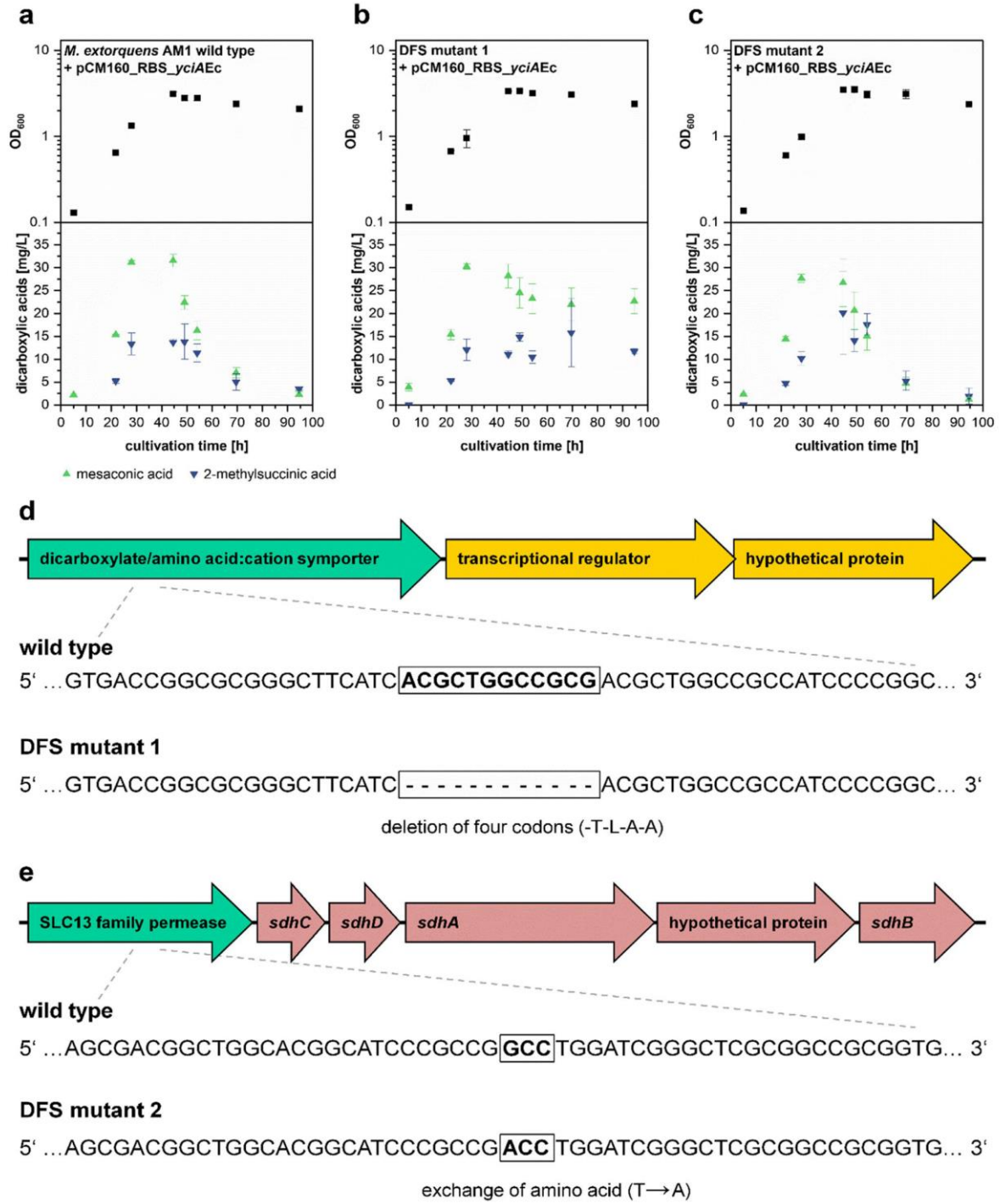
a
M. extorquens AM1 wild type
+ pCM160_RBS_yciAEc
b
DFS mutant 1
+ pCM160_RBS_yciAEc
c
DFS mutant 2
+ pCM160_RBS_yciAEc
OD600
dicarboxylic acids [mg/L]
cultivation time [h]
mesaconic acid
2-methylsuccinic acid
d
dicarboxylate/amino acid:cation symporter
transcriptional regulator
hypothetical protein
wild type
5‘ …GTGACCGGCGCGGGCTTCATC ACGCTGGCCGCG ACGCTGGCCGCCATCCCCGGC… 3‘
DFS mutant 1
5‘ …GTGACCGGCGCGGGCTTCATC - - - - - - - - - - - - ACGCTGGCCGCCATCCCCGGC… 3‘
deletion of four codons (-T-L-A-A)
e
SLC13 family permease
sdhC
sdhD
sdhA
hypothetical protein
sdhB
wild type
5‘ …AGCGACGGCTGGCACGGCATCCCGCCG GCC TGGATCGGGCTCGCGGCCGCGGTG… 3‘
DFS mutant 2
5‘ …AGCGACGGCTGGCACGGCATCCCGCCG ACC TGGATCGGGCTCGCGGCCGCGGTG… 3‘
exchange of amino acid (T⟶A)

◂**Fig. 6** Phenotypes and genotypes of DFS-resistant mutants. **a**–**c** Growth kinetics and time-dependent concentration of mesaconic acid and 2-methylsuccinic acid in supernatant of *M. extorquens* AM1 wild type + pCM160_RBS_*yciA*Ec (**a**), DFS mutant 1 + pCM160_RBS_*yciA*Ec (**b**), and DFS mutant 2 + pCM160_RBS_*yciA*Ec (**c**), growing in methanol minimal medium. Other EMCP-derived carboxylic acid products with titers insufficient for quantification (< 5 mg/L) are not displayed. Error bars represent standard deviations from three independent replicates. **d** Gene locus region of MEXAM1_RS10985-MEXAM1_RS1097, in which DFS mutant 1 has a 12 bp deletion within the dicarboxylic acid transporter MEXAM1_RS10985 (≙ *dctA2*). **e** Gene locus region MEXAM1_RS18205-MEXAM1_RS18230, in which a mutation in a SLC13 family permease encoding gene could be identified in the genome of DFS mutant 2. An additional visualization of the data in form of products per OD_{600} can be found in Online Resource Fig. S4

AM1 wild type strain also containing plasmid pCM160_RBS_*yciA*Ec. None of the strains showed a growth defect in liquid methanol minimal medium (Fig. 6a-c). Although a slight decrease in mesaconic acid concentration was still observed in the culture of DFS mutant 1 after 40 h of cultivation, it showed significantly reduced product reuptake compared to the wild type control strain. DFS mutant 2 showed production/uptake kinetics similar to the wild type control. The genomes of the wild type control strain, DFS mutant 1 and DFS mutant 2 were sequenced to identify any new mutations. A total of 11 identical mutations were found in all three strains, which differ from the NCBI reference genome sequence (Online Resource Table S2). In DFS mutant 1, an additional 12 bp deletion within the dicarboxylic acid transporter gene *dctA2* (MEXAM1_RS10985) could be identified (Fig. 6d). Although the *dctA2* gene product is probably involved in product reuptake, a residual uptake was still observed in DFS mutant 1. In DFS mutant 2, a single point mutation was identified causing an amino acid exchange in a SLC13 family permease (MEXAM1_RS18205, Fig. 6e). This mutation was probably responsible for the DFS resistance phenotype. Nevertheless, the strain did not show a decreased reuptake of mesaconic acid and 2-methylsuccinic acid behavior (Fig. 6c) observed for DFS mutant 1.

Mesaconic and 2-methylsuccinic acid production behavior of strains lacking one or several transporter-encoding genes

The 12 bp deletion in the *dctA2* gene in DFS mutant 1 conferred a reduced reuptake of mesaconic acid and 2-methylsuccinic acid, yet the reuptake was only partially prevented. This could indicate that the transporter protein variant lacking four amino acids is still partially active or that more than one import protein is involved in the reuptake of the products. Aiming at complete suppression of reuptake, we constructed single, double and triple deletion strains lacking one, two or three putative dicarboxylic acid transporter genes (start to stop codon). Besides *dctA2,* this deletion approach involved also *dctA1* and *dctA3*. Additionally, a Δ*kgtP* knockout strain was constructed and analyzed. To also obtain strains with high process suitability, we introduced the deletions not only in *M. extorquens* AM1, but also in *M. extorquens* AM1 Δ*cel*. Since the latter lacks the cellulose synthesis operon, it has been shown to be more suitable for downstream applications as biofilm formation and cell clumping are reduced (Delaney et al. 2013). Although we attempted to achieve a triple *dctA* deletion by testing different sequences of consecutive gene deletions, not all combinations could be achieved in both, the wild type and the Δ*cel* strain. Nevertheless, all possible combinations could be achieved in one of the two strains. Since production behavior did not differ significantly between both strains, the phenotypes of all combinations of transporter gene deletions could be analyzed. Since we observed that YciAHI resulted in higher product titers compared to YciAEc (e.g., Fig. 2 versus Fig. 5) and a crystal structure for YciAHI is available that may facilitate further developments (3BJK, Willis et al. 2008), the YciAHI thioesterase was chosen over the *E. coli* enzyme for the experiment. It was introduced into all constructed transporter deletion strains to investigate the effects on product reuptake during shake flask cultivations with methanol minimal medium. Single deletions of *dctA1*, *dctA3*, or *kgtP* had no effect on the production or reuptake behavior of mesaconic acid or 2-methylsuccinic acid compared to the reference strains (Fig. 7a,b). Only the effect caused by complete deletion of the *dctA2* gene is clearly evident and it is comparable to the effect caused by the 12 bp deletion in the *dctA2* gene in DFS mutant 1. The same applies to strains with double or triple deletions: Only in strains containing at least the *dctA2* deletion, a reduced dicarboxylic acid uptake could be observed after cell growth stopped, whereas additional deletions did not lead to additional phenotypes. In all Δ*dctA2* strains, product levels increased during the exponential growth phase of the cells as in the control strains. The product concentrations per biomass during the growth phase and therefore also the maximum product levels determined at the end of the exponential growth phase were, however, not higher than those observed in the production strain without transporter gene deletions (Fig S5a). Once the cells entered the stationary phase, the consumption of 2-methylsuccinic acid was clearly reduced while the mesaconic acid decrease was almost completely prevented. Therefore, in addition to a higher maintenance of the product levels, the ratio between the two products changed in the course of the stationary phase.

Investigation of transporter deletion effects on citramalic acid production

An alternative way to reduce reuptake of dicarboxylic acid products is by converting them to non-metabolizable products. By introduction of a mesaconase/fumarate hydratase

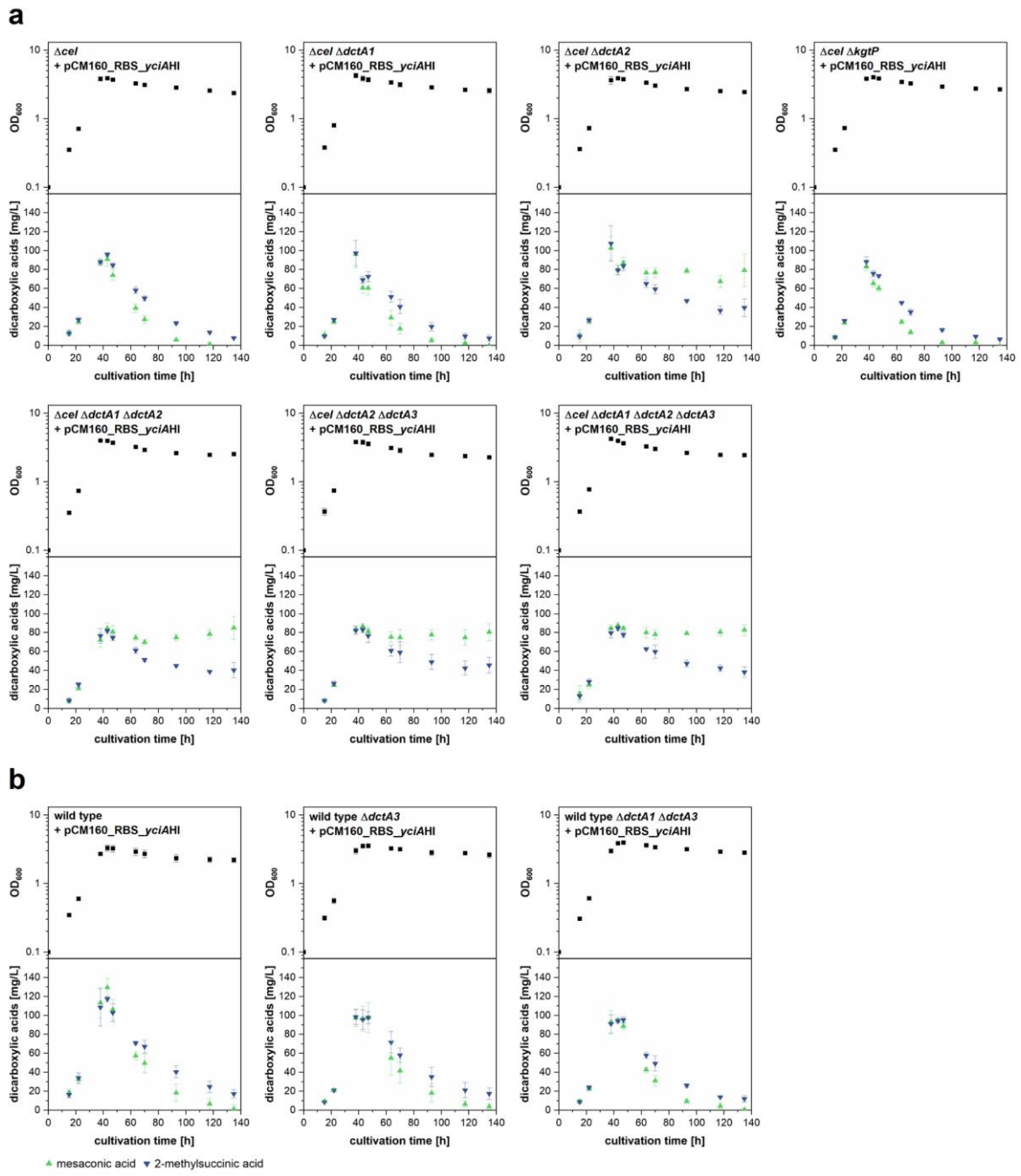

Fig. 7 Growth kinetics and time-dependent concentration of mesaconic acid and 2-methylsuccinic acid in supernatant of *M. extorquens* AM1 cells without and with single, double or triple transporter deletions. Strains heterologously express thioesterase encoding gene *yciA*HI in methanol minimal medium. Other EMCP-derived carboxylic acid products with titers insufficient for quantification (<5 mg/L) are not displayed. Error bars represent standard deviations from three independent replicates. Strains were constructed based on either **a** *M. extorquens* AM1 wild type or **b** *M. extorquens* AM1 Δ*cel* strain. An additional visualization of the data in form of products per OD_{600} can be found in Online Resource Fig. S5

from *P. xenovorans* (Kronen et al. 2015) in addition to YciAEc, we were able to convert mesaconic acid to citramalic acid by enzymatic hydration (Fig. 8a). Analytical evidence for the conversion is given in Online Resource Fig. S1. In contrast to mesaconic acid and 2-methylsuccinic acid, citramalic acid is most probably not taken up and metabolized by the cell, as its concentration stayed stable during the stationary phase (Fig. 8b,c). However, cell density values and product measurements of *M. extorquens* AM1 and *M. extorquens* AM1 Δ*cel* strains carrying pCM160_*yciA*Ec_RBS_mesaPx showed high standard deviations for the biological replicates. The maximal citramalic acid concentration measured was 164 ± 71 mg/L or 170 ± 49 mg/L, respectively (Fig. 8b,c, left graphs). Use of corresponding triple *dctA* deletion strains resulted in clearly higher citramalic acid concentrations of approximately 249 ± 5 mg/L or 241 ± 4 mg/L, respectively (Fig. 8b,c, right graphs). Moreover, in both strain backgrounds, the transporter gene deletions obviously reduced the variations observed within three independent transformants.

Discussion

In this study, we focused on the reduction of product reuptake in *M. extorquens* AM1 strains producing dicarboxylic acids as 2-methylsuccinic acid and mesaconic acid. This will serve as a basis for the development of stable and more productive strains for the future production of dicarboxylic acids from methanol.

In the past, product reuptake in the later cultivation phases reduced the product yield (Sonntag et al. 2014, 2015). It was postulated that there are two possible modes for product uptake: 1) it may be triggered upon transition from exponential to stationary growth phase or 2) the product uptake takes place over the entire course of cultivation and is masked by the high production rates during the early cultivation stages (Sonntag et al. 2014). In the second case, the productivity in the exponential growth phase would be reduced by the presence of a futile cycle. By repressing the reimport of products, one could eliminate this cycle and thus achieve higher productivity.

To identify potential import factors, we performed transcriptome analysis of a strain harboring plasmid pCM160_RBS_*yciA*HI, encoding the thioesterase YciA from *Haemophilus influenzae*. However, we could not identify genes that were clearly upregulated in stationary growth phase compared to early sampling points in the exponential growth phase and which were annotated to encode for transporters. When specifically analyzing the time-dependent expression levels of the *dctA* homologs and *kgtP* (targets suggested by Sonntag and colleagues (2014)) and comparing them with a control strain, we found slightly increased levels only for *dctA1*. After concluding that the transcriptome analysis was no appropriate approach to identify relevant transport factors, we chose a straightforward mutant selection approach using a cytotoxic dicarboxylic acid.

In preliminary tests, DFS toxicity surprisingly applied only to methanol- and acetate-grown and not to succinate-grown cells. As its toxicity could furthermore be compensated by supplementing the cells with glyoxylate, we concluded that DFS toxicity is not only mediated by the EMCP but directly targets it. Since DFS has a high structural similarity to the dicarboxylic acids that constitute the EMCP intermediates in their CoA-activated form, DFS might act as competitive inhibitor. Glyoxylate supplementation has previously been shown to fully restore methylotrophic growth of Δ*ccr*, Δ*epi*, and Δ*ecm* strains and to partially restore growth of Δ*msd* strains (Schada von Borzyskowski et al. 2018), so we can speculate that DFS acts on one or several of the corresponding EMCP enzymes.

Using a simple selection approach, we were able to isolate DFS-resistant *M. extorquens* AM1 mutants from DFS-containing methanol minimal medium or acetate minimal medium. In one of the two mutants selected for further investigations, DFS resistance was accompanied by reduced uptake of mesaconic acid and 2-methylsuccinic acid. DFS mutant 2, in which we identified a mutation in a putative dicarboxylic acid transporter encoding gene (SLC13 family), was resistant to DFS. Nevertheless, the strain showed 2-methylsuccinic acid and mesaconic acid uptake behavior comparable to a non-mutated control strain. In contrast, mutation or deletion of *dctA2*, led to strong reduction of product reuptake. The corresponding mutant strain, DFS mutant 1, not only exhibited the DFS resistance phenotype we selected for, but in addition showed clearly reduced reuptake of mesaconic acid and 2-methylsuccinic acid. Since the strain was still able to grow on succinate, we assume that *dctA2* is not identical to the open reading frame designated as A33597 in Van Dien's study (Van Dien et al. 2003).

Although we did not perform complementation experiments with dctA2, strong indications for a dicarboxylic acid uptake function of DctA2 exist. The fact that also a decreased sodium concentration resulted in a ceasing of dicarboxylic acid reuptake (Sonntag et al. 2015) is in line with this assumption, as DctA transporters are sodium-dependent (Janausch et al. 2002). The finding of identical acid uptake phenotypes with a *dctA2* deletion strain is an additional argument for DctA2 to be the causal factor for the observed reuptake defect. It furthermore demonstrated that the removal of four amino acids from the protein in the DFS mutant 1 probably results in a complete loss of function with respect to mesaconic acid and 2-methylsuccinic acid uptake. Possible explanations for the residual uptake activity observed for *dctA2* mutants were contributions of DctA2 homologs DctA1 and DctA3. After we found out that single

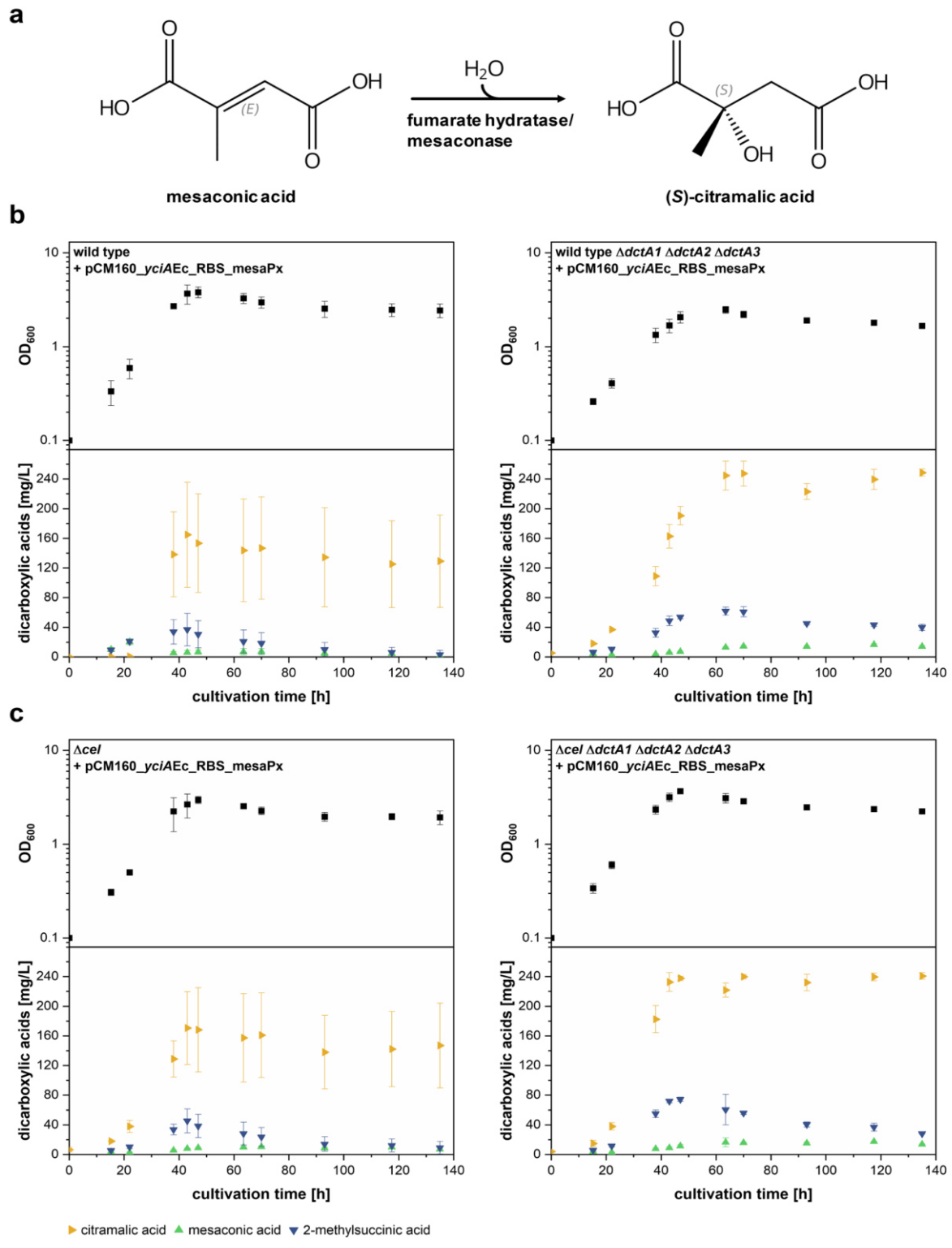
a
HO
O
OH
(E)
H2O
fumarate hydratase/
mesaconase
(S)
mesaconic acid
(S)-citramalic acid
b
wild type
+ pCM160_yciAEc_RBS_mesaPx
wild type ΔdctA1 ΔdctA2 ΔdctA3
+ pCM160_yciAEc_RBS_mesaPx
c
Δcel
+ pCM160_yciAEc_RBS_mesaPx
Δcel ΔdctA1 ΔdctA2 ΔdctA3
+ pCM160_yciAEc_RBS_mesaPx
OD600
dicarboxylic acids [mg/L]
cultivation time [h]
citramalic acid
mesaconic acid
2-methylsuccinic acid

◂**Fig. 8** Production of citramalic acid with strains lacking DctA transporters. **a** Reaction scheme for hydration of mesaconic acid to (*S*)-citramalic acid catalyzed by mesaconase/fumarate hydratase (from Kronen et al. 2015). Absolute stereochemistry and double bond geometry are labeled in gray. **b** Growth kinetics and time-dependent concentration of mesaconic acid, 2-methylsuccinic acid and citramalic acid in supernatant of *M. extorquens* AM1 wild type and triple *dctA* transporter deletion strain expressing thioesterase encoding gene *yciA*HI and mesaconase in methanol minimal medium. **c** Growth kinetics and time-dependent concentration of mesaconic acid, 2-methylsuccinic acid and citramalic acid in supernatant of Δ*cel* and Δ*cel* triple *dctA* transporter deletion strain expressing thioesterase encoding gene *yciA*HI and mesaconase from *P. xenovorans* in methanol minimal medium cultures. Other EMCP-derived carboxylic acid products with titers insufficient for quantification (< 5 mg/L) are not displayed. Error bars represent standard deviations from three independent transformants. An additional visualization of the data in form of products per OD_{600} can be found in Online Resource Fig. S6

deletions of *dctA1* or *dctA3* did not cause changes to the product uptake kinetic, we initially hypothesized that these factors might nevertheless be responsible for the residual uptake activity seen for the *dctA2* mutants. A conceivable scenario would be that transcription of their genes is activated when DctA2 is absent. However, we ruled out this possibility by testing mutant strains in which all three dctA genes were deleted. Only combinations of deletions that included the *dctA2* deletion resulted in clearly reduced product reuptake. The fact that product yields were maintained in stationary phase but that no product increase per biomass could be observed during growth for the *dctA2* mutants compared to the wild type (Fig. S5a), may suggest that uptake is likely to only occur if a threshold of product concentration is reached or carbon becomes limiting. Another aspect revealed from the analysis of the production kinetics of the *dctA2* mutant strains is based on the observation that the reduced reuptake does not apply to the two products in the same way. Expression of *yciA* from *H. influenzae* in *M. extorquens* AM1 wild type strain in our experiments usually resulted in release of similar amounts of the two dicarboxylic acid products, with a slightly higher level of 2-methylsuccinic acid. The *dctA2* deletion seems especially to prevent mesaconic acid uptake, while 2-methylsuccinic acid is still imported to a certain extent. This observation once more suggests the presence of other, yet unidentified transporters involved at least in 2-methylsuccinic acid uptake. The possibility of passive diffusion of completely protonated acids through the membrane is furthermore ruled out by the different kinetics of the two acids. As the two products have comparable pKa values and show high structural similarity, strong differences in membrane passing rates are not expected.

Besides prevention of product reuptake in the stationary phase, we also aimed at elimination of product uptake potentially taking place in the production phase during exponential growth. In the experiments conducted, the mesaconic acid and 2-methylsuccinic acid production kinetics in the exponential growth phase was the same, both with and without *dctA2* deletion. Although the overall product titer was not increased, the process is much more robust when performed in a *dctA2* deletion strain as the harvest time for achieving maximum product yield is no longer as time critical.

For the production of citramalic acid, however, the use of the *dctA* triple deletion strain resulted not only in a significant gain in robustness, but also in production yield. Citramalic acid as a non-natural product of *M. extorquens* AM1 is not reimported by the cells, as shown by the respective experiment with the control strain. Although a clear explanation for the improvements of citramalic acid production in the DctA mutant strain compared to the control strain cannot be drawn from the experiments, reduced mesaconic acid uptake is probably causal for the observed phenotypes. This reduced uptake might slow down its further metabolization and thereby increase the carbon flux towards citramalic acid. The use of a *dctA* triple deletion strain for citramalic production led to a 1.4-fold increase in mean product yield and a substantial reduction of the standard deviations. The study that first described mesaconase/fumarate hydratase from *P. xenovorans* demonstrated its enantioselectivity towards (*S*)-citramalic acid (Kronen et al. 2015). We therefore assumed that the constructed *M. extorquens* AM1 strains also produce enantiopure (*S*)-citramalic acid.

Although we were not able to achieve higher overall yields for mesaconic acid or 2-methylsuccinic acid, the use of a *dctA2* deletion strain almost completely prevented the reuptake of mesaconic acid and part of 2-methylsuccinic acid within the stationary growth phase. Furthermore, the product yield of citramalic acid was significantly increased in the *dctA2* deletion strain. Therefore, the dicarboxylic acid transporter deletion mutants provided here are excellent starting points for the creation of different dicarboxylic acid production strains.

Supplementary Information The online version contains supplementary material available at https://doi.org/10.1007/s00253-022-12161-0.

Author contribution LP and MB conceived and designed research. LP conducted experiments. EG constructed plasmid pCM160_RBS_*yciA*HI. LP and MB analyzed data and wrote the manuscript. All authors read and approved the manuscript.

Funding Open Access funding enabled and organized by Projekt DEAL. This study was supported by funds of the Federal Ministry of Education and Research (BMBF, FKZ 031B0340A, project Chiramet).

Data availability All data generated or analyzed during this study are included in this published article and its supplementary information file.

Declarations

Ethical approval This article does not contain any studies with human participants performed by any of the authors.

Conflict of interest The authors declare no competing interests.

References

Alber BE (2011) Biotechnological potential of the ethylmalonyl-CoA pathway. Appl Microbiol Biotechnol 89:17–25. https://doi.org/10.1007/s00253-010-2873-z

Alonso S, Rendueles M, Díaz M (2014) Microbial production of specialty organic acids from renewable and waste materials. Crit Rev Biotechnol 35:497–513. https://doi.org/10.3109/07388551.2014.904269

Bertani G (1951) Studies on lysogenesis I. The mode of phage liberation by lysogenic *Escherichia coli*. J Bacteriol 62:293–300. https://doi.org/10.1128/jb.62.3.293-300.1951

Chistoserdova LV, Lidstrom ME (1996) Molecular characterization of a chromosomal region involved in the oxidation of acetyl-CoA to glyoxylate in the isocitrate-lyase-negative methylotroph Methylobacterium extorquens AM1. Microbiol 142:1459–1468.https://doi.org/10.1099/13500872-142-6-1459

Delaney NF, Kaczmarek ME, Ward LM, Swanson PK, Lee M-C, Marx CJ (2013) Development of an optimized medium, strain and high-throughput culturing methods for Methylobacterium extorquens. PLoS One 8:e62957. https://doi.org/10.1371/journal.pone.0062957

Erb TJ, Berg IA, Brecht V, Müller M, Fuchs G, Alber BE (2007) Synthesis of C5-dicarboxylic acids from C2-units involving crotonyl-CoA carboxylase/reductase: the ethylmalonyl-CoA pathway. Proc Natl Acad Sci USA 104:10631–10636. https://doi.org/10.1073/pnas.0702791104

Erb TJ, Frerichs-Revermann L, Fuchs G, Alber BE (2010) The apparent malate synthase activity of *Rhodobacter sphaeroides* is due to two paralogous enzymes, (3S)-malyl-coenzyme A (CoA)/β-methylmalyl-CoA lyase and (3S)-malyl-CoA thioesterase. J Bacteriol 192:1249–1258. https://doi.org/10.1128/JB.01267-09

Grant SGN, Jessee J, Bloom FR, Hanahan D (1990) Differential plasmid rescue from transgenic mouse DNAs into *Escherichia coli* methylation-restriction mutants. Proc Natl Acad Sci 87:4645–4649. https://doi.org/10.1073/PNAS.87.12.4645

Hanahan D (1985) Techniques for transformation of *E. coli*. In: Glover DM (ed) DNA cloning: a practical approach. IRL Press, Oxford, pp 109–135

Janausch IG, Zientz E, Tran QH, Kröger A, Unden G (2002) C4-dicarboxylate carriers and sensors in bacteria. Biochim Biophys Acta - Bioenerg 1553:39–56. https://doi.org/10.1016/S0005-2728(01)00233-X

Jang Y-S, Kim B, Shin JH, Choi YJ, Choi S, Song CW, Lee J, Park HG, Lee SY (2012) Bio-based production of C2–C6 platform chemicals. Biotechnol Bioeng 109:2437–2459. https://doi.org/10.1002/bit.24599

Kiefer P, Buchhaupt M, Christen P, Kaup B, Schrader J, Vorholt JA (2009) Metabolite profiling uncovers plasmid-induced cobalt limitation under methylotrophic growth conditions. PLoS One 4:e7831. https://doi.org/10.1371/journal.pone.0007831

Kronen M, Sasikaran J, Berg IA (2015) Mesaconase activity of class I fumarase contributes to mesaconate utilization by *Burkholderia xenovorans*. Appl Environ Microbiol 81:5632–5638. https://doi.org/10.1128/AEM.00822-15

Lee JW, Kim HU, Choi S, Yi J, Lee SY (2011) Microbial production of building block chemicals and polymers. Curr Opin Biotechnol 22:758–767. https://doi.org/10.1016/j.copbio.2011.02.011

Lim CK, Villada JC, Chalifour A, Duran MF, Lu H, Lee PKH (2019) Designing and engineering *Methylorubrum extorquens* AM1 for itaconic acid production. Front Microbiol 10:1–14. https://doi.org/10.3389/fmicb.2019.01027

Marx CJ, Lidstrom ME (2001) Development of improved versatile broad-host-range vectors for use in methylotrophs and other Gram-negative bacteria. Microbiol 147:2065–2075. https://doi.org/10.1099/00221287-147-8-2065

Marx CJ, Lidstrom ME (2002) Broad-host-range cre-lox system for antibiotic marker recycling in Gram-negative bacteria. Biotechniques 33:1062–1067. https://doi.org/10.2144/02335rr01

Okubo Y, Yang S, Chistoserdova L, Lidstrom ME (2010) Alternative route for glyoxylate consumption during growth on two-carbon compounds by *Methylobacterium extorquens* AM1. J Bacteriol 192:1813–1823. https://doi.org/10.1128/JB.01166-09

Peel D, Quayle JR (1961) Microbial growth on C1 compounds. 1. Isolation and characterization of *Pseudomonas* AM 1. Biochem J 81:465–469. https://doi.org/10.1042/bj0810465

Peyraud R, Kiefer P, Christen P, Massou S, Portais J-C, Vorholt JA (2009) Demonstration of the ethylmalonyl-CoA pathway by using 13C metabolomics. Proc Natl Acad Sci USA 106:4846–4851. https://doi.org/10.1073/pnas.0810932106

Roode-Gutzmer QI, Kaiser D, Bertau M (2019) Renew Methanol Synth Chembioeng Rev 6:209–236. https://doi.org/10.1002/cben.201900012

Salem AR, Quayle JR (1971) Mutants of *Pseudomonas* AM1 that require glycollate or glyoxylate for growth on methanol or ethanol. Biochem J 124:74P. https://doi.org/10.1042/bj1240074P

Salis HM (2011) The ribosome binding site calculator. Methods Enzymol 498:19–42. https://doi.org/10.1016/B978-0-12-385120-8.00002-4

Schada von Borzyskowski L, Sonntag F, Pöschel L, Vorholt JA, Schrader J, Erb TJ, Buchhaupt M (2018) Replacing the ethylmalonyl-CoA pathway with the glyoxylate shunt provides metabolic flexibility in the central carbon metabolism of *Methylobacterium extorquens* AM1. ACS Synth Biol 7:86–97. https://doi.org/10.1021/acssynbio.7b00229

Seol W, Shatkin AJ (1991) *Escherichia coli* kgtP encodes an alpha-ketoglutarate transporter. Proc Natl Acad Sci USA 88:3802–3806

Sonntag F, Buchhaupt M, Schrader J (2014) Thioesterases for ethylmalonyl–CoA pathway derived dicarboxylic acid production in *Methylobacterium extorquens* AM1. Appl Microbiol Biotechnol 98:4533–4544. https://doi.org/10.1007/s00253-013-5456-y

Sonntag F, Müller JEN, Kiefer P, Vorholt JA, Schrader J, Buchhaupt M (2015) High-level production of ethylmalonyl-CoA pathway-derived dicarboxylic acids by *Methylobacterium extorquens* under cobalt-deficient conditions and by polyhydroxybutyrate negative

strains. Appl Microbiol Biotechnol 99:3407–3419. https://doi.org/10.1007/s00253-015-6418-3

Toyama H, Anthony C, Lidstrom ME (1998) Construction of insertion and deletion mxa mutants of *Methylobacterium extorquens* AM1 by electroporation. FEMS Microbiol Lett 166:1–7. https://doi.org/10.1111/j.1574-6968.1998.tb13175.x

Van Dien SJ, Okubo Y, Hough MT, Korotkova N, Taitano T, Lidstrom ME (2003) Reconstruction of C3 and C4 metabolism in *Methylobacterium extorquens* AM1 using transposon mutagenesis. Microbiology 149:601–609. https://doi.org/10.1099/mic.0.25955-0

Willis MA, Zhuang Z, Song F, Howard A, Dunaway-Mariano D, Herzberg O (2008) Structure of YciA from *Haemophilus influenzae* (HI0827), a hexameric broad specificity acyl-coenzyme A thioesterase. Biochem 47:2797–2805. https://doi.org/10.1021/bi702336d

Yang Y-M, Chen W-J, Yang J, Zhou Y-M, Hu B, Zhang M, Zhu L-P, Wang G-Y, Yang S (2017) Production of 3-hydroxypropionic acid in engineered *Methylobacterium extorquens* AM1 and its reassimilation through a reductive route. Microb Cell Fact 16:179. https://doi.org/10.1186/s12934-017-0798-2

Supplementary Information

Journal: Applied Microbiology and Biotechnology

Improvement of dicarboxylic acid production with *Methylorubrum extorquens* by reducing the product reuptake

Laura Pöschel[1], Elisabeth Gehr[1], Markus Buchhaupt[1]*

[1] DECHEMA-Forschungsinstitut, Microbial Biotechnology, Theodor-Heuss-Allee 25, 60486 Frankfurt am Main, Germany

[2] Department of Life Sciences of the Goethe University Frankfurt am Main, Max-von-Laue-Str. 9, 60438 Frankfurt am Main, Germany

*Corresponding author, Phone: +49-69-7564-629, e-mail address: markus.buchhaupt@dechema.de

Electronic supplementary material as Online Resource

Table S1 Details of genomic sequencing and mapping procedure

Strain	Genetic entity	Total number of mapped Illumina reads	Base coverage of reference sequence	Average base coverage [mean ± standard deviation]
***M. extorquens* AM1 wild type**	NC_012807	317 955	100 %	514.6 ± 186.0
	NC_012808	17 352 981	99.998 %	225.9 ± 212.4
	NC_012809	235 559	100 %	445.3 ± 141.6
	NC_012810	180 717	100 %	519.8 ± 180.6
	NC_012811	3 828 584	99.99 %	216.9 ± 70.7
***M. extorquens* AM1 DFS mutant 1**	NC_012807	353 562	100 %	1061.5 ± 258.9
	NC_012808	18 846 841	100 %	452.3 ± 86.2
	NC_012809	216 117	100 %	764.7 ± 110.5
	NC_012810	139 576	100 %	750.8 ± 101.3
	NC_012811	4 279 978	99.9998 %	447.9 ± 76.9
***M. extorquens* AM1 DFS mutant 2**	NC_012807	295 048	100 %	869.9 ± 195.3
	NC_012808	15 563 801	100 %	367.0 ± 83.7
	NC_012809	166 635	100 %	580.1 ± 73.9
	NC_012810	104 196	100 %	550.5 ± 76.2
	NC_012811	3 425 166	99.997 %	352.7 ± 58.6

Table S2 Genetic differences between the sequenced strains and the used reference genome. The listed mutations were found in all sequenced strains including *M. extorquens* AM1 wild type. N/A indicates that there is no annotated gene function (annotation date 04/11/2021)

Genetic entity	Locus tag	Gene	Polymorphism type	Change	Effect on open reading frame
NC_012808	MEXAM1_RS02205	N/A	Insertion	(C)3 → (C)4	Frame Shift
NC_012808	MEXAM1_RS10680	N/A	Deletion	(G)3 → (G)2	Frame Shift
NC_012808	MEXAM1_RS34015	N/A	SNP (transversion)	T → G	None
NC_012808	MEXAM1_RS12610	N/A	SNP (transition)	C → T	None
NC_012808	MEXAM1_RS12610	N/A	SNP (transition)	T → C	None
NC_012808	MEXAM1_RS13695	treS	Deletion	(C)4 → (C)3	Frame Shift
NC_012808	MEXAM1_RS14240	N/A	Deletion	(G)3 → (G)2	Frame Shift
NC_012808	MEXAM1_RS32900	N/A	Deletion	-TGCCG	Frame Shift
NC_012808	Intergenic region	N/A	SNP (transition)	A → G	None
NC_012811	MEXAM1_RS28080	N/A	Insertion	+C	Frame Shift
NC_012811	MEXAM1_RS29025	N/A	Deletion	(G)3 → (G)2	Frame Shift

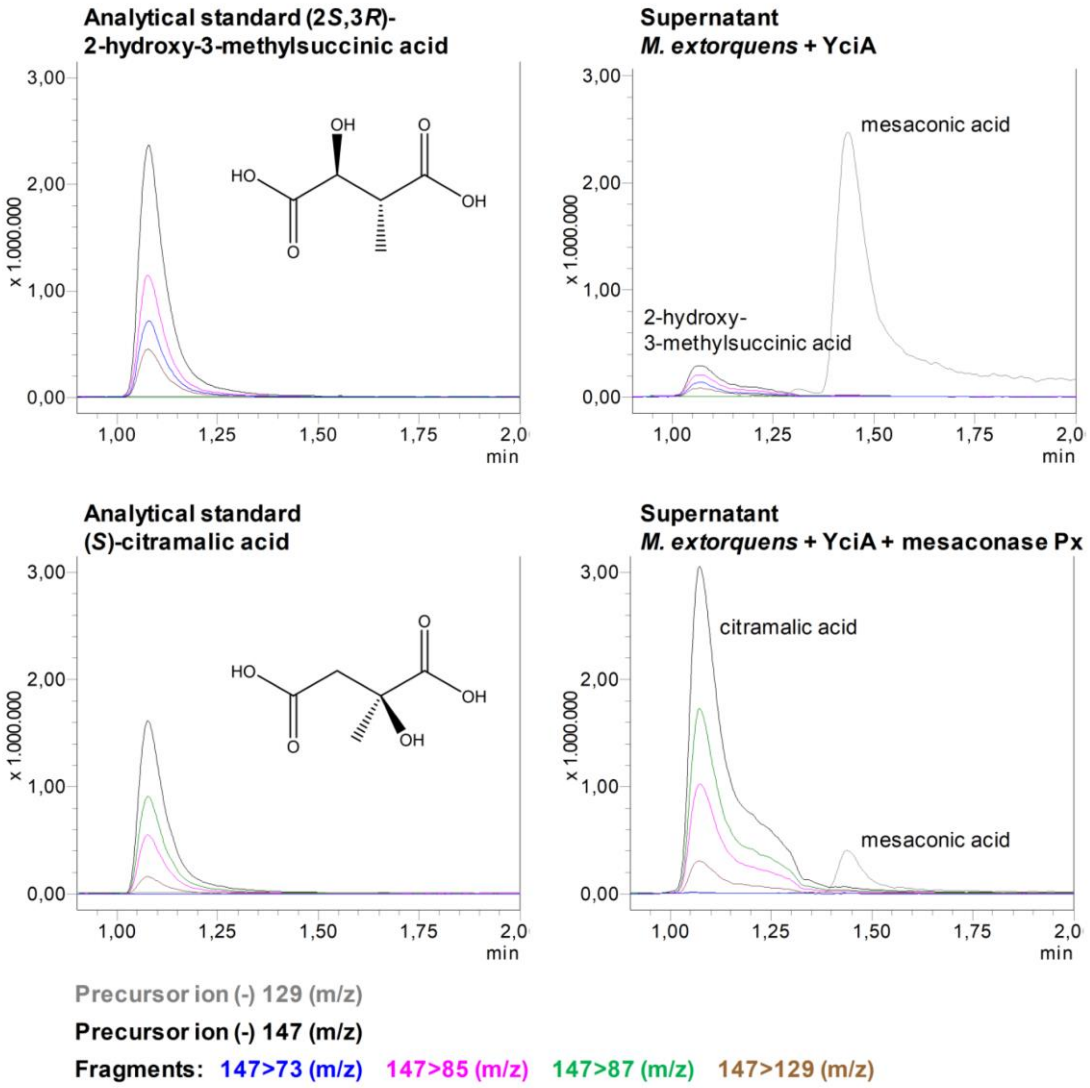

Fig. S1 Analytical evidence for production of citramalic acid by an *M. extorquens* AM1 strain expressing a mesaconase from *Paraburkholderia xenovorans* (mesaconase_Px) in addition to YciA from *Haemophilus influenzae*. Shown are chromatograms of precursor 129 m/z (mesaconic acid) and precursor 147 m/z (2-hydroxy-3-methylsuccinic acid or citramalic acid). To distinguish between 2-hydroxy-3-methylsuccinic acid (present at low concentrations in *M. extorquens* AM1 cultures) and citramalic acid, the analytes were fragmented using the identical LC-MS/MS MRM method detecting fragments 73, 85, 129 and 87. Here, the fragment of 87 (m/z) is characteristic for citramalic acid and can therefore be used for unambiguous identification. In supernatant of cultures with *M. extorquens* AM1 expressing thioesterase gene *yciA*, mesaconic acid as well as 2-hydroxy-3-methylsuccinic acid can be detected. With the additional introduction of a mesaconase, the mesaconase peak becomes smaller and conversion to citramalic acid can be observed.

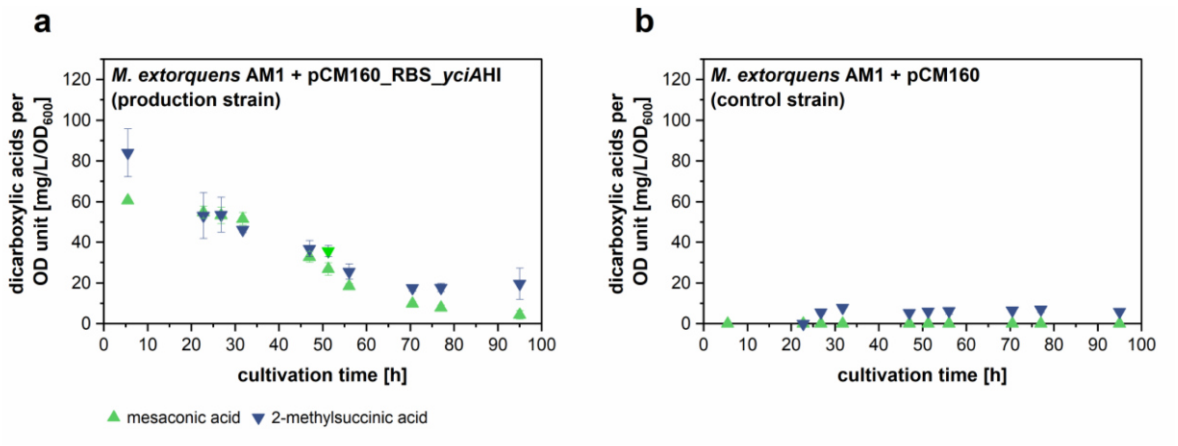

Fig. S2 Dicarboxylic acid production per OD_{600} (transformed data from figure 2). Mesaconic acid and 2-methylsuccinic acid concentrations per OD_{600} in supernatant of *M. extorquens* AM1 + pCM160_RBS_*yciAHI* (**a**) or *M. extorquens* AM1 + pCM160 (**b**) growing in methanol minimal medium. Error bars represent standard deviations from three independent replicates

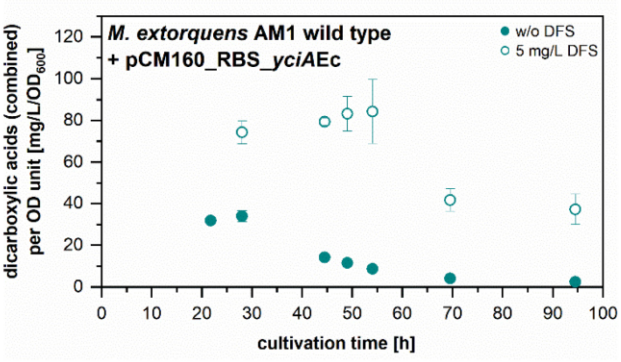

Fig. S3 Dicarboxylic acid production per OD_{600} (transformed data from figure 5). Mesaconic acid and 2-methylsuccinic acid concentrations (combined) per OD_{600} in supernatant of *M. extorquens* AM1 harboring pCM160_RBS_*yciA*Ec in methanol minimal medium (*filled symbols*) and in methanol minimal medium with addition of 5 mg/L 2,2-difluorosuccinic acid (DFS) after 5 h of cultivation (*empty symbols*). Error bars represent standard deviations from two independent replicates

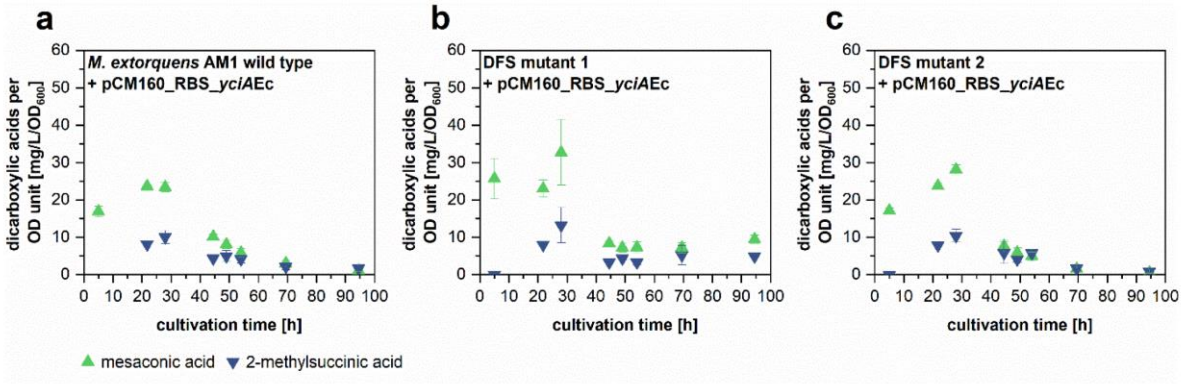

Fig. S4 Dicarboxylic acid production per OD_{600} (transformed data from figure 6). Mesaconic acid and 2-methylsuccinic acid concentrations per OD_{600} in supernatant of *M. extorquens* AM1 wild type + pCM160_RBS_*yciA*Ec (**a**), DFS mutant 1 + pCM160_RBS_*yciA*Ec (**b**) and DFS mutant 2 + pCM160_RBS_*yciA*Ec (**c**), growing in methanol minimal medium. Error bars represent standard deviations from three independent replicates

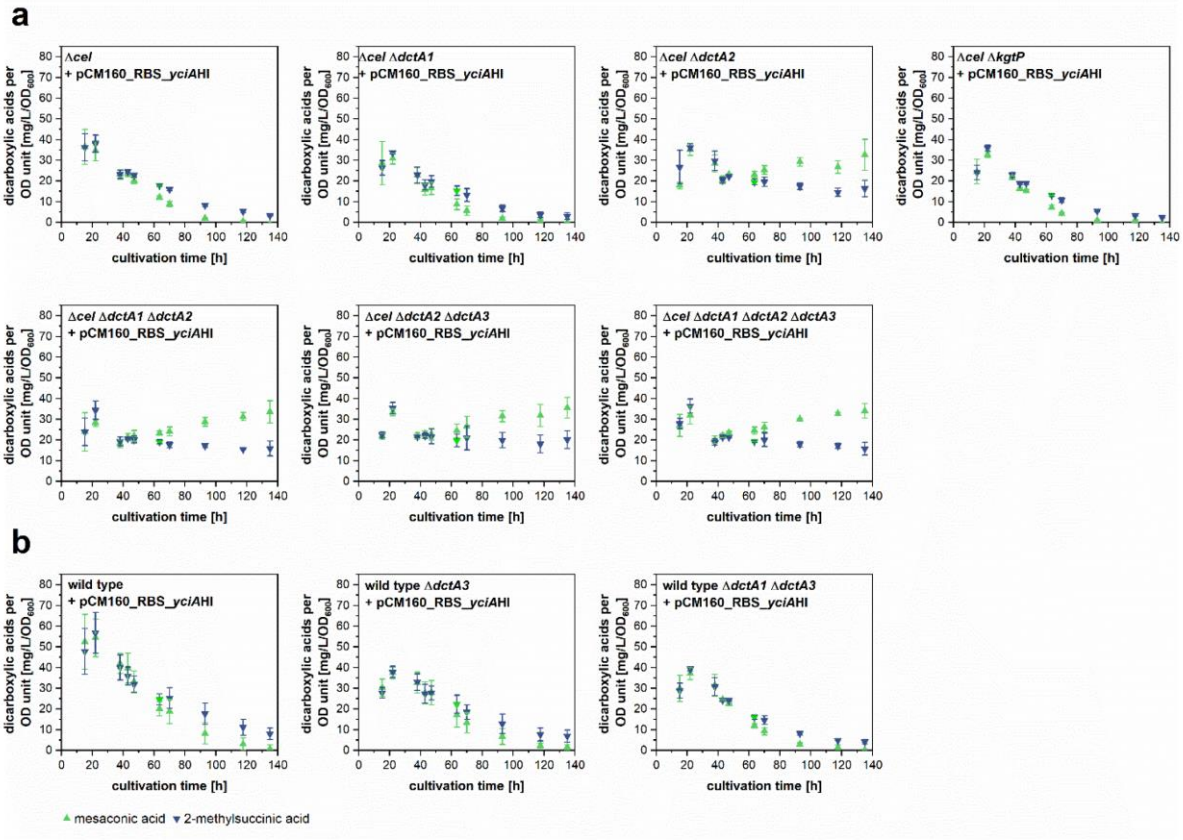

Fig. S5 Dicarboxylic acid production per OD_{600} (transformed data from figure 7). Mesaconic acid and 2-methylsuccinic acid concentrations per OD_{600} in supernatant of *M. extorquens* AM1 cells without and with single, double or triple transporter deletions. Strains heterologously express the thioesterase encoding gene *yciA*HI in methanol minimal medium. Error bars represent standard deviations from three independent replicates. Strains were constructed based on either **a** *M. extorquens* AM1 wild type or **b** *M. extorquens* AM1 Δ*cel* strain

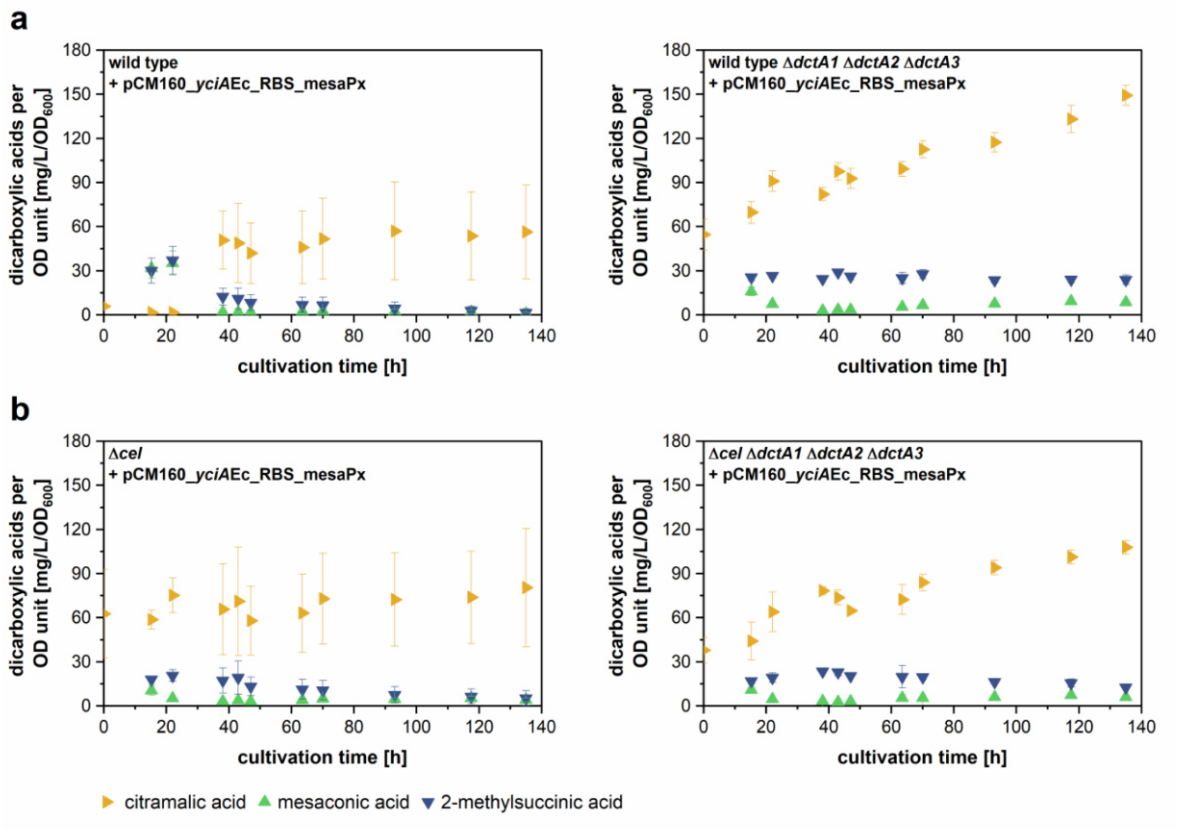

Fig. S6 Dicarboxylic acid production per OD_{600} (transformed data from figure 8). Mesaconic acid, 2-methylsuccinic acid and citramalic acid concentrations per OD_{600} in supernatant of *M. extorquens* AM1 wild type and triple *dctA* transporter deletion strain expressing thioesterase encoding gene *yciA*HI and mesaconase in methanol minimal medium

6.2 Engineering of thioesterase YciA from *Haemophilus influenzae* for production of carboxylic acids

Declaration of author contributions to the manuscript:

Engineering of thioesterase YciA from *Haemophilus influenzae* for production of carboxylic acids

Status: accepted

Name of journal: Applied Microbiology and Biotechnology

Contributing authors: Laura Pöschel (LP), Mónica Guevara-Martínez (MGM), David Hörnström (DH), Antonius van Maris (AvM), Markus Buchhaupt (MB)

What are the contributions of the doctoral candidate and his co-authors?

(1) Concept and design

Doctoral candidate:	60 %
Co-author MB:	40 %

(2) Conducting tests and experiments

Doctoral candidate:	90 %	Docking experiments, construction of mutant libraries, blotting and immunodetection, cloning experiments, production experiments with *M. extorquens* AM1, recombinant production of YciA and *in vitro* experiments
Co-author MGM:	5 %	Testing YciA_F35L for production for 3-hydroxybutyric acid production with *E. coli*
Co-author DH:	5%	Testing YciA_F35L for production for 3-hydroxybutyric acid production with *E. coli*

(3) Compilation of data sets and figures

Doctoral candidate:	90 %	Data collection, preparation of figures and tables
Co-author MGM:	5 %	Data collection
Co-author DH:	5%	Data collection

(4) Analysis and interpretation of data

Doctoral candidate:	80 %	Analysis and interpretation of data
Co-author MB:	20 %	Interpretation of data

(5) Drafting of manuscript

Doctoral candidate:	85 %
Co-author MB:	10 %
Co-author AvM:	5 %

Engineering of thioesterase YciA from *Haemophilus influenzae* for production of carboxylic acids

Laura Pöschel[1,2], Mónica Guevara-Martínez[3], David Hörnström[3], Antonius J.A. van Maris[3], Markus Buchhaupt[1]*

[1] DECHEMA-Forschungsinstitut, Microbial Biotechnology, Theodor-Heuss-Allee 25, 60486 Frankfurt am Main, Germany

[2] Faculty of Biological Sciences, Goethe University Frankfurt, Max-von-Laue-Str. 9, 60438 Frankfurt am Main, Germany

[3] Department of Industrial Biotechnology, School of Engineering Sciences in Chemistry, Biotechnology and Health, KTH Royal Institute of Technology, AlbaNova University Center, SE 10691 Stockholm, Sweden

*Corresponding author,
Phone: +49-69-7564-629, e-mail address: markus.buchhaupt@dechema.de

ORCID

Laura Pöschel: 0000-0002-8892-3998

Mónica Guevara-Martínez: 0000-0001-6501-9886

David Hörnström: 0000-0003-1442-6689

Antonius J.A. van Maris: 0000-0001-5319-7511

Markus Buchhaupt: 0000-0003-2720-5973

Abstract

Acyl-CoA-thioesterases, which hydrolyze acyl-CoA-esters and thereby release the respective acid, have essential functions in cellular metabolism and have also been used to produce valuable compounds in biotechnological processes. Thioesterase YciA originating from *Haemophilus influenzae* has been previously used to produce specific dicarboxylic acids from CoA-bound intermediates of the ethylmalonyl CoA pathway (EMCP) in *Methylorubrum extorquens*. In order to identify variants of the YciA enzyme with the capability to hydrolyze so far inaccessible CoA-esters of the EMCP or with improved productivity, we engineered the substrate-binding region of the enzyme. Screening a small semi-rational mutant library directly in *M. extorquens* yielded the F35L variant which showed a drastic product level increase for mesaconic acid (6.4-fold) and 2-methylsuccinic acid (4.4-fold) compared to the unaltered YciA enzyme. Unexpectedly, *in vitro* enzyme assays using respective *M. extorquens* cell extracts or recombinantly produced thioesterases could not deliver congruent data, as the F35L variant showed strongly reduced activity in these experiments. However, applied in an *Escherichia coli* production strain, the protein variant again outperformed the wild-type enzyme by allowing 3-fold increased 3-hydroxybutyric acid product titers. Saturation mutagenesis of the codon for position 35 led to the identification of another highly efficient YciA variant and enabled structure-function interpretations. Our work describes an important module for dicarboxylic acid production with *M. extorquens* and can guide future thioesterase improvement approaches.

Keywords

Methylorubrum extorquens
Thioesterase
Dicarboxylic acids
3-Hydroxybutyric acid
Enzyme engineering

Key Points

Substitutions at position F35 of YciAHI changed the productivity of YciA-based release of carboxylic acid products in *M. extorquens* AM1 and *E. coli*

YciAHI F35N and F35L are improved variants for dicarboxylic production of 2-methylsuccinic acid and mesaconic acid with *M. extorquens* AM1

In vitro enzyme assays did not reveal superior properties of the optimized protein variants

Introduction

Thioesterases (EC 3.1.2.1 - EC 3.1.2.27) hydrolyze thioesters to the thiol and its carboxylic acid component. They play a central role in basal cellular mechanisms of all living cells in metabolic networks and as regulatory enzymes (Swarbrick et al. 2020). Acyl-CoA thioesterases (ACOTs) are an important target for the engineering of biotechnological production strains. With their critical role in lipid metabolism, modified ACOTs have the potential to vary intracellular levels of acyl-CoAs, free fatty acids and CoA-SH in the cell (Hunt and Alexson 2002). Moreover, ACOTs have been used as key catalysts for product release of hydroxy acids and carboxylic acids in various microbial production strains (Gao et al. 2002; Lee and Lee 2003; Liu et al. 2007; Martin and Prather 2009; Tseng et al. 2009; Chung et al. 2009; Martin et al. 2013; Sonntag et al. 2014; Guevara-Martínez et al. 2015; Jarmander et al. 2015; Perez-Zabaleta et al. 2016; Guevara-Martínez et al. 2019; Pöschel et al. 2022). For example, acyl-CoA thioesterase YciAEc (EC 3.1.2.20) is used in the production of 3-hydroxybutyric acid (3HB) from (*R*)-3-hydroxybutyryl-CoA with an engineered *Escherichia coli* strain (Guevara-Martínez et al. 2015; Jarmander et al. 2015; Perez-Zabaleta et al. 2016). In this strain, the overexpression of native *yciAEc* together with nitrogen depletion and a glucose feed yielded 3HB product titers of up to 14.3 g/L (Guevara-Martínez et al. 2019). A second example for the biotechnological application of YciA is the production of dicarboxylic acids with *Methylorubrum extorquens.* Here, YciA originating from *E. coli* (YciAEc) or *Haemophilus influenzae* (YciAHI) was used to produce 2-methylsuccinic acid and mesaconic acid from CoA-ester intermediates of the ethylmalonyl-CoA-pathway (EMCP) (Sonntag et al. 2014; Pöschel et al. 2022). The authors described the production of a combined titer of 130 mg/L of 2-methylsuccinic acid and mesaconic acid in shake flask cultures of *M. extorquens* expressing *yciAEc* (Sonntag et al. 2014), which could be improved to 247 mg/L in a *yciAHI* expressing strain by minimizing product reuptake by deletion of transporter gene *dctA2* (Pöschel et al. 2022). These applications show the potential of thioesterase YciA in biotechnological processes. The broad range thioesterase YciAHI shows activity in a "physiologically relevant" range ($k_{cat}/K_m > 10^4$ $M^{-1}s^{-1}$) for a wide range of acyl-CoA thioesters (Zhuang et al. 2008) and is therefore a promising catalyst for release of various CoA-bound acids.

The crystal structure of YciAHI was elucidated and assigned the enzyme to the hot dog fold thioesterase superfamily (Willis et al. 2008). The characteristic hot dog fold motif consists of a five-stranded, antiparallel ß-fold wrapped around an elongated α-helix (Dillon and Bateman 2004; Zhuang et al. 2008). This fold diverged from an ancient archetype to fulfil a plethora of functions in the cell. Dillon and Bateman identified 18 different domain architectures for hot dog fold proteins and defined 17 subfamilies, eight of them being thioesterases (Dillon and Bateman 2004). The 3D architecture of this motif itself is highly conserved (Pidugu et al. 2009).

Nevertheless, the well-studied 4-hydroxybenzoyl-CoA thioesterases from *Arthrobacter* sp. and *Pseudomonas* sp. give an example of how diverse these enzymes can be composed. The two thioesterases differ in structure of the CoA binding site, quaternary association and the position of the catalytic residues, while showing a similar hot dog fold topology and acting on the same native substrate (Schmitz et al. 1992; Dunaway-Mariano and Babbitt 1994; Zhuang et al. 2003). In addition to the diversity in tertiary monomer structures, the superfamily of hot dog fold thioesterases includes a multitude of oligomeric structures as dimers, tetramers and hexamers with divergent inter-monomer orientation (Pidugu et al. 2009).

The hexameric structure of YciAHI is composed of a trimer of dimers, which each harbors two symmetrical equivalent binding sites for CoA-bound substrates at the dimer interface (Willis et al. 2008). The key catalytic amino acid D44 is located in a depression that accommodates the acyl chain of the ligand. This depression is formed by residues K52, 58 - 61 and 125 - 131 of monomer A and residues 29 - 35 of monomer B (Zhuang et al. 2008). The accessibility of the acyl-binding site for different substrates most probably determines the kinetic parameters for the individual substrates. Modification of this part of YciAHI might affect the affinity towards certain substrates.

In this study we engineered the substrate binding site of YciAHI aiming for improved production of dicarboxylic acids from EMCP-CoA-ester intermediates.

Material and methods

Growth conditions of bacterial cultures

E. coli cultures were grown in LB medium (Bertani 1951) at 37 °C and kanamycin sulfate was added at 30 µg/mL, if required. For cultivation of *M. extorquens* AM1 (DSM 1338, Peel and Quayle 1961), methanol minimal medium was prepared as described before (Peyraud et al. 2009), containing a $CoCl_2$ concentration of 12.6 µM (Kiefer et al. 2009; Sonntag et al. 2014) and 123 mM methanol as carbon source. If required, 50 µg/mL of kanamycin sulfate was added to the medium. For preparation of solid medium, 15 g/L agar-agar was added to the LB or methanol minimal medium. For cultivation of *M. extorquens* AM1 in liquid medium, precultures of 5 mL were grown in test tubes for 48 h at 30°C and 180 rpm on a rotary shaker. For the preparation of cell extracts, main cultures of 60 or 400 mL were inoculated to an OD_{600} of 0.1 in shake flasks and grown at 30°C and 180 rpm on a rotary shaker. For the testing of *yciAHI* expression plasmid libraries, main cultures of 1 mL were inoculated to an OD_{600} of 0.1 and grown in deep well plates in a Microtron rotary shaker (Infors, Bottmingen, Switzerland) at 900 rpm. From these cultures, 100 µL were sampled in a microtiter plate and were measured for scattered light signal on a SPARK® multimode microplate reader from TECAN (Männedorf, Switzerland).

Chemicals

If not stated differently, chemicals were purchased from Carl Roth (Karlsruhe, Germany), Merck (Darmstadt, Germany) or VWR International (Darmstadt, Germany). Substrate (2*S*)-methylsuccinyl-CoA was synthesized by GenoSynth (Berlin, Germany). DL-β-hydroxybutyryl-CoA lithium salt was bought from abcr (Karlsruhe, Germany), acetyl-CoA sodium salt was bought from Cayman Chemical (Michigan, USA).

Molecular docking of YciAHI and CoA ligands and design of *yciAHI* expression plasmid libraries

A docking simulation of YciAHI (*H. influenzae*) crystal structure (PDB entry 1YLI) and ligand was done in UCSF Chimera (Pettersen et al. 2004) using AutoDock Vina (Trott and Olson 2010). Prior to docking, the ligand (CoA) and all excess molecules such as solvents were deleted from the protein crystal structure. Hydrogens and charges were assigned to the new ligand (Gasteiger method) and the protein (AMBER force fields). Out of the resulting dockings, the four conformations with highest score (based on the hydrogen bonds formed) were selected. We then identified amino acids that might influence the substrate binding based on following information: 1) the four selected docking models 2) the crystal structure of

Thermus thermophilus acyl-CoA thioesterase PaaI with bound hexanoyl-CoA (PDB entry 1WN3, Kunishima et al. 2005) 3) the YciAHI crystal structure bound to CoA (PDB entry 1YLI) 4) the predicted location of uncleaved substrates of YciAHI from literature (Willis et al. 2008). From the set of selected amino acids, the hydrophobic ones were substituted for other hydrophobic or neutral amino acids. The corresponding gene variant sequences were synthesized and subcloned in pCM160_RBS_*yciAHI* by BioCat (Heidelberg, Germany). A saturation mutagenesis for position 35 was performed with the Q5® Site-Directed Mutagenesis Kit according to the manufacturer's protocol (NEB, Frankfurt, Germany). In this second pCM160_RBS_*YciAHI* library, the DNA triplet coding for phenylalanine at position 35 was exchanged with triplets encoding alternative amino acids (A, D, E, G, H, I, K, M, N, P, Q, S, T, Y). Oligonucleotides used for introducing mutations are listed in Table 1. All constructs were confirmed by Sanger sequencing.

Plasmid construction

Plasmid DNA was amplified in *E. coli* DH5α and purified with GeneJET Plasmid Miniprep Kit from Thermo Scientific (Waltham, USA). Transformation of *M. extorquens* AM1 was done by electroporation as described before (Toyama et al. 1998). Plasmids for C-terminal FLAG-tagged *yciAHI* expression were constructed by subcloning synthesized *yciAHI*-FLAG inserts (Table 2, Biocat, Heidelberg, Germany) with restriction enzymes SphI and NcoI. For YciaHI protein purification via N-terminal his6-tag, plasmids based on pET28awere constructed by subcloning synthesized his6-*yciAHI* inserts (Table 2, Biocat, Heidelberg, Germany) with restriction enzymes NdeI and EcoRI.

Dicarboxylic acid analysis

M. extorquens AM1 cultures were centrifuged for 5 minutes at 16000 g and the supernatants were passed through a 0.22 µm PDVF-syringe filter (Carl Roth, Karlsruhe, Germany). Analysis of the filtered supernatants was performed as described before (Pöschel et al. 2022) on a coupled Nexera X2 UHPLC / LCMS-8045 system (LC-MS/MS, Shimadzu, Duisburg, Germany) equipped with a 150 x 4.6 mm Luna Omega 3 µm PS C18 100 Å column (Phenomenex, Aschaffenburg, Germany). The analytes were negatively ionized with an APCI ion source, fragmented and finally quantified by comparing the results to calibration curves of peak areas of corresponding standards. Crotonic acid (Carl Roth, Karlsruhe, Germany), (2*S*,3*R*)-2-hydroxy-3-methylsuccinic acid (Enamine, Riga, Latvia), ethylmalonic acid, mesaconic acid, 2-methylsuccinic acid, methylmalonic acid and succinic acid (Merck, Darmstadt, Germany) were used as analytical standards.

Preparation of *M. extorquens* crude extracts

A culture (10 mL) was harvested by centrifugation (4 °C, 10 min, 4500 g) in a 5810 R Eppendorf centrifuge (Eppendorf, Hamburg, Germany) at late-exponential growth phase (at about 85 % of max. OD_{600}). Pellets were resuspended in 600 µL of 20 mM K-HEPES buffer (pH 7.5) premixed with cOmplete™ EDTA-free protease inhibitor cocktail (Roche, Basel, Switzerland). Glass beads (1.1 g of 0.25 - 0.5 mm beads, previously washed with 5 M NaOH, 5 M HCl and ddH_2O) were added and cells were disrupted at 4 °C for 9 min at 30 Hz in a MM2 mixer mill (Retsch, Haan, Germany). The lysate was centrifuged for 20 minutes at 4 °C and 14 000 g and the clear supernatant was analyzed for total protein concentration via BCA assay using the Pierce™ BCA Protein Assay Kit (Thermo Fisher Scientific, Dreieich, Germany).

SDS PAGE

For SDS PAGEs, the clarified cell extracts were mixed with 4x Laemmli Sample Buffer, boiled for 5 min and loaded on an Any kD™ Mini-PROTEAN® TGX™ SDS gel (Bio-Rad, Feldkirchen, Germany). The final samples contained 20 µg of total soluble protein. The PageRuler™ Prestained Protein Ladder (Thermo Fisher Scientific, Dreieich, Germany) was used as a size standard. The SDS PAGE was run at 80 V for 20 minutes and subsequently at 120 V for 40 minutes. If required, gels were stained with SimplyBlue™ SafeStain (Thermo Fisher Scientific, Dreieich, Germany).

Semi-quantitative detection of FLAG-tagged proteins

Immunoblotting of unstained SDS gels was done on a PVDF membrane in a Mini Trans-Blot® Electrophoretic Transfer Cell, following the manufacturer's protocol for high intensity field transfer (Bio-Rad, Feldkirchen, Germany). A transfer buffer containing 25 mM Tris, 192 mM glycine and 20% v/v methanol at pH 8.05 was used. Immunodetection was done with monoclonal ANTI-FLAG M2-Alkaline Phosphatase Clone M2 (Merck, Darmstadt, Germany) following the manufacturer's protocol. The detection buffer (pH 9.5) was prepared by dissolving a SIGMAFAST™ BCIP/NBT tablet (Merck, Darmstadt, Germany) in 10 mL deionized water. The washed PVDF membrane was developed in the detection buffer for 50 seconds. The reaction was stopped by washing the membrane in distilled water.

Production, purification and quantification of his-tagged YciAHI

For protein production, 200 mL of *E. coli* BL21(DE3) (NEB, Frankfurt, Germany) cultures harboring pET28a_his6_*yciAHI* or pET28a_his6_*yciAHI*_F35L were inoculated from

precultures to an OD_{600} of 0.1 and incubated at 37 °C. His6-*yciAHI* expression was induced by adding 0.4 mM of IPTG when OD_{600} reached 0.6. Production of N-terminal his-tagged YciAHI took place overnight at 18 °C. Cultures were chilled on ice for 5 minutes before centrifuging the cells for 30 minutes at 4 °C and 4500 g. Cell pellets were resuspended in 15 mL of equilibration buffer (20 mM K-HEPES (pH 7.5), 0.5 M NaCl, 10 mM imidazole, pH 7.5) containing cOmplete™ EDTA-free protease inhibitor cocktail (Roche, Basel, Switzerland) and 1 mg/mL lysozyme powder (~70000 U/mg, Merck, Darmstadt, Germany). Cells were chilled on ice for 30 min and disrupted with a probe sonicator (4 min total, 0.5 s pulse, 1 s pause, 25 % amplitude). The lysate was centrifuged at 4000 g for 25 min at 4 °C. Purification of N-terminal his-tagged proteins from the supernatant was done using HisPur™ Ni-NTA Spin Columns with 3 mL resin bed (Thermo Fisher Scientific, Dreieich, Germany) according to the manufacturer's protocol with the following buffers. Equilibration buffer: 20 mM K-HEPES (pH 7.5) containing 0.5 M NaCl and 10 mM imidazole, wash buffer 1/2/3: 20 mM K-HEPES (pH 7.5) containing 0.5 M NaCl and 40/50/60 mM imidazole, respectively, elution buffer: 20 mM K-HEPES (pH 7.5) containing 0.5 M NaCl and 250 mM imidazole. Imidazole concentration was reduced in the final samples by exchanging the elution buffer to protein storage buffer (20 mM K-HEPES (pH 7.5) containing 0.15 M NaCl) with Amicon Ultra-15, 3 MWCO (Merck, Darmstadt, Germany). Protein concentration was measured with Pierce™ BCA assay (Thermo Fisher Scientific, Dreieich, Germany).

DTNB thioesterase assay

The activity of N-terminal his-tagged YciAHI and YciAHI_F35L towards different CoA-thioesters was determined with a modified DTNB spectrophotometric assay (Ellman 1959; Zhuang et al. 2008). During establishment of the assay, the assay protein concentration was determined and protein concentration dependence was ensured. The final assay mixture containing 1 mM DTNB, 150 mM NaCl, 100 mM K-HEPES, 0.75 µM purified thioesterase and 0 - 150 µM CoA-thioester at pH 7.5 was set up as follows in a total reaction volume of 250 µL. First, 100 µL of assay buffer (108.9 mM K-HEPES, 337.5 mM NaCl, pH 7.5) was premixed with 25 µL DTNB stock solution (108.9 mM K-HEPES, 10 mM DTNB, pH 7.5) in a disposable micro cuvette. Subsequently, 100 µL of CoA-ester solution in 108.9 mM K-HEPES (pH 7.5) was added to the cuvette and the mixture was incubated at 25°C for 1 minute. For starting the reaction, 25 µL of protein solution (containing 20 mM K-HEPES, 150 mM NaCl, 7.5 µM purified protein, pH 7.5) was added to the assay. The formation of 5-thio-2-nitrobenzoate was monitored by measuring the absorbance at 412 nm. Crude cell extracts were assayed accordingly, using a DTNB stock solution containing 4 mM of DTNB and no NaCl. For starting

the reaction, 25 µL of clarified lysate containing 20 µg of protein in 20 mM K-HEPES buffer (pH 7.5) was used.

Production of (*R*)-3-hydroxybutyrate by overexpression of *yciAHI* variants in *E. coli*

Shake flask seed cultures of *E. coli* AF1000 containing pJBGT3Rx and additionally either pBADzwf_*yciAHI* or pBADzwf_*yciAHI*_F35L were inoculated from a -80°C glycerol stock and cultivated at 37 °C and 180 rpm. The cultivation medium used was a minimal salt medium consisting of 5 g/L $(NH_4)_2SO_4$, 1.6 g/L KH_2PO_4, 6.6 g/L $Na_2HPO_4 \cdot 2H_2O$, 0.5 g/L $(NH_4)_2$-H-citrate and separately sterilized components as 5 g/L glucose, 1 mL/L of 1 M $MgSO_4 \cdot 7H_2O$ solution, 50 mg/L kanamycin (AppliChem Panreac, Darmstadt, Germany), 25 mg/L chloramphenicol (Sigma-Aldrich) and 1 mL/L trace element stock solution (Guevara-Martínez et al. 2019). The trace element stock solution consisted of 0.5 g/L $CaCl_2 \cdot 2H_2O$, 16.7 g/L $FeCl_3 \cdot 6H_2O$, 0.18 g/L $ZnSO_4 \cdot 7H_2O$, 0.16 g/L $CuSO_4 \cdot 5H_2O$, 0.15 g/L $MnSO_4 \cdot 4H_2O$, 0.18 g/L $CoCl_2 \cdot 6H_2O$ and 20.1 g/L Na_2-EDTA (Guevara-Martínez et al. 2019). Overnight cultures were harvested (4030 g, 10 min), resuspended and subsequently used to inoculate 800 mL of fresh medium in 1L stirred tank bioreactors to an OD of 0.1 as described before (Guevara-Martínez et al. 2019). The cultivation medium was the same medium used for the shake flasks seed cultures, except it contained 1.28 g/L $(NH_4)_2SO_4$, 0.7 g/L $Na_3C_6H_5O_7 \cdot 2H_2O$, 12 g/L glucose and no $(NH_4)_2$-H-citrate. For the induction of recombinant expression, 200 µM IPTG and 0.002 %(w/w) L-arabinose were used. Samples taken during cultivation were filtered through a 0.2 µm syringe filter and corresponding supernatants were analyzed. Quantification of glucose, 3HB and acetic acid was done by ion exchange HPLC on an HPX-87H organic acid column (Bio-Rad, Hercules, Canada) using the refractive index (RI) as described before (Guevara-Martínez et al. 2019). Ammonium concentrations were determined using the Ammonia assay Kit K-AMIAR (Megazyme, Leinster, Ireland). The cell dry weight (CDW) value is a product of OD_{600} multiplied by 2.7 (previously determined).

Alignment of protein sequences

Sequences were acquired from the ThYme database (Cantu et al. 2010; Caswell et al. 2022) and aligned using the COBALT alignment tool (Papadopoulos and Agarwala 2007). Results were presented with the SnapGene software (GSL Biotech LLC, San Diego, Canada).

Results

Screening of a semi-rational mutant library of thioesterase YciAHI

M. extorquens AM1 strains can be used to produce a variety of products including the dicarboxylic acids 2-methylsuccinic acid and mesaconic acid (Sonntag et al. 2014; Sonntag et al. 2015; Pöschel et al. 2022). In these studies, the broad range thioesterase YciAHI is the key enzyme, that hydrolyzes the EMCP intermediates methylsuccinyl-CoA and mesaconyl-CoA. Aiming at YciAHI variants with the capability to hydrolyze other CoA-esters of the EMCP or with improved productivity, we tried to engineer the substrate-binding region of the enzyme. We identified hydrophobic amino acids that potentially interact with substrates using several docking models of YciAHI and 2-methylsuccinyl-CoA as well as crystal structures and overlays of models from literature (see Material and methods for detailed information). Figure 1 represents an example of a model generated in our docking studies, highlighting the catalytic residue and amino acids selected for exchange. We designed a small semi-rational *yciaHI* expression plasmid library encoding enzyme variants deviating from the wild type YciAHI enzyme at one of the selected positions. The selected hydrophobic amino acids were each exchanged for larger and smaller hydrophobic amino acids to investigate possible steric limitations of the substrate channel of the wild type enzyme.

We tested the mutant enzymes with the amino acid exchanges in the binding pocket in *in vivo* production experiments in *M. extorquens* AM1. For the expression of the respective *yciAHI* gene variants, plasmids based on pCM160, a vector for strong constitutive expression, were designed. Plasmids for the production of YciAHI and variants F35W, F35V, F35L, A48G, A48V, A48L, A51G, A51V, A51L, V59G, V59L, V59I, V60L or V60I as well as an empty pCM160 plasmid control were introduced in *M. extorquens* AM1 and the release of dicarboxylic acids into the culture medium was analyzed. While the concentration of other EMCP-derived dicarboxylic acid products was below the quantification limit, the titers of 2-methylsuccinic acid, mesaconic acid and 2-hydroxy-3-methylsuccinic acid could be quantified. The majority of YciAHI modifications lowered the amount of released dicarboxylic acid products in comparison to the wild type enzyme (Fig. 2a). Strains with YciAHI variants A51V and V59G showed similar maximum titers of 2-methylsuccinic acid and mesaconic acid compared to strains harboring unmodified YciAHI, whereas the maximum mesaconic acid titer of strains with YciAHI variant A51G was increased 1.3-fold. The most notable amino acid position was F35. Here, the F35V exchange led to a very low maximal titer of both 2-methylsuccinic acid and mesaconic acid. In contrast, exchanging F35 for W led to an increase in maximum product titer of 1.3-fold for 2-methylsuccinic acid and 1.7-fold for mesaconic acid. The YciAHI variant F35L even exceeded those values by increasing the amount of 2-methylsuccinic acid released 4.4-fold to 304 ± 52 mg/L and mesaconic acid released 6.4-fold to 295 ± 36 mg/L. The growth kinetics of

strains harboring the high level producing YciAHI F35 variants and those harboring the wild type enzyme followed a similar pattern, but F35 strains showed a slightly increased lag phase, a lower growth rate and a decreased cell density at the end of cultivation (Fig. 2b).

These experiments indicated that the F35 position may be important for substrate conversion rate and/or binding efficiency for YciAHI and its ligands. Unexpectedly, none of the enzyme variants led to a significantly enhanced release of 2-hydroxy-3-methylsuccinic acid or other EMCP derived carboxylic acids.

Investigation of YciAHI and YciAHI F35L enzyme levels via FLAG-tag

To test whether a higher cellular enzyme concentration is causative for the observed phenotype of strains harboring YciAHI F35L, protein levels were determined on a semi quantitative level. For this purpose, *M. extorquens* AM1 cells expressing a FLAG-tag-containing version of the genes *yciAHI* or *yciAHI*_F35L together with an empty vector control were cultivated and harvested in the late exponential growth phase. Extracts were prepared and clarified by centrifugation. Subsequently, the clear supernatant of extracted samples were loaded onto SDS gels. Two SDS-PAGEs were performed simultaneously, generating two identical gels, containing 20 µg of total protein per lane. One of the gels was stained and the other gel was blotted on a PVDF membrane. On the stained gel, no apparent differences could be identified between the SDS-PAGE patterns of the total protein extracts of the three different strains (Fig. 3). The blotted membrane was treated with monoclonal ANTI-FLAG M2-Alkaline phosphatase antibodies and the YciAHI thioesterases were detected with a BCIP/NBT staining reaction. The bands of C-terminal FLAG-tagged proteins were clearly visible and corresponded to the predicted mass of 17.8 kDa (molecular weight of untagged enzyme is 16.8 kDa, Zhuang et al. 2008). The bands of C-terminal FLAG-tagged YciAHI F35L were not as strongly visible as the bands of C-terminal FLAG-tagged YciAHI, which demonstrates lower protein levels of the F35L variant enzyme. Consequently, the substantially higher dicarboxylic acid product titers of strains carrying this enzyme variant (Online Resource Fig. S2) did not originate from higher protein concentrations.

Determination of activity of YciAHI and YciAHI F35L (untagged) in crude cell extracts

The activity of untagged YciAHI and untagged YciAHI F35L was analyzed in crude cell extracts. *M. extorquens* AM1 was transformed with pCM160_RBS_*yciAHI,* pCM160_RBS_*yciAHI*_F35L or the empty vector control pCM160, respectively. Cell cultures were harvested in late exponential growth phase, lyzed and clarified by centrifugation. Thioesterase activity was measured with a photometric DTNB assay. In this assay, DTNB

reacts with free CoA to 5-thio-2-nitrobenzoate which is then quantified at 412 nm. Three CoA-ester metabolites were tested, namely (2*S*)-methylsuccinyl-CoA, acetyl-CoA and 3-hydroxybutyryl-CoA (Fig. 4). With acetyl-CoA, no activity was detected with either cell extract. With (2*S*)-methylsuccinyl-CoA or 3-hydroxybutyryl-CoA, activity was detectable only for cells producing the wild type YciAHI, but not for the cells producing the F35L variant.

DTNB assay of purified YciAHI and YciAHI F35L (N-terminal His-tagged)

Since activity of untagged YciAHI F35L towards the tested CoA-esters was unexpectedly not detectable in crude cell extracts, we additionally tested the purified enzymes. Wild type YciAHI and the F35L variant were produced in *E. coli* and purified via a *his6*-tag. The conversion with different (2*S*)-methylsuccinyl-CoA concentrations was tested in a DTNB assay (Fig. 5).

Substrate concentrations in the physiological sub-µM range for EMCP intermediates (personal communication Patrick Kiefer) and concentrations far beyond the physiological level were tested. The datasets showed a similar behavior to the results acquired with *M. extorquens* extracts containing the respective enzymes (Fig. 4). The reaction rates of purified N-terminal His-tagged YciAHI are substantially higher than the values obtained with purified N-terminal His-tagged YciAHI F35L (Fig. 5).

Application of untagged YciAHI variant F35L for 3-hydroxybutyric acid production with *E. coli*

Although our *in vitro* enzyme assays failed to verify a higher specific activity of the F35L variant, the improved productivity in the *M. extorquens* strain encouraged us to test its utility in another production system. Therefore, we used an *E. coli* strain engineered for 3HB production (Guevara-Martínez et al. 2019) to test YciAHI and the variant YciAHI F35L (both untagged) *in vivo* in a different environment. We tested *E. coli* AF1000 strains (over-)expressing genes *t3* (encoding a thiolase, WP_007111820), *rx* (encoding a reductase, WP_007111780), *zwf* (encoding a glucose-6-phosphate dehydrogenase, UKY30849) and additionally *yciAHI* or *yciAHI* F35L in an ammonium depleted batch cultivation as already done for the *E. coli yciAEc* gene in previous works (Guevara-Martínez et al. 2019). The cultivation comprised two phases. While in the first phase biomass and the main product 3HB as well as the by-product acetic acid were formed, in the second, nitrogen depleted phase (> 8h of cultivation), the carbon flux towards 3HB production was favored and part of the acetic acid was consumed (Fig. 6). While the strains harboring the YciAHI wild type enzyme produced up to 0.54 ± 0.06 g/L 3HB (Fig. 6a), the strain harboring the F35L variant produced 1.86 ± 0.06 g/L (Fig. 6b). The 3HB yields (per biomass or glucose) are substantially higher for the F35L variant. These

experiments again showed a more than 3-fold improved productivity caused by the F35L exchange in YciAHI.

Screening of other YciAHI F35 variants

As the F35L variant of YciAHI showed enormous productivity improvements in two different biotechnological production systems, we constructed another plasmid library for expression of *yciAHI* by saturation mutagenesis of the F35 position. Except for gene variants *yciAHI*_F35C and *yciAHI*_F35R we successfully cloned expression constructs for the investigation of all possible YciAHI F35 variants (all untagged). The generated constructs were introduced into *M. extorquens* AM1 and the respective strains were cultivated and analyzed for dicarboxylic acid production. Most enzyme variants, namely YciAHI F35A, F35D, F35E, F35G, F35H, F35I, F35K, F35M, F35P, F35S, F35T and F35V showed reduced or abolished ability to release 2-methylsuccinic acid and mesaconic acid (Fig. 7a). Despite product titers that were slightly higher with unmodified YciaHI and lower with the F35L variant compared to what was observed in Fig. 2, also in this experiment expression of variant F35L, together with F35N and F35Q, led to substantially increased titers of 2-methylsuccinic acid and mesaconic acid compared to the strain expressing the wild type thioesterase gene. The highest values obtained in the experiments shown in Fig. 7b were obtained with *yciAHI*_F35N resulting in titers of 289 ± 20 mg/L 2-methylsuccinic acid and 213 ± 16 mg/L mesaconic acid after 45.5 h of cultivation.

Discussion

In two previous studies, several thioesterases for EMCP-derived dicarboxylic acid production were tested in *M. extorquens* AM1 by overexpressing the corresponding genes (Sonntag et al. 2014; Pöschel et al. 2022). Out of the seven candidates (TesBec thioesterase B from *E. coli*, TesBext thioesterase B from *M. extorquens*, YciAEc ACOT from *E. coli*, YciAHI ACOT from *H. influenzae,* ACOT4 succinyl-CoA hydrolase from *Mus musculus*, PaaI phenylacetate thioesterase from *Azoarcus evansii* and Bch 3-hydroxyisobutyryl-CoA hydrolase from *Bacillus cereus*) only strains harboring the YciAEc or YciAHI thioesterase released notable amounts of two EMCP-derived products, namely 2-methylsuccinic acid and mesaconic acid.

The objective of this work was to engineer YciAHI for improved production of EMCP-derived carboxylic acids with *M. extorquens.* The YciAEc homolog from *E. coli* was not considered, since up to now there is no crystal structure available in the publicly accessible databases. We designed YciAHI variants semi-rationally based on docking models of enzyme and ligand and published crystal structures of related thioesterases. For overexpression of the corresponding gene variants, we constructed a small plasmid library and screened for the carboxylic acid production *in vivo*.

In all *M. extorquens* production experiments, we analyzed the culture supernatants for new EMCP-CoA-ester products such as (2*S*,3*R*)-2-hydroxy-3-methylsuccinic acid, 3HB, ethylmalonic acid and methylmalonic acid. For none of the YciAHI variants were we able to detect amounts of these products above the quantification limit. Although the concentrations of all CoA intermediates in the EMCP in methanol-grown *M. extorquens* AM1 cells are similar (Sonntag et al. 2015), there appears to be no considerable conversion of the potential substrates other than (2*S*)-methylsuccinyl-CoA and mesaconyl-CoA. The semi-rational exchange of hydrophobic amino acids in the binding region of YciAHI carried out in this work does not seem to influence the product spectrum regarding EMCP derived carboxylic acid products. Predicting substrate selectivity for potential substrates with high similarity as the short-chain EMCP thioesters based on the 3D enzyme structure is rather difficult. Therefore, for accessing new EMCP-derived carboxylic acid products with *M. extorquens* in the future, we suggest a random mutagenesis approach for YciAHI (even neglecting the polarity of residues) followed by *in vivo* testing or the screening of other heterologous ACOTs with short chain specificity.

In our work, we could identify two variants of YciAHI which led to higher release of 2-methylsuccinic acid and mesaconic acid, namely F35N and F35L, of which the latter was characterized more closely. In general, growth of high performing strains was impaired as carbon is drained from the anaplerotic EMCP. Although the levels and trends of carboxylic acid

production were similar, the exact titers varied between our experiments. This phenomenon may be caused by slightly different growth conditions or product reuptake. The latter could be avoided in the future by using recently described acid transporter deletion mutants (Pöschel et al. 2022).

The observed low *in vitro* activities of YciAHI F35L measured in this work did not match the *in vivo* results of substantially higher productivity compared to strains harboring the wild type enzyme. This low activity could indicate that the enzyme may be too unstable for *in vitro* analysis. We can only hypothesize that the F35L mutation may affect the structural integrity of the hexameric or monomeric structure resulting in an unstable or inactive enzyme under *in vitro* conditions. There is also the possibility that the observed low activity could be the result of stronger feedback inhibition of the F35L enzyme. Bound CoA or accumulating carboxylic acid products may reduce the activity in the *in vitro* assays. Unbound CoA in the assay solution should not play a role in this context since it reacts rapidly with DTNB to 5-thio-2-nitrobenzoate.

Although no enhanced productivity for YciAHI F35L could be proven *in vitro*, we could measure a substantially increased product release in *in vivo* experiments of 2-methylsuccinic acid and mesaconic acid with *M. extorquens* AM1 and of 3HB with *E. coli* production strains. We suspect this to be the result of a change of the conformation of the enzymes binding pocket.

To find possible explanations for the enhanced productivity of YciAHI variants F35L and F35N *in vivo*, we will discuss the crystal structure of YciAHI and other, closely related thioesterases in the following. Based on their similarity in primary and tertiary structures and the position and identity of the catalytic residues, the superfamily of thioesterases were sorted in families TE1-TE35 in the ThYme database (https://thyme.engr.unr.edu/v2.0/, Cantu et al. 2010; Caswell et al. 2022). YciAHI belongs to the TE6 family ACOTs that act on short- to long-chain acyl-CoAs (C4 - C18 products). Prokaryotic TE6 enzymes assemble a functional unit from two identical monomers (topology β1-α1-β2-β3-β4-β5), while eukaryotic TE6 enzymes contain a fused domain of double hotdogs (topology β1-α1-β2-β3-β4-β5-α2-*β6-α3-β7-β8-β9-β10-α4*) as functional unit (Swarbrick et al. 2020). TE6 thioesterases typically co-crystallize with a tightly bound CoA molecule at one of the two potential active sites in a dimer or the equivalent monomeric double hot dog (e.g. PDB entries 1YLI, 1Y7U, 3B7K, 1VPM, Willis et al. 2008; Swarbrick et al. 2014). For YciAHI, the role of CoA as a strong feedback inhibitor was demonstrated by determination of the inhibition constant and attributed to the necessity of regulating the cytoplasmic acyl-CoA hydrolyzing enzyme in the living cell (Zhuang et al. 2008). To date, no structure with an uncleaved substrate is publicly available, so the CoA-bound model (PDB entry 1YLI) is discussed in the following.

YciAHI harbors a hydrophobic pocket in which the thiol group of CoA is tightly anchored. This pocket is not spacious enough to accommodate an acyl-group of a CoA-bound substrate (Willis et al. 2008). Therefore, the thiol group of the thioester substrate must be flipped such that the acyl group is located in the depression leading towards the catalytic amino acid. F35 is located on the edge of the CoA-binding pocket and the depression. From our experiments we cannot conclude if the higher product release of F35L and F35N variants is caused by changes in the catalytic depression or the hydrophobic CoA pocket.

In the crystal structure of YciAHI, F35 is located at the N-terminus of the central α-helix (α1). The phenyl sidechain of F35 is facing away from the binding pocket (Fig. 8a). In all published crystal structures of TE6 ACOTs, the start of α1 (and α3 for eukaryotic enzymes) is highly conserved at sequence (Fig. 8e) and topology level. As example for the latter, crystal structures of eukaryotic ACOT12 (*Homo sapiens*, PDB entry 3B7K) and procaryotic ACOT (*Alkalihalobacillus halodurans*, PDB entry 1VPM) are shown in Fig. 8b and 8c. As in YciAHI, a phenylalanine residue can be found at the N-terminus of helix α1. In ACOT7 enzymes, instead of a phenylalanine, a histidine residue is positioned at the end of α1 and α3. As an example, the α1 domain of ACOT7 from *Mus musculus* (PDB entry 2V1O) is given in Fig. 8d. In all crystal structures available, glycine is marking positions 2 and 3 of the α-helix. An alignment of all TE6 family members from the ThYme database confirms a conserved triplet of F-G-G or H-G-G in the α1/α3 domains (Online Resource Fig. S5). This conservation indicates an important role of the triplet in binding site constitution. Interestingly, the consensus triplet with phenylalanine or equivalent histidine at the start of a α-helix can also be found TE families 4, 7, 8, 11 and 31 (Online Resource Fig. S6-S10). The function of this triplet in other TE families is not part of this study but could be an interesting target for modification of enzymes belonging to these groups.

The comparison of the available TE6 crystal structures indicates that the phenyl or imidazole moiety of the amino acid at the α1 N-terminus does not interact directly with the substrate due to its orientation. Based on a structure overlay of YciAHI and the hexanoyl-CoA ligand from a *H. thermophilus* PaaI model (PDB entry 1WN3), Willis and coworkers speculated that the carbonyl oxygen of the thioester substrate interacts with G36 in analogy to Y24 (*Pseudomonas* enzyme) *or* G65 (*Arthrobacter* enzyme) of 4-hydroxybenzoyl-CoA thioesterases (Willis et al. 2008). Assuming a nucleophilic mode of catalysis, the formation of a hydrogen bond between the backbone NH amide of G36 and the thioester would polarize the C=O group for a nucleophilic attack (Zhuang et al. 2002). Based on our results, we can only hypothesize that the F35 variation may influence the polarization in some way by either taking part itself or bringing G36 in a more favorable position. Another conceivable scenario is that F35 is modulating the size of the CoA binding pocket or the catalytic depression. In either case, we assume that the position of the polypeptide backbone at the N-terminus of helix α1 is crucial.

This assumption is also supported by the fact that in our experiments the physical-chemical side-chain properties of the supplementing amino acid were not the decisive factor for *in vivo* enzyme activity. F35 could be substituted with nonpolar (F35L, F35I), polar (F35Q, F35W, F35N), acidic (F35E, F35D) or basic (F35K, F35H) amino acids while still remaining active. Instead of chemical properties, rather the length of side chain at the F35 position was critical. For all substitutions tested, (except for F35M) it seemed that medium length side chains were favorable for enzyme activity, while short side chains abolished it. Leucine and asparagine might provide the optimal chain length for positioning of the polypeptide backbone.

Although the exact reason for enhanced *in vivo* characteristics of YciAHI variants F35L and F35N stays unclear, the higher productivity was proven by application in an alternative system. Also in *E. coli* strains engineered for 3HB production, the F35L variant led to substantially higher product titers compared to unmodified YciAHI and even reached the yields and titers of the overexpressed native YciAEc homolog (Guevara-Martínez et al. 2019). With currently available *in vitro* assay techniques we would not have been able to identify the variants. Therefore, although it is more laborious, testing new and engineered thioesterases *in vivo* in the production host can be a valuable strategy.

Besides providing more productive YciAHI variants, we contributed new insights into the understanding the structure of TE6 thioesterases. The discussed consensus triplet can be also found in thioesterases from other families such as TesB from TE4 (Swarbrick et al. 2015) or *Arthrobacter* 4-hydroxybenzoyl-CoA from TE11 (Song et al. 2012). A closer examination of this position by investigation of corresponding mutant enzymes might reveal new insights in thioesterase mechanisms in general and might also help to develop improved thioesterase variants for biotechnological applications.

Statements and Declarations

Data availability

All data generated or analyzed during this study are included in this published article and its supplementary information file.

Author Contribution Statement

LP and MB conceived and designed the research, whilst MGM, DH and AJAvM contributed to the design of the research using *E. coli*. LP, MGM and DH conducted experiments. LP and MB analyzed data and wrote the manuscript. All authors read and approved the manuscript.

Compliance with Ethical Standards

Funding

LP and MB were supported by funds of the Federal Ministry of Education and Research (BMBF, FKZ 031B0340A, project Chiramet and FKZ 031B0904B, project SynBioTech). DH was funded by grant VR-621-2014-5293 from the Swedish Research council. MGM was supported by the Swedish International Development Agency (SIDA).

Disclosure of potential conflicts of interest

All authors declare that they have no conflict of interest.

Ethical approval

This article does not contain any studies with human participants performed by any of the authors.

Reference list

Bertani G (1951) Studies on Lysogenesis I. The Mode of Phage Liberation by Lysogenic *Escherichia coli*. J Bacteriol 62:293–300. https://doi.org/10.1128/jb.62.3.293-300.1951

Cantu DC, Chen Y, Reilly PJ (2010) Thioesterases: A new perspective based on their primary and tertiary structures. Protein Sci 19:1281–1295. https://doi.org/10.1002/pro.417

Caswell BT, Carvalho CC, Nguyen H, Roy M, Nguyen T, Cantu DC (2022) Thioesterase enzyme families: Functions, structures, and mechanisms. Protein Sci 31:652–676. https://doi.org/10.1002/pro.4263

Chung A, Liu Q, Ouyang S-P, Wu Q, Chen G-Q (2009) Microbial production of 3-hydroxydodecanoic acid by *pha* operon and *fadBA* knockout mutant of *Pseudomonas putida* KT2442 harboring *tesB* gene. Appl Microbiol Biotechnol 83:513–519. https://doi.org/10.1007/s00253-009-1919-6

Dillon SC, Bateman A (2004) The Hotdog fold: Wrapping up a superfamily of thioesterases and dehydratases. BMC Bioinform 5:1–14. https://doi.org/10.1186/1471-2105-5-109

Dunaway-Mariano D, Babbitt PC (1994) On the origins and functions of the enzymes of the 4-chlorobenzoate to 4-hydroxybenzoate converting pathway. Biodegradation 5:259–276. https://doi.org/10.1007/BF00696464

Ellman GL (1959) Tissue sulfhydryl groups. Arch Biochem Biophys 82:70–77. https://doi.org/10.1016/0003-9861(59)90090-6

Gao H-J, Wu Q, Chen G-Q (2002) Enhanced production of D-(-)-3-hydroxybutyric acid by recombinant *Escherichia coli*. FEMS Microbiol Lett 213:59–65. https://doi.org/10.1111/j.1574-6968.2002.tb11286.x

Grant SGN, Jessee J, Bloom FR, Hanahan D (1990) Differential plasmid rescue from transgenic mouse DNAs into *Escherichia coli* methylation-restriction mutants. Proc Natl Acad Sci U S A 87:4645–4649. https://doi.org/10.1073/PNAS.87.12.4645

Guevara-Martínez M, Perez-Zabaleta M, Gustavsson M, Quillaguamán J, Larsson G, van Maris AJA (2019) The role of the acyl-CoA thioesterase "YciA" in the production of (*R*)-3-hydroxybutyrate by recombinant *Escherichia coli*. Appl Microbiol Biotechnol 103:3693–3704. https://doi.org/10.1007/s00253-019-09707-0

Guevara-Martínez M, Sjöberg Gällnö K, Sjöberg G, Jarmander J, Perez-Zabaleta M, Quillaguamán J, Larsson G (2015) Regulating the production of (*R*)-3-hydroxybutyrate in *Escherichia coli* by N or P limitation. Front Microbiol 6:1–9. https://doi.org/10.3389/fmicb.2015.00844

Hanahan D (1985) Techniques for transformation of *E. coli*. In: Glover DM (ed) DNA cloning: a practical approach. IRL Press, Oxford, pp 109–135

Hunt MC, Alexson SEH (2002) The role Acyl-CoA thioesterases play in mediating intracellular lipid metabolism. Prog Lipid Res 41:99–130. https://doi.org/10.1016/S0163-7827(01)00017-0

Jarmander J, Belotserkovsky J, Sjöberg G, Guevara-Martínez M, Pérez-Zabaleta M, Quillaguamán J, Larsson G (2015) Cultivation strategies for production of (*R*)-3-hydroxybutyric acid from simultaneous consumption of glucose, xylose and arabinose

by *Escherichia coli*. Microb Cell Factories 14:1–12. https://doi.org/10.1186/s12934-015-0236-2

Kiefer P, Buchhaupt M, Christen P, Kaup B, Schrader J, Vorholt JA (2009) Metabolite Profiling Uncovers Plasmid-Induced Cobalt Limitation under Methylotrophic Growth Conditions. PLOS ONE 4:e7831. https://doi.org/10.1371/journal.pone.0007831

Kunishima N, Asada Y, Sugahara M, Ishijima J, Nodake Y, Sugahara M, Miyano M, Kuramitsu S, Yokoyama S, Sugahara M (2005) A Novel Induced-fit Reaction Mechanism of Asymmetric Hot Dog Thioesterase PaaI. J Mol Biol 352:212–228. https://doi.org/10.1016/j.jmb.2005.07.008

Lee SY, Lee Y (2003) Metabolic Engineering of *Escherichia coli* for Production of Enantiomerically Pure (*R*)-(−)-Hydroxycarboxylic Acids. Appl Environ Microbiol 69:3421–3426. https://doi.org/10.1128/AEM.69.6.3421-3426.2003

Liu Q, Ouyang S-P, Chung A, Wu Q, Chen G-Q (2007) Microbial production of *R*-3-hydroxybutyric acid by recombinant *E. coli* harboring genes of *phbA*, *phbB*, and *tesB*. Appl Microbiol Biotechnol 76:811–818. https://doi.org/10.1007/s00253-007-1063-0

Martin CH, Dhamankar H, Tseng H-C, Sheppard MJ, Reisch CR, Prather KLJ (2013) A platform pathway for production of 3-hydroxyacids provides a biosynthetic route to 3-hydroxy-γ-butyrolactone. Nat Commun 4:1414. https://doi.org/10.1038/ncomms2418

Martin CH, Prather KLJ (2009) High-titer production of monomeric hydroxyvalerates from levulinic acid in *Pseudomonas putida*. J Biotechnol 139:61–67. https://doi.org/10.1016/j.jbiotec.2008.09.002

Marx CJ, Lidstrom ME (2001) Development of improved versatile broad-host-range vectors for use in methylotrophs and other Gram-negative bacteria. Microbiology 147:2065–2075. https://doi.org/10.1099/00221287-147-8-2065

Papadopoulos JS, Agarwala R (2007) COBALT: constraint-based alignment tool for multiple protein sequences. Bioinformatics 23:1073–1079. https://doi.org/10.1093/bioinformatics/btm076

Peel D, Quayle JR (1961) Microbial growth on C1 compounds. 1. Isolation and characterization of *Pseudomonas* AM 1. Biochem J 81:465–469. https://doi.org/10.1042/bj0810465

Perez-Zabaleta M, Sjöberg G, Guevara-Martínez M, Jarmander J, Gustavsson M, Quillaguamán J, Larsson G (2016) Increasing the production of (*R*)-3-hydroxybutyrate in recombinant *Escherichia coli* by improved cofactor supply. Microb Cell Factories 15:1–10. https://doi.org/10.1186/s12934-016-0490-y

Pettersen EF, Goddard TD, Huang CC, Couch GS, Greenblatt DM, Meng EC, Ferrin TE (2004) UCSF Chimera-A visualization system for exploratory research and analysis. J Comput Chem 25:1605–1612. https://doi.org/10.1002/jcc.20084

Peyraud R, Kiefer P, Christen P, Massou S, Portais J-C, Vorholt JA (2009) Demonstration of the ethylmalonyl-CoA pathway by using ^{13}C metabolomics. Proc Natl Acad Sci U S A 106:4846–51. https://doi.org/10.1073/pnas.0810932106

Pidugu LS, Maity K, Ramaswamy K, Surolia N, Suguna K (2009) Analysis of proteins with the “hot dog” fold: Prediction of function and identification of catalytic residues of hypothetical proteins. BMC Struct Biol 9:37. https://doi.org/10.1186/1472-6807-9-37

Pöschel L, Gehr E, Buchhaupt M (2022) Improvement of dicarboxylic acid production with *Methylorubrum extorquens* by reduction of product reuptake. Appl Microbiol Biotechnol 106:6713–6731. https://doi.org/10.1007/s00253-022-12161-0

Sandén AM, Prytz I, Tubulekas I, Förberg C, Le H, Hektor A, Neubauer P, Pragai Z, Harwood C, Ward A, Picon A, de Mattos JT, Postma P, Farewell A, Nyström T, Reeh S, Pedersen S, Larsson G (2003) Limiting factors in *Escherichia coli* fed-batch production of recombinant proteins. Biotechnol Bioeng 81:158–166. https://doi.org/10.1002/bit.10457

Schmitz A, Gartemann KH, Fiedler J, Grund E, Eichenlaub R (1992) Cloning and sequence analysis of genes for dehalogenation of 4-chlorobenzoate from *Arthrobacter* sp. strain SU. Appl Environ Microbiol 58:4068–4071. https://doi.org/10.1128/aem.58.12.4068-4071.1992

Song F, Thoden JB, Zhuang Z, Latham J, Trujillo M, Holden HM, Dunaway-Mariano D (2012) The Catalytic Mechanism of the Hotdog-fold Enzyme Superfamily 4-Hydroxybenzoyl-CoA Thioesterase from *Arthrobacter* sp. Strain SU. Biochemistry 51:7000–7016. https://doi.org/10.1021/bi301059m

Sonntag F, Buchhaupt M, Schrader J (2014) Thioesterases for ethylmalonyl–CoA pathway derived dicarboxylic acid production in *Methylobacterium extorquens* AM1. Appl Microbiol Biotechnol 98:4533–4544. https://doi.org/10.1007/s00253-013-5456-y

Sonntag F, Müller JEN, Kiefer P, Vorholt JA, Schrader J, Buchhaupt M (2015) High-level production of ethylmalonyl-CoA pathway-derived dicarboxylic acids by *Methylobacterium extorquens* under cobalt-deficient conditions and by polyhydroxybutyrate negative strains. Appl Microbiol Biotechnol 99:3407–3419. https://doi.org/10.1007/s00253-015-6418-3

Swarbrick CMD, Nanson JD, Patterson EI, Forwood JK (2020) Structure, function, and regulation of thioesterases. Prog Lipid Res 79:101036. https://doi.org/10.1016/j.plipres.2020.101036

Swarbrick CMD, Perugini MA, Cowieson N, Forwood JK (2015) Structural and functional characterization of TesB from *Yersinia pestis* reveals a unique octameric arrangement of hotdog domains. Acta Crystallogr D 71:986–995. https://doi.org/10.1107/S1399004715002527

Swarbrick CMD, Roman N, Cowieson N, Patterson EI, Nanson J, Siponen MI, Berglund H, Lehtiö L, Forwood JK (2014) Structural Basis for Regulation of the Human Acetyl-CoA Thioesterase 12 and Interactions with the Steroidogenic Acute Regulatory Protein-related Lipid Transfer (START) Domain. J Biol Chem 289:24263–24274. https://doi.org/10.1074/jbc.M114.589408

Toyama H, Anthony C, Lidstrom ME (1998) Construction of insertion and deletion *mxa* mutants of *Methylobacterium extorquens* AM1 by electroporation. FEMS Microbiol Lett 166:1–7. https://doi.org/10.1111/j.1574-6968.1998.tb13175.x

Trott O, Olson AJ (2010) AutoDock Vina: Improving the speed and accuracy of docking with a new scoring function, efficient optimization, and multithreading. J Comput Chem 31:455–461. https://doi.org/10.1002/jcc.21334

Tseng H-C, Martin CH, Nielsen DR, Prather KLJ (2009) Metabolic Engineering of *Escherichia coli* for Enhanced Production of (*R*)- and (*S*)-3-Hydroxybutyrate. Appl Environ Microbiol 75:3137–3145. https://doi.org/10.1128/AEM.02667-08

Willis MA, Zhuang Z, Song F, Howard A, Dunaway-Mariano D, Herzberg O (2008) Structure of YciA from *Haemophilus influenzae* (HI0827), a Hexameric Broad Specificity Acyl-Coenzyme A Thioesterase. Biochemistry 47:2797–2805. https://doi.org/10.1021/bi702336d

Zhuang Z, Gartemann K-H, Eichenlaub R, Dunaway-Mariano D (2003) Characterization of the 4-Hydroxybenzoyl-Coenzyme A Thioesterase from *Arthrobacter* sp. Strain SU. Appl Environ Microbiol 69:2707–2711. https://doi.org/10.1128/AEM.69.5.2707-2711.2003

Zhuang Z, Song F, Zhang W, Taylor K, Archambault A, Dunaway-Mariano D, Dong J, Carey PR (2002) Kinetic, Raman, NMR, and Site-Directed Mutagenesis Studies of the *Pseudomonas* Sp. Strain CBS3 4-Hydroxybenzoyl-CoA Thioesterase Active Site. Biochemistry 41:11152–11160. https://doi.org/10.1021/bi0262303

Zhuang Z, Song F, Zhao H, Li L, Cao J, Eisenstein E, Herzberg O, Dunaway-Mariano D (2008) Divergence of Function in the Hot Dog Fold Enzyme Superfamily: The Bacterial Thioesterase YciA. Biochemistry 47:2789–2796. https://doi.org/10.1021/bi702334h

Figures and figure captions

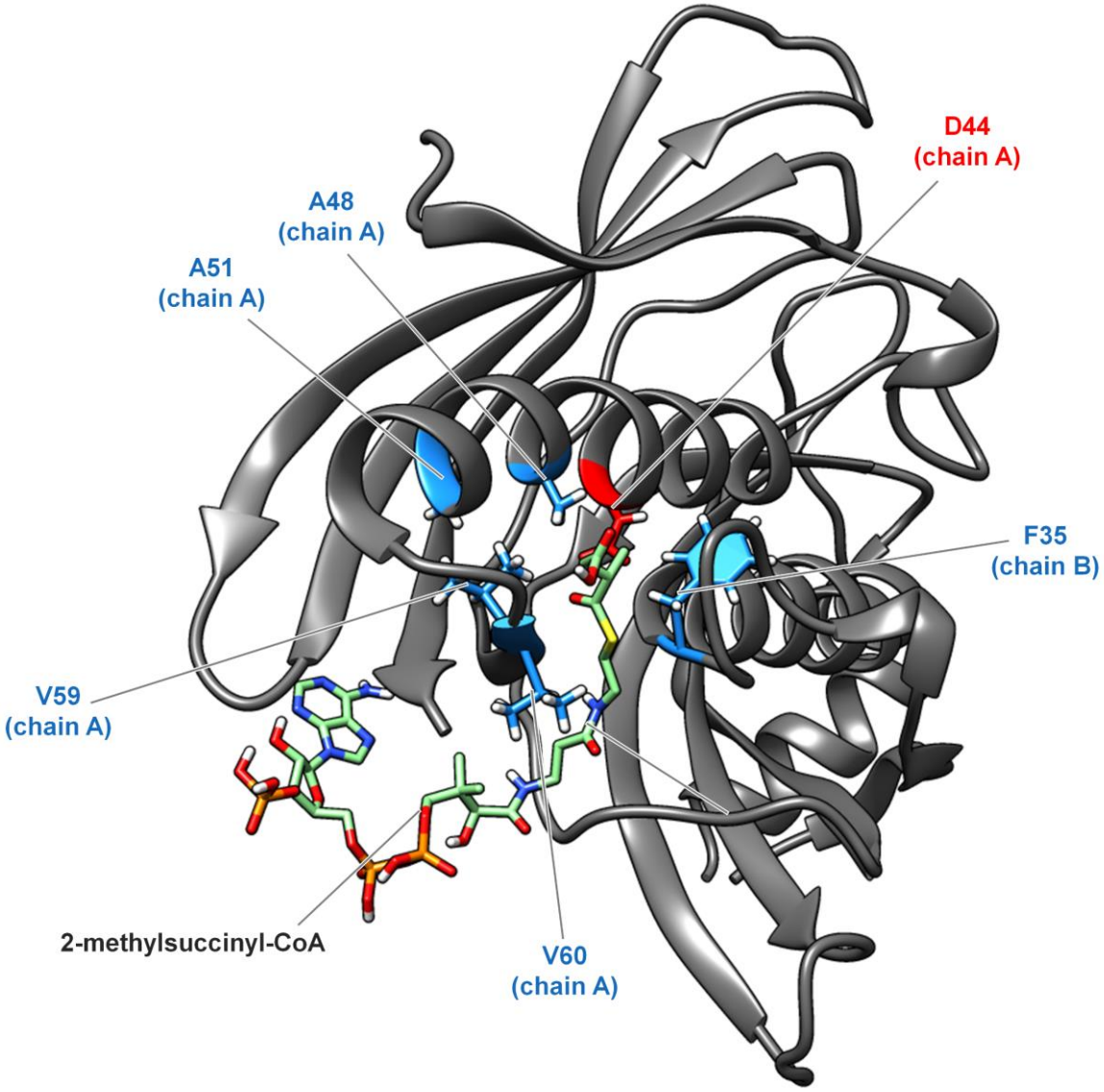

Fig. 1 Molecular docking model of (2*S*)-methylsuccinyl-CoA and YciAHI with targeted amino acids. The ligand is docking at the interface of two hot dog folded monomers. The shown protein section consists of parts of monomer A (amino acid 11-125) and monomer B (amino acid 14-151). Catalytic residue D44 is colored in red, amino acids selected for exchange are colored in light blue. The respective chain is indicated in brackets. For better illustration, only one of the two symmetrically equivalent active site channels of the dimer is highlighted

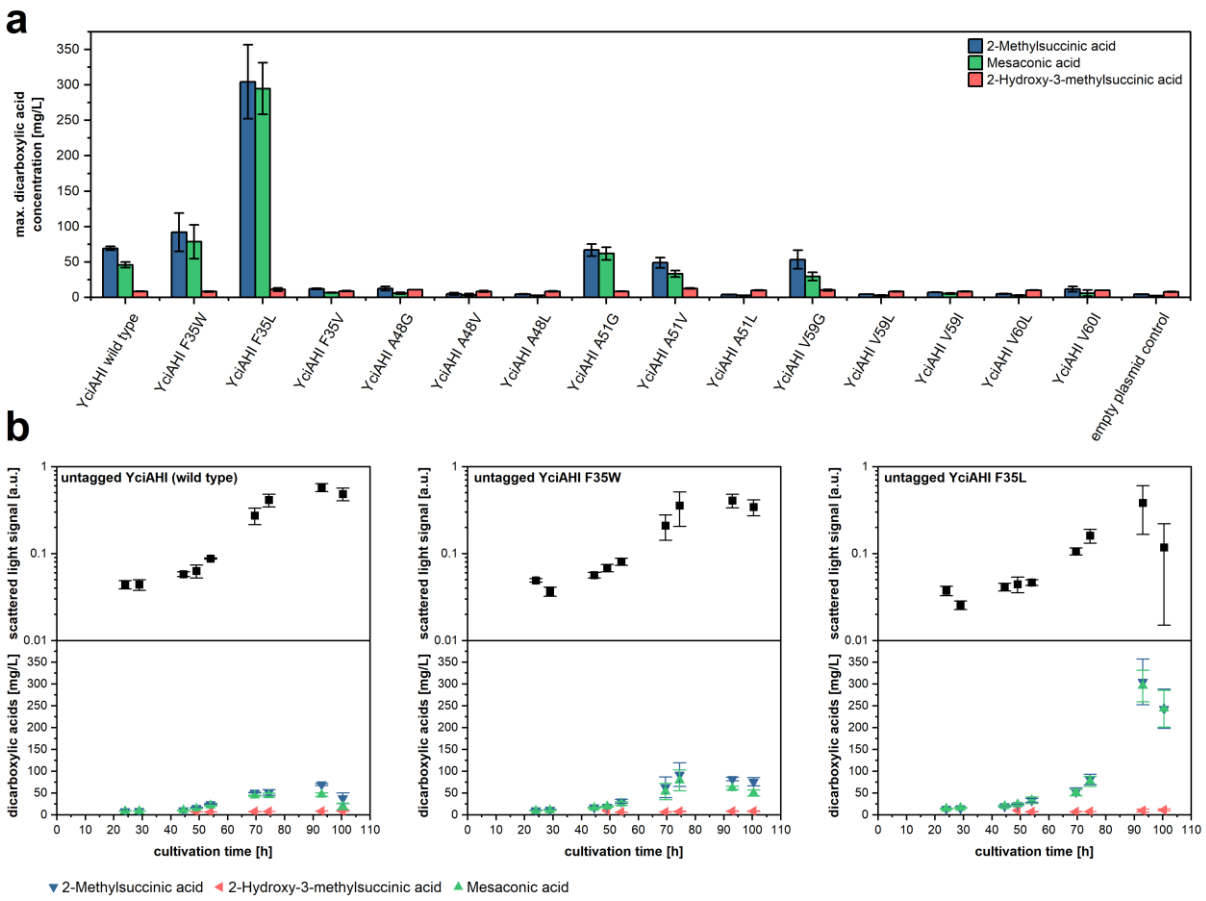

Fig. 2 Production of 2-methylsuccinic acid and mesaconic acid with YciAHI variants in *M. extorquens* AM1 *in vivo*. **a** Maximum product titers of 2-methylsuccinic acid, mesaconic acid and 2-hydroxy-3-methylsuccinic produced by *M. extorquens* AM1 harboring YciAHI variants. **b** Growth kinetics and time-dependent concentration of mesaconic acid, 2-methylsuccinic acid and 2-hydroxy-3-methylsuccinic in supernatants of *M. extorquens* AM1 harboring YciAHI, variant F35W or variant F35L (all untagged). Error bars represent standard deviations from three independent replicates. Production kinetics for all strains are shown in Online Resource Fig. S1

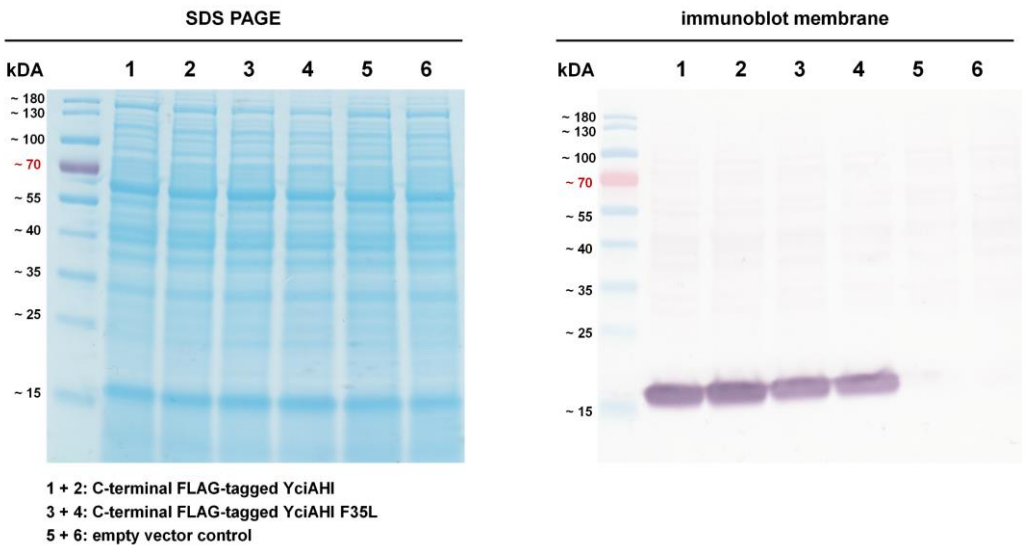

Fig. 3 Semi quantitative detection of C-terminal FLAG-tagged YciAHI and C-terminal FLAG-tagged YciAHI F35L in cell extracts of *M. extorquens* AM1. Coomassie stained SDS-PAGE gel and immunoblot membrane of whole protein extracts (20 µg of total protein per lane) of *M. extorquens* AM1 expressing *yciAHI*_FLAG, *yciAHI*_F35L_FLAG or harboring an empty pCM160 vector control. The PVDF membrane was treated with monoclonal ANTI-FLAG M2-Alkaline phosphatase antibody and stained with BCIP/NBT. Duplicate samples were harvested from two individual strains. Growth and dicarboxylic acid production kinetics for all strains are shown in Online Resource Fig. S2

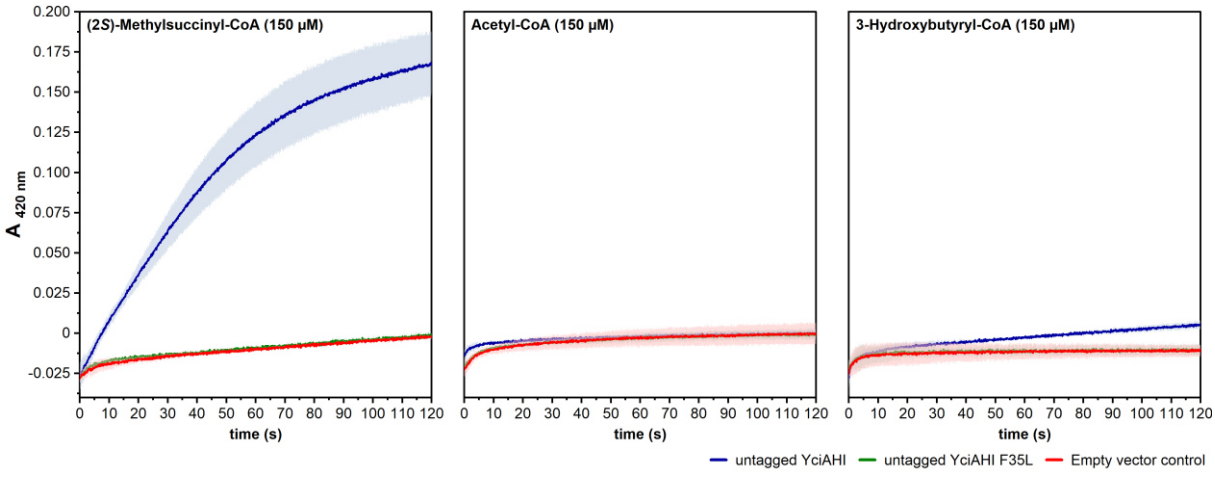

Fig. 4 Activity of untagged YciAHI and untagged YciAHI F35L towards EMCP-CoA esters in crude cell extracts. DTNB assays of crude cell extracts of *M. extorquens* overexpressing genes encoding untagged YciAHI or untagged YciAHI F35L or harboring an empty pCM160 vector as a control. As substrate, 150 µM of either (2*S*)-methylsuccinyl-CoA, acetyl-CoA or 3-hydroxybutyryl-CoA was used. The assay was set up at pH 7.5 in a micro cuvette and

contained 0.4 mM DTNB and 20 µg of total protein. The formation of DTNB-derived 5-thio-2-nitrobenzoate was measured at 412 nm. Prior to addition of the lysate, the assay mixture containing all other components was equilibrated to 25 °C. The signal obtained in equilibration phase was set to zero. Lightly colored areas represent standard deviations from three independent replicates

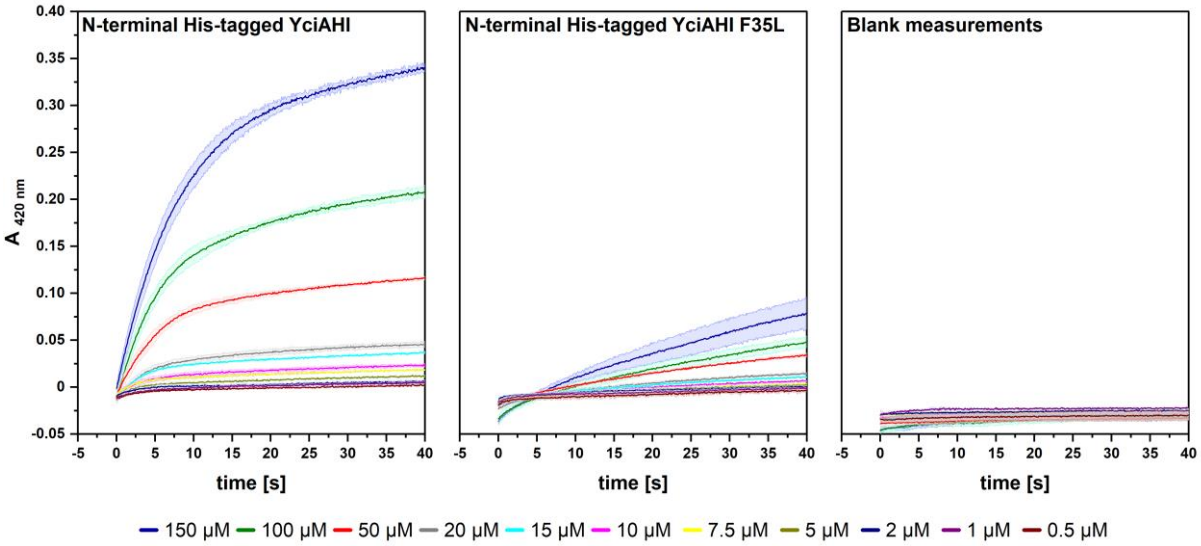

Fig. 5 (2*S*)-Methylsuccinyl-CoA conversion tests with purified N-terminal His-tagged YciAHI,N-terminal His-tagged YciAHI F35L thioesterases and without enzyme addition. Values were determined with a DTNB assay at pH 7.5 and 25°C using 1-150 µM of (2*S*)-methylsuccinyl-CoA as substrate (color coded concentrations) and 7.5 µM of purified enzyme. Prior to addition of the protein, the assay mixture containing all other components was equilibrated to 25 °C. For blank measurements, no enzyme was added. The formation of DTNB-derived 5-thio-2-nitrobenzoate was measured at 412 nm. Values were corrected by setting the baseline before protein addition (not shown) to zero. Uncorrected values can be found in Online Resource Fig. S3. All measurements were done in triplicates

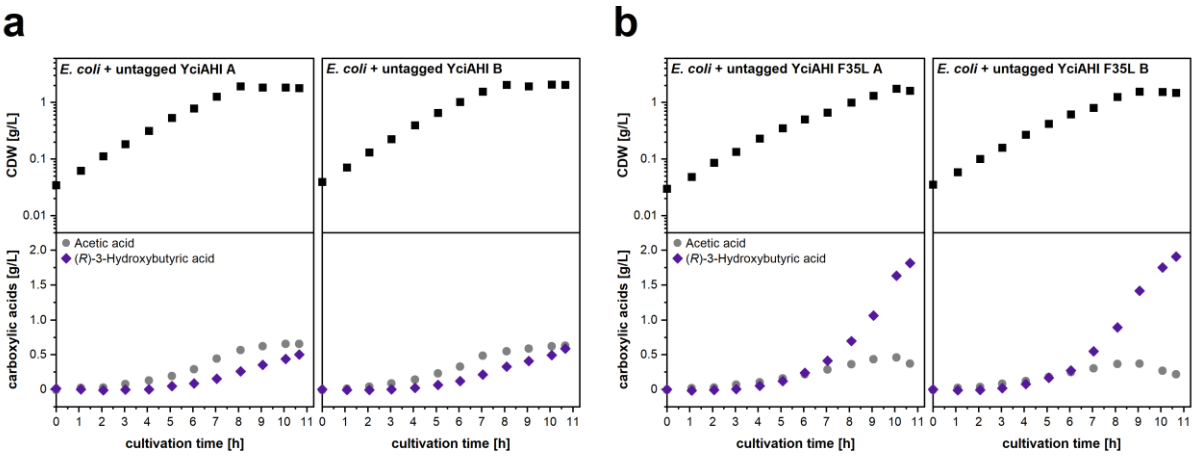

	μ [1/h]	3HB titer [g/L]	q_{3HB} [g_{3HB} /h*$g_{biomass}$]	$Y_{3HB/Glc}$ [g_{3HB}/ $g_{glucose}$]
Batch phase	0.52 ± 0.01	0.18 ± 0.04	0.083 ± 0.01	0.06
Depletion phase	-	0.54 ± 0.06	0.05	0.20 ± 0.01

	μ [1/h]	3HB titer [g/L]	q_{3HB} [g_{3HB} /h*$g_{biomass}$]	$Y_{3HB/Glc}$ [g_{3HB}/ $g_{glucose}$]
Batch phase	0.44 ± 0.01	0.79 ± 0.14	0.40	0.19 ± 0.01
Depletion phase	-	1.86 ± 0.06	0.28 ± 0.12	0.33 ± 0.01

Fig. 6 Growth and product formation kinetics during batch cultivations of *E. coli* AF1000 engineered for production of 3HB *in vivo*. On the expression vectors used, the untagged versions of thioesterases were encoded. All cultivations were performed in duplicates and in parallel. Identical media composition was used in all reactors. Complete nitrogen depletion was detected between 8 and 10 hours of cultivation. **a** Duplicates (A and B) of *E. coli* AF1000 containing pJBGT3Rx pBAD*_zwf_yciAHI* **b** Duplicates (A and B) of *E. coli* AF1000 containing pJBGT3Rx pBAD*_zwf_yciAHI_F35L*

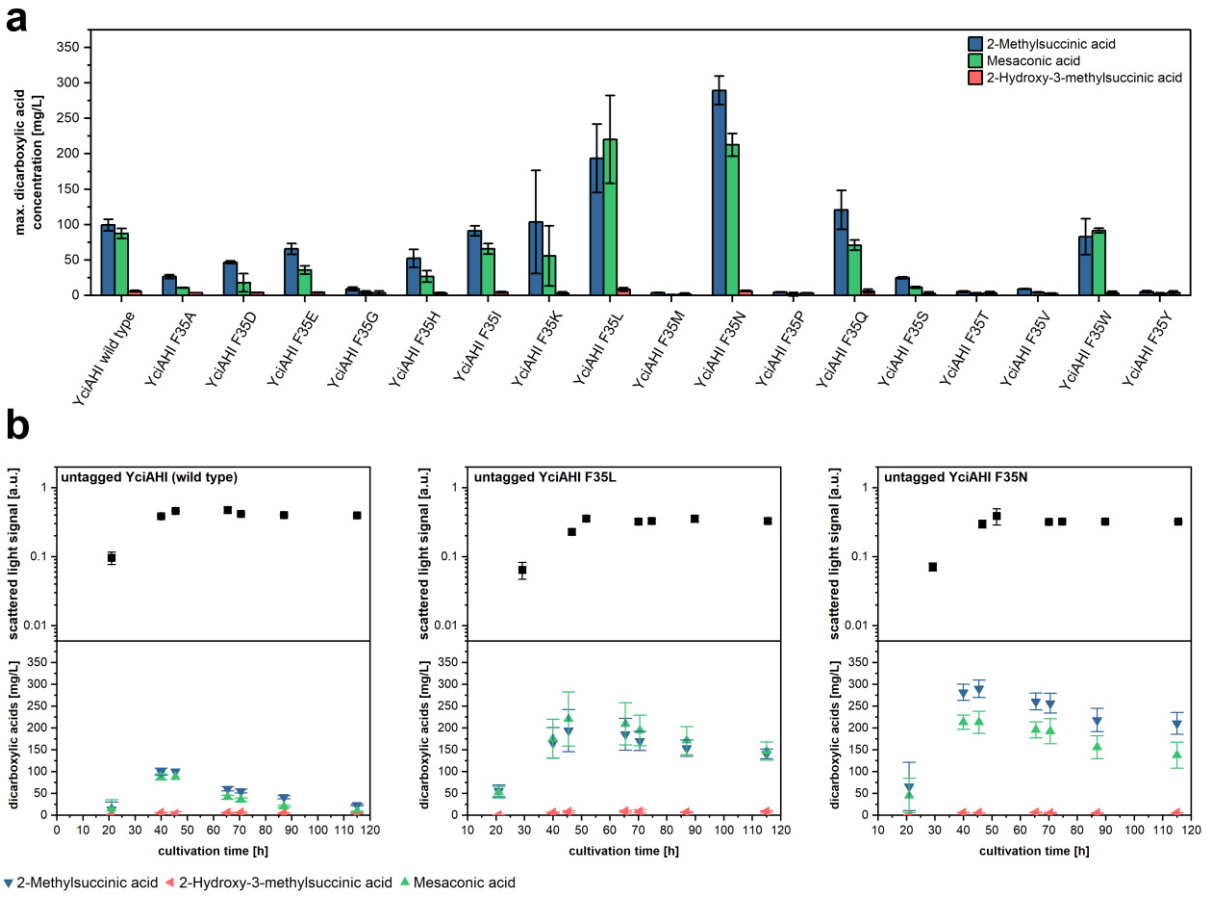

Fig. 7 Production of 2-methylsuccinic acid and mesaconic acid with YciAHI F35 variants in *M. extorquens* AM1 *in vivo*. **a** Maximum product titers of 2-methylsuccinic acid, mesaconic acid and 2-hydroxy-3-methylsuccinic produced by *M. extorquens* AM1 harboring untagged YciAHI F35 variants. **b** Growth kinetics and time-dependent concentration of mesaconic acid, 2-methylsuccinic acid and 2-hydroxy-3-methylsuccinic in supernatant of *M. extorquens* AM1 harboring YciAHI, variant F35L or variant F35N (all untagged). Error bars represent standard deviations from three independent replicates. Production kinetics of all strains are shown in Online Resource Fig. S4

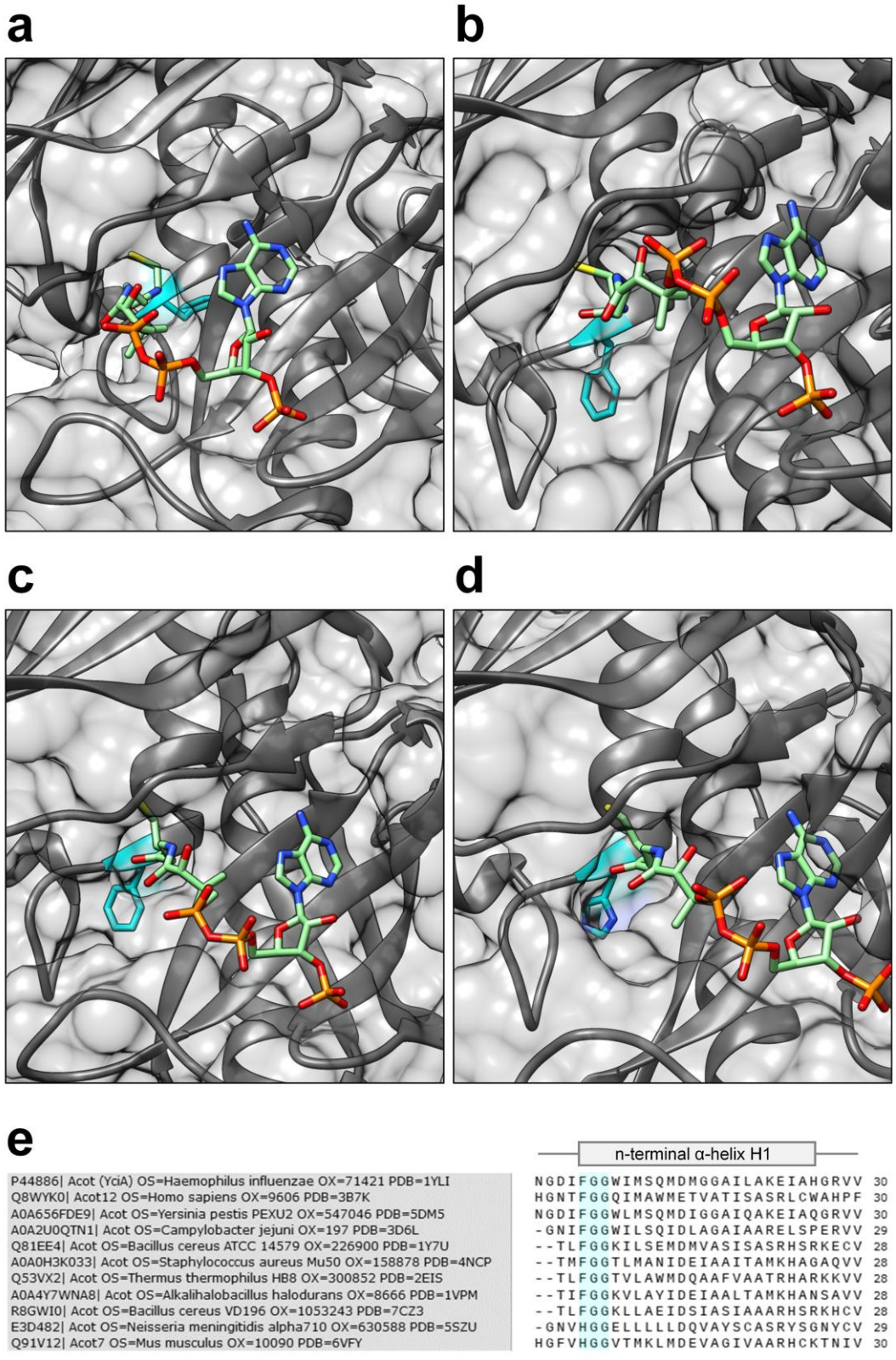

Fig. 8 Comparison of CoA binding site of representative TE6 thioesterases YciAHI, ACOT12 (Hs), ACOT (Ah) and ACOT7 (Mm) **a** Crystal structure of YciAHI (*H. influenzae*, PDB number 1YLI) with bound CoA. Phenylalanine 35 at the N-terminus of helix α1 is highlighted in blue. **b** Crystal structure of ACOT12 (*H. sapiens*, PDB number 3B7K) with bound CoA. Phenylalanine

201 at the N-terminus of helix α1 is highlighted in blue. **c** Crystal structure of ACOT from *Alkalihalobacillus halodurans* (PDB number 1VPM) with bound CoA. Phenylalanine 30 at the N-terminus of helix α1 is highlighted in blue. **d** Crystal structure of ACOT7 N-domain (*M. musculus*, PDB number 2V1O) with bound CoA. Histidine 30 at the N-terminus of helix α1 is highlighted in blue. **e** Sequence alignment of CoA-proximal α-helices of TE6 family members with available crystal structures. Consensus sequence at the N-terminus of the α-helix is highlighted in blue. Sequences, Uniprot identifiers, protein names, organism names (OS) and identifiers (OX), as well as PDB accession numbers were acquired through the ThYme database (https://thyme.engr.unr.edu/v2.0/)

Tables

Table 1 Strains, plasmids and oligonucleotides used in this work. Bold and underlined letters indicated introduced mutations in pCM160_RBS_*yciAHI*. Oligonucleotides were purchased from Merck (Darmstadt, Germany)

Name	Description	Reference
Bacterial strains		
E. coli DH5α	F⁻ φ80*lac*ZΔM15 Δ(*lac*ZYA-*arg*F)U169 *rec*A1 *end*A1 *hsd*R17(r_K^-, m_K^+) *pho*A *sup*E44 λ⁻*thi*-1 *gyr*A96 *rel*A1	Hanahan 1985; Grant et al. 1990
E. coli BL21(DE3)	*fhuA2 [lon] ompT gal (λ DE3) [dcm] ΔhsdS λ DE3 = λ sBamHIo ΔEcoRI-B int::(lacI::PlacUV5::T7 gene1) i21 Δnin5*	NEB (Frankfurt, Germany)
E. coli AF1000	*MC4100, relA+*	Sandén et al. 2003
M. extorquens AM1 (DSM 1338)	Cm^R, Gram-negative, facultative methylotrophic, obligate aerobic, α-proteobacterium	Peel and Quayle 1961
Plasmids		
pCM160	Kan^R, p_{mxaF}, oriT, pBR322ori, *M. extorquens* expression vector	Marx and Lidstrom 2001
pCM160_RBS_*yciA*HI	pCM160 containing codon-optimized for *M. extorquens* thioesterase gene *yciA* from *Haemophilus influenzae*, optimized RBS	Pöschel et al. 2022
pCM160_RBS_*yciAHI*_I34A pCM160_RBS_*yciAHI*_I34F pCM160_RBS_*yciAHI*_F35W pCM160_RBS_*yciAHI*_F35L pCM160_RBS_*yciAHI*_F35V pCM160_RBS_*yciAHI*_A48G pCM160_RBS_*yciAHI*_A48V pCM160_RBS_*yciAHI*_A48L pCM160_RBS_*yciAHI*_A51G pCM160_RBS_*yciAHI*_A51V pCM160_RBS_*yciAHI*_A51L pCM160_RBS_*yciAHI*_V59G pCM160_RBS_*yciAHI*_V59L pCM160_RBS_*yciAHI*_V59I pCM160_RBS_*yciAHI*_V60L pCM160_RBS_*yciAHI*_V60I pCM160_RBS_*yciAHI*_F35A pCM160_RBS_*yciAHI*_F35D pCM160_RBS_*yciAHI*_F35E pCM160_RBS_*yciAHI*_F35G pCM160_RBS_*yciAHI*_F35H pCM160_RBS_*yciAHI*_F35I pCM160_RBS_*yciAHI*_F35K pCM160_RBS_*yciAHI*_F35M pCM160_RBS_*yciAHI*_F35N pCM160_RBS_*yciAHI*_F35P pCM160_RBS_*yciAHI*_F35Q pCM160_RBS_*yciAHI*_F35S	pCM160_RBS_*yciAHI* for production of YciAHI variants, modified at positions I34, F35, A48, A51, V59 or V60	This work

pCM160_RBS_*yciAHI*_F35T pCM160_RBS_*yciAHI*_F35Y		
pCM160_RBS_*yciAHI* _FLAG pCM160_RBS_*yciAHI*_F35L_FLAG	Vectors for production of C-terminal FLAG-tagged YciAHI variants	This work
pET28a_his6_*yciAHI* pET28a_his6_*yciAHI*_F35L	Vectors for production of N-terminal his-tagged YciAHI variants	This work
pJBGT3Rx	*t3* and *rx* from *H. boliviensis* under p_{lacUV5} and *lacI* control (p15A/ Cm^R)	Jarmander et al. 2015
pBAD_*zwf_yciAHI*	*yciAHI* and *zwf* from AF1000 under control of p_{araBAD} (pBR22/Kan^R)	This work
pBAD_*zwf_yciAHI*_F35L	*yciAHI*_F35L and *zwf* from AF1000 under control of p_{araBAD} (pBR22/Kan^R)	This work

Oligonucleotides

LP01_35A_fw	CGGCGACATC**GCC**GGCGGCTGGA	This work
LP02_35D_fw	CGGCGACATC**GAC**GGCGGCTGGA	
LP03_35E_fw	CGGCGACATC**GAG**GGCGGCTGGATC	
LP04_35G_fw	CGGCGACATC**GGC**GGCGGCTGGA	
LP05_35H_fw	CGGCGACATC**CAC**GGCGGCTGGA	
LP06_35K_fw	CGGCGACATC**AAG**GGCGGCTGGATC	
LP07_35M_fw	CGGCGACATC**ATG**GGCGGCTGGA	
LP08_35N_fw	CGGCGACATC**AAC**GGCGGCTGGA	
LP09_35P_fw	CGGCGACATC**CCG**GGCGGCTGGATC	
LP10_35Q_fw	CGGCGACATC**CAG**GGCGGCTGGATC	
LP11_35S_fw	CGGCGACATC**TCG**GGCGGCTGGA	
LP12_35T_fw	CGGCGACATC**ACC**GGCGGCTGGA	
LP13_35W_fw	CGGCGACATC**TGG**GGCGGCTGGA	
LP14_35_rev	TTGGCGTTGGTGTCCGAC	
LP15_35I_fw	CGGCGACATC**ATC**GGCGGCTGGA	
LP16_35L_fw	CGGCGACATC**CTC**GGCGGCTGGA	
LP17_35V_fw	CGGCGACATC**GTC**GGCGGCTGGA	
LP18_35Y_fw	CGGCGACATC**TAC**GGCGGCTGGA	
LP19_35ILVY_rev	TTGGCGTTGGTGTCCGACGG	

Table 2 Synthetic sequences used for plasmid construction. For pCM160 constructs, the codon optimized sequence of *yciAHI* (Pöschel et al. 2022) for *M. extorquens* was used. FLAG tag sequences are written in bold. Restriction sites for subcloning are indicated by underlined letters (*Sph*I and *Nco*I for pCM160 constructs, *Nde*I and *Eco*RI for pET28a constructs)

Name of target construct	Sequence
pCM160_RBS_*yciAHI*_FLAG (C-terminal tagged)	GCATGCCAACAAGTATCTAAAAGATTAAAGGAGGAATAACAATGTCGGCCA ACTTCACCGACAAGAACGGCCGCCAGTCGAAGGGCGTCCTCCTCCTCCG CACCCTCGCCATGCCGTCGGACACCAACGCCAACGGCGACATCTTCGGC GGCTGGATCATGTCGCAGATGGACATGGGCGGCGCCATCCTCGCCAAGG AGATCGCCCACGGCCGCGTCGTCACCGTCGCCGTCGAGTCGATGAACTTC ATCAAGCCGATCTCGGTCGGCGACGTCGTCTGCTGCTACGGCCAGTGCCT CAAGGTCGGCCGCTCGTCGATCAAGATCAAGGTCGAGGTCTGGGTCAAGA AGGTCGCCTCGGAGCCGATCGGCGAGCGCTACTGCGTCACCGACGCCGT GTTCACCTTCGTCGCCGTGGACAACAACGGCCGCTCGCGCACCATCCCGC GCGAGAACAACCAGGAGCTGGAGAAGGCCCTCGCCCTCATCTCGGAGCA GCCGCTC**GACTACAAGGACGACGACGACAAG**TGACCATGG
pCM160_RBS_*yciAHI*_F35L_ FLAG (C-terminal tagged)	GCATGCCAACAAGTATCTAAAAGATTAAAGGAGGAATAACAATGTCGGCCA ACTTCACCGACAAGAACGGCCGCCAGTCGAAGGGCGTCCTCCTCCTCCG CACCCTCGCCATGCCGTCGGACACCAACGCCAACGGCGACATCCTCGGC GGCTGGATCATGTCGCAGATGGACATGGGCGGCGCCATCCTCGCCAAGG AGATCGCCCACGGCCGCGTCGTCACCGTCGCCGTCGAGTCGATGAACTTC ATCAAGCCGATCTCGGTCGGCGACGTCGTCTGCTGCTACGGCCAGTGCCT CAAGGTCGGCCGCTCGTCGATCAAGATCAAGGTCGAGGTCTGGGTCAAGA AGGTCGCCTCGGAGCCGATCGGCGAGCGCTACTGCGTCACCGACGCCGT GTTCACCTTCGTCGCCGTGGACAACAACGGCCGCTCGCGCACCATCCCGC GCGAGAACAACCAGGAGCTGGAGAAGGCCCTCGCCCTCATCTCGGAGCA GCCGCTC**GACTACAAGGACGACGACGACAAG**TGACCATGG
pET28a_his6_*yciAHI* (N-terminal tagged)	CATATGTCTGCCAATTTTACTGATAAAAATGGTCGCCAATCAAAAGGAGTTC TTTTACTACGAACTTTGGCGATGCCTTCTGACACCAATGCTAACGGAGATA TTTTTGGTGGCTGGATTATGTCTCAAATGGATATGGGCGGCGCGATTTTAG CGAAAGAAATCGCACACGGACGCGTGGTTACTGTCGCCGTTGAAAGTATG AATTTTATCAAACCAATCTCTGTGGGCGATGTGGTTTGTTGCTACGGTCAAT GTCTCAAAGTTGGGCGTTCTTCCATTAAAATTAAAGTAGAAGTATGGGTAA AAAAAGTGGCGAGTGAGCCAATTGGCGAACGTTATTGTGTCACCGATGCG GTATTTACTTTTGTTGCAGTTGATAATAATGGTCGCTCTCGCACGATTCCCC GTGAAAATAACCAAGAGTTAGAAAAAGCATTAGCCTTAATTTCAGAACAAC CCTTGTAAGAATTC
pET28a_his6_*yciAHI*_F35L (N-terminal tagged)	CATATGTCTGCCAATTTTACTGATAAAAATGGTCGCCAATCAAAAGGAGTTC TTTTACTACGAACTTTGGCGATGCCTTCTGACACCAATGCTAACGGAGATA TTTTAGGTGGCTGGATTATGTCTCAAATGGATATGGGCGGCGCGATTTTAG CGAAAGAAATCGCACACGGACGCGTGGTTACTGTCGCCGTTGAAAGTATG AATTTTATCAAACCAATCTCTGTGGGCGATGTGGTTTGTTGCTACGGTCAAT GTCTCAAAGTTGGGCGTTCTTCCATTAAAATTAAAGTAGAAGTATGGGTAA AAAAAGTGGCGAGTGAGCCAATTGGCGAACGTTATTGTGTCACCGATGCG GTATTTACTTTTGTTGCAGTTGATAATAATGGTCGCTCTCGCACGATTCCCC GTGAAAATAACCAAGAGTTAGAAAAAGCATTAGCCTTAATTTCAGAACAAC CCTTGTAAGAATTC

Online Resource - Supplementary Information

Engineering of thioesterase YciA from *Haemophilus influenzae* for production of carboxylic acids

Laura Pöschel[1,2], Mónica Guevara-Martínez[3], David Hörnström[3], Antonius J.A. van Maris[3], Markus Buchhaupt[1]*

[1] DECHEMA-Forschungsinstitut, Microbial Biotechnology, Theodor-Heuss-Allee 25, 60486 Frankfurt am Main, Germany

[2] Faculty of Biological Sciences, Goethe University Frankfurt, Max-von-Laue-Str. 9, 60438 Frankfurt am Main, Germany

[3] Department of Industrial Biotechnology, School of Engineering Sciences in Chemistry, Biotechnology and Health, KTH Royal Institute of Technology, AlbaNova University Center, SE 10691 Stockholm, Sweden

*Corresponding author,

Phone: +49-69-7564-629, e-mail address: markus.buchhaupt@dechema.de

Fig. S1 Growth kinetics and time-dependent concentration of 2-methylsuccinic acid, 2-hydroxy-3-methylsuccinic acid and mesaconic acid in supernatant of *M. extorquens* AM1 harboring YciAHI variants

Fig. S2 Growth kinetics and time-dependent concentration of 2-methylsuccinic acid and mesaconic acid in supernatant of *M. extorquens* AM1 harboring plasmids encoding YciAHI FLAG, YciAHI F35L FLAG or an empty pCM160 vector

Fig. S3 Uncorrected (2*S*)-methylsuccinyl-CoA conversion tests with purified YciAHI and YciAHI F35L thioesterases

Fig. S4 Growth kinetics and time-dependent concentration of 2-methylsuccinic acid, 2-hydroxy-3-methylsuccinic acid and mesaconic acid in supernatant of *M. extorquens* AM1 harboring YciAHI F35 variants

Fig. S5 Alignment of TE6 family members (α-helix domain)

Fig. S6 Alignment of TE4 family members (α-helix domain)

Fig. S7 Alignment of TE7 family members (presumed α-helix domain)

Fig. S8 Alignment of TE8 family members (α-helix domain)

Fig. S9 Alignment of TE11 family members (α-helix domain)

Fig. S10 Alignment of TE31 family members (α-helix domain)

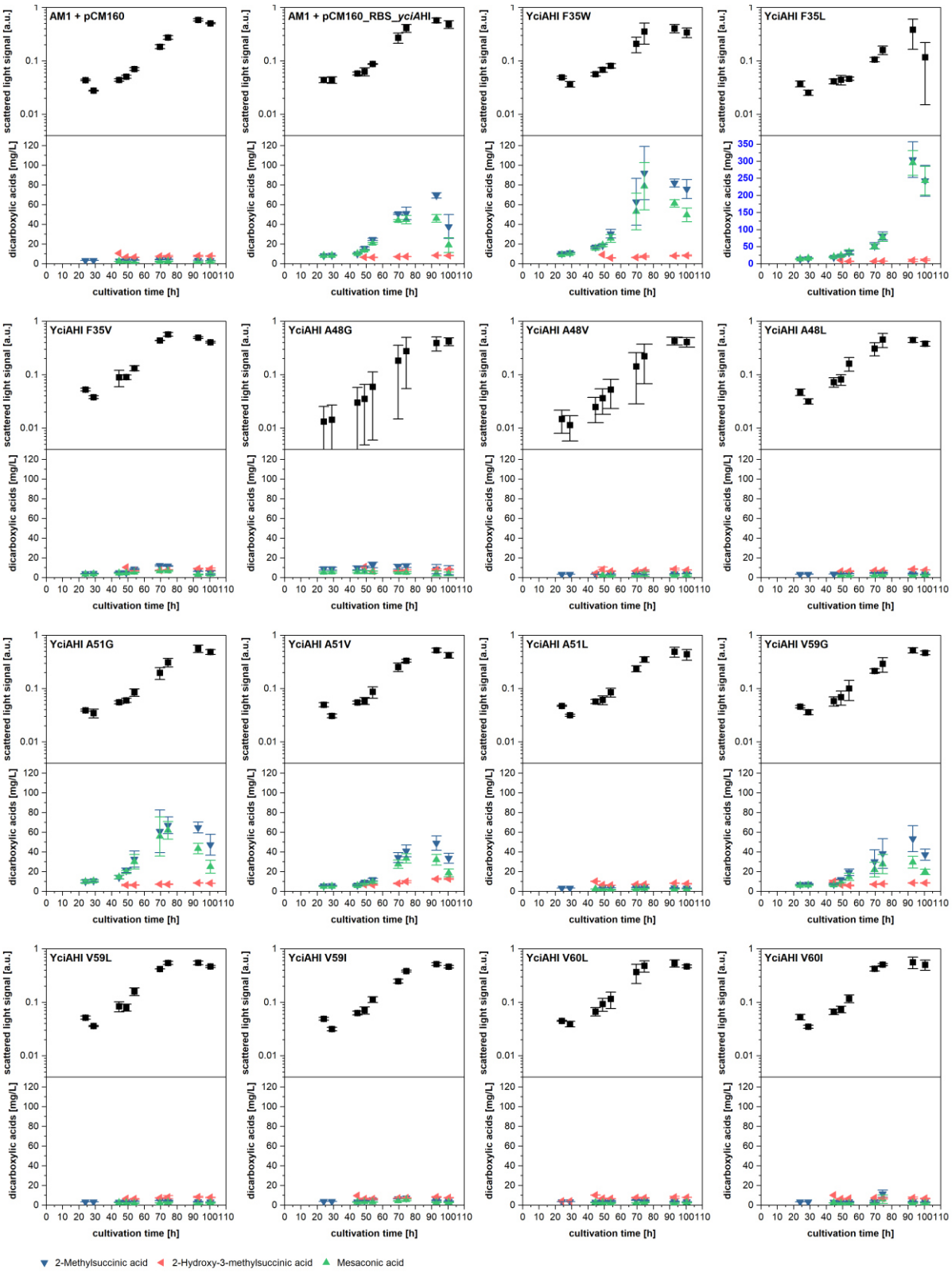

Fig. S1 Growth kinetics and time-dependent concentration of 2-methylsuccinic acid, 2-hydroxy-3-methylsuccinic acid and mesaconic acid in supernatant of *M. extorquens* AM1 harboring YciAHI variants (untagged). EMCP-derived carboxylic acid products with titers insufficient for quantification (< 5 mg/L) are not displayed. Error bars represent standard deviations from three independent replicates

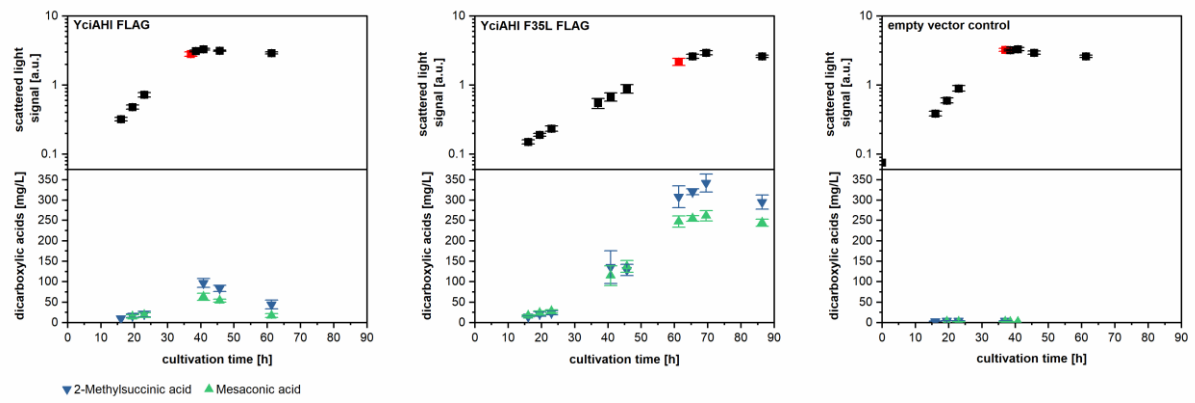

Fig. S2 Growth kinetics and time-dependent concentration of 2-methylsuccinic acid and mesaconic acid in supernatant of *M. extorquens* AM1 harboring plasmids encoding C-terminal FLAG-tagged YciAHI, C-terminal FLAG-tagged YciAHI F35L or an empty pCM160 vector. Red squares indicate the sampling time points for SDS-PAGE samples. Error bars represent standard deviations from three independent replicates

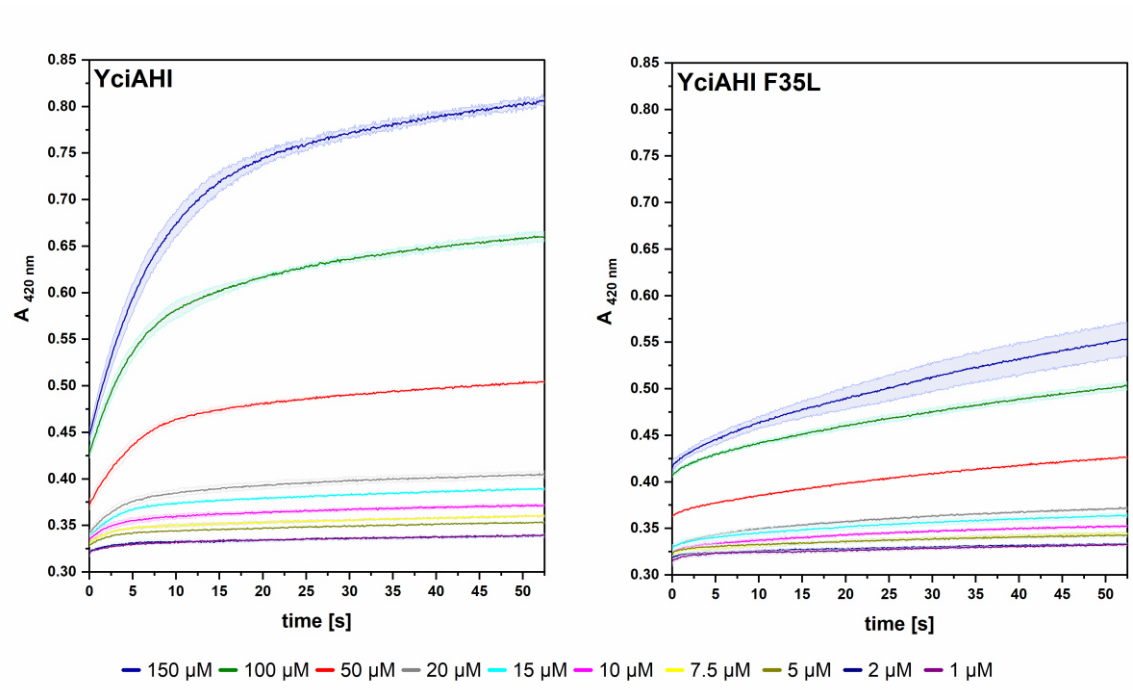

Fig. S3 Uncorrected (2*S*)-methylsuccinyl-CoA conversion tests with purified N-terminal His-tagged YciAHI and N-terminal His-tagged YciAHI F35L thioesterases. Values were determined with a DTNB assay at pH 7.5 and 25°C using 1-150 µM of (2*S*)-methylsuccinyl-CoA as substrate (color coded concentrations) and 7.5 µM of purified enzyme. Prior to addition of the protein, the assay mixture containing all other components was equilibrated to 25 °C. The formation of DTNB-derived 5-thio-2-nitrobenzoate was measured at 412 nm. All measurements were done in triplicates

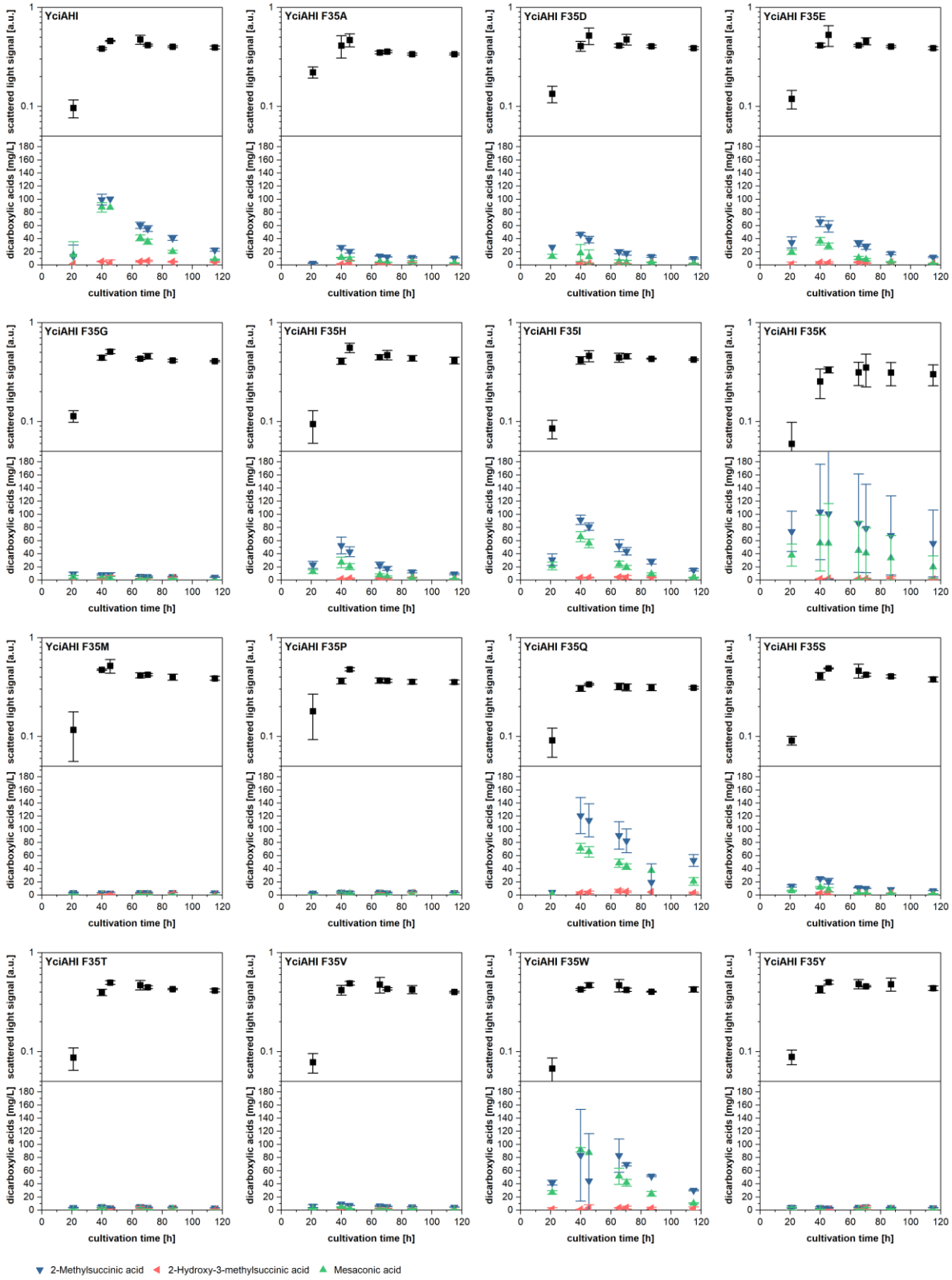

Fig. S4 Growth kinetics and time-dependent concentration of 2-methylsuccinic acid, 2-hydroxy-3-methylsuccinic acid and mesaconic acid in supernatant of *M. extorquens* AM1 harboring YciAHI F35 variants (untagged). EMCP-derived carboxylic acid products with titers insufficient for quantification (< 5 mg/L) are not displayed. Error bars represent standard deviations from three independent replicates

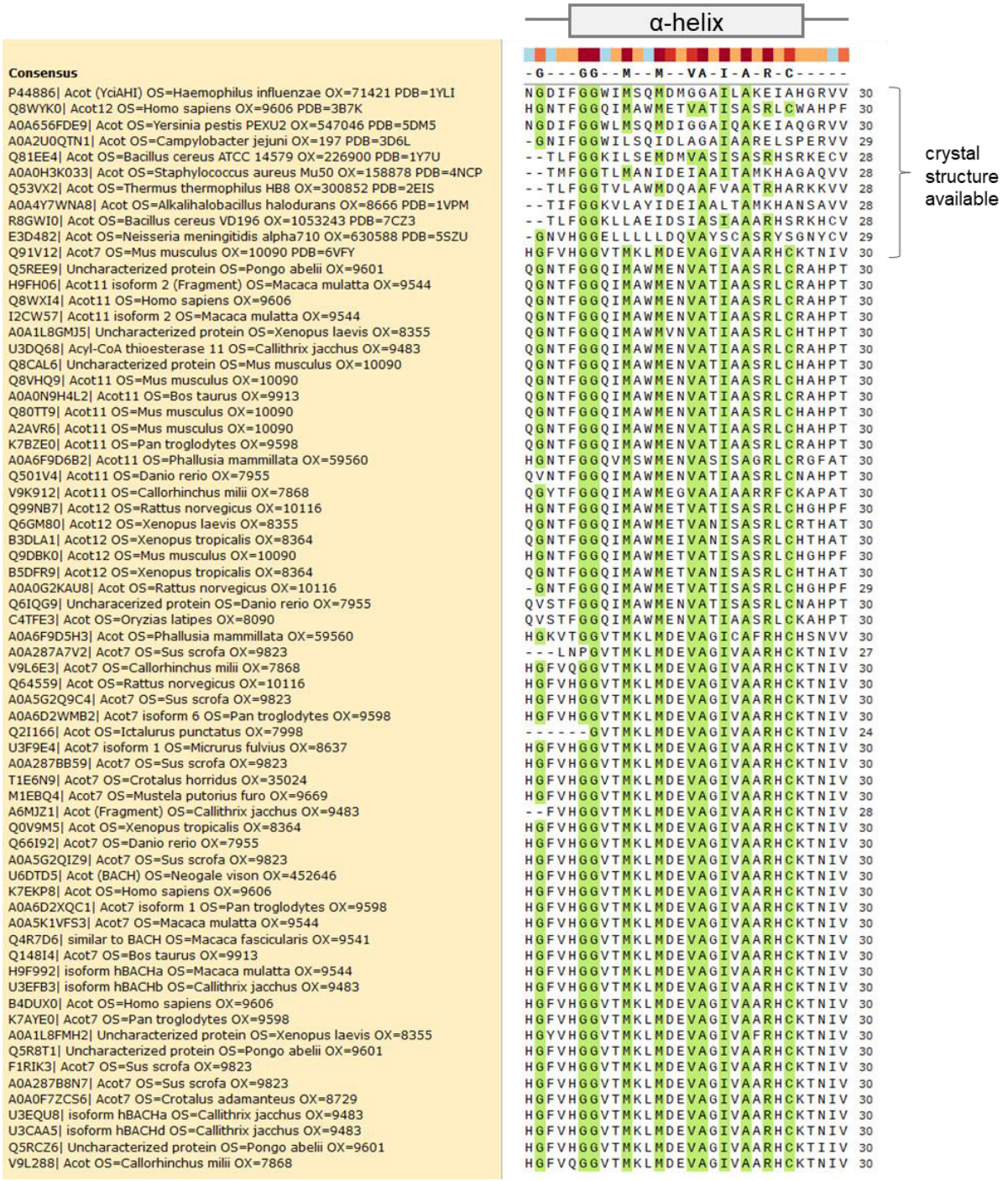

Fig. S5 Alignment of TE6 family members (α-helix domain). Sequences were acquired from ThYme (https://thyme.engr.unr.edu/v2.0/). Alignment was done in COBALT (Papadopoulos and Agarwala 2007) and visualized with SnapGene (GSL Biotech LLC, San Diego, Canada). Consensus with a threshold of 80% is shown. Amino acids corresponding to consensus are highlighted in green

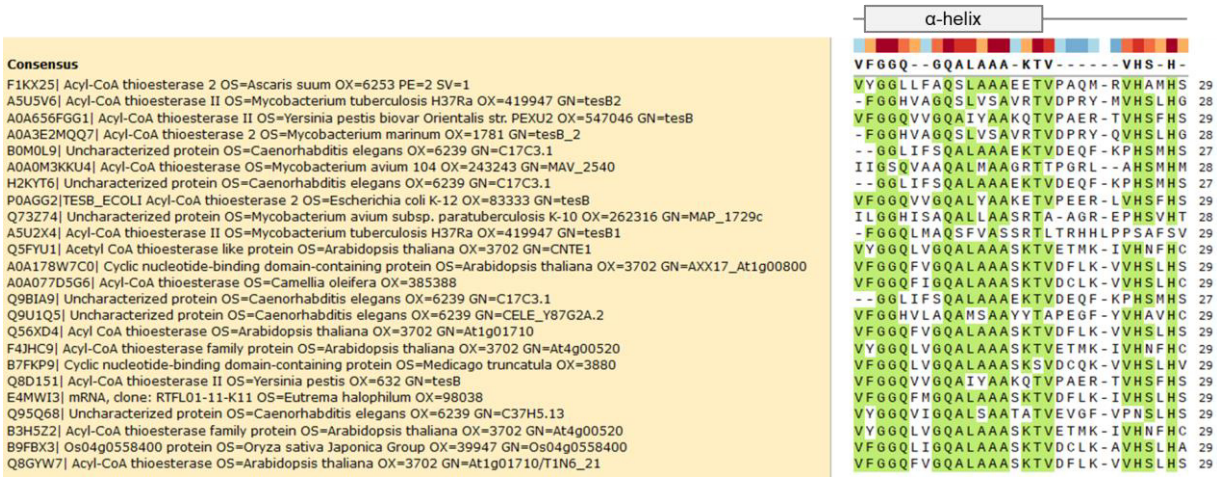

Fig. S6 Alignment of TE4 family members (α-helix domain). Sequences were acquired from ThYme (https://thyme.engr.unr.edu/v2.0/). Alignment was done in COBALT (Papadopoulos and Agarwala 2007) and visualized with SnapGene (GSL Biotech LLC, San Diego, Canada). Consensus with a threshold of 80% is shown. Amino acids corresponding to consensus are highlighted in green

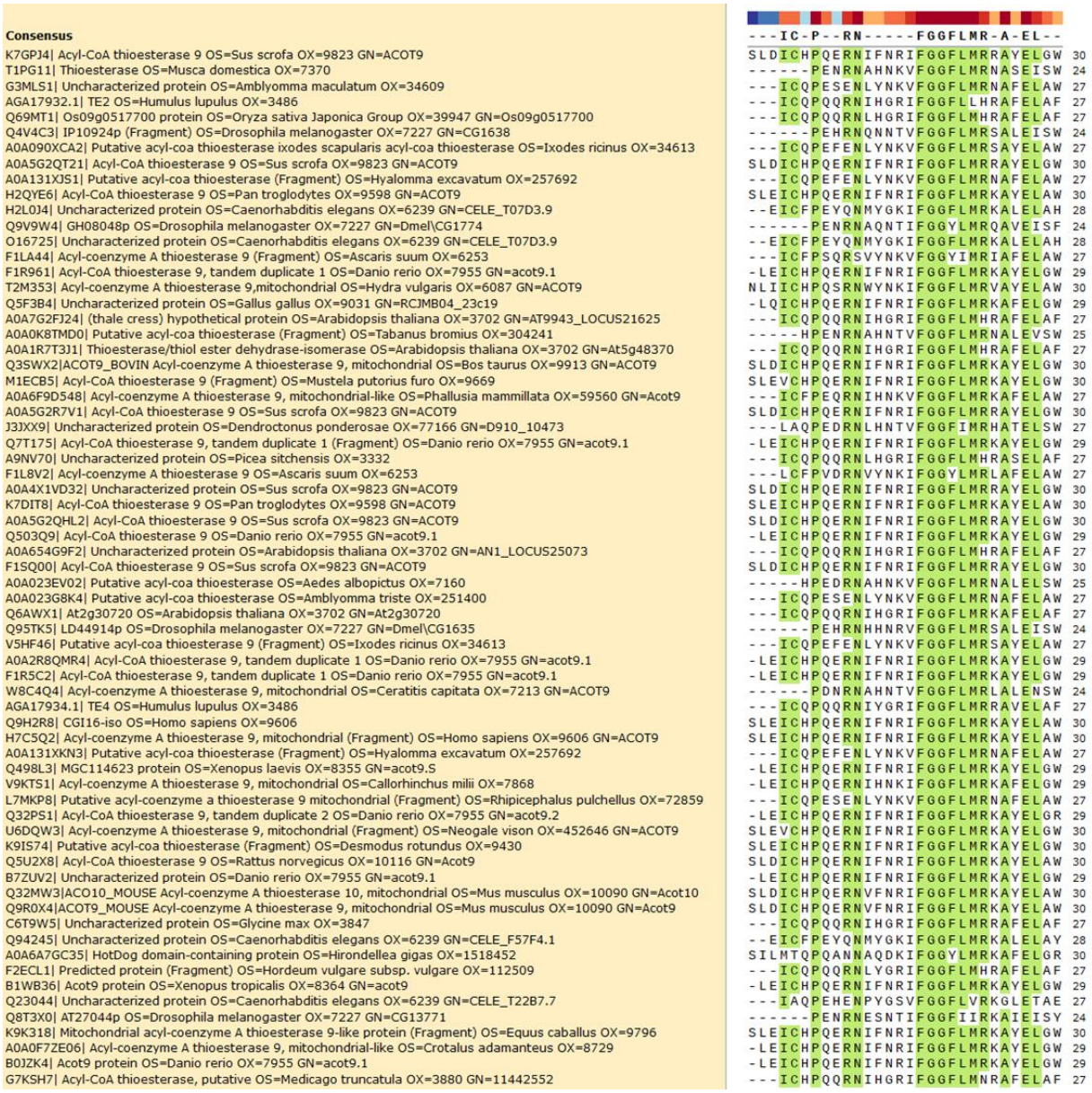

Fig. S7 Alignment of TE7 family members (presumed α-helix domain). Sequences were acquired from ThYme (https://thyme.engr.unr.edu/v2.0/). Alignment was done in COBALT (Papadopoulos and Agarwala 2007) and visualized with SnapGene (GSL Biotech LLC, San Diego, Canada). Consensus with a threshold of 80% is shown. Amino acids corresponding to consensus are highlighted in green

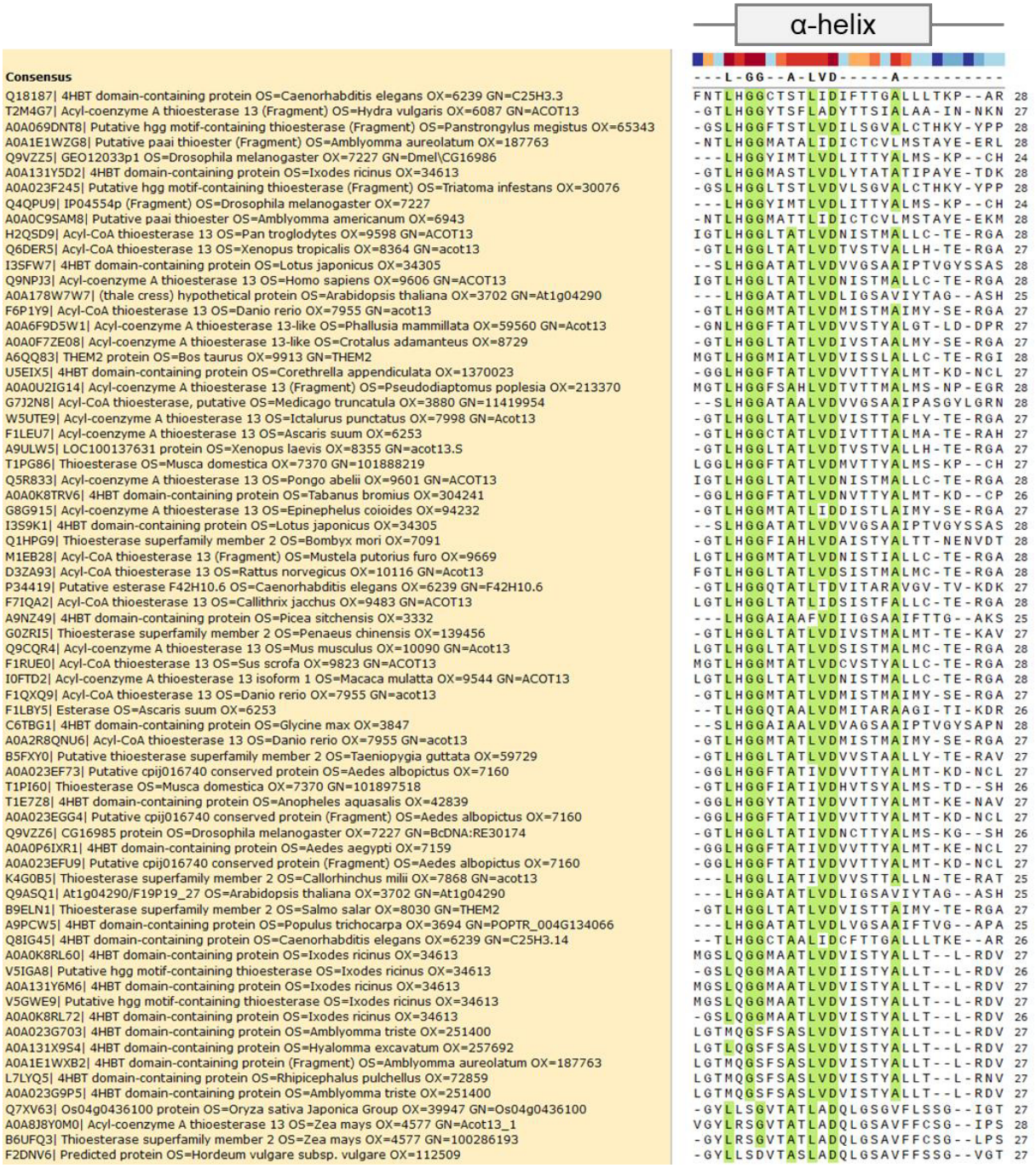

Fig. S8 Alignment of TE8 family members (α-helix domain). Sequences were acquired from ThYme (https://thyme.engr.unr.edu/v2.0/). Alignment was done in COBALT (Papadopoulos and Agarwala 2007) and visualized with SnapGene (GSL Biotech LLC, San Diego, Canada). Consensus with a threshold of 80% is shown. Amino acids corresponding to consensus are highlighted in green

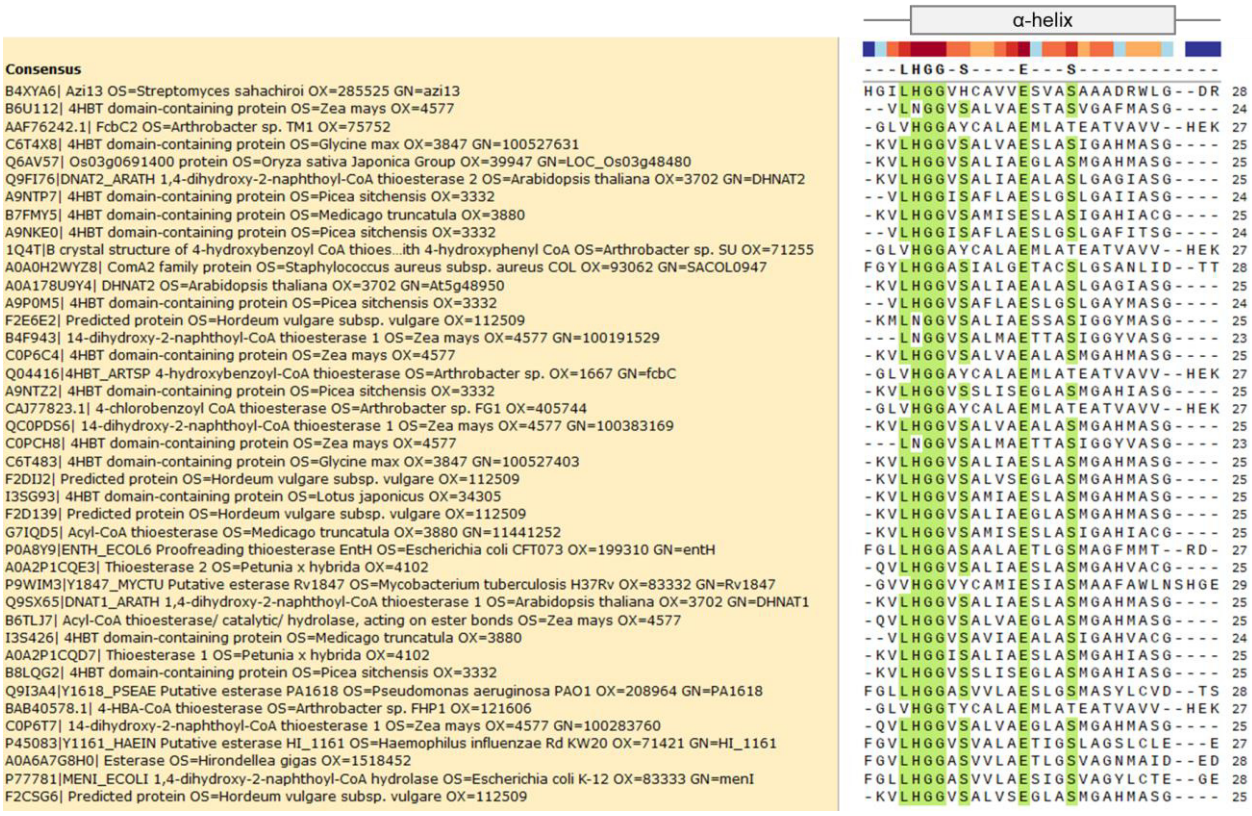

Fig. S9 Alignment of TE11 family members (α-helix domain). Sequences were acquired from ThYme (https://thyme.engr.unr.edu/v2.0/). Alignment was done in COBALT (Papadopoulos and Agarwala 2007) and visualized with SnapGene (GSL Biotech LLC, San Diego, Canada). Consensus with a threshold of 80% is shown. Amino acids corresponding to consensus are highlighted in green

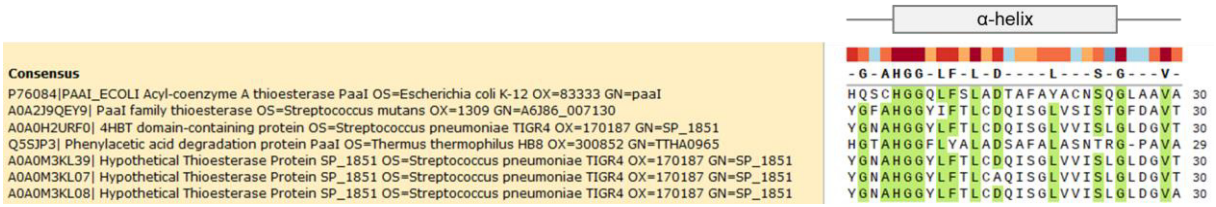

Fig. S10 Alignment of TE31 family members (α-helix domain). Sequences were acquired from ThYme (https://thyme.engr.unr.edu/v2.0/). Alignment was done in COBALT (Papadopoulos and Agarwala 2007) and visualized with SnapGene (GSL Biotech LLC, San Diego, Canada). Consensus with a threshold of 80% is shown. Amino acids corresponding to consensus are highlighted in green

Reference list

Papadopoulos JS, Agarwala R (2007) COBALT: constraint-based alignment tool for multiple protein sequences. Bioinformatics 23:1073–1079. https://doi.org/10.1093/bioinformatics/btm076

6.3 A pBBR1-based vector with IncP group plasmid compatibility for *Methylorubrum extorquens*

Declaration of author contributions to the publication:

A pBBR1-based vector with IncP group plasmid compatibility for *Methylorubrum extorquens*

Status: published

Name of journal: MicrobiologyOpen

Contributing authors: Laura Pöschel (LP), Elisabeth Gehr (EG), Markus Buchhaupt (MB)

What are the contributions of the doctoral candidate and his co-authors?

(1) Concept and design

Doctoral candidate:	33.3 %	
Co-author EG:	33.3 %	
Co-author MB:	33.3 %	

(2) Conducting tests and experiments

Doctoral candidate:	50 %	Characterization of pMis1_1B as single and co-expression vector: cloning experiments, reporter gene experiments, transformation efficiency determination, determination of PCN
Co-author EG:	50 %	Initial testing of pBB1MCS-2 derivatives and isolation of pMis1_1B, initial co-transformation experiments

(3) Compilation of data sets and figures

Doctoral candidate:	80 %	Data collection, preparation of figures and tables
Co-author EG:	20 %	Data collection

(4) Analysis and interpretation of data

Doctoral candidate:	70 %	Analysis and interpretation of data
Co-author EG:	5 %	Analysis of data
Co-author MB:	25 %	Interpretation of data

(5) Drafting of manuscript

Doctoral candidate:	90 %
Co-author MB:	10 %

Received: 9 August 2022 | Accepted: 23 September 2022

DOI: 10.1002/mbo3.1325

COMMENTARY

MicrobiologyOpen Open Access WILEY

A pBBR1-based vector with IncP group plasmid compatibility for *Methylorubrum extorquens*

Laura Pöschel[1,2] | **Elisabeth Gehr**[1] | **Markus Buchhaupt**[1]

[1]DECHEMA-Forschungsinstitut, Microbial Biotechnology, Frankfurt am Main, Germany

[2]Department of Life Sciences, Goethe University Frankfurt, Frankfurt am Main, Germany

Correspondence
Markus Buchhaupt, DECHEMA-Forschungsinstitut, Microbial Biotechnology, Theodor-Heuss-Allee 25, 60486 Frankfurt am Main, Germany.
Email: markus.buchhaupt@dechema.de

Funding information
Bundesministerium für Bildung und Forschung, Grant/Award Number: FKZ 031B0340A

Abstract

Plasmids are one of the most important genetic tools for basic research and biotechnology, as they enable rapid genetic manipulation. Here we present a novel pBBR1-based plasmid for *Methylorubrum extorquens*, a model methylotroph that is used for the development of C1-based microbial cell factories. To develop a vector with compatibility to the so far mainly used pCM plasmid system, we transferred the pBBR1-based plasmid pMiS1, which showed an extremely low transformation rate and caused a strong growth defect. Isolation of a suppressor mutant with improved growth led to the isolation of the variant pMis1_1B. Its higher transformation rate and less pronounced growth defect phenotype could be shown to be the result of a mutation in the promotor region of the *rep* gene. Moreover, cotransformation of pMis1_1B and pCM160 was possible, but the resulting transformants showed stronger growth defects in comparison with a single pMis1_1B transformant. Surprisingly, cotransformants carrying pCM160 and a pMis1_1B derivative containing a *mCherry* reporter construct showed higher fluorescence levels than strains containing only the pMis1_1B-based reporter plasmids or a corresponding pCM160 derivative. Relative plasmid copy number determination experiments confirmed our hypothesis of an increased copy number of pMis1_1B in the strain carrying both plasmids. Despite the slight metabolic burden caused by pMis1_1B, the plasmid strongly expands the genetic toolbox for *M. extorquens*.

KEYWORDS
cotransformation, expression system, *Methylorubrum extorquens* AM1, plasmid, plasmid copy number, Rep gene

1 | INTRODUCTION

Methylorubrum extorquens has great potential to become a universal production strain for the C1-based bioeconomy (Chen & Lan, 2020; Ochsner et al., 2014; Zhang et al., 2019). In the last decade, several *M. extorquens* strains with heterologously expressed metabolic pathways were described for the biotechnological production of various products including 1-butanol, 3-hydroxypropionic acid, mono- and dicarboxylic acids, mevalonate or α-humulene (Hu & Lidstrom, 2014; Liang et al., 2017; Lim et al., 2019; Schada von Borzyskowski et al., 2018; Sonntag et al., 2014, Sonntag, Kroner, et al., 2015; Sonntag, Müller, et al., 2015; Yang et al., 2017). The development of production strains, however, is limited by the organism's

restricted genetic accessibility. Although the bacterium has served as a model organism for methylotrophy for many decades and is therefore well described, only a few genetic tools have been developed. Plasmids are a key tool for the biotechnological applicability of a strain. The simultaneous use of two independent plasmids provides experimental flexibility and simplifies screenings and production strain developments. The compatibility of two or more plasmids in a single bacterial cell requires not only different selection markers but, more importantly, different origins of replication and partitioning systems (del Solar et al., 1998; Novick, 1987). As part of their characterization, plasmids are divided into Inc groups: plasmids from the same group are usually incompatible.

For *M. extorquens* AM1, besides a recently described set of mini chromosomes (Carrillo et al., 2019), derivatives of the pCM plasmid system (Marx & Lidstrom, 2001) were used almost exclusively as episomal vectors for heterologous gene expression. The expression vectors pCM80 (tc^R) and pCM160 (kan^R) are based on pDN19, a small IncP vector (Marx & Lidstrom, 2001). The authors of the respective study isolated the derivative pDN19X from *M. extorquens* AM1 transformed with pDN19. This derivative could be efficiently maintained and retransferred in *M. extorquens* AM1 and was used as a basis for the development of the pCM system (Marx & Lidstrom, 2001). In their work, the authors also showed that pBBR1MCS-2, a vector derived from *Bordetella bronchiseptica* pBBR1, could be transferred into *M. extorquens* with very low transformation efficiency and a significantly reduced transformant growth rate. Since this vector is known to be compatible with IncP group plasmids (Antoine & Locht, 1992; Kovach et al., 1994, 1995), we chose it as a starting point for the development of a plasmid with compatibility with the pCM vector system. The GC content of 64.6% seems to be applicable to *M. extorquens* AM1 (overall GC content of 68.5% [Vuilleumier et al., 2009]) and its diverse usability as a broad range vector can be also useful for certain applications. Here, we describe a pBBR1-derived plasmid with a mutation upstream of the *rep* gene that confers suitability for cotransformation with established pCM plasmids.

2 | MATERIALS AND METHODS

2.1 | Plasmids and bacterial strains

A list of all used plasmids and bacterial strains is given in Table 1. Reporter gene plasmids were constructed by subcloning synthesized DNA fragments (BioCat) into plasmid backbones. Used sequences and restriction enzymes are listed in Table 2. Analysis of sequences and creation of plasmid map was done with SnapGene (www.snapgene.com). Transformation of *M. extorquens* AM1 with plasmid DNA was performed as previously described (Toyama et al., 1998). If not stated differently, 100 ng of plasmid DNA was used for transformations.

2.2 | Media and culture conditions

Escherichia coli DH5α (NEB) was used for plasmid amplification and cloning. *E. coli* cultures were grown in LB (lysogeny broth) medium (Bertani, 1951). *M. extorquens* AM1 (Peel & Quayle, 1961)

TABLE 1 Plasmids and bacterial strains used in this study

Name	Relevant features	Reference
Bacterial strains		
Escherichia coli DH5α	F^- φ80*lac*ZΔM15, Δ(*lac*ZYA-*arg*F)U169, *rec*A1, *end*A1, *hsd*R17 (r_K^-, m_K^+) *pho*A, *sup*E44, λ^-, *thi*-1 *gyr*A96 *rel*A1	ATCC
Methylorubrum extorquens AM1	Cm^R, gram-negative, facultatively methylotrophic, obligate aerobic α-proteobacterium	Peel and Quayle (1961)
Plasmids		
pCM160	Constitutive expression vector for *M. extorquens*; Kan^R, pmxaF (IncP)	Marx and Lidstrom (2001)
pCM80	Constitutive expression vector for *M. extorquens*; Tc^R, pmxaF (IncP)	Marx and Lidstrom (2001)
pMis1	*Pseudomonas putida* expression vector, Kan^R	Mi et al. (2014)
pMis4	*P. putida* expression vector; pMis1 derivative with mutated *rep* gene, Kan^R	Mi et al. (2016)
pBBR1MCS-2	broad-host-range expression vector, Kan^R	Kovach et al. (1995)
pMis1_1B	pMis1 derivative, Kan^R	This study (GenBank OP441404)
pCM160_*mCherry*	pCM160-based mCherry reporter plasmid	This study
pMis1_1B_P_{mxaF}_*mCherry*	pMis1_1B based mCherry reporter plasmid, promoter *rha*P_{BAD} was exchanged with P_{mxaF}	This study

TABLE 2 Synthetic sequences used for cloning of reporter plasmids. DNA was synthesized by BioCat (Heidelberg, Germany). Underlined nucleotides mark restriction sites for cloning

Plasmids/Sequences	Restriction enzymes used	Backbone
pMis1_1B_P_{mxaF}_*mCherry*		
GAATTCCCCGCTTGGTCGGGCCGCTTCGCGAGGGCCCGTTGACGACAACGGTGCGATGGGTCCCGGCCCCGGTCAAGACGATGCCAA- TACGTTGCGACACTACGCCTTGGCACTTTTAGAATTGCCTTATCGTCCTGATAAGAAATGTCCGACCAGCTAAAGACATCGCGTCCAAT- CAAAGCCTAGAAAATATAGGCGAAGGGACGCTAATAAGTCTTTCATAAGACCGCGCAAATCTAAAAATATCCTTAGATTCACGATGCGG- CACTTCGGATGACTTCCGAGCGAGCCTGGAACCTCAGAAAAACGTCTGAGAGATACCGCGGAGACGTCATGGTGAGCAAGGGCGAGGAGGA- TAACATGGCCATCATCAAGGAGTTCATGCGCTTCAAGGTGCACATGGAGGGCTCCGTGAACGGCCACGAGTTCGAGATCGAGGGCGAGGGC- GAGGGCGCCCCCTACGAGGGCACCCAGACCGCCAAGCTGAAGGTGACCAAGGGTGGCCCCCTGCCCTTCGCCTGGGACATCCTGTCCCCT- CAGTTCATGTACGGCTCCAAGGCCTACGTGAAGCACCCCGCCGACATCCCCGACTACTTGAAGCTGTCCTTCCCCGAGGGCTTCAAGTGG- GAGCGCGTGATGAACTTCGAGGACGGCGGCGTGGTGACCGTGACCCAGGACTCCTCCCTGCAGGACGGCGAGTTCATCTACAAGGT- GAAGCTGCGCGGCACCAACTTCCCCTCCGACGGCCCCGTAATGCAGAAGAAGACCATGGGCTGGGAGGCCTCCTCCGAGCGGATGTACCCC- GAGGACGGCGCCCTGAAGGGCGAGATCAAGCAGAGGCTGAAGCTGAAGGACGGCGGCCACTACGACGCTGAGGTCAAGACCACCTACAAGGC- CAAGAAGCCCGTGCAGCTGCCCGGCGCCTACAACGTCAACATCAAGTTGGACATCACCTCCCACAACGAGGACTACACCATCGTGGAACAG- TACGAACGCGCCGAGGGCCGCCACTCCACCGGCGGCATGGACGAGCTGTACAAGTAATCTAGA	*EcoR*I + *Xba*I	pMis1_1B
pCM160_*mCherry*		
GCATGCATGGTGAGCAAGGGCGAGGAGGATAACATGGCCATCATCAAGGAGTTCATGCGCTTCAAGGTGCACATGGAGGGCTCCGT- GAACGGCCACGAGTTCGAGATCGAGGGCGAGGGCGAGGGCCGCCCCTACGAGGGCACCCAGACCGCCAAGCTGAAGGTGAC- CAAGGGTGGCCCCCTGCCCTTCGCCTGGGACATCCTGTCCCCTCAGTTCATGTACGGCTCCAAGGCCTACGTGAAGCACCCCGCCGA- CATCCCCGACTACTTGAAGCTGTCCTTCCCCGAGGGCTTCAAGTGGGAGCGCGTGATGAACTTCGAGGACGGCGGCGTGGTGACCGTGACC- CAGGACTCCTCCCTGCAGGACGGCGAGTTCATCTACAAGGTGAAGCTGCGCGGCACCAACTTCCCCTCCGACGGCCCCGTAATGCAGAAGAA- GACCATGGGCTGGGAGGCCTCCTCCGAGCGGATGTACCCCGAGGACGGCGCCCTGAAGGGCGAGATCAAGCAGAGGCTGAAGCTGAAG- GACGGCGGCCACTACGACGCTGAGGTCAAGACCACCTACAAGGCCAAGAAGCCCGTGCAGCTGCCCGGCGCCTACAACGTCAACAT- CAAGTTGGACATCACCTCCCACAACGAGGACTACACCATCGTGGAACAGTACGAACGCGCCGAGGGCCGCCACTCCACCGGCGGCATGGAC- GAGCTGTACAAGTAAGCATGC	*Sph*I	pCM160

Name	Sequence	Target of amplification
LPoe144_qPCR_fw_ref	GATCAGCGTGACGTACTG	Parts of gene *kgtP* (genomic DNA = "Ref")
LPoe145_qPCR_rev_ref	CCGGTTCTTCTCGTGATC	
LPoe150_qPCR_fw_pMis	CGAGGATCTCGTCGTGACC	Parts of Kan^R cassette on pMis (plasmid DNA = "target")
LPoe151_qPCR_rev_pMis	TATCACGGGTAGCCAACGC	

TABLE 3 Primers used for real-time polymerase chain reactions

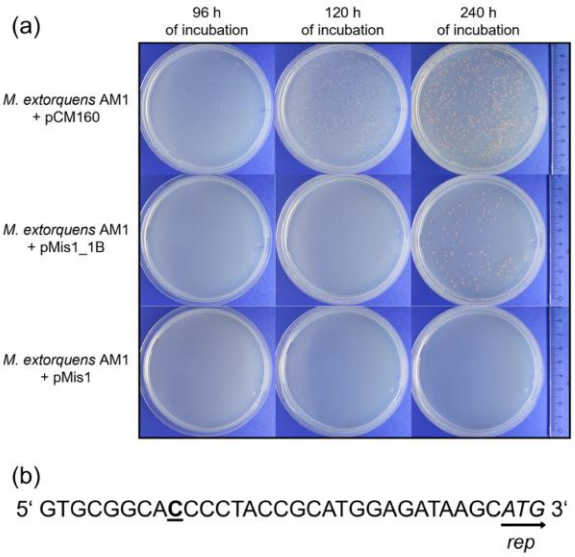

FIGURE 1 Growth of *Methylorubrum extorquens* AM1 after transformation with pCM160 or pBBR derivatives and DNA sequence differences between the used pBBR derivatives pMis1 and pMis1_1B. (a) Transformation plates after transformation of *M. extorquens* AM1 with 30 fmol of pMis1, pMis1_1B, or pCM160. Transformation plates were photographed after 96, 120, and 240 h of incubation. (b) Mutation in the sequence of pMis1_1B. The inserted nucleotide (cytosine) is located 22 bp upstream of the *rep* gene, whose start codon is indicated by italic letters.

cultivations were performed in a liquid minimal medium (Peyraud et al., 2009) with 123 mM methanol and a final concentration of 12.6 µM CoCl2 (Kiefer et al., 2009; Sonntag et al., 2014). Solid medium contained 1.5% [w/v] agar-agar. Antibiotics were used in concentrations of 50 µg/ml for kanamycin or 10 µg/ml for tetracycline hydrochloride. All media components were purchased from Carl Roth or Merck. *M. extorquens* AM1 main cultures were inoculated to an OD_{600} value of 0.1 with precultures grown for 48 h at 30°C and 180 rpm on a rotary shaker.

2.3 | Growth monitoring and fluorescence assays

For the high-resolution monitoring of growth and mCherry fluorescence signals, *M. extorquens* AM1 cultures were grown in a BioLector® microbioreactor system (m2p-labs GmbH). Main cultures were grown in Flowerplate® wells at 30°C, 1000 rpm, and 85% humidity. The final cultivation volume was 1 ml. The level of mCherry reporter protein was measured via its fluorescence signal at 580/610 nm [ex/em]. Growth was monitored via scattered light signals.

2.4 | Determination of relative plasmid copy numbers

The relative plasmid copy number (PCN) of pMis1_1B_*mCherry* was determined by comparing plasmid-specific real-time PCR fluorescence signals in strains containing two plasmids (=sample) to strains containing one plasmid (=control). The main cultures of respective strains were inoculated and cultivated as described above. Cells were harvested in the mid to late exponential growth phase after 45 h of cultivation. DNA was isolated with a QIAamp® DNA Mini kit (Qiagen) following the manufacturer's instructions for bacterial cells. Real-time PCR primers pairs (Table 3) were designed for amplification of a specific region of the resistance markers on the plasmids (=target) as well as for amplification of a genomic reference sequence (=Ref), all yielding amplicons of 140–143 nucleotides in length. Real-time PCR experiments were performed using QuantiTect® SYBR® Green PCR Kit in a PikoReal™ System (Thermo Scientific) according to the manufacturer's instructions. The following PCR protocol was used: 15 min at 95°C followed by 45 cycles of 94°C/15 s, 50°C/30 s, and 72°C/30 s. The specificity of primers was confirmed by melting curves and gel electrophoresis. The dynamic range of reaction was validated by testing a tenfold serial dilution of DNA template ranging from 50 ng to 5 pg. The efficiency (E) was subsequently calculated with Equation (1) (Higuchi et al., 1993; Rasmussen, 2001).

$$E = 10^{-1/\text{slope}} \quad (1)$$

The amount of starting material for the final experiments was 500 pg of template DNA. All reactions were performed in biological triplicates. The relative ratio (R) was calculated with the Pfaffl efficiency-corrected model with averaged controls (Equation 2): (Pfaffl, 2004).

$$R = \frac{(E_{target})^{\Delta Cp\ target(MEAN\ \ control-sample)}}{(E_{Ref})^{\Delta Cp\ Ref(MEAN\ \ control-sample)}} \quad (2)$$

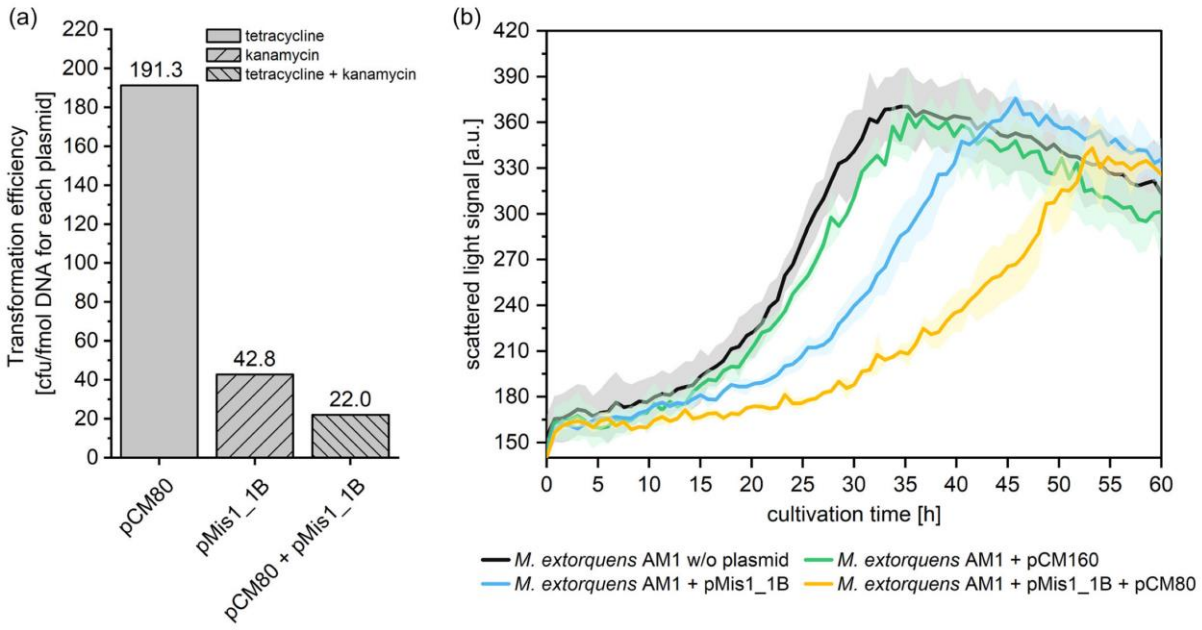

FIGURE 2 Compatibility of pMis1_1B and pCM80. (a) Transformation efficiencies of pCM80 and pMis1_1B for single and double transformations. Transformation mixtures contained 30 fmol plasmid DNA for single plasmid transformations and 30 fmol plasmid DNA of each plasmid in double transformations. Transformation mixtures were plated on a solid medium with antibiotics for the corresponding plasmid(s). Antibiotics used are indicated by the bar pattern. Colonies of single transformants were counted after 144 h of growth, while colonies of cotransformants were counted after 192h of growth. (b) Growth of *Methylorubrum extorquens* AM1 in a microbioreactor system containing no plasmid, pCM160, pMis1_1B, or pMis1_1B and pCM80 in combination, respectively. Selective antibiotics were used as follows: w/o plasmid: none; pCM160 or pMis1_1B: kanamycin; pMis1_1B + pCM80: kanamycin + tetracycline. Three independent biological replicates were measured. Colored areas indicate the standard deviation (SD).

3 | RESULTS AND DISCUSSION

3.1 | Increased transformation efficiency of pMis variant pMis1_1B

We tested different variants of pBBR1 (Antoine & Locht, 1992) for transformability in *M. extorquens* AM1, as pBBR1MCS-2 was transferred into *M. extorquens* AM1 already, albeit with very low efficiency (Marx & Lidstrom, 2001). Plasmids pMis1 and pMis4 are derivatives of pBBR1MCS-2 carrying a rhamnose-inducible promoter (Mi et al., 2016). In pMis4, a mutation in the *rep* gene leads to a G159S modification in the Rep protein. This mutation prevented the plasmid burden caused by pMis1 in *Pseudomonas putida* (Mi et al., 2016). The named plasmids and a pCM160 control were transferred into *M. extorquens* AM1, and an aliquot of 100 µl of the transformation mix was spread on selective agar plates. Although transformation of *M. extorquens* AM1 with pCM160 yielded almost a lawn of colonies after 96 h of incubation, other plasmids yielded a low number of transformants after 192 h of incubation: On the pBBR1MCS-2 transformation plate, only 2 very small colonies were visible, indicating a severe growth defect of the respective transformants. Transformation with pMis1 yielded in a sole, big colony, and transformation with pMis4 in a small number of big colonies. The respective plasmids of these colonies were isolated and 30 fmol of pDNA was retransformed into *M. extorquens* AM1 along with pCM160 as a control. Only the plasmid isolated from the pMis1 transformant showed a clear increase in transformation efficiency compared to pMis1 and was named pMis1_1B (Figure 1a). Colonies of pMis1_1B transformants were clearly visible after 96 h of incubation, with inconsistent colony size, whereas colonies of pMis1 transformants were not visible even after 240 h of cultivation. Complete sequencing of pMis1_1B revealed an insertion of one cytosine residue 22 bp upstream of the *rep* gene (Figure 1b). This insertion upstream of the rep region has likely altered the plasmid copy number (PCN). For pBBR1-based plasmids, the Rep protein is known to play a crucial role in PCN control by binding to the origin of replication (ori) (Antoine & Locht, 1992; del Solar et al., 1998). Consequently, modifications in the *rep* gene region have been shown to influence the PCN (Mi et al., 2016; Tao et al., 2005; Wadood et al., 1997). Interestingly, the currently used pCM system is based on a similar experiment with the plasmid pDN19 (Marx & Lidstrom, 2001). pDN19 was transferred into *M. extorquens* AM1 with low efficiency, but a mutated derivative (pDN19X) could be isolated from a transformant. pDN19X was efficiently maintained and showed enhanced transformation efficiency. The described single-point mutation in *traJ* led to changes in transformability even though all

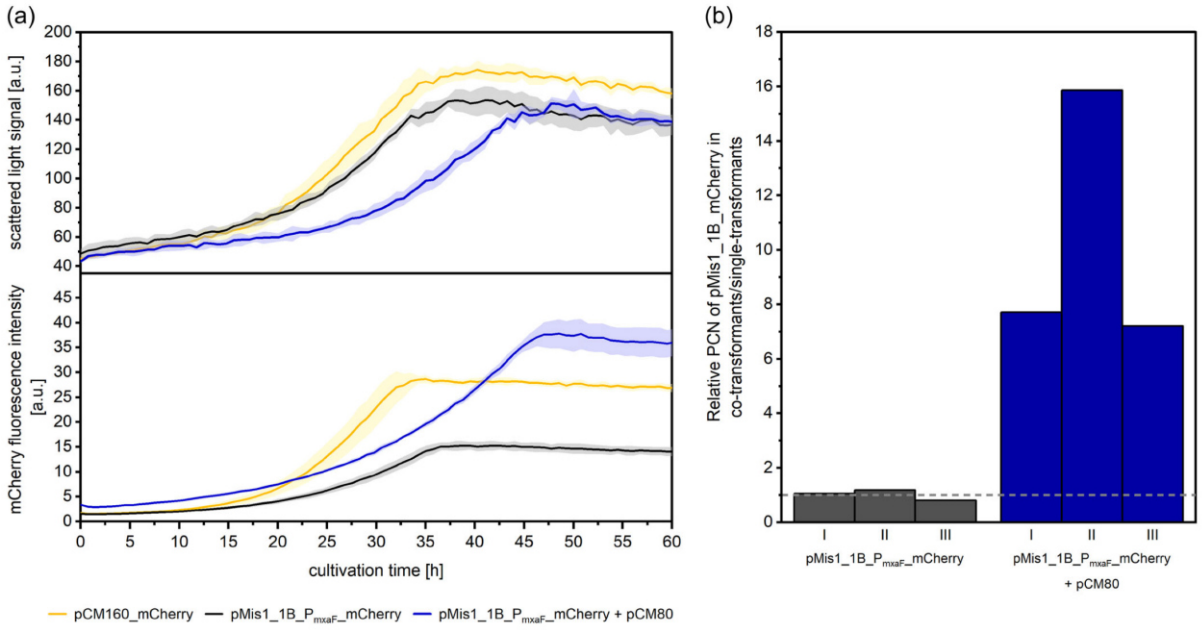

FIGURE 3 Investigation of phenotypes for *Methylorubrum extorquens* AM1 strains carrying pCM160 and pMis1_1B_P_{mxaF}_*mCherry*. (a) Growth and mCherry fluorescence signal of *M. extorquens* AM1 containing pCM160, pMis1_1B_P_{mxaF}_*mCherry*, or both plasmids in combination. Three independent biological replicates were investigated in a microbioreactor system. Colored areas indicate the standard deviation (SD). (b) Ratio of relative PCN of pMis1_1B_P_{mxaF}_*mCherry* in *M. extorquens* AM1 + pMis1_1B_P_{mxaF}_*mCherry* + pCM80 to the same plasmid in *M. extorquens* AM1 + pMis1_1B_P_{mxaF}_*mCherry*. The chromosomal housekeeping gene was used as a reference. The mean value of relative pMis1_1B_P_{mxaF} _*mCherry* PCN of the control strain (= 1) is shown by a dashed line. For each strain, three independent transformants (I–III) were measured.

traJ functions were provided by helper plasmids. The authors, therefore, speculated that transformability was not enhanced by changes in TraJ but by a change in PCN. This confirms that the PCN is an extremely important factor for *M. extorquens* plasmids.

3.2 | Compatibility of pMis1_1B with the established pCM plasmids

For testing the compatibility of pMis1_1B with the pCM system, *M. extorquens* AM1 was transformed with pMis1_1B and pCM80 simultaneously. The cotransformation did lower the transformation efficiency by 2-fold compared to transformation of pMis1_1B alone (Figure 2a). Furthermore, colonies of cotransformants were only clearly visible after 8 days of growth, indicating an increased metabolic burden caused by the presence of both plasmids. Detailed growth monitoring in liquid growth medium confirmed these results: While *M. extorquens* AM1 harboring pMis1_1B already showed a reduced growth rate compared to the pCM160-containing strain or the plasmid-free strain, cotransformation with both plasmids strongly reduced the growth rate (Figure 2b). Plasmid-induced reduction of growth rates under methylotrophic growth conditions due to metabolite limitations have already been described for *M. extorquens* AM1 (Kiefer et al., 2009). We, therefore, tested increased amounts of several media components but were unable to identify any medium-related limitation (data not shown). Only a reduction in the kanamycin concentration resulted in an increased growth rate, but most probably reduced plasmid maintenance stability or copy number, as revealed by fluorescence quantification experiments using an mCherry reporter derivative of pMis1_1B (Figure A1). Mutations in the *rep*-gene region were already successfully used to increase the copy number of pBBR-based broad host range plasmids and the growth rate of corresponding transformants (Mi et al., 2016; Tao et al., 2005). A more directed screening of *rep* gene expression level variants might identify a more suitable expression level associated with less plasmid burden.

3.3 | Characterization of pMis1_1B as pCM coexpression vector

Despite the lower growth rates of the cotransformants, pMis1_1B is nevertheless a promising candidate for simultaneous gene expression from two plasmids in *M. extorquens* AM1. To investigate the plasmid stability and general expression levels from pMis1_1B, we used pMis1_P_{mxaF}_*mCherry* containing the reporter gene under the control of the strong native constitutive promotor P_{mxaF}. Expression of *mCherry* did not change the growth behavior of the respective strains

(Figure A2). We investigated the *mCherry* expression levels from respective pCM and pMis1_1B constructs in strains with one or two plasmids, respectively. The previously described growth defect of the cotransformants was also visible in this experiment (Figure 3a). However, there was a clear synergistic effect in terms of expression: The mCherry signal originating from pMis1_1B_P_{mxaF}_*mCherry* was substantially increased if pCM80 was additionally present. The maximal mCherry fluorescence signal of the cotransformants even exceeded the values from pCM160_*mCherry* single transformants. One explanation for this finding could be an increased PCN. We, therefore, determined the relative PCN of pMis1_1B_*mCherry* for strains containing two plasmids and strains containing only a single plasmid by real-time PCR. Since the efficiency of the used primer pairs varied from 1.73 to 1.96, the E-corrected Pfaffl-method was used (Pfaffl, 2004). Although the values determined for each of the three replicate strains containing two plasmids showed a strong variation, a clear increase in PCN was detectable when both plasmids are present in *M. extorquens* AM1 (Figure 3b). Thus, the presence of pCM80 led to a strong increase in the pMis1_1B copy number.

4 | CONCLUSIONS

The pBBR1 derivative pMis1_1B, which we characterized in this study represents a novel plasmid for *M. extorquens*, which is compatible with the widely used pCM system. Even though the growth rate of *M. extorquens* AM1 was affected when both plasmids were present in the cells, pMis1_1B could be a powerful tool for certain applications. For example, it provides enormous facilitation for the combinatorial testing of multiple enzymes during the development of synthetic pathways. Moreover, a new plasmid system that is not as stably maintained as pCM could be useful for applications where an expression plasmid is only needed transitionally as for the expression of Cre-recombinase in a Cre/*loxP* recombination system or for CRISPR gene editing. With pMis1_1B, a new useful tool has been added to the expanding genetic toolbox for *M. extorquens*.

AUTHOR CONTRIBUTIONS

Laura Pöschel: Conceptualization (equal); investigation (equal); methodology (equal); visualization (lead); writing–original draft (lead); writing–review and editing (equal); **Elisabeth Gehr**: Conceptualization (equal), investigation (equal), methodology (equal); writing–original draft (supporting); **Markus Buchhaupt**: Conceptualization (equal); methodology (equal); funding acquisition (lead); project administration (lead); writing–original draft (supporting); writing–review and editing (equal).

ACKNOWLEDGMENTS

This study was funded by the German Federal Ministry of Education and Research ("Bundesministerium für Bildung und Forschung," BMBF) in the project ChiraMet (FKZ 031B0340A). Open Access funding enabled and organized by Projekt DEAL.

CONFLICT OF INTEREST

None declared.

DATA AVAILABILITY STATEMENT

The plasmid sequence of pMis1_1B is available in the NCBI GenBank under accession number OP441404: https://www.ncbi.nlm.nih.gov/nuccore/OP441404. The plasmid itself has been deposited to Addgene. All other data generated or analyzed during this study are included in this published article.

ETHICS STATEMENT

None required.

ORCID

Markus Buchhaupt http://orcid.org/0000-0003-2720-5973

REFERENCES

Antoine, R., & Locht, C. (1992). Isolation and molecular characterization of a novel broad-host-range plasmid from *Bordetella bronchiseptica* with sequence similarities to plasmids from gram-positive organisms. *Molecular Microbiology*, *6*(13), 1785–1799. https://doi.org/10.1111/j.1365-2958.1992.tb01351.x

Bertani, G. (1951). Studies on lysogenesis I. the mode of phage liberation by lysogenic *Escherichia coli*. *Journal of Bacteriology*, *62*(3), 293–300. https://doi.org/10.1128/jb.62.3.293-300.1951

Carrillo, M., Wagner, M., Petit, F., Dransfeld, A., Becker, A., & Erb, T. J. (2019). Design and control of extrachromosomal elements in *Methylorubrum extorquens* AM1. *ACS Synthetic Biology*, *8*(11), 2451–2456. https://doi.org/10.1021/acssynbio.9b00220

Chen, A. Y., & Lan, E. I. (2020). Chemical production from methanol using natural and synthetic methylotrophs. *Biotechnology Journal*, *15*(6), 1900356. https://doi.org/10.1002/biot.201900356

Higuchi, R., Fockler, C., Dollinger, G., & Watson, R. (1993). Kinetic PCR analysis: Real-time monitoring of DNA amplification reactions. *Nature Biotechnology*, *11*(9), 1026–1030. https://doi.org/10.1038/nbt0993-1026

Hu, B., & Lidstrom, M. E. (2014). Metabolic engineering of *Methylobacterium extorquens* AM1 for 1-butanol production. *Biotechnology for Biofuels*, *7*(1), 156. https://doi.org/10.1186/s13068-014-0156-0

Kiefer, P., Buchhaupt, M., Christen, P., Kaup, B., Schrader, J., & Vorholt, J. A. (2009). Metabolite profiling uncovers plasmid-induced cobalt limitation under methylotrophic growth conditions. *PLoS One*, *4*(11), e7831. https://doi.org/10.1371/journal.pone.0007831

Kovach, M. E., Elzer, P. H., Steven Hill, D., Robertson, G. T., Farris, M. A., Roop, R. M., & Peterson, K. M. (1995). Four new derivatives of the broad-host-range cloning vector pBBR1MCS, carrying different antibiotic-resistance cassettes. *Gene*, *166*(1), 175–176. https://doi.org/10.1016/0378-1119(95)00584-1

Kovach, M. E., Phillips, R. W., Elzer, P. H., Roop, R. M., & Peterson, K. M. (1994). pBBR1MCS: A broad-host-range cloning vector. *Biotechniques*, *16*(5), 800–802. http://www.ncbi.nlm.nih.gov/pubmed/8068328

Liang, W. F., Cui, L. Y., Cui, J. Y., Yu, K. W., Yang, S., Wang, T. M., Guan, C. G., Zhang, C., & Xing, X. H. (2017). Biosensor-assisted transcriptional regulator engineering for *Methylobacterium extorquens* AM1 to improve mevalonate synthesis by increasing the acetyl-CoA supply. *Metabolic Engineering*, *39*(2016), 159–168. https://doi.org/10.1016/j.ymben.2016.11.010

Lim, C. K., Villada, J. C., Chalifour, A., Duran, M. F., Lu, H., & Lee, P. (2019). Designing and engineering *Methylorubrum extorquens* AM1 for

itaconic acid production. *Frontiers in Microbiology*, *10*, 1027. https://doi.org/10.3389/fmicb.2019.01027

Marx, C. J., & Lidstrom, M. E. (2001). Development of improved versatile broad-host-range vectors for use in methylotrophs and other gram-negative bacteria. *Microbiology*, *147*(8), 2065–2075. https://doi.org/10.1099/00221287-147-8-2065

Mi, J., Becher, D., Lubuta, P., Dany, S., Tusch, K., Schewe, H., Buchhaupt, M., & Schrader, J. (2014). De novo production of the monoterpenoid geranic acid by metabolically engineered *Pseudomonas putida*. *Microbial Cell Factories*, *13*, 170(1). https://doi.org/10.1186/S12934-014-0170-8

Mi, J., Sydow, A., Schempp, F., Becher, D., Schewe, H., Schrader, J., & Buchhaupt, M. (2016). Investigation of plasmid-induced growth defect in *Pseudomonas putida*. *Journal of Biotechnology*, *231*, 167–173. https://doi.org/10.1016/J.JBIOTEC.2016.06.001

Novick, R. P. (1987). Plasmid incompatibility. *Microbiological Reviews*, *51*(4), 381–395.

Ochsner, A. M., Sonntag, F., Buchhaupt, M., Schrader, J., & Vorholt, J. A. (2014). *Methylobacterium extorquens*: Methylotrophy and biotechnological applications. *Applied Microbiology and Biotechnology*, *99*(2), 517–534. https://doi.org/10.1007/s00253-014-6240-3

Peel, D., & Quayle, J. (1961). Microbial growth on C1 compounds. 1. isolation and characterization of *pseudomonas* AM 1. *Biochemical Journal*, *81*(3), 465–469. https://doi.org/10.1042/bj0810465

Peyraud, R., Kiefer, P., Christen, P., Massou, S., Portais, J.-C., & Vorholt, J. A. (2009). Demonstration of the ethylmalonyl-CoA pathway by using 13C metabolomics. *Proceedings of the National Academy of Sciences*, *106*(12), 4846–4851. https://doi.org/10.1073/pnas.0810932106

Pfaffl, M. W. (2004). Quantification strategies in real-time PCR. In S. A. Bustin (Ed.), *A-Z of quantitative PCR* (pp. 87–112). International University Line.

Rasmussen, R. (2001). Quantification on the LightCycler. In S. Meuer, C. Wittwer, & K. I. Nakagawara (Eds.), *Rapid cycle real-time PCR* (pp. 21–34). Springer Berlin Heidelberg.

Schada von Borzyskowski, L., Sonntag, F., Pöschel, L., Vorholt, J. A., Schrader, J., Erb, T. J., & Buchhaupt, M. (2018). Replacing the ethylmalonyl-CoA pathway with the glyoxylate shunt provides metabolic flexibility in the central carbon metabolism of *Methylobacterium extorquens* AM1. *ACS Synthetic Biology*, *7*(1), 86–97. https://doi.org/10.1021/acssynbio.7b00229

del Solar, G., Giraldo, R., Ruiz-Echevarría, M, Espinosa, M., & Díaz-Orejas, R. (1998). Replication and control of circular bacterial plasmids. *Microbiology and Molecular Biology Reviews*, *62*(2), 434–464. https://doi.org/10.1128/MMBR.62.2.434-464.1998

Sonntag, F., Buchhaupt, M., & Schrader, J. (2014). Thioesterases for ethylmalonyl–CoA pathway derived dicarboxylic acid production in *Methylobacterium extorquens* AM1. *Applied Microbiology and Biotechnology*, *98*(10), 4533–4544. https://doi.org/10.1007/s00253-013-5456-y

Sonntag, F., Kroner, C., Lubuta, P., Peyraud, R., Horst, A., Buchhaupt, M., & Schrader, J. (2015). Engineering *Methylobacterium extorquens* for de novo synthesis of the sesquiterpenoid α-humulene from methanol. *Metabolic Engineering*, *32*, 82–94. https://doi.org/10.1016/j.ymben.2015.09.004

Sonntag, F., Müller, J. E. N., Kiefer, P., Vorholt, J. A., Schrader, J., & Buchhaupt, M. (2015). High-level production of ethylmalonyl-CoA pathway-derived dicarboxylic acids by *Methylobacterium extorquens* under cobalt-deficient conditions and by poly-hydroxybutyrate negative strains. *Applied Microbiology and Biotechnology*, *99*(8), 3407–3419. https://doi.org/10.1007/s00253-015-6418-3

Tao, L., Jackson, R. E., & Cheng, Q. (2005). Directed evolution of copy number of a broad host range plasmid for metabolic engineering. *Metabolic Engineering*, *7*(1), 10–17. https://doi.org/10.1016/j.ymben.2004.05.006

Toyama, H., Anthony, C., & Lidstrom, M. E. (1998). Construction of insertion and deletion mxa mutants of *Methylobacterium extorquens* AM1 by electroporation. *FEMS Microbiology Letters*, *166*(1), 1–7. https://doi.org/10.1111/j.1574-6968.1998.tb13175.x

Vuilleumier, S., Chistoserdova, L., Lee, M.-C., Bringel, F., Lajus, A., Zhou, Y., Gourion, B., Barbe, V., Chang, J., Cruveiller, S., Dossat, C., Gillett, W., Gruffaz, C., Haugen, E., Hourcade, E., Levy, R., Mangenot, S., Muller, E., Nadalig, T., … Lidstrom M.E. (2009). *Methylobacterium* genome sequences: A reference blueprint to investigate microbial metabolism of C1 compounds from natural and industrial sources. *PLoS One*, *4*(5), e5584. https://doi.org/10.1371/journal.pone.0005584

Wadood, A., Dohmoto, M., Sugiura, S., & Yamaguchi, K. (1997). Characterization of copy number mutants of plasmid pSC101. *The Journal of General and Applied Microbiology*, *43*, 309–316.

Yang, Y.-M., Chen, W.-J., Yang, J., Zhou, Y.-M., Hu, B., Zhang, M., Zhu, L.-P., Wang, G.-Y., & Yang, S. (2017). Production of 3-hydroxypropionic acid in engineered *Methylobacterium extorquens* AM1 and its reassimilation through a reductive route. *Microbial Cell Factories*, *16*(1), 179. https://doi.org/10.1186/s12934-017-0798-2

Zhang, M., Yuan, X., Zhang, C., Zhu, L., Mo, X., Chen, W., & Yang, S. (2019). Bioconversion of methanol into value-added chemicals in native and synthetic methylotrophs. *Current Issues in Molecular Biology*, *33*, 225–236. https://doi.org/10.21775/cimb.033.225

How to cite this article: Pöschel, L., Gehr, E., & Buchhaupt, M. (2022). A pBBR1-based vector with IncP group plasmid compatibility for *Methylorubrum extorquens*. *MicrobiologyOpen*, 11, e1325. https://doi.org/10.1002/mbo3.1325

APPENDIX

FIGURE A1 Effect of variation of kanamycin concentration on the growth of *Methylorubrum extorquens* AM1 pCM80/pMis1_1B_P_{mxaF}_*mCherry* cotransformants. The maximal mCherry fluorescence signal is a measure of pMis1_1B_P_{mxaF}_*mCherry* abundance, while the maximal slope of the scattered light signal is an indicator of growth rate. Three independent biological replicates were measured; standard deviations are indicated by error bars.

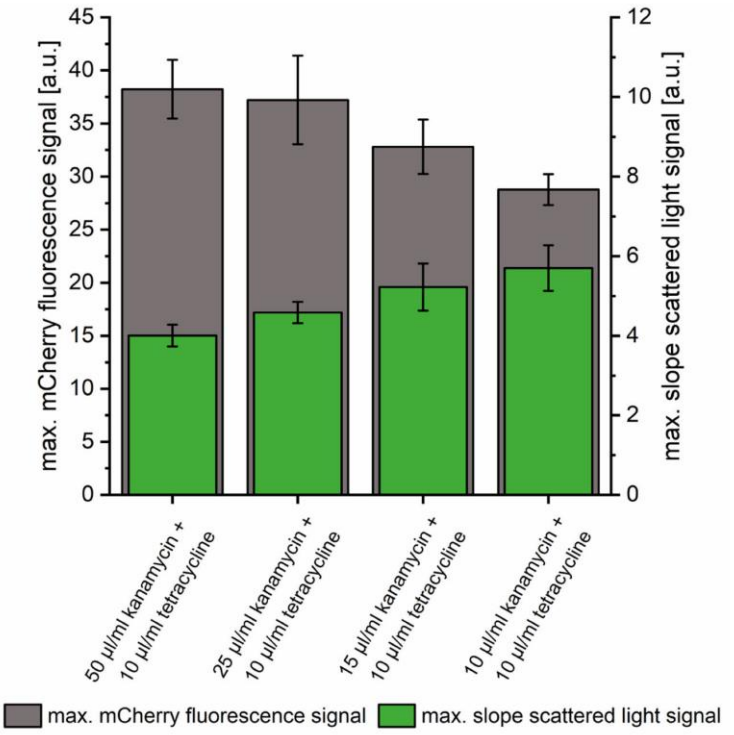

FIGURE A2 Comparison of scattered light measurements of *Methylorubrum extorquens* AM1 cotransformants containing pCM80 combined with either pMis1_1B or pMis1_1B_P_{mxaF}_*mCherry*. Measurements of biological triplicates are shown.

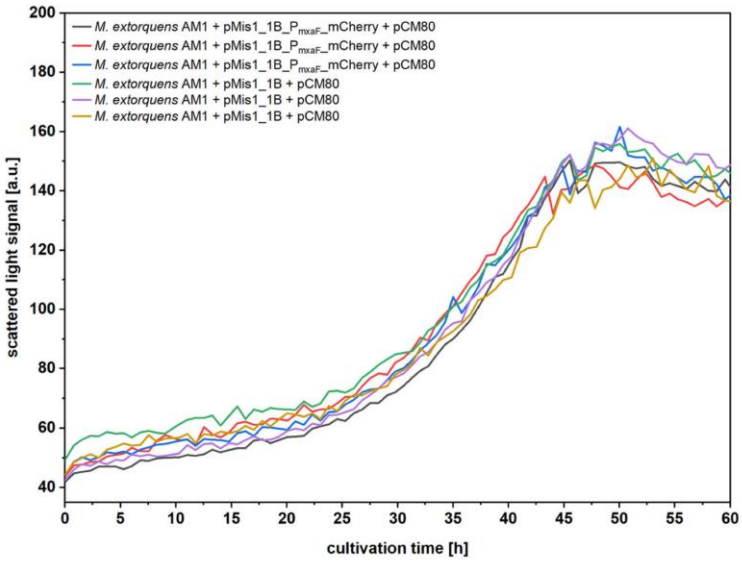

6.4 Expression of toxic genes in *Methylorubrum extorquens* with a tightly repressed, cumate-inducible promoter

Declaration of author contributions to the manuscript:

Expression of toxic genes in *Methylorubrum extorquens* with a tightly repressed, cumate-inducible promoter

Status: submitted

Contributing authors: Laura Pöschel (LP), Elisabeth Gehr (EG), Paulina Jordan (PJ), Frank Sonntag (FS), Markus Buchhaupt (MB)

What are the contributions of the doctoral candidate and his co-authors?

(1) Concept and design

Doctoral candidate:	30%
Co-author EG:	20%
Co-author PJ:	10 %
Co-author FS:	10 %
Co-author MB:	30 %

(2) Conducting tests and experiments

Doctoral candidate:	30 %	Characterization of promotor P_{s6}
Co-author EG:	30 %	Isolation of suppressor mutants and respective plasmids, terpenoid production experiments, characterization of promotor P_{s6}
Co-author PJ:	30 %	Isolation of suppressor mutants and respective plasmids, terpenoid production experiments
Co-author FS:	10 %	Terpenoid production experiments

(3) Compilation of data sets and figures

Doctoral candidate:	90 %	Data collection, preparation of figures and tables
Co-author EG:	5 %	Data collection, preparation of figures
Co-author MB:	5 %	Preparation of figures

(4) Analysis and interpretation of data

Doctoral candidate:	50 %	Analysis and interpretation of data
Co-author EG:	10 %	Analysis of data
Co-author PJ:	10 %	Analysis of data
Co-author FS:	10 %	Analysis of data
Co-author MB:	20 %	Analysis and interpretation of data

(5) Drafting of manuscript

Doctoral candidate:	90 %
Co-author MB:	10 %

Expression of toxic genes in *Methylorubrum extorquens* with a tightly repressed, cumate-inducible promoter

Laura Pöschel[1,2], Elisabeth Gehr[1], Paulina Jordan[1], Frank Sonntag[1], Markus Buchhaupt[1]*

[1] DECHEMA-Forschungsinstitut, Microbial Biotechnology, Theodor-Heuss-Allee 25, 60486 Frankfurt am Main, Germany

[2] Faculty of Biological Sciences, Goethe University Frankfurt, Max-von-Laue-Str. 9, 60438 Frankfurt am Main, Germany

*Corresponding author,

e-mail address: markus.buchhaupt@dechema.de

ORCID

Laura Pöschel: 0000-0002-8892-3998

Markus Buchhaupt: 0000-0003-2720-5973

Abstract

Methylorubrum extorquens is an important model methylotroph and has enormous potential for the development of C1-based microbial cell factories. During strain construction, regulated promoters with a low background expression level are important genetic tools for expression of potentially toxic genes. Here we present an accordingly optimised promoter, which can be used for that purpose. During construction and testing of terpene production strains harbouring a recombinant mevalonate pathway, strong growth defects were observed which made strain development impossible. After isolation and characterisation of suppressor mutants, we discovered a variant of the cumate-inducible promoter P_{Q2148} used in this approach. Deletion of 28 nucleotides resulted in an extremely low background expression level, but also reduced the maximal expression strength by about 30 %. This tightly repressed promoter version is a powerful module for controlled expression of potentially toxic genes in *M. extorquens*.

Keywords

Inducible Promoter

Methylorubrum extorquens AM1

Alphaproteobacteria

Cumate

Background expression

Acknowledgment

This study was funded by the German Federal Ministry of Education and Research (BMBF) in the project ChiraMet (FKZ 031B0340A).

We thank J. A. Vorholt for providing us with plasmid pQ2148. We further thank T. J. Erb for providing us with pTE105_mCherry.

Introduction

Methylotrophs are organisms which use reduced one carbon compounds as sole carbon and energy source. *Methylorubrum extorquens* AM1 serves as model organism for bacterial methylotrophy research since its isolation in 1961 (Peel and Quayle 1961). Furthermore, the organism has gained importance in recent years as a platform organism for C1-biotechnology. Hence, several production routes for bulk and fine chemicals as 1-butanol, 3-hydroxypropionic acid, dicarboxylic acids, mevalonate and α-humulene have been described (Sonntag et al. 2014, 2015a, b; Hu and Lidstrom 2014; Liang et al. 2017; Yang et al. 2017; Schada von Borzyskowski et al. 2018; Lim et al. 2019). Nevertheless, the full potential of *M. extorquens* AM1 as a production platform has not yet been reached (Ochsner et al. 2015). The implementation of new synthetic production routes requires a broad set of molecular tools for DNA introduction, genome manipulation and recombinant gene expression. For many years, only P_{mxaF}-based expression vectors were used for gene overexpression in *M. extorquens* AM1 (Marx and Lidstrom 2001). The *mxaF* gene, encoding the methanol dehydrogenase in *M. extorquens*, is highly expressed during methylotrophic growth (Liu et al. 2006) and P_{mxaF} is among the strongest known native promoters of *M. extorquens* (Choi et al. 2006). Besides P_{mxaF}, a variety of synthetic constitutive promoters with different expression strengths have been described (Schada von Borzyskowski et al. 2015). Yet, constitutive expression is not always useful during construction of highly efficient production strains. Inducible and adjustable expression can be necessary to separate growth and production phases or to express toxic genetic constructs. Different inducible promoters with the possibility of tuning the expression level have been described for *M. extorquens* (Choi et al. 2006; Chubiz et al. 2013; Kaczmarczyk et al. 2013; Carrillo et al. 2019; Sathesh-Prabu et al. 2021). In two of the developments, expression levels comparable to or even exceeding those of P_{mxaF} were achieved (Carrillo et al. 2019; Sathesh-Prabu et al. 2021). However, the development of promoters which are suitable for fine-tuned low expression of toxic genes in *M. extorquens* AM1, has not been the subject of studies so far.

In this study, we report on the use of inducible promoters for expression of a gene cluster for *cis*-abienol production in *M. extorquens* AM1. The organism has been described to be especially suited for production of terpenoids via the mevalonic acid (MVA) pathway due to the occurrence of the MVA pathway starting intermediate acetoacetyl-CoA in its primary metabolism (Sonntag et al. 2015a). While in this publication the sesquiterpene α-humulene was the target product, we now aimed at construction of a strain able to synthesise the diterpene alcohol *cis*-abienol. This compound serves as a valuable bioproduct material for the fragrance industry. For production of *cis*-abienol with *M. extorquens* AM1 we planned on using P_{Q5} derivative P_{Q2148} (Kaczmarczyk et al. 2013). The original cumate-inducible promoter system P_{Q5} was designed for expression in *Sphingomonas* species (Kaczmarczyk et al. 2013). For this synthetic promoter, P_{syn2} was combined with control elements of the *Pseudomonas putida* F1 *cym/cmt* system to make it responsive to cumate induction (Eaton 1997; Kaczmarczyk et al. 2013). In the original study, P_{syn2} -32 and -10 regions were exchanged with *M. extorquens* specific sequences. This yielded in P_{Q2148}, that can be used to drive gene expression in *M. extorquens.* Surprisingly, in our study P_{Q2148} was not tight enough for using it with the *cis*-abienol synthesis gene cluster and caused strong growth inhibition. Hence, we present P_{Q2148}-derivative P_{s6}, which is tightly repressible and whose activity is tuneable with different inducer concentrations. With this optimised promoter, we expand the genetic toolkit of *M. extorquens* to promote its use as platform organism for C1 biotechnology.

Results and discussion

Terpene production with P_{Q2148}-based plasmids

Inducible expression of toxic genes or pathways with toxic intermediates can be essential during the implementation of novel production routes. For instance, previous studies have shown that it is beneficial for terpene production in *M. extorquens* AM1 to increase IPP supply as a metabolic substrate of FPP synthases (Sonntag et al. 2015a). Thereby, constitutive expression of the heterologous MVA pathway had a lethal effect on the cells, and no transformants carrying the corresponding expression plasmid could be isolated in the named study. To overcome this problem, the authors chose the cumate-inducible expression plasmid pQ2148. Although transformation of the construct was successful and product concentrations of the product α-humulene could be increased, the cells still showed a growth defect in the absence of the inducer, which indicates a certain leakiness of the P_{Q2148} promoter (Sonntag et al. 2015a).

When we attempted to replicate the experiments of the corresponding study (Sonntag et al. 2015a), the amount of α-humulene production surprisingly varied strongly between the different pFS62b-transformants of the AM1 strain (Figure 1). These strong differences in productivity might be the result of toxic effects of the terpene production gene cluster, which probably caused a strong selection pressure against high carbon flux through the pathway. A non-induced control strain produced 8.7 % of the α-humulene titer from the original study (Sonntag et al. 2015a). Another clone showed the same level of production even when induced, probably due to early occurrence of a suppressor mutation. These results indicated that the MVA pathway-encoding plasmid pFS62b exerts some toxic effect on the host strain in the absence of the inducing agent cumate.

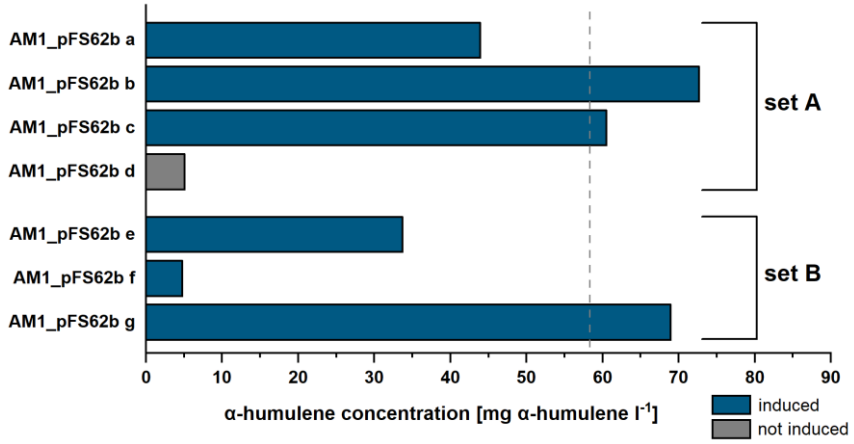

Fig. 1 Two datasets (set A and set B) demonstrating α-humulene production with *M. extorquens* AM1 + pFS62b. Different clones, designated a-g, were used in the experiment. All cultures except the one using clone d were induced with 100 µM cumate. The dashed line marks the previously observed product concentration of 58 mg α-humulene l^{-1} reported by Sonntag et al. (2015a)

These effects became even more evident during an approach to further broaden the terpene product spectrum of *M. extorquens* AM1. The introduction of a *cis*-abienol synthesis operon on plasmid ppjo16 resulted in a very poor transformation efficiency. After transformation of 400 ng of plasmid DNA and six days of incubation, only two colonies appeared on agar plates with medium containing tetracycline, but no cumate, whereas a control transformation of vector pQ2148F yielded over 3000 colonies. This low transformation efficiency rate and the fact that some small colonies appeared on the transformation plates after eight days of incubation led us to the conclusion that the promoter P_{Q2148F} does not tightly regulate the expression of the obviously toxic *cis*-abienol synthesis operon. Striking out some of the small colonies on a new agar plate resulted in the formation of faster growing strains, which probably contained suppressor mutations and were isolated.

Investigation of suppressor mutants

In order to gain knowledge about the underlying cause for growth inhibition mediated by the plasmid ppjo16, the suppressor mutants were thoroughly analysed. First, their sensitivity towards fosmidomycin was tested. Fosmidomycin inhibits the DXP pathway (Shigi 1989; Jomaa et al. 1999), which represents the native terpenoid biosynthesis route of *M. extorquens*. Since IPP and DMAPP supply is crucial for growth of the cells, the suppressor clones were tested for a functional, alternative mevalonate pathway with this assay (Figure 2A). To further characterise the suppressor mutants, terpene production yields were determined (Figure 2A), the respective plasmids were isolated and the genes encoding the *cis*-abienol production pathway were sequenced (Figure 2B). As positive control, an *M. extorquens* AM1 strain harbouring the α-humulene synthesis plasmid pFS62b was used.

The two suppressor mutants unable to grow on fosmidomycin and to produce *cis*-abienol (AM1_ppjo16s1 and AM1_ppjo16s4) were probably able to overcome the plasmid-imposed toxicity by deletion of MVA pathway genes. Additionally, the *cis*-abienol synthase gene *AbCAS* and GGPP synthase gene *ERG20F96C* were partly or completely deleted on the respective plasmids, leading to the inability to produce *cis*-abienol. Only three of the suppressor strains tested were resistant to fosmidomycin, namely AM1_ppjo16L1, AM1_ppjo16s3 and AM1_ppjo16s6. In AM1_ppjo16L1 *AbCAS* and *ERG20F96C* were partly deleted and no *cis*-abienol production was detectable for the respective strain. As the deletion can also affect mRNA stability or translation efficiency of the MVA pathway genes, reduction of MVA pathway flux might be the suppression mechanism also in this mutant. This assumption is supported by the fact that *cis*-abienol itself was found to be not toxic for *M. extorquens* AM1 (Figure S1, Online Resource 1). No plasmid could be isolated from strain AM1_ppjo16s3, so we assume that genomic integration of the entire gene cluster or at least of genes indispensable for *cis*-abienol production has occurred. AM1_ppjo16s6 in fact was able to produce 5.3 mg *cis*-abienol l^{-1} and was resistant to fosmidomycin. The isolated plasmid showed no mutations in any of the genes necessary for *cis*-abienol production or the MVA pathway-encoding genes.

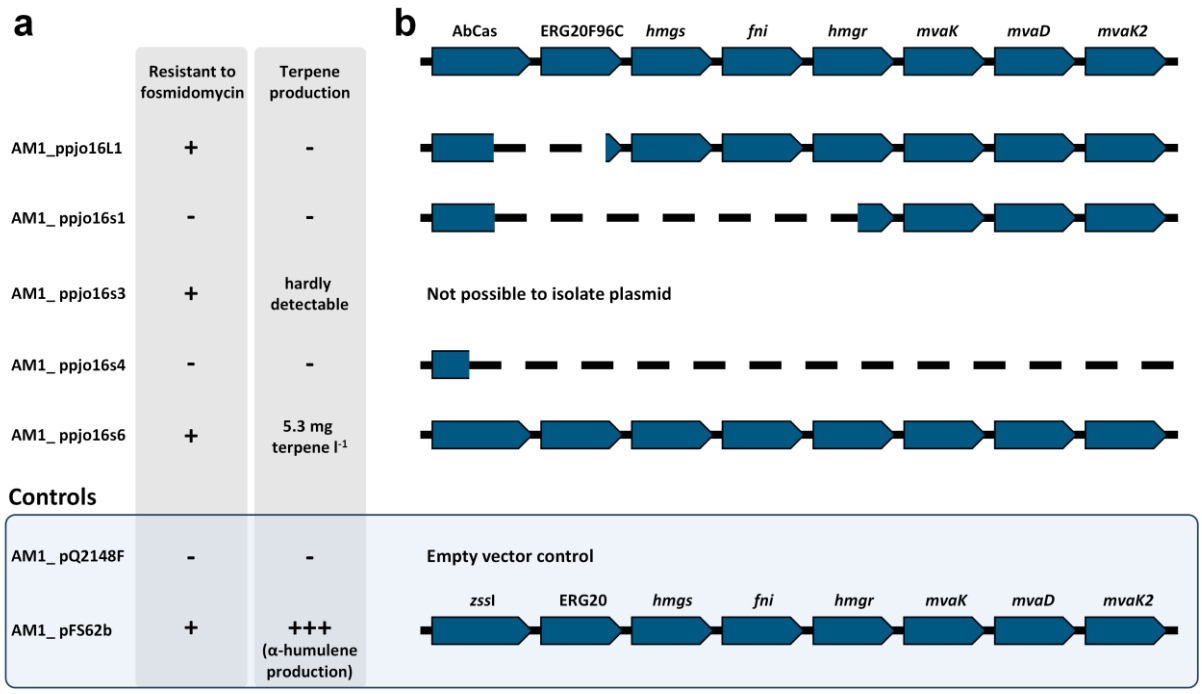

155

156 **Fig. 2** Phenotypes and genotypes of suppressor strains. **a**) Phenotypes of suppressor strains
157 regarding fosmidomycin resistance and terpene production. **b**) Schematic sequence of terpene
158 synthesis gene cluster (*cis*-abienol synthase gene *AbCAS* and GGPP synthase gene
159 *ERG20F96C*) and MVA gene cluster on plasmid ppjo16 and positions of deletions observed in
160 the plasmid sequences isolated from suppressor mutants

161

162 The original cumate-dependent promoter system P_{Q2148} was already used for inducible gene
163 expression in *M. extorquens* (Kaczmarczyk et al. 2013). In our experiments, expression of the
164 genes encoding the toxic *cis*-abienol production pathway was not tightly repressed by CymR,
165 which is supposed to bind to CuO operator sites as long as no cumate is present.
166 AM1_ppjo16s6 overcame the toxicity of the plasmid while harbouring an intact synthesis
167 operon (Figure 2B). Sequencing the upstream region of the gene cluster on ppjo16s6 revealed
168 a deletion of 28 nucleotides in the promoter region (Figure 3). This promoter variant (henceforth
169 P_{s6}) lacks parts of the $P_{bla\text{-}mut1T}$ -35 and the adjacent CuO operator sequence. This modification

probably leads to higher expression of the CymR repressor protein or enhanced binding efficiency to the repressor site.

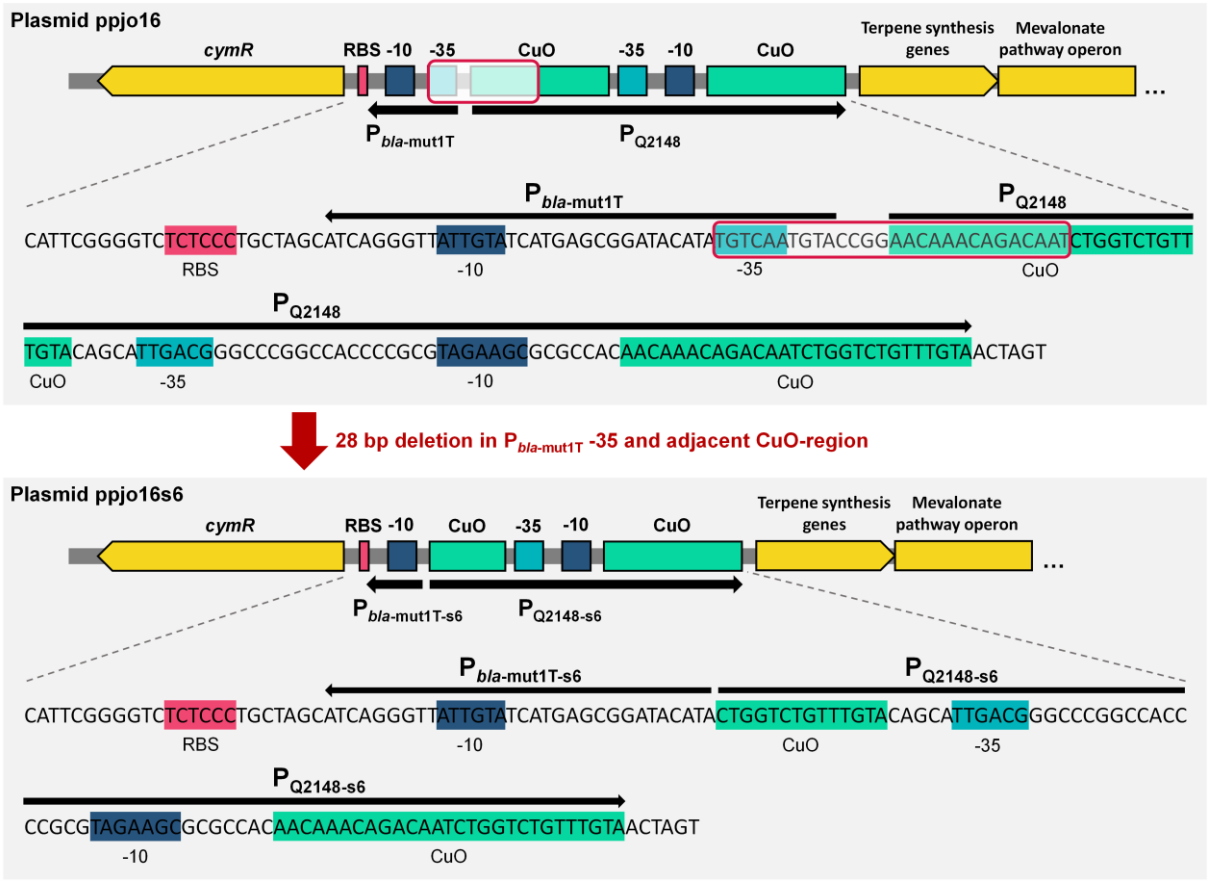

Fig. 3 Schematic illustration of *cymR*, the two promoter regions ($P_{bla\text{-}mut2T1}$ and P_{Q2148}) and the terpene synthesis genes on ppjo16 and ppjo16s6. Sequences of coding DNA strands are given in detail for promoter regions. Important features are marked with coloured boxes. $P_{bla\text{-}mut2T1}$ and P_{Q2148} are indicated by arrows. In ppjo16s6, 28 nucleotides within $P_{bla\text{-}mut2T1}$ and the close operator region (CuO) in P_{Q2148} are deleted, yielding $P_{bla\text{-}mut2T1\text{-}s6}$ and $P_{Q2148\text{-}s6}$, in this study collectively referred to as P_{s6}

Characterisation of P_{s6}

To further characterise P_{s6}, we conducted reporter assays with different cumate concentrations. Therefore, we designed mCherry-reporter constructs pQ2148_mCherry and pQ2148-s6_mCherry and monitored fluorescence of respective *M. extorquens* AM1 transformants in a microbioreactor system. The cumate concentrations we used (up to 150 µM) did not affect cell growth (Figure 4). A high mCherry signal was already detectable at the begin of cultivation of AM1_pQ2148_mCherry and showed a linear increase in strength even before induction with cumate (Figure 4A). This confirms that P_{Q2148} in its original confirmation is not as tight as assumed. Induction at 3 µM cumate did not affect fluorescence. Addition of higher inducer levels resulted in induction, although a tuneability with different cumate concentrations was not distinctly evident. In comparison, when investigating AM1_pQ2148-s6_mCherry, the initial fluorescence signal was 5-fold lower (Figure 4B). The signal remained nearly stable until induction (at t_0: 0.38 ± 0.01; at t_{i-1}: 0.45 ± 0.1) and did quickly respond to cumate addition, while tunability was evident. With addition of the highest tested cumate concentration of 150 µM a 40-fold enhanced signal (determined at t_{max} = 33.2 h) compared to the non-induced control could be reached. Moreover, the maximum mCherry fluorescence signal at this high inducer concentration was 54-fold higher (t_{max} = 33.2 h) than immediately before induction (t_{i-1} = 18.3 h).

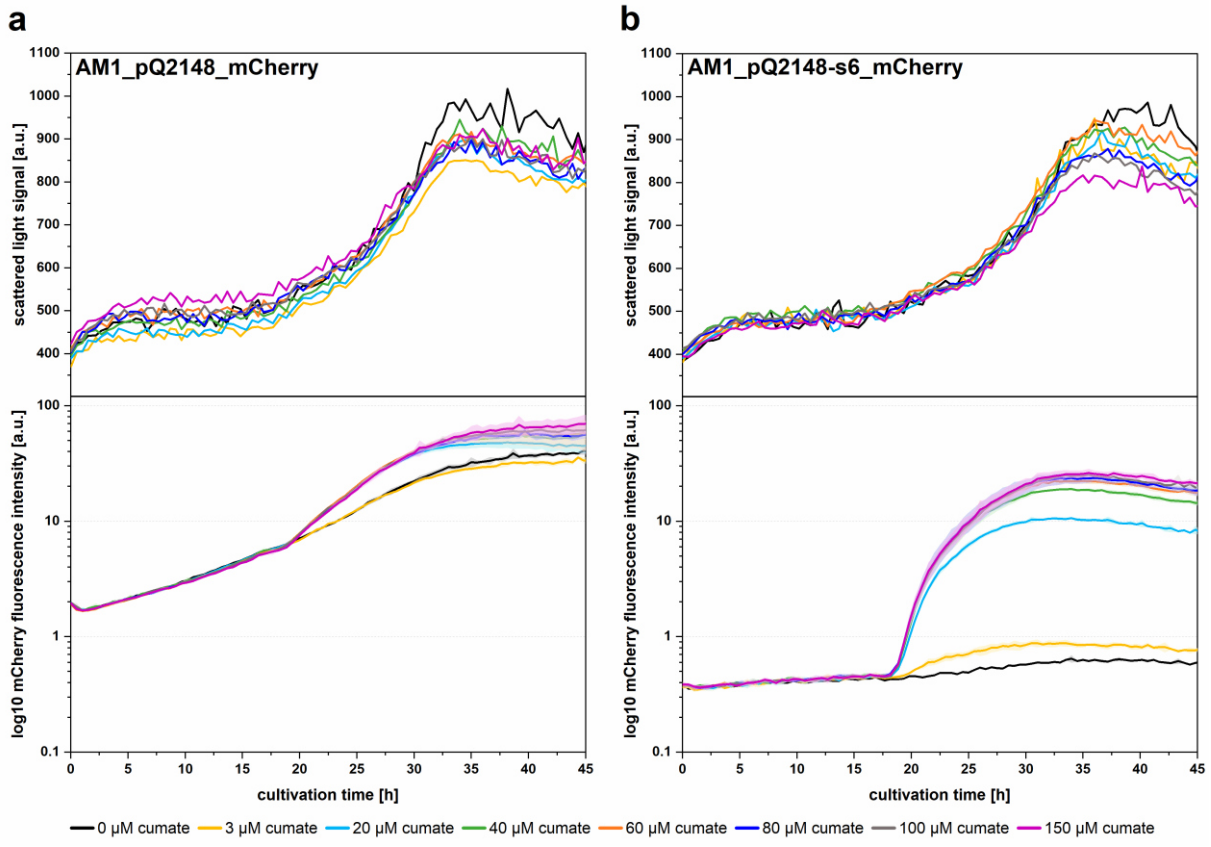

198

199 **Fig. 4** Promoter study of cumate inducible promoter on plasmid pQ2148_mCherry (**a**) and
200 pQ2148_mCherry-s6 (modified promoter P_{s6}) (**b**) in a microbioreactor system. *M. extorquens*
201 AM1 cultures containing respective plasmids were induced with cumate after 17.5 h in early
202 exponential growth phase. Top graphs represent cell density measured via scattered light
203 signal at 700 nm, bottom graphs represent mCherry fluorescence signal. Shown datasets are
204 representative for three independent experimental replicates

205

206 P_{Q2148} was shown to be tight and inducible in *M. extorquens* AM1 in previous studies
207 (Kaczmarczyk et al. 2013). Our reporter plasmids carried a different reporter gene, a different
208 selection marker (Tc^r instead of Km^r) and a different linker sequence between promoter and
209 reporter gene due to distinct genesis of the constructs. To validate our observations made with
210 P_{Q2148} and to assure that the sequence differences in the inter-promoter-gene region did not
211 change promoter characteristics, we constructed plasmids pQ2148L_mCherry and pQ2148L-
212 s6_mCherry with the according linker sequence (Figure 5A). The monitored mCherry

fluorescence signals for the new constructs were nearly identical to the previous results. Whereas P_{Q2148} on pQ2148L_mCherry was leaky and promoted mCherry expression even before induction (Figure 5B), P_{s6} on pQ2148L-s6_mCherry repressed expression without inducer and exhibited quick response to cumate addition with induction at various levels (Figure 5C).

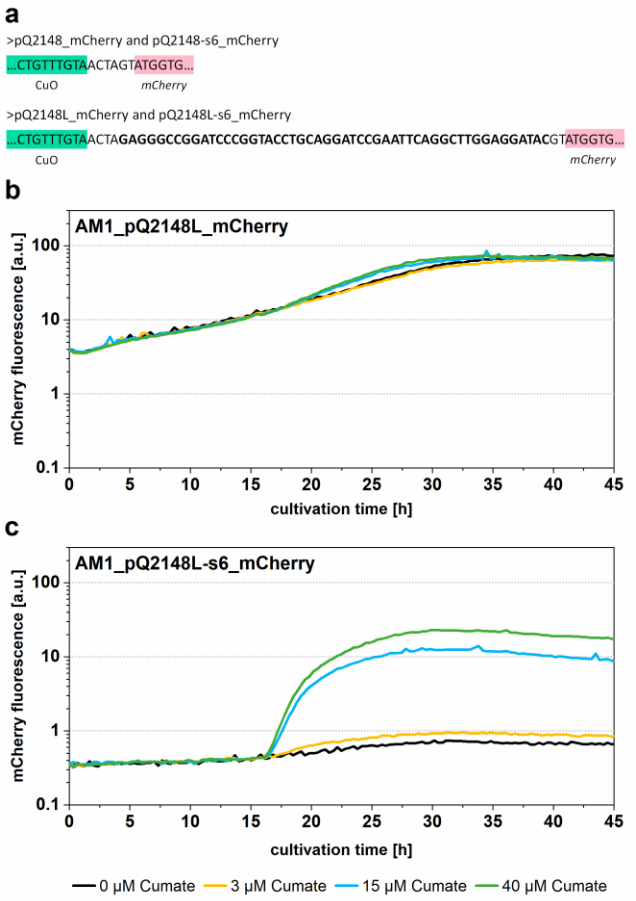

Fig. 5 Investigation of P_{s6} promoter variant with the originally described linker region between promoter and controlled gene. **a**) Linker region from P_{Q2148}-*luxCDABE* (Kaczmarczyk et al. 2013), that was introduced in pQ2148_mCherry and pQ2148-s6_mCherry to yield pQ2148L_mCherry and pQ2148L-s6_mCherry, respectively. Introduced nucleotides are in bold. **b**) and **c**) Fluorescence study of cumate inducible promoter from plasmid pQ2148L_mCherry (**b**) and pQ2148L_mCherry-s6 (modified promoter P_{s6}) (**c**) in a microbioreactor system. Cultures were induced with cumate after 15.5 h in early exponential

growth phase. Shown datasets are representative for three independent experimental replicates. Growth was monitored with scattered light signal at 620 nm (data not shown)

In either version of the reporter gene constructs, the overall mCherry expression driven by the P_{s6} promoter was considerably lower than with P_{Q2148} (~30 % of the maximal pQ2148 expression strength). Testing P_{s6} in α-humulene synthesis plasmid led to similar results. Production experiments with the according construct pFS62b-s6 only yielded 28 ± 4 mg α-humulene l^{-1} (three replicates), which is a lower titer compared to experiments with the original plasmid pFS62b. Nevertheless, in the case of *cis*-abienol production, this property of P_{s6} was highly beneficial. The avoidance of pathway-encoding operon expression under non-induced conditions only enabled plasmid transformation and strain cultivation without strong selection for terpene synthesis pathway destruction. P_{s6} furthermore allowed production of *cis*-abienol and will facilitate metabolic engineering approaches towards a more balanced pathway.

Conclusion

Here, we provide P_{s6}, a modified version of the P_{Q2148} promoter (Kaczmarczyk et al. 2013) for cumate inducible gene expression in *M. extorquens*. While P_{s6} is less efficient with regard to strong overexpression, it is a powerful tool for controlled expression of potentially toxic genes or pathways. We successfully demonstrated its application for the development of a *cis*-abienol production strain. Confirmatively, reporter experiments detected essentially no background expression for uninduced constructs. This property makes P_{s6} a valuable addition to the emerging genetic toolbox for *M. extorquens*.

Material and methods

Bacterial strains and growth conditions

Escherichia coli DH5α (Gibco-BRL, Rockville, USA) was used for cloning and amplification of all plasmids. *E. coli* cultures were grown in LB medium (Bertani 1951) at 37 °C. Liquid minimal medium for *M. extorquens* AM1 (Peel and Quayle 1961) was prepared using 123 mM methanol as previously described (Peyraud et al. 2009) with a $CoCl_2$ concentration of 12.6 µM (Kiefer et al. 2009; Sonntag et al. 2014). For preparation of solid growth medium, 1.5 % [w/v] agar-agar was added. If necessary, tetracycline was added at a concentration of 10 µg tetracycline hydrochloride ml^{-1} for both *E. coli* and *M. extorquens* AM1 cultures. For cultivation of *M. extorquens* AM1, precultures were grown in test tubes for 48 h at 30 °C and main cultures were subsequently inoculated to an OD_{600} of 0.1. If not stated differently, gene expression was induced after 16 h of cultivation by cumate addition. Cumate (4-isopropylbenzoic acid) was prepared as a 100 mM stock solution in ethanol and diluted prior to use. Fosmidomycin sensitivity of suppressor mutants was tested by striking out cells on solid medium containing 20 mg fosmidomycin l^{-1}. All chemicals used for media preparation were purchased from Carl Roth (Karlsruhe, Germany) or Merck KGaA (Darmstadt, Germany).

Plasmid construction

All standard cloning procedures were performed in *E. coli* DH5α. Plasmids (see Table S1, Online Resource 1) were constructed as follows. For ppjo16, *cis*-abienol synthase gene *AbCAS* (Zerbe et al. 2012) and GGPP synthase gene *ERG20F96C* (Ignea et al. 2015) were codon optimised and a new RBS sequence was calculated (Salis 2011) and inserted. For the detailed sequence information of genes see international patent WO 2016/142503 (Schrader et al. 2016). Plasmids ppjo16s1, ppjo16s3, ppjo16s4, ppjo16s6 and ppjo16L1 were isolated from AM1_ppjo16 suppressor mutants. To construct pFS62b-s6, a fragment containing P_{s6} was subcloned from ppjo16s6 into pFS62b using NheI and SpeI restriction sites. Reporter

plasmids were constructed via Gibson assembly (Gibson et al. 2009): Assembly of PCR product of primers EGe119 and EGe121 on template pTE105_mCherry (Schada von Borzyskowski et al. 2015) and SpeI/EcoRI linearised backbone pQ2148F or ppjo16s6 yielded pQ2148_mCherry or pQ2148-s6_mCherry, respectively. pQ2148L_mCherry was constructed by assembly of PCR products of primers LPoe1 and LPoe2 on template pQ2148 and product of primers LPoe3 and LPoe4 on template pQ2148_mCherry. Accordingly, assembly of PCR products of primers LPoe6 and LPoe7 on template pQ2148_mCherry and product of primers LPoe5 and LPoe8 on template pQ2148_mCherry yielded pQ2148L-s6_mCherry. The sequences of final genetic constructs were confirmed by Sanger sequencing at Eurofins Scientific (Luxembourg, Luxembourg). All used oligonucleotides were purchased from Merck KGaA (Darmstadt, Germany) and are listed in Table S2 (Online Resource 1). PCRs were performed with Q5 Polymerase from NEB (Frankfurt, Germany) according to the manufacturer's instructions. Subsequently, PCR products were purified with the DNA Clean & Concentrator Kit from Zymo Research Europe (Freiburg, Germany). Transformation of final constructs in *M. extorquens* AM1 was performed as previously described (Toyama et al. 1998).

Terpene production and analysis

Terpenes produced by *M. extorquens* AM1 strains harbouring respective terpene synthesis plasmids, were extracted *in situ* with a dodecane overlay as described before (Sonntag et al. 2015a). The analysis of the extracted terpenes was performed on a GC-MS (GC17A with Q5050 mass spectrometer, Shimadzu, Kyoto, Japan) equipped with an Equity 5 column (Supelco, 30 m x 0.25 mm x 0.25 µM) as previously described (Sonntag et al. 2015a). For *cis*-abienol analysis the split ratio was reduced from 1:8 to 1:1 and the overall measuring time was prolonged to 17.5 minutes. Retention time for *cis*-abienol was 14.1 minutes. The *cis*-abienol analytical standard was purchased from Toronto Research Chemicals (Toronto, CA).

301 **Fluorescence assisted promoter studies**

302 For high-resolution measurements of growth curves and mCherry fluorescence signals, cells
303 were cultivated in a BioLector® microbioreactor system (m2p-labs GmbH, Baesweiler,
304 Germany). First, precultures of *M. extorquens* AM1 containing respective reporter plasmids
305 were grown in MeOH minimal medium with 10 µg tetracycline-hydrochloride ml^{-1} for 48 h at
306 30 °C. Subsequently, 1 ml of fresh medium was inoculated to an OD of 0.1 in 48-well
307 Flowerplates® in the microbioreactor and incubated at 30 °C, 1000 rpm and 85 % humidity.
308 The growth was monitored via scattered light signal intensity at 700 nm. The fluorescence
309 signal of mCherry was measured at 580/610 nm [ex/em]. Gene expression was induced by
310 adding 20 µL of cumate stock solutions (solved in ethanol, the final ethanol concentration in
311 the medium was 51 mM).

312

313 **Supplementary tables and figures (uploaded as Online Resource 1)**

314 **Table S1** Bacterial strains and plasmids used in this work

315 **Table S2** Oligonucleotides used in this study

316 **Figure S1** Tolerance of *M. extorquens* AM1 towards *cis*-abienol dissolved in aqueous phase

317 **References**

318 Bertani G (1951) Studies on Lysogenesis I. The Mode of Phage Liberation by Lysogenic
319 *Escherichia coli*. J Bacteriol 62:293–300. https://doi.org/10.1128/jb.62.3.293-300.1951

320 Carrillo M, Wagner M, Petit F, et al (2019) Design and Control of Extrachromosomal
321 Elements in *Methylorubrum extorquens* AM1. ACS Synth Biol 8:2451–2456.
322 https://doi.org/10.1021/acssynbio.9b00220

323 Choi YJ, Morel L, Bourque D, et al (2006) Bestowing Inducibility on the Cloned Methanol
324 Dehydrogenase Promoter (P_{mxaF}) of *Methylobacterium extorquens* by Applying
325 Regulatory Elements of *Pseudomonas putida* F1. Appl Environ Microbiol 72:7723–7729.
326 https://doi.org/10.1128/AEM.02002-06

327 Chubiz LM, Purswani J, Carroll SM, Marx CJ (2013) A novel pair of inducible expression
328 vectors for use in *Methylobacterium extorquens*. BMC Res Notes 6:1–8.
329 https://doi.org/10.1186/1756-0500-6-183

330 Eaton RW (1997) *p*-Cymene catabolic pathway in *Pseudomonas putida* F1: cloning and
331 characterization of DNA encoding conversion of *p*-cymene to *p*-cumate. J Bacteriol
332 179:3171–3180. https://doi.org/10.1128/jb.179.10.3171-3180.1997

333 Gibson DG, Young L, Chuang RY, et al (2009) Enzymatic assembly of DNA molecules up to
334 several hundred kilobases. Nat Methods 6:343–345.
335 https://doi.org/10.1038/NMETH.1318

336 Hu B, Lidstrom ME (2014) Metabolic engineering of *Methylobacterium extorquens* AM1 for 1-
337 butanol production. Biotechnol Biofuels 7:156. https://doi.org/10.1186/s13068-014-0156-
338 0

339 Ignea C, Trikka FA, Nikolaidis AK, et al (2015) Efficient diterpene production in yeast by
340 engineering Erg20p into a geranylgeranyl diphosphate synthase. Metab Eng 27:65–75.
341 https://doi.org/10.1016/j.ymben.2014.10.008

342 Jomaa H, Wiesner J, Sanderbrand S, et al (1999) Inhibitors of the Nonmevalonate Pathway
343 of Isoprenoid Biosynthesis as Antimalarial Drugs. Science (80-) 285:1573–1576.
344 https://doi.org/10.1126/science.285.5433.1573

345 Kaczmarczyk A, Vorholt JA, Francez-Charlot A (2013) Cumate-Inducible Gene Expression
346 System for Sphingomonads and Other *Alphaproteobacteria*. Appl Environ Microbiol
347 79:6795–6802. https://doi.org/10.1128/AEM.02296-13

348 Kiefer P, Buchhaupt M, Christen P, et al (2009) Metabolite Profiling Uncovers Plasmid-
349 Induced Cobalt Limitation under Methylotrophic Growth Conditions. PLOS ONE
350 4:e7831. https://doi.org/10.1371/journal.pone.0007831

351 Liang WF, Cui LY, Cui JY, et al (2017) Biosensor-assisted transcriptional regulator
352 engineering for *Methylobacterium extorquens* AM1 to improve mevalonate synthesis by
353 increasing the acetyl-CoA supply. Metab Eng 39:159–168.
354 https://doi.org/10.1016/j.ymben.2016.11.010

355 Lim CK, Villada JC, Chalifour A, et al (2019) Designing and Engineering *Methylorubrum*
356 *extorquens* AM1 for Itaconic Acid Production. Front Microbiol 10:1–14.
357 https://doi.org/10.3389/fmicb.2019.01027

358 Liu Q, Kirchhoff JR, Faehnle CR, et al (2006) A rapid method for the purification of methanol
359 dehydrogenase from *Methylobacterium extorquens*. Protein Expr Purif 46:316–320.
360 https://doi.org/10.1016/j.pep.2005.07.014

361 Marx CJ, Lidstrom ME (2001) Development of improved versatile broad-host-range vectors
362 for use in methylotrophs and other Gram-negative bacteria. Microbiology 147:2065–
363 2075. https://doi.org/10.1099/00221287-147-8-2065

364

Ochsner AM, Sonntag F, Buchhaupt M, et al (2015) *Methylobacterium extorquens*: methylotrophy and biotechnological applications. Appl Microbiol Biotechnol 99:517–534. https://doi.org/10.1007/s00253-014-6240-3

Peel D, Quayle JR (1961) Microbial growth on C_1 compounds. 1. Isolation and characterization of *Pseudomonas* AM 1. Biochem J 81:465–469. https://doi.org/10.1042/bj0810465

Peyraud R, Kiefer P, Christen P, et al (2009) Demonstration of the ethylmalonyl-CoA pathway by using ^{13}C metabolomics. Proc Natl Acad Sci U S A 106:4846–51. https://doi.org/10.1073/pnas.0810932106

Salis HM (2011) The ribosome binding site calculator. Methods Enzymol 498:19–42. https://doi.org/10.1016/B978-0-12-385120-8.00002-4

Sathesh-Prabu C, Ryu YS, Lee SK (2021) Levulinic Acid-Inducible and Tunable Gene Expression System for *Methylorubrum extorquens*. Front Bioeng Biotechnol 9:1–10. https://doi.org/10.3389/fbioe.2021.797020

Schada von Borzyskowski L, Remus-Emsermann M, Weishaupt R, et al (2015) A Set of Versatile Brick Vectors and Promoters for the Assembly, Expression, and Integration of Synthetic Operons in *Methylobacterium extorquens* AM1 and Other Alphaproteobacteria. ACS Synth Biol 4:430–443. https://doi.org/10.1021/sb500221v

Schada von Borzyskowski L, Sonntag F, Pöschel L, et al (2018) Replacing the Ethylmalonyl-CoA Pathway with the Glyoxylate Shunt Provides Metabolic Flexibility in the Central Carbon Metabolism of *Methylobacterium extorquens* AM1. ACS Synth Biol 7:86–97. https://doi.org/10.1021/acssynbio.7b00229

Schrader J, Buchhaupt M, Sonntag F, et al (2016) PROCESS FOR DE NOVO MICROBIAL SYNTHESIS OF TERPENES. WO 2016/142503 A1 (Patent)

Shigi Y (1989) Inhibition of bacterial isoprenoid synthesis by fosmidomycin, a phosphonic acid-containing antibiotic. J Antimicrob Chemother 24:131–145. https://doi.org/10.1093/jac/24.2.131

Sonntag F, Buchhaupt M, Schrader J (2014) Thioesterases for ethylmalonyl–CoA pathway derived dicarboxylic acid production in *Methylobacterium extorquens* AM1. Appl Microbiol Biotechnol 98:4533–4544. https://doi.org/10.1007/s00253-013-5456-y

Sonntag F, Kroner C, Lubuta P, et al (2015a) Engineering *Methylobacterium extorquens* for de novo synthesis of the sesquiterpenoid α-humulene from methanol. Metab Eng 32:82–94. https://doi.org/10.1016/j.ymben.2015.09.004

Sonntag F, Müller JEN, Kiefer P, et al (2015b) High-level production of ethylmalonyl-CoA pathway-derived dicarboxylic acids by *Methylobacterium extorquens* under cobalt-deficient conditions and by polyhydroxybutyrate negative strains. Appl Microbiol Biotechnol 99:3407–3419. https://doi.org/10.1007/s00253-015-6418-3

Toyama H, Anthony C, Lidstrom ME (1998) Construction of insertion and deletion *mxa* mutants of *Methylobacterium extorquens* AM1 by electroporation. FEMS Microbiol Lett 166:1–7. https://doi.org/10.1111/j.1574-6968.1998.tb13175.x

Yang Y-M, Chen W-J, Yang J, et al (2017) Production of 3-hydroxypropionic acid in engineered *Methylobacterium extorquens* AM1 and its reassimilation through a reductive route. Microb Cell Factories 16:179. https://doi.org/10.1186/s12934-017-0798-2

Zerbe P, Chiang A, Yuen M, et al (2012) Bifunctional *cis*-Abienol Synthase from *Abies balsamea* Discovered by Transcriptome Sequencing and Its Implications for Diterpenoid Fragrance Production. J Biol Chem 287:12121–12131. https://doi.org/10.1074/jbc.M111.317669

Statements and Declarations

Funding

This study was funded by the German Federal Ministry of Education and Research (BMBF) in the project ChiraMet (FKZ 031B0340A).

Competing Interests

Part of this work is published in the international patent WO2016/142503 A1 (BASF, Ludwigshafen, Germany).

Author Contribution

All authors contributed to the study conception, design and data analysis. Material preparation and data collection were performed by Laura Pöschel, Elisabeth Gehr, Paulina Jordan and Frank Sonntag. The manuscript was written by Laura Pöschel and Markus Buchhaupt. All authors read and approved the final manuscript.

Data Availability

All data generated or analysed during this study are included in this published article and its supplementary information file.

Supplementary Information (Online Resource 1)

Expression of toxic genes in Methylorubrum extorquens with a tightly repressed, cumate-inducible promoter

Laura Pöschel[1,2], Elisabeth Gehr[1], Paulina Jordan[1], Frank Sonntag[1], Markus Buchhaupt[1]*

[1] DECHEMA-Forschungsinstitut, Microbial Biotechnology, Theodor-Heuss-Allee 25, 60486 Frankfurt am Main, Germany

[2] Faculty of Biological Sciences, Goethe University Frankfurt, Max-von-Laue-Str. 9, 60438 Frankfurt am Main, Germany

*Corresponding author,
e-mail address: markus.buchhaupt@dechema.de

Description of content:

Table S1 Bacterial strains and plasmids used in this work.

Name	Relevant features/Cloning strategy	Application/Source	Reference
Bacterial strains			
E. coli DH5α	F⁻ φ80*lac*ZΔM15, Δ(*lac*ZYA-*arg*F)U169, *rec*A1, *end*A1, *hsd*R17(r_K^-, m_K^+) *pho*A, *sup*E44, λ⁻, *thi*-1 *gyr*A96 *rel*A1	Standard cloning applications	ATCC
M. extorquens AM1	Cm^R, gram-negative, facultative methylotrophic, obligate aerobic, α-proteobacterium		Peel and Quayle 1961
Plasmids			
pFS62b	pQ2148F-*zssI-ERG20-hmgs*-MVA	Expression vector for *M. extorquens* AM1 for α-humulene synthesis	Sonntag et al. 2015
pFS62b-s6	pQ2148-s6-*zssI-ERG20-hmgs*-MVA	α-humulene synthesis under P_{s6}-control	This work
pTE105_mCherry	Tet^R	mCherry expression vector for *M. extorquens* AM1	Schada von Borzyskowski et al. 2015
ppjo16	pQ2148F-*AbCAS-ERG20F96C*-MVA, *AbCAS* (Zerbe et al. 2012) and *ERG20F96C* (Ignea et al. 2015) were codon optimized and a new RBS[a] was inserted. For detailed sequence information see international patent WO 2016/142503 (Schrader et al.)	*cis*-abienol production plasmid	This work
ppjo16s1	pQ2148F_*AbCAS*(mut.)_MVA(mut.)	Isolated from ppjo16-suppressor mutant	This work
ppjo16s3	pQ2148F_*AbCAS_ERG20F96C*_MVA	Isolated from ppjo16-suppressor mutant	This work
ppjo16s4	pQ2148F_*AbCAS*(mut.)	Isolated from ppjo16-suppressor mutant	This work
ppjo16s6	pQ2148F_*AbCAS_ERG20F96C*_MVA (mutated P_{Q2148})	Isolated from ppjo16-suppressor mutant	This work
ppjo16L1	pQ2148F_*AbCAS*(mut.)_*ERG20F96C* (mut.)_MVA	Isolated from ppjo16-suppressor mutant	This work
pQ2148	P_{Q2148}, Tet^R, oriT, pBR322ori	Expression vector for *M. extorquens* harboring cumate inducible promoter	Kaczmarczyk et al. 2013
pQ2148F	pQ2148 with adapted multiple cloning site, Tet^R, oriT, pBR322ori	Expression vector for *M. extorquens* harboring cumate inducible promoter	Sonntag et al. 2015
pQ2148_mCherry	P_{Q2148}, mCherry, Tet^R, oriT, pBR322ori	mCherry reporter plasmid for P_{Q2148}	This work
pQ2148-s6_mCherry	P_{s6}, mCherry, Tet^R, oriT, pBR322ori	mCherry reporter plasmid for P_{s6}	This work

pQ2148L_mCherry	P_{Q2148}, mCherry, Tet^R, oriT, pBR322ori, contains linker region of pQ2148-lux (Kaczmarczyk et al. 2013)	mCherry reporter plasmid for P_{Q2148} with same GOI-upstream sequence like pQ2148-lux (Kaczmarczyk et al. 2013)	This work
pQ2148L-s6_mCherry	P_{s6}, mCherry, Tet^R, oriT, pBR322ori, contains linker region of pQ2148-lux (Kaczmarczyk et al. 2013)	mCherry reporter plasmid for P_{s6} with same GOI-upstream sequence like pQ2148-lux (Kaczmarczyk et al. 2013)	This work

[a] Optimization of RBS sequences was done with the RBS Calculator (Salis 2011)

Table S2 Oligonucleotides used in this study[a].

EGe119	ACAATCTGGTCTGTTTGTAACTAGTATGGTGAGCAAGGGCGAG	Construction of pQ2148F_mCherry and pQ2148F-s6_mCherry
EGe121	TTGTAAAACGACGGCCAGTGAATTCTTACTTGTACAGCTCGTCCATGCC	
LPoe1	AGCCTGAATTCGGATCCTGCAGGTACCGGGATCCGGCCCTCTAGTTACAAACAGACCAGATTGTCTGTTTGTTGTGGCGCGCTTCTAC	Construction of pQ2148_mCherry and pQ2148-s6_mCherry
LPoe2	CATGGACGAGCTGTACAAGTAAGAATTCACTGGCCGTCGTTTTACAACGTCGTGACTGG	
LPoe3	CGGTACCTGCAGGATCCGAATTCAGGCTTGGAGGATACGTATGGTGAGCAAGGGCGAGG	
LPoe4	GTAAAACGACGGCCAGTGAATTCTTACTT	
LPoe5	GTATCATGAGCGGATACATACTGGTCTGTTTGTACAGCATTGACG	
LPoe6	TATGTATCCGCTCATGATACAATAACCCTGATGC	
LPoe7	GCCTCGCGCGGGATTTTCTT	
LPoe8	CTGTTCACCACGCGCAACAAG	
PJo113	TTCGGCGACATGATGAC	Sequencing of constructs

[a] For oligonucleotides and PCR templates used for construction of ppjo16, see international patent WO 2016/142503 (Schrader et al.)

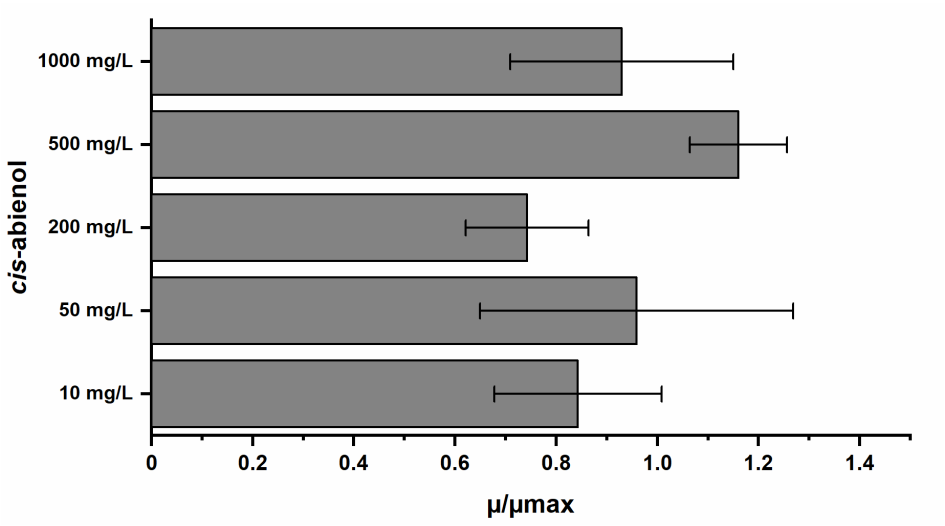

Fig. S1 Tolerance of *M. extorquens* AM1 towards *cis*-abienol. Maximum growth rates (μ_{max}) in medium without *cis*-abienol were compared to growth rates (μ) with different *cis*-abienol concentrations dissolved in aqueous phase. Three to four independent replicates were measured. Error bars represent standard deviations

References

Ignea C, Trikka FA, Nikolaidis AK, et al (2015) Efficient diterpene production in yeast by engineering Erg20p into a geranylgeranyl diphosphate synthase. Metab Eng 27:65–75. https://doi.org/10.1016/j.ymben.2014.10.008

Kaczmarczyk A, Vorholt JA, Francez-Charlot A (2013) Supplemental material Cumate-inducible gene expression system for sphingomonads and other Alphaproteobacteria. Appl Environ Microbiol 79:6795–6802. https://doi.org/10.1128/AEM.02296-13

Peel D, Quayle JR (1961) Microbial growth on C_1 compounds. 1. Isolation and characterization of *Pseudomonas* AM 1. Biochem J 81:465–469. https://doi.org/10.1042/bj0810465

Salis HM (2011) The ribosome binding site calculator. Methods Enzymol 498:19–42. https://doi.org/10.1016/B978-0-12-385120-8.00002-4

Schada von Borzyskowski L, Remus-Emsermann M, Weishaupt R, et al (2015) A Set of Versatile Brick Vectors and Promoters for the Assembly, Expression, and Integration of Synthetic Operons in *Methylobacterium extorquens* AM1 and Other Alphaproteobacteria. ACS Synth Biol 4:430–443. https://doi.org/10.1021/sb500221v

Schrader J, Buchhaupt M, Sonntag F, et al PROCESS FOR DE NOVO MICROBIAL SYNTHESIS OF TERPENES. WO 2016/142503 A1, 2016

Sonntag F, Kroner C, Lubuta P, et al (2015) Engineering *Methylobacterium extorquens* for de novo synthesis of the sesquiterpenoid α-humulene from methanol. Metab Eng 32:82–94. https://doi.org/10.1016/j.ymben.2015.09.004

Zerbe P, Chiang A, Yuen M, et al (2012) Bifunctional *cis*-Abienol Synthase from *Abies balsamea* Discovered by Transcriptome Sequencing and Its Implications for Diterpenoid Fragrance Production. J Biol Chem 287:12121–12131. https://doi.org/10.1074/jbc.M111.317669